

this document downloaded from

vulcanhammer.net

Since 1997, your complete on-line resource for information geotechnical engineering and deep foundations:

The Wave Equation Page for Piling

The historical site for Vulcan Iron Works Inc.

Online books on all aspects of soil mechanics, foundations and marine construction

Free general engineering and geotechnical software

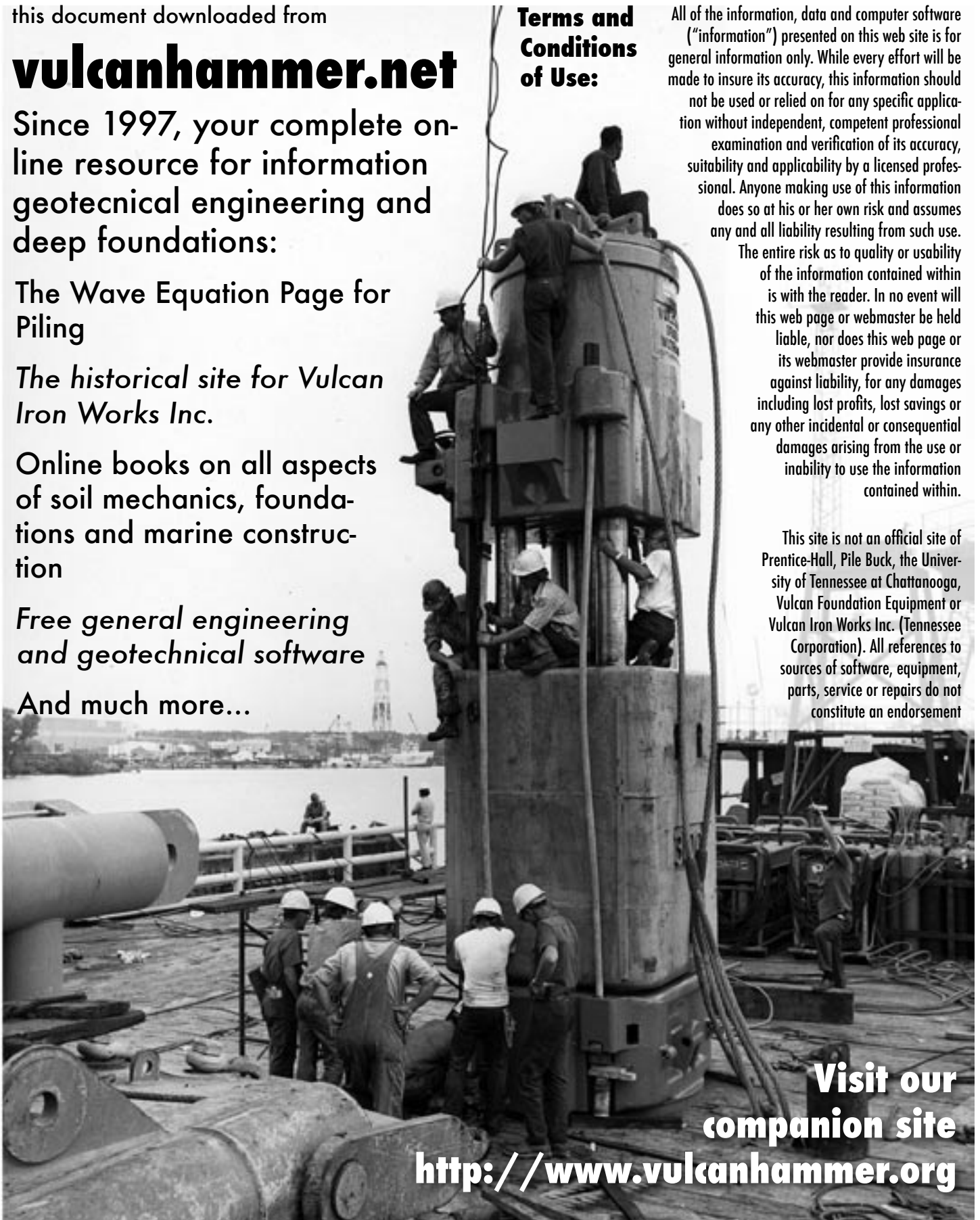
And much more...

Terms and Conditions of Use:

All of the information, data and computer software ("information") presented on this web site is for general information only. While every effort will be made to insure its accuracy, this information should not be used or relied on for any specific application without independent, competent professional examination and verification of its accuracy, suitability and applicability by a licensed professional. Anyone making use of this information does so at his or her own risk and assumes any and all liability resulting from such use.

The entire risk as to quality or usability of the information contained within is with the reader. In no event will this web page or webmaster be held liable, nor does this web page or its webmaster provide insurance against liability, for any damages including lost profits, lost savings or any other incidental or consequential damages arising from the use or inability to use the information contained within.

This site is not an official site of Prentice-Hall, Pile Buck, the University of Tennessee at Chattanooga, Vulcan Foundation Equipment or Vulcan Iron Works Inc. (Tennessee Corporation). All references to sources of software, equipment, parts, service or repairs do not constitute an endorsement



**Visit our
companion site**

<http://www.vulcanhammer.org>

MECHANICS OF DIESEL PILE DRIVING

BY

DAVID MAHER REMPE

B.C.E., Cornell University, 1960
M.S., University of Illinois, 1969

THESIS

Submitted in partial fulfillment of the requirements
for the degree of Doctor of Philosophy in Civil Engineering
in the Graduate College of the
University of Illinois at Urbana-Champaign, 1975

Urbana, Illinois

1954

June

1954

1954

1954

1954

1954

1954

1954

1954

1954

1954

1954

1954

1954

1954

1954

1954

1954

1954

1954

1954

1954

1954

1954

1954

1954

1954

1954

1954

1954

1954

1954

1954

1954

1954

1954

1954

1954

1954

1954

1954

MECHANICS OF DIESEL PILE DRIVING

David Maher Rempe, Ph.D.
Department of Civil Engineering
University of Illinois at Urbana-Champaign, 1975

Research was conducted into the mechanics of pile driving with diesel hammers. The first step consisted of an investigation of the mechanical and operational details of diesel pile hammers. Then, a mathematical simulation of diesel hammer operation was developed for purposes of wave equation analysis, which is an analytical method for prediction of pile load capacity and driving stress on the basis of driving resistance (pile penetration per hammer-blow). Finally, the performance characteristics of diesel pile hammers and the factors affecting performance were studied.

The details of diesel hammer design and operation are described. Differences in design and operation among the various types of diesel hammer are discussed as they relate to pile-driving effectiveness. Design features related to inclined operation and soft-ground operation are discussed.

The mathematical model of the diesel hammer is described in detail, with emphasis on the simulation of diesel combustion, steel-on-steel impact, and interaction of hammer operation with the dynamic response of pile and soil. In wave equation analysis of diesel pile driving, the mathematical hammer model is combined with models of the pile and soil to produce a total simulation of the hammer-pile-soil system.

1947

1948

1949

1950

1951

1952

1953

1954

1955

1956

1957

1958

1959

1960

1961

1962

1963

1964

1965

1966

1967

1968

1969

1970

1971

1972

1973

1974

1975

The simulation has three principal applications: prediction of the load-carrying capacity of the pile; stress analysis of the pile during driving; and detailed study of hammer operation. Prediction of pile capacity and stress analysis are of great practical importance in the design and construction of pile foundations. The detailed study of hammer operation is potentially useful in the design of diesel pile hammers for optimum performance. On the basis of comparisons of measured and simulated hammer performance, it is concluded that the hammer simulation method developed in the current research is sufficiently accurate for each of the foregoing applications.

Fundamental characteristics of diesel hammer performance are discussed. Energy available in the hammer, transmission of energy to the pile, and the form of the energy at the pile head are considered.

The results of an investigation of the factors affecting hammer performance are presented and discussed. The factors considered include those related to operational conditions, such as pile characteristics, soil resistance, inclination, and fuel volume, and those related to the design of the hammer and associated equipment.

ACKNOWLEDGMENT

The writer acknowledges the guidance of Professor M. T. Davisson in the conception and execution of the research and in the preparation of this manuscript. Several manufacturers and distributors of diesel pile hammers provided information and test data; special acknowledgment is extended to the following: Mr. T. R. Morris of International Construction Equipment, distributors of BSP hammers; Mr. A. G. MacKinnon of The Foundation Equipment Corporation, distributors of Delmag hammers; Mr. E. T. Houk of L. B. Foster Company, distributors of Kobe hammers; Messrs. K. E. Bailey and T. M. Leigh of Link-Belt Speeder Division of FMC Corp., manufacturers of Link-Belt hammers; and Messrs. G. R. Compton, Jr. and G. Kurylko of MKT Division of Koehring Company, manufacturers of MKT hammers.

The writer received National Defense Education Act fellowship support during part of the research. Computer facilities and assistance were provided by the Department of Civil Engineering and the Civil Engineering Systems Lab. Financial assistance in the drafting of the thesis figures was provided by Dames & Moore.

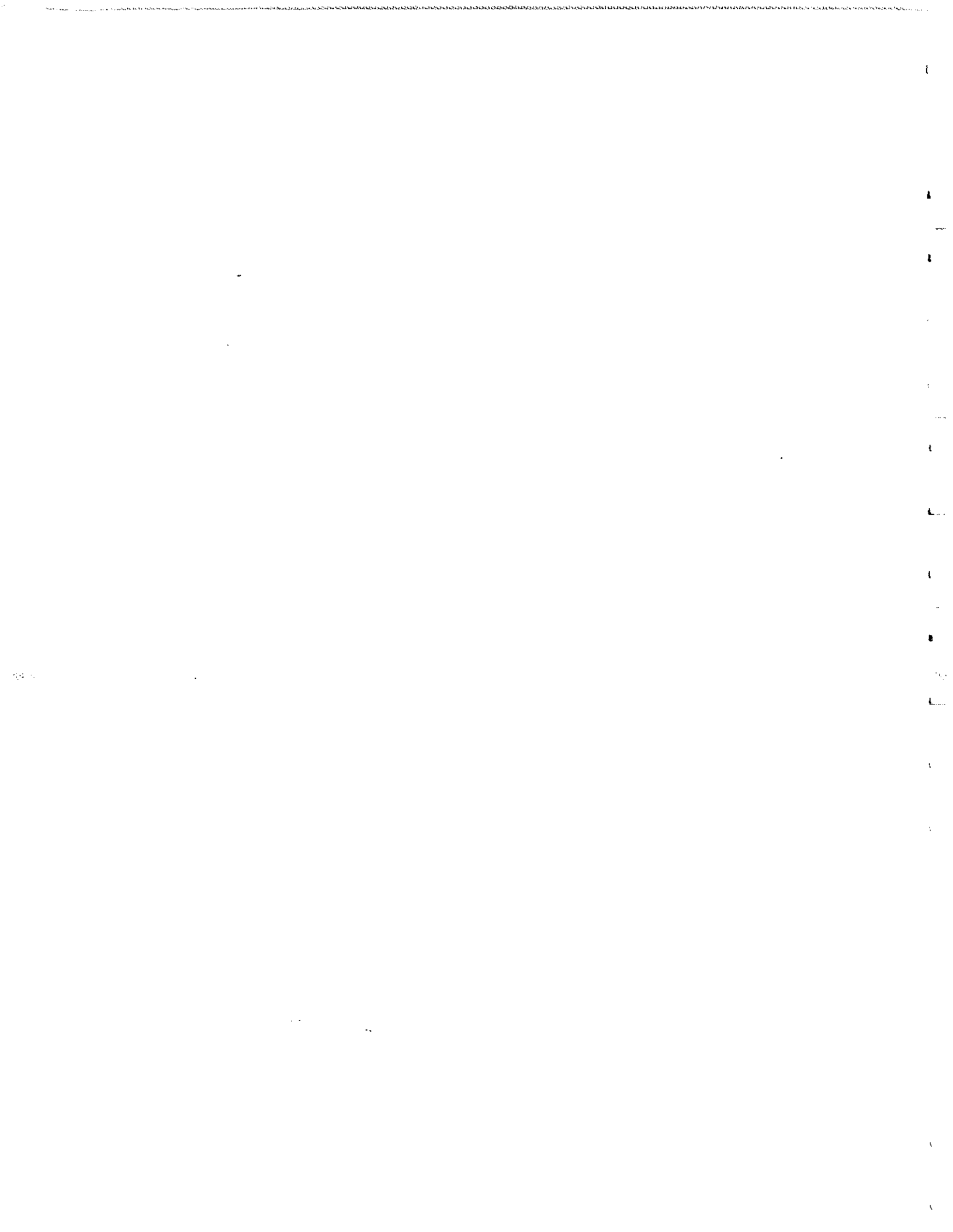


TABLE OF CONTENTS

CHAPTER		Page
1.	INTRODUCTION	1
	1.1 OVERVIEW	1
	1.2 ADVANTAGES OF DIESEL HAMMERS	6
	1.3 DISADVANTAGES OF DIESEL HAMMERS	8
	1.4 ANALYTICAL MODEL	9
	1.5 WAVE EQUATION ANALYSIS	12
	1.6 TEST DATA	14
	1.7 PREVIEW	15
2.	DETAILS OF DESIGN AND OPERATION	16
	2.1 INTRODUCTION	16
	2.2 COMPONENTS AND OPERATION	16
	2.3 GAS FORCE	21
	2.4 DESIGN DETAILS AND VARIATIONS	27
	2.5 FEATURES RELATED TO INCLINED DRIVING	47
	2.6 FEATURES RELATED TO SOFT-GROUND OPERATION.	49
	2.7 FEATURES AFFECTING PERFORMANCE	54
3.	COMPUTER SIMULATION	56
	3.1 INTRODUCTION	56
	3.2 WAVE EQUATION ANALYSIS	57
	3.3 MODELING THE DIESEL HAMMER	68
	3.4 IMPROVED MODEL	74
	3.5 GAS FORCE SIMULATION	79

CHAPTER	Page
3.6 STEEL-ON-STEEL IMPACT	95
3.7 FRICTION	98
3.8 INCLINED DRIVING	99
3.9 RESULTS OF WAVE EQUATION ANALYSIS, MULTIPLE RAM-STROKES	101
3.10 EVALUATION OF COMPUTER SIMULATION	103
4. FUNDAMENTAL ASPECTS OF DIESEL HAMMER PERFORMANCE .	118
4.1 INTRODUCTION	118
4.2 AVAILABLE ENERGY	118
4.3 TRANSMISSION OF ENERGY	120
4.4 FORM OF ENERGY	131
5. FACTORS AFFECTING DIESEL HAMMER PERFORMANCE . .	141
5.1 INTRODUCTION	141
5.2 PROCEDURE	141
5.3 JOB-CONTROLLED FACTORS	150
5.4 HAMMER-CONTROLLED FACTORS	174
6. CONCLUSIONS AND RECOMMENDATIONS FOR RESEARCH . .	219
6.1 CONCLUSIONS	219
6.2 RECOMMENDATIONS FOR RESEARCH	226
REFERENCES	229
APPENDIX	
A. OSCILLATION ERROR IN SPRING-MASS MODEL	231
A.1 INTRODUCTION	231
A.2 CAUSE OF OSCILLATION	231

APPENDIX	Page
A.3 DAMPING	232
A.4 EXAMPLE	235
A.5 CONCLUSION	241
B. SUMMARY FLOW CHART FOR DIESEL1 PROGRAM	243
VITA	245



LIST OF FIGURES

Figure		Page
1.1	COMPARISON OF IMPACT AND DIESEL PILE DRIVING . . .	3
1.2	COMPARISON OF REAL SYSTEM WITH MODEL	11
1.3	SUMMARY OF RESULTS OF WAVE EQUATION ANALYSIS . . .	13
2.1	COMPONENTS OF TYPICAL OPEN-TOP DIESEL HAMMER (SCHEMATIC)	17
2.2	OPERATIONAL CYCLE OF DIESEL HAMMER	19
2.3	THREE PHASES OF GAS-FORCE PULSE	22
2.4	RAM CONFIGURATION (SCHEMATIC)	29
2.5	CROSS-SECTION OF POWER CYLINDER (SCHEMATIC) . . .	35
2.6	CLOSED-TOP HAMMERS (SCHEMATIC)	43
2.7	INCLINED OPERATION	48
2.8	SOFT-GROUND OPERATION	51
3.1	RAM-PILE IMPACT	58
3.2	CONSTRUCTION OF MASS-SPRING-DASHPOT MODEL . . .	61
3.3	EXAMPLE PLOT OF RESULTS	65
3.4	EXAMPLE PLOT OF PILE-HEAD FORCE PULSE	67
3.5	DIESEL HAMMER MODEL (EDWARDS, 1967)	70
3.6	PREDICTED VS MEASURED FORCE-PULSE, EXISTING HAMMER MODEL	73
3.7	IMPROVED HAMMER MODEL	76
3.8	MEASURED PRESSURE VS VOLUME, COMPRESSION PHASE .	82
3.9	THREE TYPES OF ATOMIZATION TIMING (IDEALIZED) . .	83
3.10	SIMULATION OF GAS FORCE, COMBUSTION PHASE . . .	86

Figure		Page
3.11	MEASURED PRESSURE VS VOLUME, EXPANSION PHASE . . .	90
3.12	EFFECT OF CHANGE IN PEAK GAS FORCE ON GAS-FORCE PULSE	92
3.13	EXAMPLE RESULTS, ENERGY-INPUT ANALYSIS	94
3.14	OSCILLATION ERROR IN PREDICTION OF FORCE PULSE	97
3.15	SUMMARY OF RESULTS, WAVE EQUATION ANALYSIS, MULTIPLE RAM-STROKES	102
3.16	PREDICTED VS MEASURED GAS-FORCE PULSE, MANUFACTURER'S DATA	105
3.17	PREDICTED VS MEASURED ANVIL DEFLECTION, MANUFACTURER'S DATA	106
3.18	PREDICTED VS MEASURED CUSHION FORCE, MANUFACTURER'S DATA	107
3.19	PREDICTED VS MEASURED FORCE PULSE, ABERDEEN TEST PILE, 12.5 PSIG BOUNCE-CHAMBER PRESSURE	110
3.20	PREDICTED VS MEASURED FORCE PULSE, ABERDEEN TEST PILE, 20 PSIG BOUNCE-CHAMBER PRESSURE	111
3.21	PREDICTED VS MEASURED FORCE PULSE, ABERDEEN TEST PILE, 25 PSIG BOUNCE-CHAMBER PRESSURE	112
3.22	PREDICTED VS MEASURED FORCE PULSE, ABERDEEN TEST PILE, 25 PSIG BOUNCE-CHAMBER PRESSURE, SIMULATED TIP DAMAGE	114
3.23	PREDICTED VS MEASURED FORCE PULSE, PURDUE TEST PILE	115
3.24	PREDICTED VS MEASURED PILE CAPACITY	117
4.1	HAMMER-PILE-SOIL SYSTEM	121
4.2	ENERGY VS TIME, HAMMER-PILE-SOIL SYSTEM	123
4.3	EXAMPLE ENERGY CHART FOR DIESEL HAMMER	125
4.4	FORM OF ENERGY, FORCE-PULSE SHAPES	133
4.5	EFFECTS OF PILE IMPEDANCE AND SOIL RESISTANCE ON GAS-FORCE PULSE, CONSTANT STROKE	136

Figure	Page
4.6	INFLUENCE OF SOIL RESISTANCE ON FORM OF ENERGY 139
5.1	SIMULATION OF DRIVING INFINITELY LONG PILE 146
5.2	TRANSMITTED ENERGY VS PILE LENGTH 151
5.3	PEAK FORCE VS PILE LENGTH 152
5.4	PILE DEFLECTION VS PILE LENGTH 153
5.5	NET EXPENDED FUEL ENERGY VS PILE LENGTH 154
5.6	IMPEDANCE EFFECTS, INFINITELY LONG PILE 158
5.7	COMPONENTS OF WORK DONE ON ANVIL, INFINITELY LONG PILE 159
5.8	IMPEDANCE EFFECTS, 40 FT PILE, 240 TONS SOIL RESISTANCE 160
5.9	EFFECTS OF INCLINATION, 40 FT PILE, 240 TONS SOIL RESISTANCE 163
5.10	EFFECTS OF INCLINATION, 160 FT PILE, 240 TONS SOIL RESISTANCE 164
5.11	SOIL RESISTANCE EFFECTS, 40 FT PILE 166
5.12	SOIL RESISTANCE EFFECTS, 160 FT PILE 167
5.13	EFFECTS OF VARIATION IN SOIL RESISTANCE, CONSTANT FUEL ENERGY 170
5.14	COMPARISON OF FORCE PULSES - VARYING SOIL RESISTANCE, CONSTANT FUEL ENERGY, 40 FT PILE 171
5.15	EFFECTS OF VARIATION IN FUEL ENERGY, CONSTANT SOIL RESISTANCE 173
5.16	PREIGNITION EFFECTS, INFINITELY LONG PILE, 8 FT STROKE 175
5.17	EFFECTS OF PREIGNITION DISTANCE ON CONTRIBUTION OF GAS AND IMPACT TO HAMMER OUTPUT, INFINITELY LONG PILE, 8 FT STROKE 176
5.18	PREIGNITION EFFECTS, INFINITELY LONG PILE, 5 FT STROKE 177

Figure	Page
5.19	PREIGNITION EFFECTS, 40 FT PILE, 8 FT STROKE, 240 TONS SOIL RESISTANCE 178
5.20	EFFECTS OF PREIGNITION DISTANCE ON RELATIVE CONTRIBUTION OF GAS AND IMPACT TO HAMMER OUTPUT, 40 FT PILE, 8 FT STROKE, 240 TONS SOIL RESISTANCE 179
5.21	EFFECTS OF POWER-CYLINDER AREA, INFINITELY LONG PILE 183
5.22	COMPARISON OF FORCE PULSES - VARYING POWER- CYLINDER AREA, INFINITELY LONG PILE 184
5.23	EFFECTS OF POWER-CYLINDER AREA, 160 FT PILE, 300 TONS SOIL RESISTANCE 185
5.24	EFFECTS OF POWER-CYLINDER AREA, 40 FT PILE, 120 TONS SOIL RESISTANCE 186
5.25	EFFECTS OF POWER-CYLINDER AREA, 40 FT PILE, 300 TONS SOIL RESISTANCE 187
5.26	EFFECTS OF COMPRESSION RATIO, INFINITELY LONG PILE 191
5.27	COMPARISON OF FORCE PULSES - VARYING COMPRESSION RATIO, INFINITELY LONG PILE 192
5.28	EFFECTS OF COMPRESSION RATIO, 40 FT PILE, 120 TONS SOIL RESISTANCE 193
5.29	EFFECTS OF COMPRESSION RATIO, 40 FT PILE, 300 TONS SOIL RESISTANCE 194
5.30	EFFECTS OF RAM WEIGHT, INFINITELY LONG PILE, CONSTANT RATED ENERGY 198
5.31	COMPARISON OF FORCE PULSES - VARYING RAM WEIGHT, INFINITELY LONG PILE 199
5.32	EFFECTS OF RAM WEIGHT, 40 FT PILE, 120 TONS SOIL RESISTANCE, CONSTANT RATED ENERGY 200
5.33	EFFECTS OF RAM WEIGHT, 40 FT PILE, 300 TONS SOIL RESISTANCE, CONSTANT RATED ENERGY 201
5.34	EFFECTS OF ANVIL WEIGHT, INFINITELY LONG PILE 204

Figure	Page
5.35	COMPARISON OF FORCE PULSES - VARYING ANVIL WEIGHT, INFINITELY LONG PILE 205
5.36	EFFECTS OF ANVIL WEIGHT, 40 FT PILE, 120 TONS SOIL RESISTANCE 206
5.37	EFFECTS OF ANVIL WEIGHT, 40 FT PILE, 300 TONS SOIL RESISTANCE 207
5.38	EFFECTS OF DRIVEHEAD WEIGHT, INFINITELY LONG PILE 209
5.39	COMPARISON OF FORCE PULSES - VARYING DRIVEHEAD WEIGHT, INFINITELY LONG PILE 210
5.40	EFFECTS OF DRIVEHEAD WEIGHT, 40 FT PILE, 120 TONS SOIL RESISTANCE 211
5.41	EFFECTS OF DRIVEHEAD WEIGHT, 40 FT PILE, 300 TONS SOIL RESISTANCE 212
5.42	EFFECTS OF HAMMER-CUSHION STIFFNESS, INFINITELY LONG PILE 215
5.43	COMPARISON OF FORCE PULSES - VARYING HAMMER-CUSHION STIFFNESS, INFINITELY LONG PILE 216
5.44	EFFECTS OF HAMMER-CUSHION STIFFNESS ON PERFORMANCE, 40 FT PILE, VARYING IMPEDANCE 218
A.1	DAMPING ELEMENT FOR CONTROL OF SPURIOUS OSCILLATION 233
A.2	HYPOTHETICAL PROBLEM AND ANALYTICAL MODELS 236
A.3	HYPOTHETICAL PROBLEM, DIESEL1 SOLUTION USING MODEL I 238
A.4	HYPOTHETICAL PROBLEM, DIESEL1 SOLUTION USING MODEL II 239
A.5	HYPOTHETICAL PROBLEM, DIESEL1 SOLUTION USING MODEL III 240
A.6	HYPOTHETICAL PROBLEM, DIESEL1 SOLUTION USING MODEL IV 242
B.1	SUMMARY FLOW CHART FOR DIESEL1 PROGRAM 244

NOTATION

Symbol		Units
A_d	Effective acceleration of ram due to gravity and friction during downward movement of ram.	L/T^2
A_u	Effective acceleration of ram due to gravity and friction during upward movement of ram.	L/T^2
A_{pc}	Power-cylinder area in plane normal to axis of hammer.	L^2
a	Cross-sectional area of pile.	L^2
BPI	Blows per inch of penetration.	1/L
C_d	Damping constant.	FT
C_f	Friction factor pertinent to vertical operation of hammer.	1
C_{fb}	Friction factor pertinent to increase in friction resulting from inclined operation.	1
C_p	Percentage of critical damping.	1
C_r	Compression ratio.	1
c	Velocity of wave propagation.	L/T
D_h	Deflection of pile head.	L
D_{hm}	Maximum value of D_h .	L
D_p	Preignition distance.	L
D_t	Deflection of pile tip.	L
D_{tm}	Maximum deflection of pile tip.	L
D_{tn}	Net deflection of pile tip.	L
E	Young's modulus of elasticity.	F/L^2
E_a	Work done on anvil (energy).	FL
E_{ag}	Work done on anvil by gas force (energy).	FL

Symbol		Units
E_{agm}	Maximum value of E_{ag} .	FL
E_{am}	Maximum value of E_a .	FL
E_{an}	Net value of E_a , at completion of hammer cycle.	FL
E_{ar}	Work done on anvil by ram-impact force (energy).	FL
E_{arm}	Maximum value of E_{ar} .	FL
E_{avn}	Available net energy.	FL
E_{avp}	Available peak energy.	FL
E_{gl}	Gas energy lost by exhaust.	FL
E_{gn}	Net work done on ram and anvil by gas force (energy).	FL
E_{gt}	Total gas energy released by combustion.	FL
E_h	Work done on pile head (energy).	FL
E_{hm}	Maximum value of E_h .	FL
E_{hn}	Net value of E_h , at completion of hammer cycle.	FL
E_{lf}	Latent energy of fuel.	FL
E_{rg}	Work done on ram by gas force (energy).	FL
E_{wh}	Rated energy of pile-driving hammer.	FL
e	Coefficient of restitution of bilinear cushion.	1
e_f	Efficiency of energy transmission.	1
e_h	Hammer efficiency.	1
\dot{e}	Strain rate.	1/T
F	Force.	F
F_a	Force applied to anvil.	F
F_{ag}	Force applied to anvil by gas.	F

Symbol		Units
F_g	Gas force.	F
F_{gm}	Maximum value of F_g .	F
F_h	Force in pile head.	F
F_{hm}	Maximum value of F_h .	F
F_i	Impact force on anvil.	F
F_p	Peak force.	F
F_s	Total soil resistance force under dynamic loading.	F
F_{su}	Ultimate value of F_s .	F
F_t	Force in pile tip.	F
F_{tm}	Maximum value of F_t .	F
g	Acceleration due to gravity.	L/T^2
I_a	Impulse on top of anvil.	FT
I_{ag}	Impulse on top of anvil due to gas force.	FT
I_{ar}	Impulse on top of anvil due to ram-impact force.	FT
I_h	Impulse on pile head.	FT
I_r	Ratio of hammer impedance to pile impedance.	1
J_s	Viscous damping factor for soil along the side of the pile.	T/L
J_t	Viscous damping factor for soil at the pile tip.	T/L
K_c	Spring stiffness of hammer cushion.	F/L
K_{pc}	Spring stiffness of pile cushion.	F/L
L_p	Length of pile.	L
M_1	Mass of ram.	FT^2/L
M_2	Mass of anvil.	FT^2/L
M_3	Mass of drivehead.	FT^2/L

Symbol		Units
n_c	Constant pertinent to compression of gas.	1
n_e	Constant pertinent to expansion of gas.	1
p	Gas pressure.	F/L^2
p_1	Gas pressure at the beginning of compression.	F/L^2
p_3	Gas pressure at the beginning of expansion	F/L^2
Q_s	Soil quake at side of pile.	L
Q_t	Soil quake at tip of pile.	L
R_u	Total ultimate soil resistance under static loading.	F
r_u	Ultimate soil resistance under static loading, for single soil spring.	F
S_p	Power stroke of ram.	L
S_t	Total stroke of ram.	L
T_d	Delay time of gas force.	T
T_h	Hold time of gas force.	T
T_r	Rise time of gas force.	T
t	Time.	T
u	Longitudinal displacement of bar in x direction.	L
V_o	Velocity of ram at impact.	L/T
V_{cc}	Volume of combustion chamber.	L^3
V_{pc}	Volume of power cylinder.	L^3
V_s	Swept volume.	L^3
v	Velocity.	L/T
v	Volume.	L^3
v_1	Volume of gas at beginning of compression.	L^3
v_3	Volume of gas at beginning of expansion.	L^3

Symbol		Units
W_1	Weight of ram.	F
W_2	Weight of anvil.	F
W_3	Weight of drivehead.	F
x	Distance from pile head.	L
α	Angle of inclination of hammer, measured from the vertical.	Deg.
β	Fraction of E_{wh} available for transmission to pile.	1
γ	Fraction of R_u used in determination of effective force-pulse duration.	1
ρ	Pile mass per unit volume.	FT^2/L^4
ρ_{ca}	Pile impedance.	FT/L
ω	Frequency of vibration, radians per second.	$1/T$

CHAPTER 1
INTRODUCTION

1.1 OVERVIEW

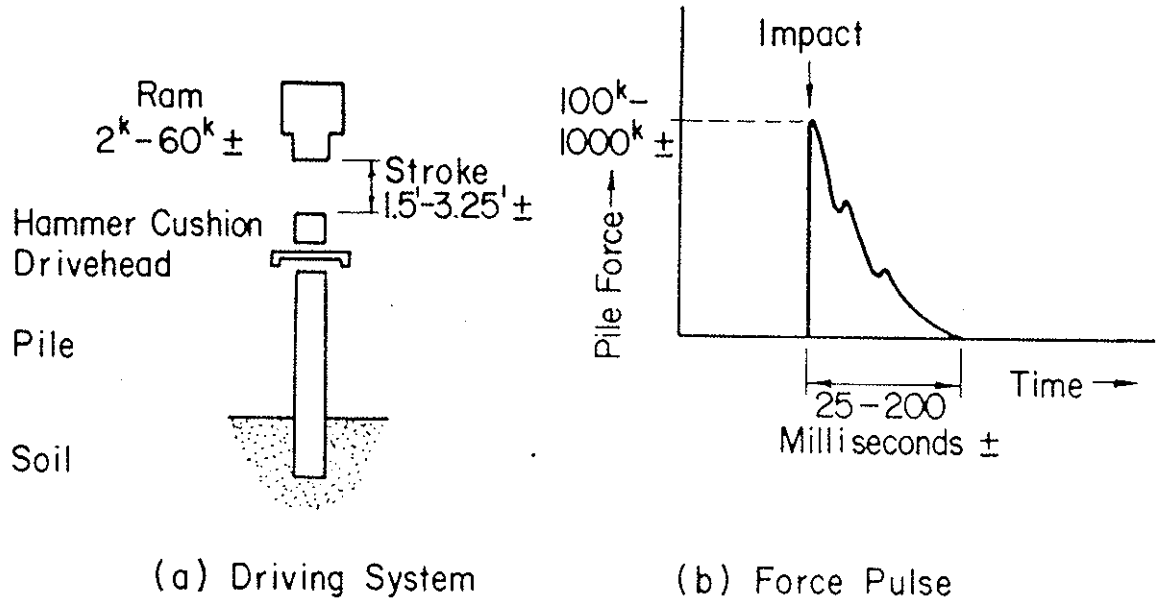
This dissertation summarizes the results of a study of diesel pile-driving hammer performance. The research was motivated by a need within the engineering and contracting professions for a basic understanding of the mechanics of diesel pile driving. The need arises partly from the practice of using the pile driving hammer as both a contractor's tool and as an engineer's measuring instrument. As a tool, the pile hammer serves to force the pile into the ground by repeated application of impulsive force. It functions as a measuring instrument when, as is normally the case, the engineer predicts or verifies the axial load capacity of the pile on the basis of the net penetration for each hammer blow at final driving. Competent use of a pile hammer in either function requires that both the engineer and contractor have thorough knowledge of the performance characteristics of the particular hammer being used. In the case of the diesel hammer this knowledge heretofore has not been available. A peculiar situation exists wherein diesels are widely used because of their economic advantages, but are regarded with suspicion and/or discriminated against by engineers.

The research described herein has led to both a fundamental explanation of the performance characteristics of diesel

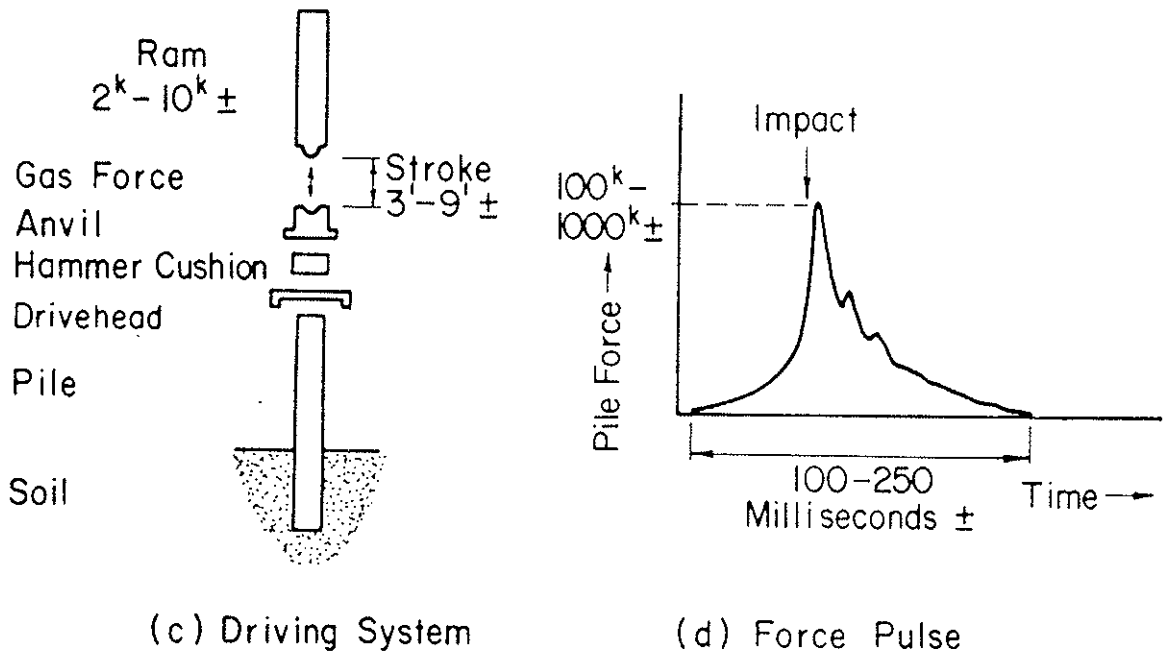
hammers and a method for quantitative analysis of diesel pile driving. Hopefully this will help bring about more competent use of diesel hammers and, consequently, more efficient pile installation.

There are three types of pile hammer in use today, each having distinct performance characteristics. In this dissertation, the three types will be designated as impact, diesel and vibratory hammers. The last, vibratory hammers, are specialized tools which are radically different from the other hammer types; they are not widely used for bearing-pile installation and will not be discussed further herein. The interested reader is referred to Smart (1969) for a complete study of vibratory hammer performance.

Impact hammers employ a falling mass of steel, called a ram, which impacts a hammer cushion consisting of a block of wood, plastic or other material softer than steel (Figure 1.1a). Force is transmitted through the hammer cushion to a second steel mass, called the drivehead, and then to the pile. Between hammer blows the ram is raised to the starting position by steam, compressed air or hydraulic fluid supplied by a remote power source. The force pulse generated in the pile head by the ram impact is typified in Figure 1.1b. Pile-head force increases rapidly at the time of impact, then decays either rapidly or slowly, depending upon the dynamic response of the pile and soil. The mechanics of pile driving with this type of hammer have previously been investigated by Parola (1960) and will be discussed later as they relate to the mechanics of diesel pile driving.



Impact Driving



Diesel Driving

Figure 1.1 COMPARISON OF IMPACT AND DIESEL PILE DRIVING

Diesel hammers resemble impact hammers in that they employ a falling ram to generate force in the pile. In the diesel, however, the ram impacts a steel mass known as an anvil (Figure 1.1c). Prior to impact, air is compressed between the ram and anvil, and fuel is injected; upon impact the fuel-air mixture ignites and the resulting combustion force drives the ram upward to the starting position. Because the gas forces act equally upon the ram and anvil, and because the ignition is nearly simultaneous with impact, the total generated pile force is affected by combustion. As indicated in Figure 1.1d, generated pile force begins to increase prior to impact due to compression of air, increases sharply at the time of impact and ignition, then decays. It will be demonstrated that combustion has an important effect on the pile driving performance of diesel hammers.

In diesel pile driving, the complex interaction of impact force, combustion force, and dynamic response of pile and soil produces hammer performance characteristics which in some ways are totally different from those of impact hammers. At present the only practical mathematical tool for accurately describing the foregoing characteristics is known as the wave equation analysis. This is a technique utilizing the one-dimensional wave equation for mathematical modeling of hammer operation and the resulting movements and forces generated in the pile and soil (Cummings, 1940; Smith, 1962). Wave equation analysis supersedes the so-called dynamic formulas, such as

the Engineering News Formula, the use of which is no longer justifiable (Cummings, 1940; Parola, 1970; Davisson, 1974).

Utilization of the wave equation analysis with impact pile hammers is a straight-forward procedure. Impact hammers employ a compact mass of steel impacting a hammer cushion which is soft relative to the drivehead and pile. The mechanics of this event can be described with acceptable accuracy by simple equations of motion (Smith, 1955; Parola, 1970) and, therefore, are easily incorporated into a mathematical simulation.

Operational characteristics of diesel hammers, however, pose serious analytical problems with respect to wave equation methods. The gas force at any point in the hammer cycle is dependent upon pile characteristics, soil resistance, and other factors, such that accurate prediction of gas force without consideration of these factors is impossible. An additional complicating factor is encountered in the simulation of the impact of the steel ram on the steel anvil. Steel-on-steel impact is more difficult to treat mathematically than the ram-on-cushion (steel-on-softer material) impact of the impact hammer.

The following steps were taken to identify and explain the performance characteristics of diesel hammers:

1. Study of diesel hammer design details and cycle of operation.
2. Construction of an analytical model for simulation of diesel hammer operation in wave equation analysis of pile driving.

3. Study of hammer performance characteristics employing wave equation analysis, hammer test data, and field observations of hammer behavior.

The results of this investigation pertain to diesel hammers in general because all diesel hammers are fundamentally similar in operation. Differences exist among the various hammer models currently in use, but these differences are adequately accounted for in the analysis presented herein. Other details not directly related to pile-driving performance, such as lifting hardware, fuel storage, and maintenance are not discussed. For historical information relative to the use of diesel hammers in the U.S.A., the reader is directed to a brochure published by Link-Belt, a manufacturer of diesel hammers (Link-Belt, undated).

The balance of this chapter is devoted to introductory information relating to diesel hammers, the fundamentals of the problem to be solved, and the methods used in arriving at a solution.

1.2 ADVANTAGES OF DIESEL HAMMERS

Advantages associated with diesel hammers as compared with impact hammers can be summarized as follows:

1. Self-contained operation.
2. Variable ram stroke.
3. Reduced weight.
4. Simplified cold weather operation.

Self-contained operation leads to several important economies. Whereas an impact hammer is dependent upon a remote energy source such as a boiler, air compressor, hydraulic pump or power winch, a diesel hammer operates independently of such accessory equipment. As a result, total equipment cost may be reduced and the cost of labor required for operation of the auxiliary energy source if eliminated. Mobilization is cheaper due to lower freight costs and rapid assembly of equipment at the jobsite. Fuel consumption is decreased as a result of improved overall mechanical and thermal efficiency. In general, polluting gas emissions are reduced as compared to those of the remote power source required for impact hammers.

The ram stroke of a diesel hammer is variable and, as a result, the peak force applied to the pile is also variable. This allows a greater flexibility of operation than is now available with impact hammers. Variable stroke is especially useful, for instance, in the driving of precast concrete piles. Such piles are susceptible to tensile cracking under conditions of "easy driving", that is, low soil resistance. In this situation a reduced ram stroke leads to a decrease in peak tensile force in the pile and therefore to a reduction in the potential for pile damage.

A commonly used basis for the comparison of the weights of hammers of different types is the energy per hammer blow, where energy is defined as the ram weight multiplied by the free-fall distance (stroke). To avoid confusion with other

definitions of energy, the product of ram weight and stroke is referred to herein as rated energy. For a given rated energy, diesel hammers typically weight less than impact hammers. As a result the contractor is able to use smaller crane and hammer-supporting equipment, thus lowering his equipment costs.

The diesel hammer can be operated efficiently in sub-zero weather, without the problems of freezing associated with steam-driven impact hammers.

1.3 DISADVANTAGES OF DIESEL HAMMERS

The most important disadvantages often associated with diesel hammers are as follows:

1. Lack of information relative to performance.
2. Failure to operate continuously in soft-ground driving.
3. Low blow rate.
4. Head room requirements.

The performance characteristics of diesel hammers are widely misunderstood as a result of the lack of available information. Thus, these hammers are often used inefficiently and in inappropriate situations, or their use is denied in situations where they would be appropriate.

When resistance to penetration is low, that is, soft-ground driving, diesel hammers may not operate continuously and thus require frequent restarting. Innovations in hammer

design have largely eliminated this problem. In some cases where the problem does exist it may be solved by changing to a hammer of the same type but of lower rated energy. Operation in soft-ground conditions will be examined in later chapters.

The number of hammer blows per minute (blow rate) is of importance to the contractor because it determines the total driving time per pile. An increased blow rate results in reduced costs of equipment and labor. Although blow rates vary from hammer to hammer, diesel hammers in general are slightly slower than impact hammers. The typical range of blow rates for diesel hammers is 40 to 60 blows per minute, depending on stroke, whereas comparable impact hammers operate at 50 to 60 blows per minute. One type of diesel hammer, known as "closed-top", operates at 80 to 100 blows per minute; a comparable impact hammer is the differential-acting hammer which operates at approximately 90 to 120 blows per minute.

Because of the comparatively long ram and high stroke, the diesel hammer requires more operating head room. This may be a disadvantage where head room is restricted due to leader dimensions or limited overhead clearance.

1.4 ANALYTICAL MODEL

Diesel hammer performance cannot be studied without reference to the dimensions and material of the pile being driven and the magnitude and distribution of the soil resistance

on the pile. This situation arises from the interdependence of hammer force output and the dynamic response of the pile and soil. As a result of the interaction phenomena, analysis of diesel pile driving must take into account many variables apart from the hammer.

As a first step in studying hammer performance, all the significant factors controlling performance were incorporated into an analytical model. An idealized version of the model, in comparison to the real elements of the hammer-pile-soil system which it simulates, is presented in Figure 1.2.

In the model, mechanical hammer components are replaced by concentrated masses, massless springs, or combinations of the two. Gas force is introduced as a function of several variables, including time and the relative position of the ram and anvil.

The pile is represented in the model as a series of masses and springs. Although a pile of uniform cross-section is shown in the example, the method can be applied with equal validity to any configuration.

Soil resistance is simulated in the model by pairs of elastic-plastic springs and dashpots attached to selected mass points at the tip and along the side of the pile. The magnitude and distribution of soil resistance on the pile is controlled by the peak force assigned to each soil spring.

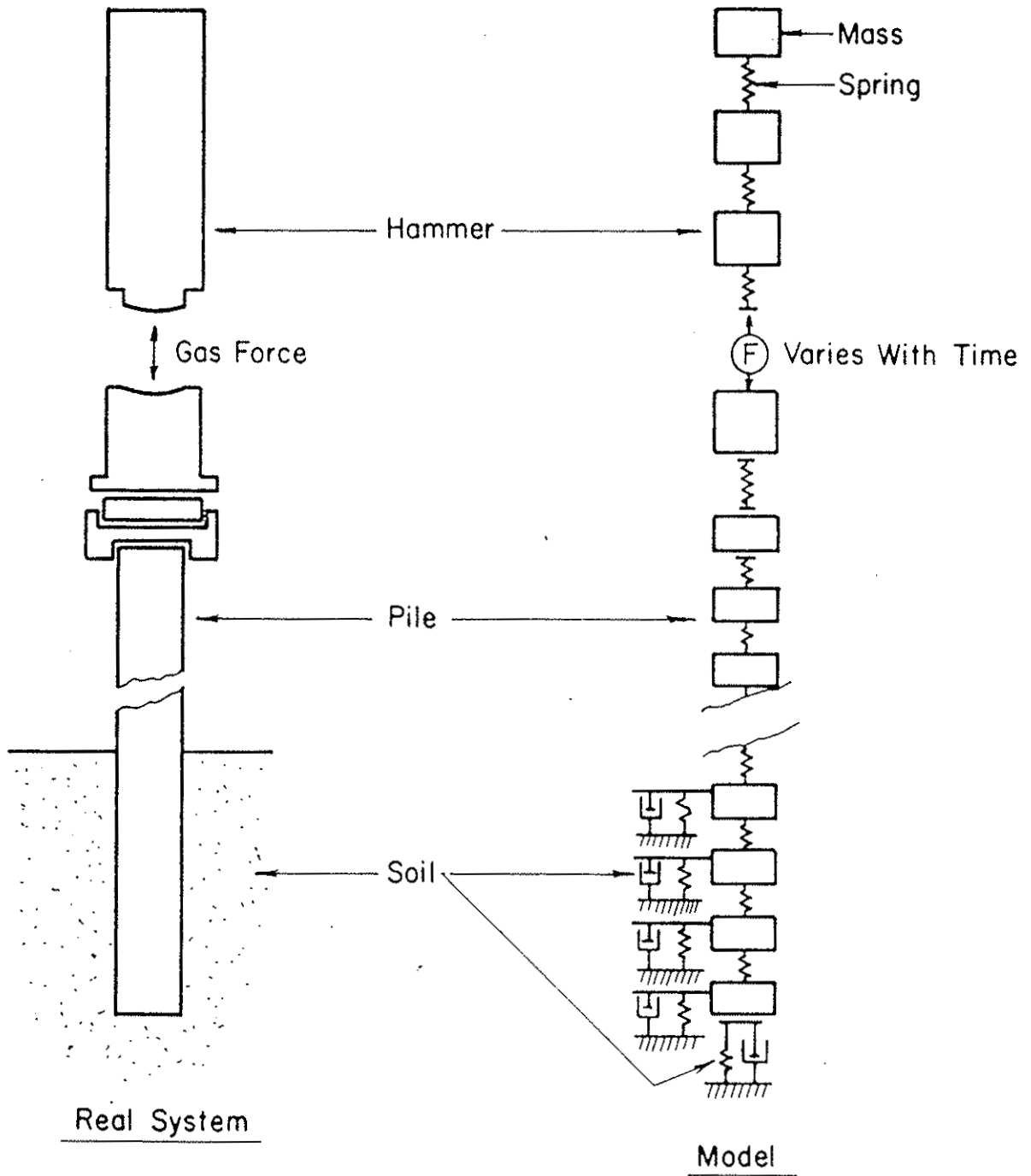


Figure 1.2 COMPARISON OF REAL SYSTEM WITH MODEL

1.5 WAVE EQUATION ANALYSIS

Forces and deflections within the analytical model are calculated by means of wave equation analysis, on the assumption that the motions of the discrete masses within the model proceed according to the physical law governing stress wave propagation in a slender rod, that is, the one-dimensional wave equation. A variety of hammer types, pile configurations, and soil conditions can be simulated by insertion of appropriate masses, spring stiffness and damping constants into the model. Details of the calculation procedure are discussed in Chapter 3.

The end product of the calculation is a prediction of net pile penetration, expressed as blows/inch, and peak stresses and displacements generated in the pile as a result of a single hammer blow. Each solution is based on an assumed total static soil resistance, which is the ultimate pile load capacity, R_u , at the time of driving. If solutions are obtained for various values of R_u , a curve of R_u vs blows/inch is generated (Figure 1.3). Peak pile stresses, compressive and tensile, can also be plotted on this graph. Thus, wave equation analysis provides the correlation between penetration data and pile capacity which is required by the foundation engineer. The stress data makes possible the optimum exploitation of pile drivability without pile damage, resulting in economical pile design.

For research purposes, such as the current study of diesel hammer performance, wave equation analysis is equally useful. It allows a thorough study of the operational

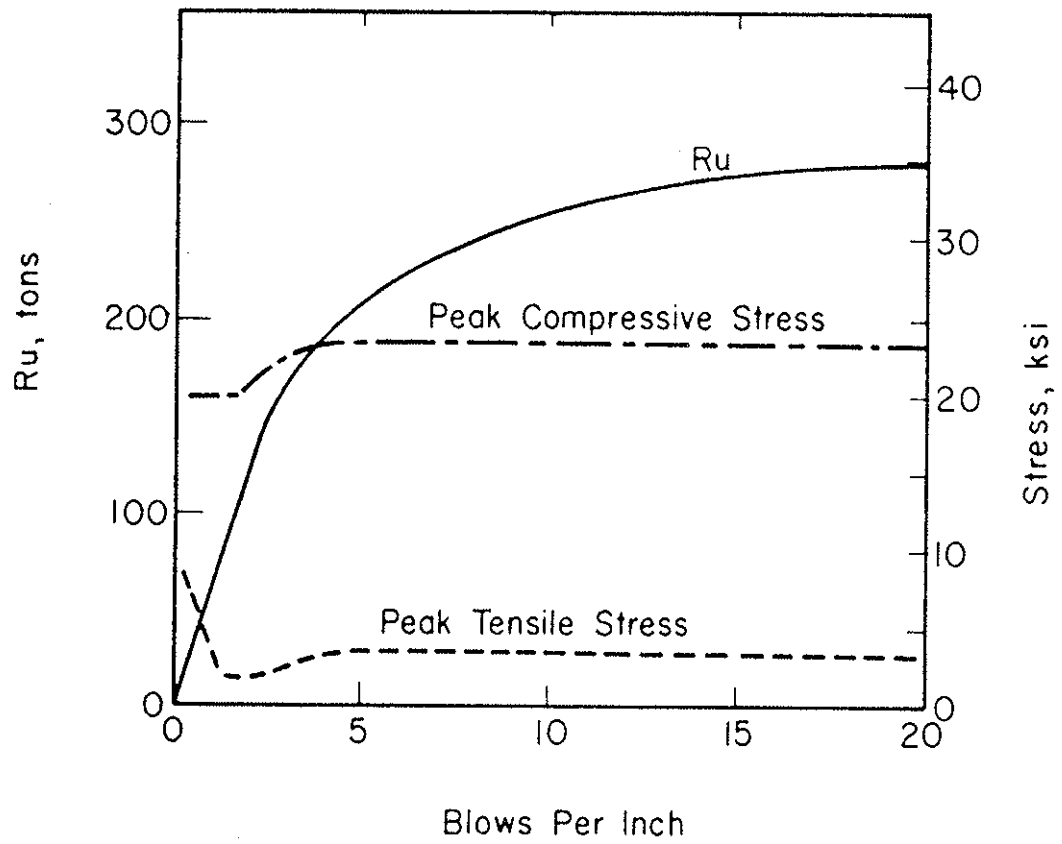


Figure 1.3 SUMMARY OF RESULTS OF WAVE EQUATION ANALYSIS

characteristics of each hammer component under a variety of simulated driving conditions, without the prohibitive expense of prototype testing.

1.6 TEST DATA

The analytical methods developed in this investigation are based on well established theoretical concepts of mechanics and thermodynamics. However, there are a great number of variables involved, many of which are difficult or impossible to quantify. It has been necessary, therefore, to make reasonable assumptions relative to these variables and then to check the net result by comparison of the predicted and measured hammer performance.

Hammer performance measurements are of two basic types: field checks and instrumented tests. Field checks consist of jobsite measurements of gross and net pile movements during driving, static tests of pile load capacity, and observations of hammer behavior under various driving conditions. Instrumented tests of diesel pile-driving hammers provide detailed data regarding combustion-chamber pressures, ram and anvil motions, and other facets of hammer performance. Unfortunately, very little data of this type is available either in the literature or from hammer manufacturers. Such data is potentially of great value, but it is strongly affected by test conditions which, in most cases, are not fully documented. As a consequence,

useful detailed test data relative to hammer performance is scarce; samples of available data are included in later chapters.

1.7 PREVIEW

The results of the investigation will be summarized in the chapters to follow. In Chapter 2 design details and operating features of diesel hammers are discussed; the emphasis is on hammer features relating to pile-driving effectiveness.

Chapter 3 consists of a discussion of the application of wave equation analysis to diesel pile driving, with emphasis on mathematical simulation of diesel hammer operation.

Chapter 4 is devoted to the fundamental aspects of diesel hammer performance including the energy available in the hammer, transmission of the energy to the pile, and the form of the energy as it occurs at the pile head.

In Chapter 5 the results of a study of the major factors influencing diesel hammer performance are presented and discussed.

Conclusions drawn from the research and proposals for further research and data collection are presented in Chapter 6.

Appendices include a discussion of oscillation errors associated with simulation of steel-on-steel impact and a summary flow chart describing the DIESEL1 computer program.



CHAPTER 2

DETAILS OF DESIGN AND OPERATION

2.1 INTRODUCTION

As a first step in the study of diesel hammer performance it was necessary to investigate the details of hammer design and operation. Emphasis was placed on those details which affect the force output of the hammer, that is, the force which the hammer applies to the pile.

This chapter will summarize the results of the investigation, thus providing a basis for discussions of computer simulation and hammer performance in later chapters. Hammer components are identified and the operational cycle is examined with emphasis on gas force phenomena. Design details and variations, inclined and soft-ground driving, and other factors affecting hammer performance are presented.

2.2 COMPONENTS AND OPERATION

Most diesel hammers are of the open-top design as shown schematically in Figure 2.1. The ram is a solid mass of steel which moves as a free piston within the steel cylinder and impacts another steel mass known as the anvil, or impact block. Beneath the anvil is the hammer cushion, which is made of plastic, asbestos, wood or other material softer than steel.

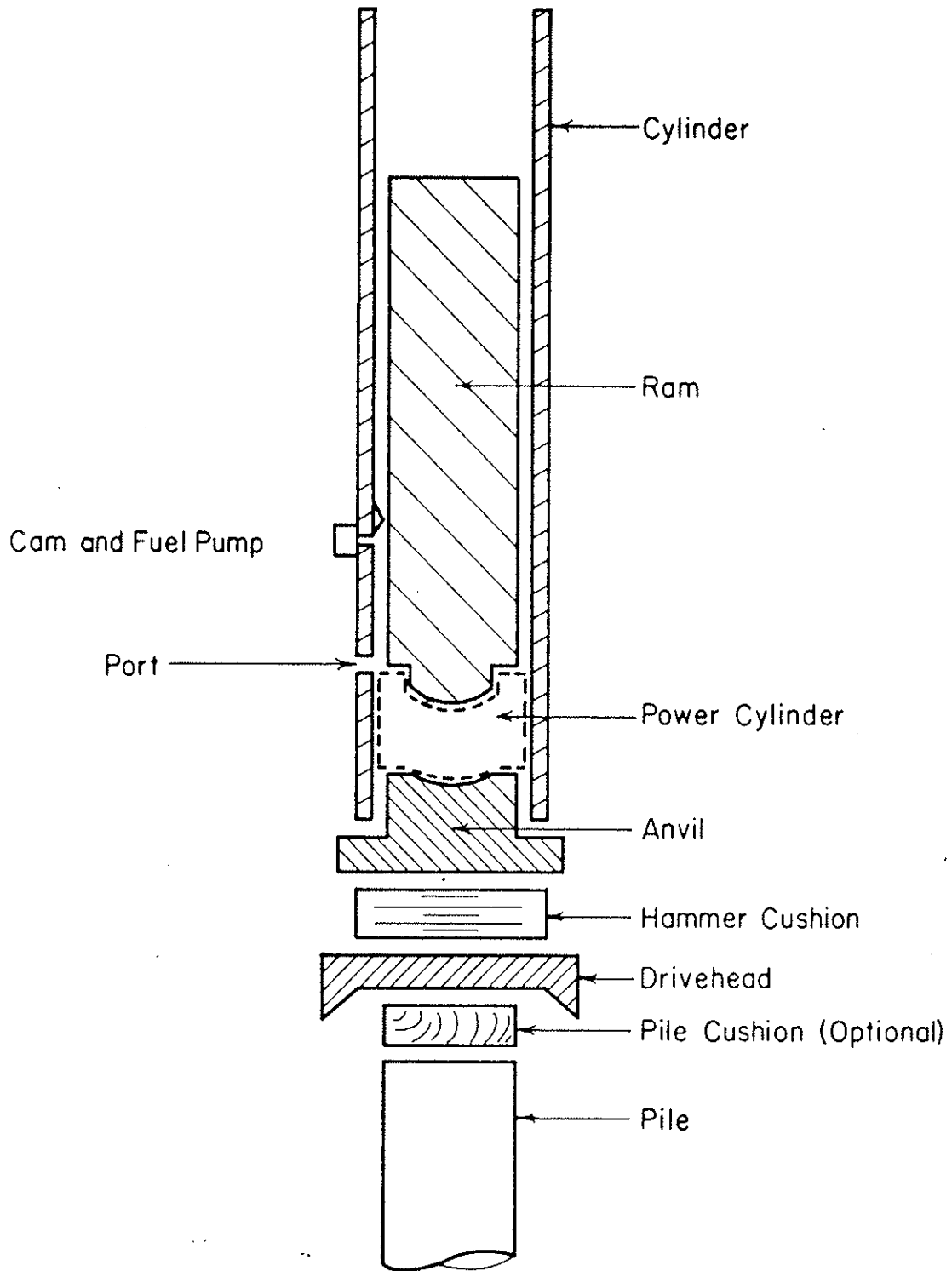


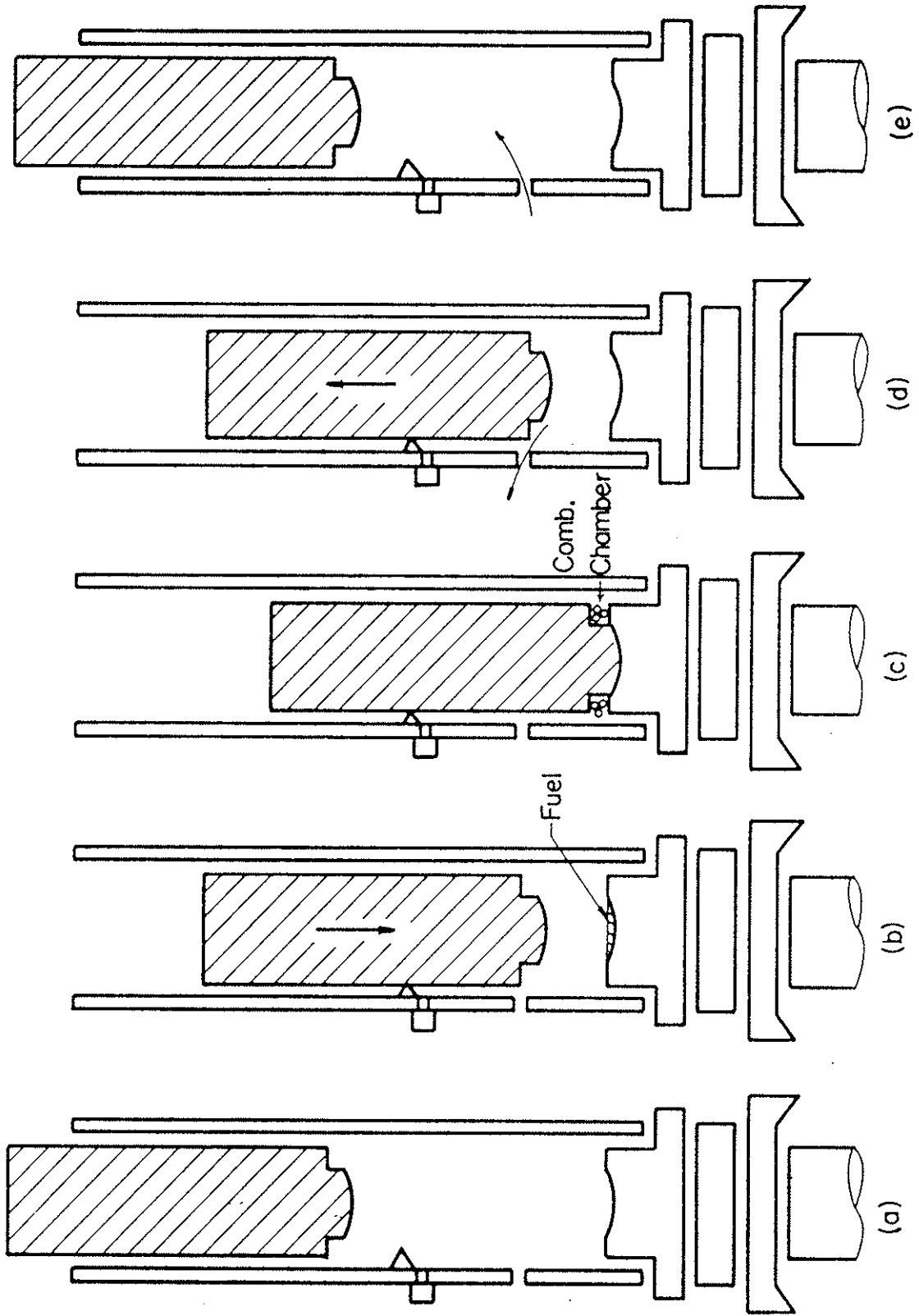
Figure 2.1 COMPONENTS OF TYPICAL OPEN-TOP DIESEL HAMMER (SCHEMATIC)

The cushion rests on the drivehead, a third steel mass which is designed to fit the top of the pile. In some cases a second cushioning element, called a pile cushion, is inserted between the drivehead and pile. For convenience the elements between ram and pile head will be referred to collectively as interface equipment.

Openings in the cylinder wall above the top surface of the anvil are known as ports. The zone enclosed by the cylinder between the ports, the bottom of the ram at port closure, and the top surface of the anvil is known as the power cylinder. A fuel pump and activating cam are built into the cylinder wall.

Figure 2.2 is a schematic representation of the operational cycle of the hammer depicted in Figure 2.1. To initiate hammer operation the ram is lifted to the top-of-stroke position (Figure 2.2a) by crane line or other accessory mechanism. This lifting is required only for the first hammer cycle, after which the ram is raised by diesel combustion.

When the ram is released from top-of-stroke, it accelerates downward under the force of gravity. Atmospheric pressure acts equally on the top and bottom surfaces of the ram; thus the only resistance to downward motion is provided by friction between the ram and the cylinder walls. On the way downward the ram contacts the fuel-pump activating cam, causing fuel to be pumped onto the concave top surface of the anvil, where it collects in a pool. As the falling ram passes the port it seals the power cylinder zone and thus prevents further escape of air (Figure 2.2b).



Top-Of-Stroke

Exhaust

Impact, Ignition

Port Closure

Top-Of-Stroke

Figure 2.2 OPERATIONAL CYCLE OF DIESEL HAMMER

As the ram continues downward the power-cylinder air is compressed into a progressively decreasing volume. The resulting increased gas force acts on the lower surface of the ram, in opposition to the force of gravity; thus the ram velocity at the instant of impact on the anvil is reduced. Pre-impact gas force acts equally on the anvil, accelerating it downward and further reducing the relative velocity of ram and anvil at impact.

As indicated in Figure 2.2c the lower ram surface and upper anvil surface are designed such that, upon impact, an annular clearance space known as a combustion chamber remains. The fuel which was pooled on the anvil is splashed into this combustion chamber where it mixes with the compressed air and ignites spontaneously. The result is a rapid increase of gas pressure, approximately simultaneous with impact.

The ram is in contact with the anvil for several milliseconds, during which time the reaction force of the anvil and the gas force first decelerate the ram to zero downward velocity, then accelerate it upward. After separation of ram and anvil the accelerating force is provided solely by the gas. The gas force decreases as the ram moves upward and drops to zero when the bottom of the ram passes the port, opening the power cylinder to the atmosphere and allowing exhaust (Figure 2.2d). Further upward movement of the ram creates suction within the cylinder and thus draws fresh air in through the ports, such that when the ram reaches the top-of-stroke position another cycle can begin (Figure 2.2e).

A single cycle for the hammer described above typically consumes approximately 1.0 to 1.5 seconds, corresponding to a blow rate of 40 to 60 blows per minute in continuous operation. Each blow generates a force pulse in the anvil, which is transmitted through the hammer cushion and drivehead to the pile, causing penetration of the pile into the soil.

The generated pile force is a result of both gas and impact forces on the anvil. The gas component of the force begins to act as soon as the ram enters the power cylinder and starts to compress the air within. Gas force and thus pile force continue to increase up to the time of impact, at which time ignition and impact combine to cause an additional sharp rise in force. The gas force remains after impact forces are dissipated. As the ram moves upward this force decreases steadily until exhaust occurs; the generated pile force then drops to zero. The duration of the generated force, for the type of hammer described above, is approximately 125 to 225 milliseconds.

2.3 GAS FORCE

The gas force developed within a diesel hammer is the focal point of this investigation; it is this force, as it affects hammer operation and force output, which results in most of the analytical problems relating to diesel hammers. In the following paragraphs the three phases of the gas-force pulse, namely, compression, combustion, and expansion (Figure 2.3), are examined in detail. Mathematical simulation of each of these phases will be discussed in Chapter 3.

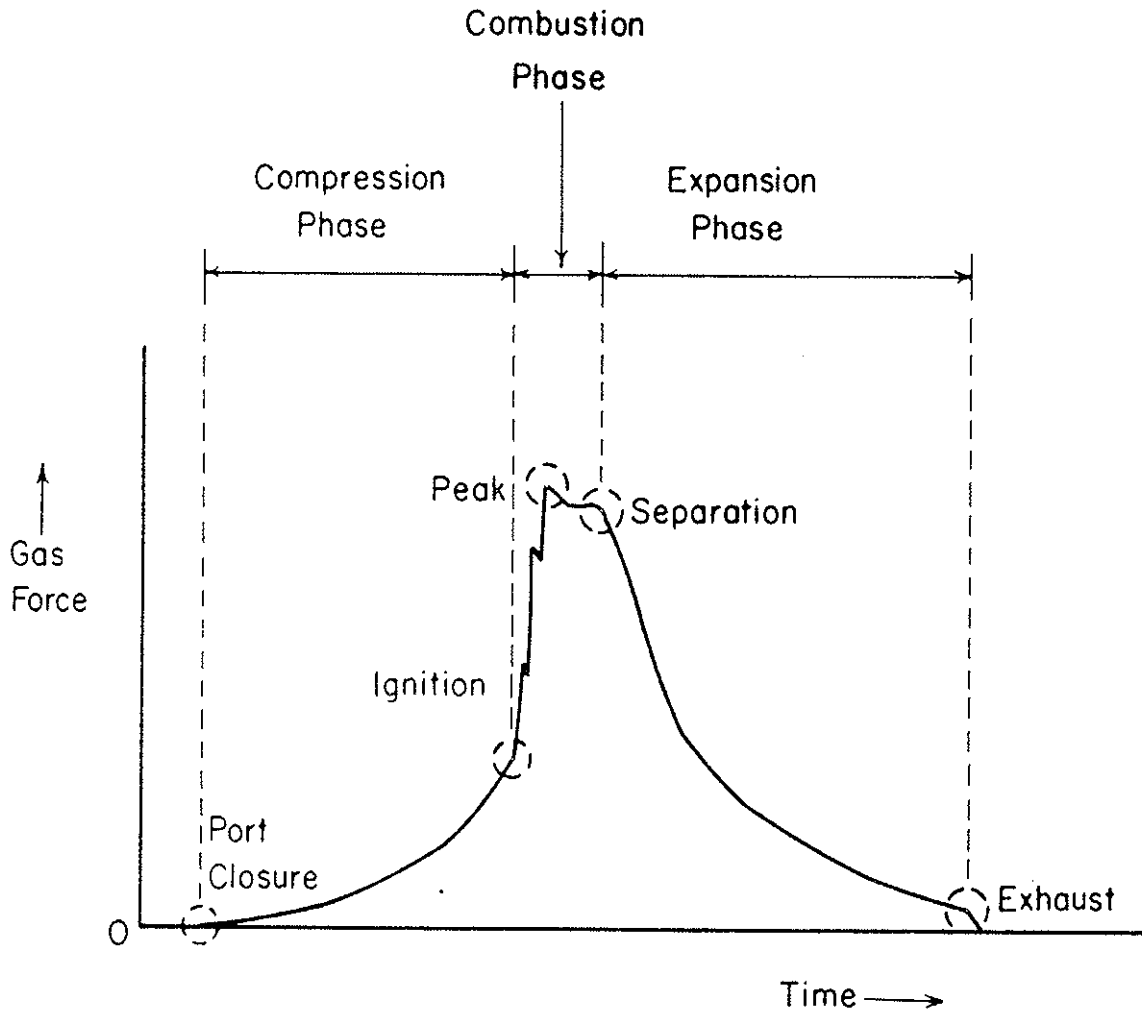


Figure 2.3 THREE PHASES OF GAS-FORCE PULSE

Compression

The compression phase is defined to begin at port closure on the downstroke of the ram and to end when ignition occurs or, in the case of delayed ignition, when ram-anvil impact occurs. During this phase the air initially occupying the full power-cylinder volume is compressed to the combustion-chamber volume. According to customary internal combustion engine terminology, the ratio of these volumes is known as the compression ratio.

Within the range of compression ratios encountered in diesel hammers, the pressures and temperatures generated in the power cylinder during compression can be calculated on the assumption that the process is approximately adiabatic and reversible. It will be shown in Chapter 3 that predictions on this basis are reasonably accurate.

Combustion

The combustion phase is considered for purposes of this discussion to begin with ignition and to end with final separation of ram and anvil. Requirements for ignition, timing of ignition relative to impact, and force-time relationships during combustion will be discussed. It will be demonstrated in Chapter 3 that prediction of peak combustion pressures is not required for wave equation analysis of diesel pile driving. Only the general shape of the force-time curve during combustion need

be estimated. Therefore, detailed discussion of the thermodynamics of combustion is unnecessary.

Ignition, that is, the onset of rapid general combustion of the fuel-air mixture, begins when the following requirements are met:

1. Air attains sufficiently high temperature and pressure.
2. Fuel is present in proper proportion to the amount of air.
3. The air and the fuel are mixed such that adequate air-fuel interface area is present.

Compression of the power-cylinder air by the ram fulfills the first requirement. The second requirement is met by the action of the fuel pump and injection system. Finally, mixing of fuel and air is caused by the impact of ram on anvil, which displaces the fuel laterally into the combustion chamber with such force that the fuel is atomized, that is, separated into many small globules which mix readily with the air. This process is known as impact atomization.

Another method for atomization of the fuel, known as spray atomization, employs a high-pressure nozzle to inject and atomize in a single operation. With this system, which will be discussed later in this chapter, the ignition is not necessarily coincidental with impact.

Ignition occurring prior to impact is known as preignition. This will occur whenever the three requirements for

ignition mentioned above are met within the power cylinder before the moment of impact. Normally, in hammers employing impact atomization, sufficient mixing of fuel and air does not occur prior to impact. There is evidence, however, that high cylinder temperatures resulting from prolonged continuous operation may lead to vaporization of the raw fuel as it is injected onto the top surface of the anvil. The result is varying degrees of pre-ignition. In hammers employing spray atomization, ignition occurs when the spray begins; thus if the spray is initiated prior to impact, preignition will occur.

The effect of preignition is a sharp rise in gas pressure just prior to impact, and a consequent decrease in ram impact velocity. Overall hammer performance may be strongly affected by preignition; this will be discussed in Chapters 3 and 4. In hammers wherein significant preignition occurs it may be possible to operate the hammer continuously at low stroke without ram-anvil impact. In this case preignition produces sufficient gas force to reduce ram velocity to zero before the ram strikes the anvil. This phenomenon has been observed in field tests on a Link-Belt 520 diesel hammer (Davisson and McDonald, 1969).

After ignition there is a period in which gas pressure increases sharply to a peak value. The duration of this period, from ignition to peak pressure, will be referred to as the rise time. The rise time is primarily a function of two factors, namely, the duration of fuel atomization and the rate of burning.

In impact-atomization hammers, atomization is essentially instantaneous whereas in spray-atomization hammers the duration of injection may exceed several milliseconds. The rate of burning of the fuel-air mixture is a function of compression ratio, combustion chamber configuration, injection spray pattern, initial combustion chamber temperature, fuel characteristics and other factors. The state-of-the-art of diesel hammer technology is such that most of these factors cannot be predicted accurately without extensive testing.

Because so many unknown factors affect rise time, it is not possible to make accurate predictions on the basis of theoretical calculations. Therefore it is necessary to rely on the available force-pulse measurements; samples of these will be presented and discussed in Chapter 3. As will be demonstrated later, reasonable assumptions relative to rise time yield solutions of acceptable accuracy.

Expansion

Expansion begins when the ram and anvil separate at the beginning of the upstroke and continues until the power-cylinder gases are exhausted. During this phase the power cylinder is filled with the products of combustion, initially at temperatures possibly in excess of 3000°F and pressures up to or somewhat greater than 1500 psi. In this state the gases will not expand precisely according to the thermodynamic laws governing expansion of an ideal gas. However, the data presented in

Chapter 3 indicate that the process approximates adiabatic reversible expansion.

At least one type of diesel hammer, manufactured by I.H.I. of Japan, incorporates spray atomization which is timed to begin at impact and to continue after impact. It is quite possible with this type of ignition that combustion will continue into the expansion phase. In this case gas pressures during expansion will be increased by the continued burning.

Exhaust occurs as the lower edge of the ram uncovers the ports in the cylinder wall. At this time the power cylinder gases are released to the atmosphere and pressure in the power cylinder drops to zero (gage).

2.4 DESIGN DETAILS AND VARIATIONS

The force-output characteristics of a diesel hammer can be affected by the design of certain of its component parts. Therefore design details of the currently available diesel hammers were investigated and evaluated in terms of their influence on hammer performance as indicated by computer simulation. In the paragraphs to follow the most important of these hammer-design features are identified and discussed. The means for accounting for these features in the wave equation analysis of diesel pile driving will be discussed in Chapter 3.

Ram

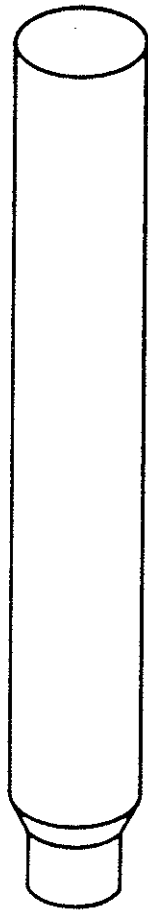
The most important aspect of ram design is weight relative to rated energy. In order to achieve a given rated energy

the hammer manufacturer can provide a heavy ram with a short stroke, or a lighter ram with a longer stroke. In diesel hammers the ratio of ram weight to rated energy is lower than in impact hammers; typically the diesel hammer will have a ram weight which is 35 to 60 percent of that in an impact hammer of equal rated energy. The reasons for the use of a light ram in diesel hammers include the following:

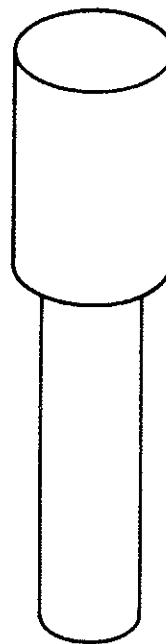
1. A reduction in ram weight results in a reduction in total hammer weight because the additional cylinder length required to accommodate a longer ram stroke introduces less weight than would a heavier ram.
2. A reduction in ram weight allows a smaller ram and cylinder diameter; thus the hammer is more compact and leader size requirements are reduced.
3. Reduced ram diameter can lead to improved operation under easy-driving conditions.

Ram length relative to diameter is much greater in diesel hammers than in impact hammers. For a given rated energy, the effect of the increased ram length is a slight reduction of peak generated pile force in some driving situations, particularly where stiff hammer cushions are employed.

Most diesel hammers employ a ram of constant diameter, as shown in Figure 2.4a. With this configuration the power-cylinder area, in a plane normal to the hammer axis, is equal to the ram area. One manufacturer, Link-Belt, produces two



(a) Constant Diameter



(b) Stepped Diameter

Figure 2.4 RAM CONFIGURATION (SCHEMATIC)

hammer models which feature a ram of stepped-diameter design as shown schematically in Figure 2.4b. The portion of the ram which enters the power cylinder has a reduced diameter, such that the power-cylinder area is less than the area of the upper section of the ram. The reduced power-cylinder area has important effects on the force-output characteristics of the hammer under conditions of high and low soil resistance.

Ram lubrication systems and wear rings can have only a negative influence on force output. That is, if they fail to reduce friction between cylinder and ram to an acceptable amount, hammer efficiency will be reduced. Deficient lubrication becomes particularly important when the hammer is used for inclined, or "batter" driving. Inclined driving will be discussed later in this chapter.

Anvil

Earlier in this chapter it was shown that the top surface of the anvil serves as the lower surface of the power cylinder and transmits force from the power cylinder to the hammer cushion below. In order to withstand the repeated high stresses induced during driving, the anvil is designed as a massive block of steel. Because of its mass, the presence of the anvil influences the force output of a diesel hammer. In general, however, the effect of the anvil mass does not vary widely among the various types of hammers and, therefore, is not an important factor in hammer selection.

Hammer Cushion

Hammer cushions were originally incorporated into pile driving hammers in order to protect the hammer components from high stresses during hammer operation. Over the years foundation engineers and contractors have come to the realization that the hammer cushion also plays a large role in controlling pile stresses and, therefore, in determining hammer effectiveness.

Commonly used cushioning materials include hardwood, plywood, micarta plastic, pressed paper, rubber, coiled wire rope and asbestos. Aluminum or steel wafers are often included in the cushion in order to improve heat conductivity.

Selection of proper cushioning from the variety of available materials is one of the most important, but often neglected, functions of the foundation engineer and contractor. Criteria for selection of cushioning can be summarized as follows:

1. Force-deflection characteristics should be such that hammer energy and peak force transmitted to the pile are adequate for achieving pile penetration without causing pile damage due to dynamic stresses.
2. Compressive strength and heat conductivity of the cushioning material should be adequate to prevent rapid deterioration.

3. Availability, initial cost and service life of the cushion should be favorable as compared to other suitable materials.

The first of these criteria is of primary importance relative to the force-output performance of the hammer. Parola (1970) investigated the force-deflection behavior of cushioning materials and the effect on the performance of impact hammers. In the case of diesel hammers, generalization is more difficult due to the increased complexity of the dynamic phenomena and, therefore, Parola's conclusions should be applied with a degree of caution and checked by wave equation analysis. It is sufficient here to state that selection of cushioning deserves the attention of the foundation engineer and contractor.

Unfortunately, the contractor may not have the ability to change the overall dimensions of the hammer cushion sufficiently to obtain a desired stiffness, as a result of the inflexible dimensions of the cushion receptacle built into the hammer. In diesel hammers these dimensions are such that overall cushion stiffness is sometimes higher than the desired value, no matter which of the available cushion materials is used. One solution is to fabricate a new cushion receptacle; this is an expensive process but has been done on large projects. An alternative is to employ a pile cushion, between the pile and drivehead, which will simulate the effect of a lower hammer-cushion stiffness.

Drivehead

The drivehead, sometimes known as "helmet", is a detachable hammer accessory which is inserted between the hammer cushion and the head of the pile. Its function is to transmit force from the hammer cushion to the pile. The primary requirement of a drivehead is that it contain a receptacle on the underside which closely fits the top of the pile, ensuring an even distribution of driving stresses over the pile head. An ill-fitting drivehead may cause pile damage by applying eccentric or concentrated loads to portions of the pile head.

In the case of driving precast concrete piles the drivehead should not fit the pile tightly. A tight fit might cause pile damage due to torsional stresses induced by pile flexing. This problem can be minimized by the incorporation of a spherical lubricated bearing-surface between the hammer-cushion receptacle and drivehead; Link-Belt hammers have this feature.

Parola (1970) demonstrated that variation in drivehead weight, within the range of ram-to-drivehead weight ratios normally used, does not have an important effect on force output. Therefore weight is normally not a consideration in drivehead selection (see Chapter 5).

Pile Cushion

The pile cushion is an optional element in the driving system which can be inserted between the drivehead and pile. The functions of the pile cushion are to provide additional

cushioning and to ensure an even stress distribution over the head of the pile. Pile cushions are commonly used in driving precast concrete piles.

Plywood is the most commonly used pile cushion material because it is relatively soft and easily fabricated into the desired configuration. Plywood compresses and deteriorates quickly under repeated hammer blows; thus plywood cushions are replaced at frequent intervals. A new cushion for each pile is common.

Power Cylinder

Power-cylinder design considerations include compression ratio, combustion-chamber volume, cylinder diameter, power stroke and combustion-chamber configuration. These factors will be discussed insofar as they influence the force-output characteristics of a hammer. This will establish a basis for the mathematical simulation of hammer combustion described in Chapter 3.

With reference to Figure 2.5, the compression ratio, C_r , is equal to the ratio of total power-cylinder volume, V_{pc} , to combustion-chamber volume, V_{cc} . V_{pc} is equal to the sum of the swept volume, V_s , and V_{cc} . Therefore,

$$C_r = \frac{V_{pc}}{V_{cc}} = \frac{V_s + V_{cc}}{V_{cc}}$$

Current diesel hammers have compression ratios ranging from

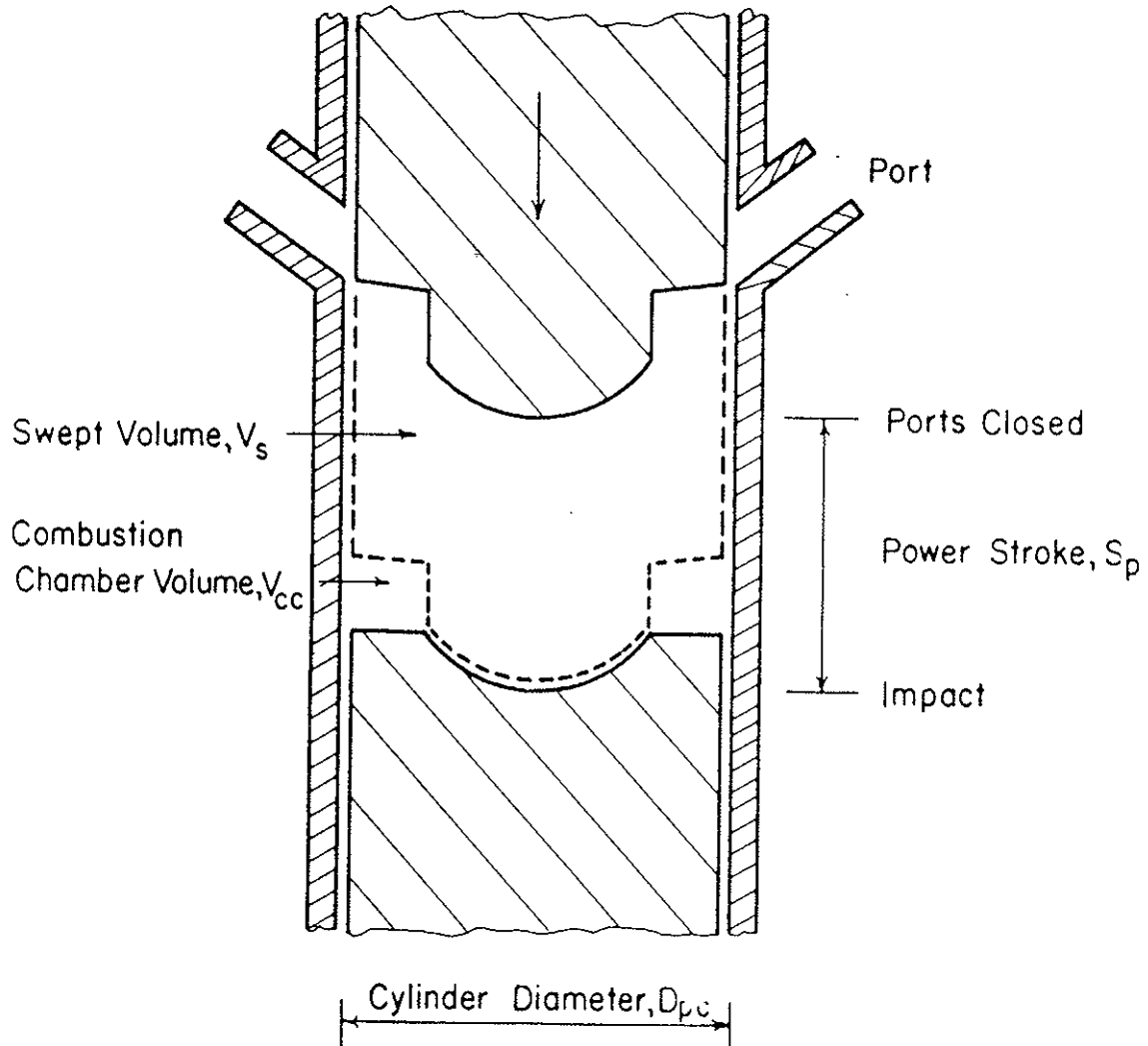


Figure 2.5 CROSS-SECTION OF POWER CYLINDER (SCHEMATIC)

11.0 to 16.5, thus exhibiting a considerable range of design philosophy.

Combustion-chamber volume is an important factor in overall hammer performance. For a given compression ratio there is a limited range of fuel-to-air ratios which can be used effectively. The combustion-chamber volume, therefore, determines the maximum and minimum amounts of fuel which can be burned in a given hammer blow and thus controls the maximum and minimum amounts of energy which can be released. Maximum energy release normally occurs during soft-ground running at maximum obtainable stroke, when a large percentage of the available gas energy is expended in downward anvil movement. Minimum energy release corresponds to driving with reduced stroke against high resistance, wherein nearly all the gas energy is available for upward ram acceleration. Ideally the combustion-chamber volume is such that acceptable fuel-to-air ratios are obtainable under both maximum and minimum energy conditions.

The diameter of the portion of the ram which enters the power cylinder determines A_{pc} , the area of the power cylinder normal to the hammer axis. Because total gas force is equal to gas pressure multiplied by power-cylinder area, the power-cylinder area is an important factor in hammer performance; this will be discussed further in Chapter 5.

For purposes of this discussion the power stroke, S_p , is defined as the distance which the ram travels from the point of port closure to impact, assuming no anvil movement. In many diesel hammers the ratio of S_p to power-cylinder diameter is

approximately equal to unity; however, ratios in the range of 0.5 to 1.4 are encountered. In an effort to increase the energy rating of existing hammer models, some manufacturers have increased power stroke while maintaining the power-cylinder diameter. In combination with increases in combustion chamber volume or compression ratio, the increased power stroke allows the combustion of greater volumes of fuel per hammer blow. Ram weight is increased by lengthening the ram while maintaining original diameter; thus the additional rated energy is obtained without increasing the lateral dimensions of the hammer. A potential benefit of the increased power stroke is improved soft-ground operation.

A variety of combustion-chamber shapes can be found in diesel hammers. These configurations have been determined by the manufacturers in order to provide optimum fuel-air mixing, turbulence, and combustion characteristics for the particular fuel injection system employed. It is probable that the configuration used in a given hammer is not an important factor in hammer performance with respect to force output. Therefore, the effects of combustion-chamber configuration were excluded from this investigation.

Fuel System

Diesel fuel and kerosene are generally used as fuel for diesel hammers, depending upon the manufacturer's recommendation. Use of a lighter, more volatile fuel as an alternative to

recommended fuels may provide easier starting in cold weather. However, it also may lead to preignition problems.

Fuel is normally stored in a tank mounted on the hammer cylinder near the top of the hammer. It flows by gravity to a metering fuel pump and then is injected into the power cylinder. The mechanisms required to store, meter, pump and inject the fuel comprise the fuel system of a diesel hammer.

Several types of fuel system are encountered; common to all are the mechanisms mentioned above. Differences and innovations can be grouped according to their characteristics, as follows:

1. Variable vs fixed volume metering.
2. Spray vs impact atomization.
3. Injection timing and duration.

Because these characteristics have an important effect on hammer performance, each will be discussed in detail.

Metering. All diesel hammers employ some means of metering the fuel flow to the power cylinder. Some models provide a constant volume of fuel per hammer blow by use of a constant-volume metering pump. Increasingly, however, manufacturers are fitting their hammers with variable-volume metering devices which incorporate an adjustable fuel setting, accessible to the operator while the hammer is operating. This permits a greater flexibility in operation and, as a result, greater rate of production and reduced potential for pile damage.

At least one hammer manufacturer, Mitsubishi (Japan), produces hammers incorporating a variable-volume fuel pump

which automatically adjusts fuel volume, maintaining relatively constant ram stroke under varying driving conditions. Although the writer has not investigated the effectiveness of this feature, it potentially relieves the hammer operator of the responsibility for continual adjustment of the fuel flow for constant stroke. To be useful, however, it should include a mechanism to allow the operator to override the automatic control when necessary. This is particularly important, for instance, when driving precast concrete piles through soft soil, in which case it is desirable to maintain a low ram stroke in order to prevent pile damage.

Ideally, control of fuel flow should be available to pile driving personnel at all times during the driving operation in order that fuel flow can be changed instantaneously to meet varying soil resistance. This requirement is not met by mechanisms which can be adjusted only while the hammer is stopped or at ground level. Remote controls are generally preferable. For optimum efficiency the person controlling the fuel flow should be in position to observe ram stroke and pile penetration per blow. This is critical when driving precast concrete piles.

Atomization. In the previous discussion of gas force a distinction was made between impact and spray atomization systems. With impact systems the efficiency of the atomization process depends upon the relative velocity of ram and anvil at impact, the distribution of the fuel in liquid form on the top

of the anvil prior to impact, and the mating of the contact surfaces of the ram and anvil. In general, efficiency decreases with a decrease in relative velocity, uneven distribution of fuel, and mismatching of impact surfaces due to wear and carbon deposits.

One disadvantage of impact atomization is that the presence of liquid fuel in the power cylinder prior to impact may, under certain conditions, lead to uncontrolled preignition. The results are erratic hammer performance and decreased peak generated force. One hammer manufacturer has presented evidence in sales literature that preignition occurs under conditions of overheating (I.H.I., 1970). This evidence was accumulated under artificial test conditions; no data taken during actual construction conditions has been published. Field experience of the writer supports the conclusion that severe overheating does affect hammer performance and that this is probably due to preignition. Other factors, such as possible vapor lock in the fuel lines, might in some cases be responsible for the deterioration in performance of overheated hammers. More research relative to preignition is necessary (see Chapter 6).

Spray atomization is accomplished by injection of fuel directly into the combustion chamber through one or more spray nozzles under pressures in excess of 2000 psi. As compared to impact atomization, spray atomization affords more flexibility with respect to ignition timing and duration of combustion. Because ignition is approximately simultaneous with the beginning of injection, the hammer designer has the option of

initiating combustion prior to, simultaneous with, or after impact. If prolonged combustion is desired, this can be accomplished by provision for an extended period of injection.

There is a delay between the beginning of injection and the onset of general combustion. Available measurements, however, indicate that the delay is not significant. This subject will be discussed further in Chapter 3.

Currently, two manufacturers (Link-Belt and I.H.I.) have incorporated spray atomization into their hammers. Link-Belt hammers feature spray injection which is timed to begin when the ram is approximately one inch from the anvil and to end prior to impact. Controlled preignition is produced by the injection timing. A constant-start type of Bosch injector is employed wherein injection begins at the same ram-to-anvil spacing regardless of fuel volume setting. At reduced fuel volumes the duration of injection is reduced.

Hammers produced by I.H.I. feature spray injection beginning approximately at the instant of impact and continuing for several milliseconds thereafter. In this system the injector is pressurized by combustion chamber gas. The apparent result is to provide a gas-force pulse of lower peak value and longer duration.

Injection timing and duration must be taken into account in the prediction of hammer performance. For this purpose a general acquaintance with the injection system of each hammer is required. The effects of timing and duration of injection on hammer performance are discussed in Chapters 3 and 4.

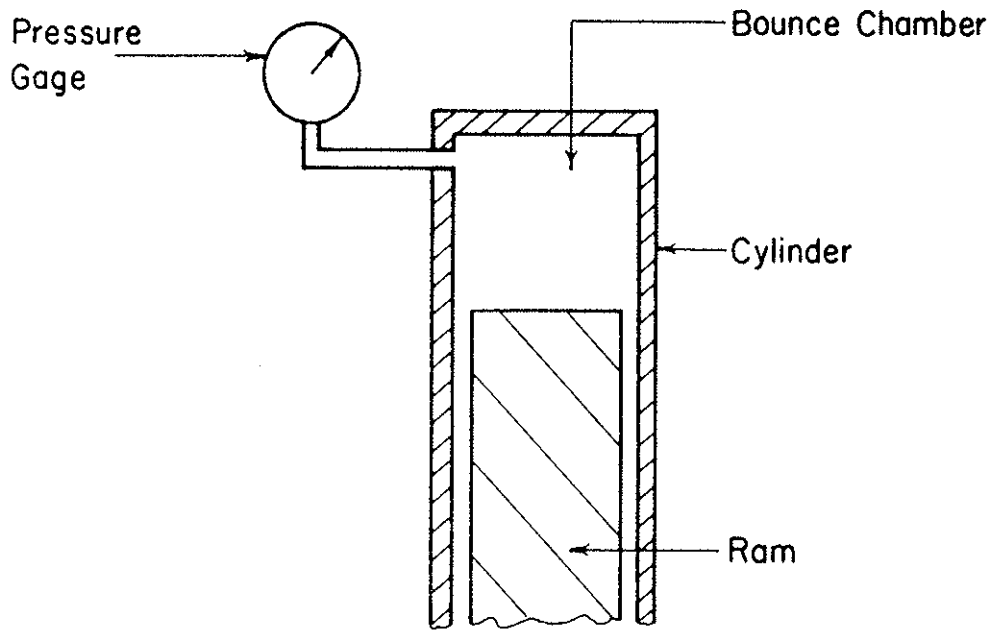
Closed Top

Hammers with a closed top differ from the open-top types previously discussed in that they employ an air-tight cover on the top of the cylinder, as indicated schematically in Figure 2.6a. Air initially at atmospheric pressure is displaced by the ram on the upstroke and is trapped and compressed in the bounce chamber, the result being temporary storage of energy and deceleration of the ram. The energy required to compress the air on the upstroke is returned to the ram on the downstroke, thus providing an accelerating force in addition to that of gravity. The net result is a reduction in the overall cycle time, which translates into an increased blow rate. Hammers with this feature typically operate at blow rates approximately twice that of comparable open-top hammers.

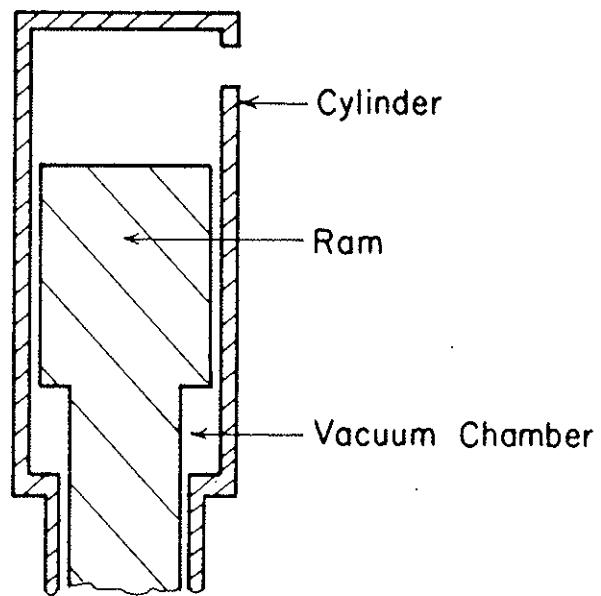
Note that the hammer weight provides a reaction to the upward force in the bounce chamber. Maximum bounce-chamber pressure, which determines maximum equivalent ram stroke, is limited by the hammer weight available for reaction. In some hammers maximum stroke can be increased by addition of weight to the hammer.

Closed-top hammers of the bounce-chamber type as described above are produced by Link-Belt and MKT. The MKT models are convertible from open-top to closed-top operation.

In order to gage the output of a bounce-chamber hammer it is convenient to calculate an equivalent stroke, that is, the height to which the ram would rise if the hammer were of



a. Bounce-Chamber Hammer



b. Vacuum-Chamber Hammer

Figure 2.6 CLOSED-TOP HAMMERS (SCHEMATIC)

the open-top type. This is accomplished by calculations based on the peak pressure developed in the bounce chamber. A bourdon gage is normally provided with this type of hammer so that bounce-chamber pressures can be observed. Pressure readings are converted to equivalent stroke by means of correlation charts. In the case of gages remote from the hammer and connected by hose, the charts provide a correction for hose length.

A different type of closed-top hammer, designated herein as a vacuum-chamber hammer, is produced by BSP (England). In this design, as illustrated schematically in Figure 2.6b, the rise of the ram creates a vacuum in the annular chamber below the shoulder on the ram. Pressure in the chamber approaches zero (absolute) after a short upward movement; for additional upward movement, the downward force on the ram is constant. If the weight of the hammer is sufficient to provide reaction for this constant force, maximum stroke is limited only by the length of the cylinder.

Because vacuum-chamber pressure is essentially independent of ram position, means other than a pressure gage must be employed to measure stroke. BSP recommends measurement of the blow rate and correlation of blow rate to stroke. An electronic device for automatic measurement of blow rate is provided with the hammer.

Closed-top hammers are generally shorter and, because the actual ram stroke is reduced, require less head room. Friction losses are lower due to a reduction in the actual stroke.

Cooling

The cooling system of a diesel hammer is of major importance in hammer performance only if it fails. Overheating can lead to preignition and reduced density of air in the power cylinder. The result is a deterioration in hammer effectiveness, as manifested by erratic stroke and reduced generated peak pile force. For this reason, the use of an overheated hammer should not be allowed.

Cylinder heat is generated by the combustion of fuel. The rate of heat production is proportional to the rate that fuel is burned; therefore, overheating is most likely to occur in continuous full-throttle operation, especially in hot weather.

Heat is dissipated by discharge of exhaust gas and by conduction through the cylinder walls to cooling surfaces, from where it is transferred to the atmosphere by convection and radiation. At least two hammer manufacturers, Kobe and Mitsubishi produce water-cooled hammers which are claimed to be relatively immune to overheating. Water cooling may lead to maintenance problems such as leakage and freezing in cold weather. The majority of diesel hammers are air cooled.

Port Design; Scavenging

Scavenging is the replacement of burned power-cylinder gases with fresh air between hammer blows. Poor scavenging results in low volumetric efficiency and incomplete combustion.

In most hammers scavenging occurs as a result of the negative cylinder pressure that is created during the upstroke of the ram, and which draws in fresh air to dilute the products of combustion remaining in the cylinder after exhaust. The subsequent downstroke of the ram forces most of the diluted mixture out through the ports, leaving relatively pure air in the power cylinder for the next combustion cycle.

At low ram stroke, however, scavenging efficiency is reduced because a smaller volume of air is drawn into the cylinder during the upstroke. The result is inefficient combustion and, possibly, a failure of the hammer to operate continuously.

One manufacturer, Link-Belt, produces a hammer incorporating a positive system for replacement of burned power-cylinder gases with fresh air; this is known as self-scavenging. Other hammer designs incorporate optimum design and location of exhaust ports for improved scavenging.

In some hammers it is possible to operate with one or more of the ports covered. This will affect performance characteristics by altering the effective power stroke and, possibly, by reducing scavenging efficiency. At least one hammer manufacturer, Delmag (Germany) incorporates two sets of ports in certain hammer models in order to provide for easy conversion of the cylinder for use with different ram sizes.

2.5 FEATURES RELATED TO INCLINED DRIVING

Piles driven at an inclination to the vertical are known as batter piles (Figure 2.7a). The degree of inclination can be stated as the ratio of vertical distance to horizontal distance; thus a pile inclined at 14° from vertical is on a 4:1 batter (Figure 2.7b). For general use, a hammer should have the capability of driving piles on a batter of 3:1, or less.

Both impact and diesel hammers rely on gravity for at least part of the necessary ram acceleration. When driving on a batter, however, only that component of gravity which is colinear with the hammer axis is effective in accelerating the ram (Figure 2.7c). For a given ram stroke as measured along the hammer axis, batter operation reduces impact velocity relative to vertical operation. Furthermore, the component of gravity normal to the hammer axis acts to increase the force between the ram and cylinder wall, thus increasing friction losses and causing a decrease in impact velocity.

Measurements are not available which allow an accurate, quantitative estimate of the effect of batter operation on ram impact velocity. However, the following conclusions can be drawn regarding the effect of inclined driving on the force-output performance of various types of diesel hammers:

1. Hammers with longer actual stroke will be most affected by increased friction.
2. Hammers incorporating positive lubrication systems and friction-reducing "wear" rings between ram and cylinder are likely to be less affected.

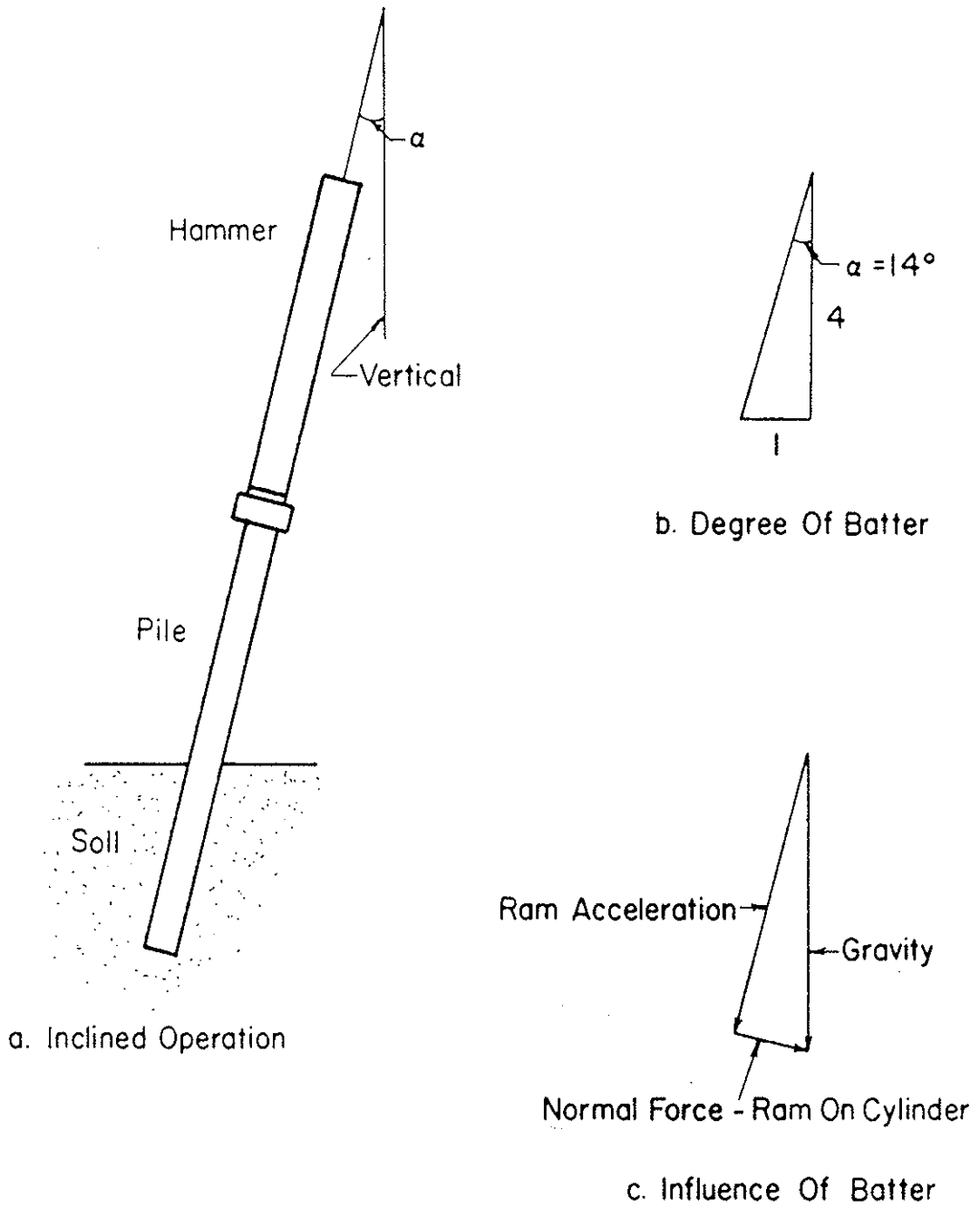


Figure 2.7 INCLINED OPERATION

3. Impact-atomization hammers are probably more affected than spray-atomization hammers, because the inclined attitude of the fuel receptacle in the impact-atomization models is likely to produce uneven distribution of atomized fuel in the combustion chamber.

In general, diesel hammers will tend to increase stroke automatically to compensate for the inclination of the hammer axis, such that the product of ram weight and vertical drop remains approximately constant. Some open-top hammers can be fitted with a cylinder extension to accommodate a longer stroke for batter operation. In closed-top hammers of the bounce-chamber type, additional reaction weight must be added in order to maintain rated energy.

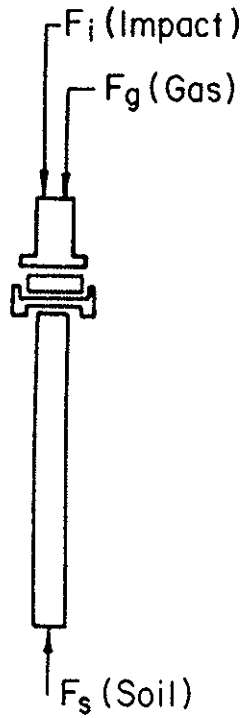
2.6 FEATURES RELATED TO SOFT-GROUND OPERATION

A diesel hammer will fail to operate continuously if total soil resistance falls below a certain threshold value. either the fuel-air mixture will not ignite on the initial downstroke or, if ignition does occur, the stroke on succeeding cycles will decrease progressively until the hammer stops altogether. When this happens the ram must be lifted by a crane line for each stroke until the pile penetrates to firmer soil. This is a time-consuming and annoying process which should, and can, be minimized or avoided by proper hammer selection.

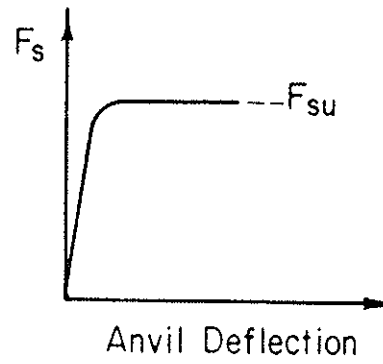
The two symptoms of soft-ground operational problems, failure to ignite and insufficient stroke, are both caused by excessive anvil movement. In Figure 2.8a, the forces acting on the anvil-cushion-drivehead-pile system are the power-cylinder gas force, F_g , the impact force, F_i , and the soil resistance force, F_s . Inertial forces and wave phenomena are of secondary importance in this case and have been neglected for simplicity. Large downward anvil movement will occur when the sum of F_g and F_i exceeds F_{su} , which is defined as the ultimate value of F_s (Figure 2.8b).

Failure to ignite results when preimpact anvil acceleration is so great that impact either does not occur, or occurs at low relative velocity. Hammers employing impact atomization require the relative velocity of ram and anvil at impact to be sufficiently high so that fuel and air will be thoroughly mixed. A low impact velocity may result in incomplete atomization of the fuel and consequent failure to ignite.

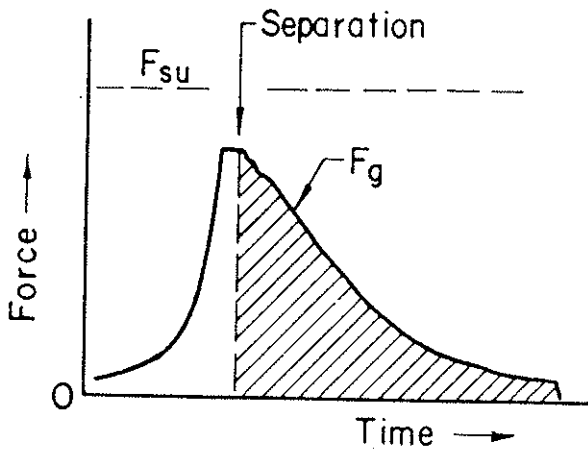
Insufficient stroke is caused by excessive anvil movement during the critical period between ram-anvil separation and exhaust. When soil resistance is high compared to the peak gas force the anvil movement during this period is small and nearly all the gas energy is expended in accelerating the ram upward (Figure 2.8c). In soft ground, however, F_g exceeds F_{su} and the anvil moves downward as the pile penetrates the soil. In the process, gas energy is consumed and the force pulse on the ram is insufficient for ram acceleration (Figure 2.8d); the result is a reduced upstroke.



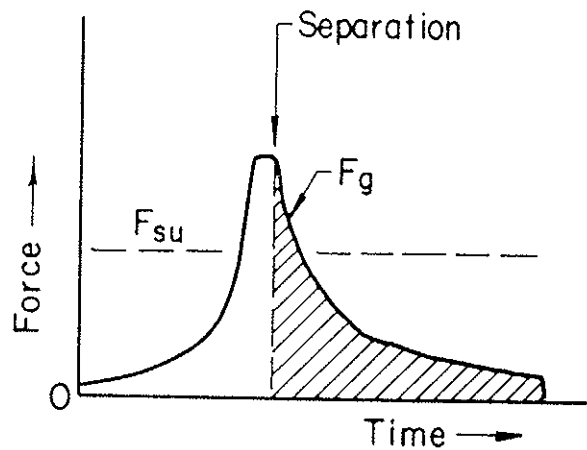
(a) Forces



(b) Soil Force vs Anvil Deflection



(c) High Soil Resistance



(d) Low Soil Resistance

Note: Impulse Effective In Raising Ram Is Indicated By Shaded Area

Figure 2.8 SOFT-GROUND OPERATION

At the reduced stroke the ram may fail to actuate the fuel pump, or scavenging efficiency may be reduced to a great extent. In either case, ignition will not occur on the subsequent downstroke and the hammer must be restarted.

To overcome the soft-ground operation problem it is necessary to select a hammer which will operate at a low threshold value of F_{su} . Very little definitive data is available relative to the soft-ground running of various hammer types and sizes. However, it is possible on the basis of field observations and knowledge of hammer operational details to identify a number of hammer characteristics which tend to lower the threshold soil resistance of a hammer. These characteristics can be summarized as follows:

1. Low rated energy.
2. Variable fuel volume.
3. Spray atomization.
4. Efficient scavenging at low stroke.
5. High ratio of power stroke to power-cylinder diameter.
6. Delayed fuel injection.
7. Low compression ratio.

In general, hammers of low energy rating have a lower threshold soil resistance than larger hammers of similar design. Although combustion pressures are equal to those in a large hammer, the power-cylinder area is smaller and therefore the total gas force is lower throughout the hammer blow. Thus, if

soft-ground running is critical, one of the most obvious remedies is to change to the smallest hammer consistent with the minimum hammer size required for development of pile bearing capacity. In the driving of offshore piles through great depths of soft soil, a small hammer is sometimes used for initial driving and a larger hammer is employed for final driving.

Variable fuel volume allows the hammer operator to increase the amount of fuel burned to compensate for the energy consumed by anvil movement.

Spray atomization and efficient low-stroke scavenging allow a hammer to operate at a lower stroke. Because spray atomization is not dependent on ram-anvil impact for efficiency, the fuel-air mixture required for ignition can be achieved in the event of low impact velocity or, possibly, when impact does not occur. Efficient low-stroke scavenging will provide sufficient fresh air in the power cylinder for combustion.

If the power stroke is long in comparison to the power-cylinder diameter, the effect is to lessen the peak gas force and prolong the gas-force pulse, such that F_g exceeds F_{su} for only a small portion of the time between ram-anvil separation and exhaust. Delayed, prolonged fuel injection has a similar effect. A low compression ratio reduces pre-impact anvil movement. Each of these features serves to lower the threshold soil resistance for a given hammer.

It should be noted that the gas-force pulse characteristics which are optimum for soft-ground running are not optimum for peak hammer output under conditions of high soil resistance. This is discussed further in Chapter 5.

One additional measure, available to the engineer and contractor for purposes of improving soft-ground operation, is to increase drivehead weight. The added mass provides inertial reaction to the gas force, thus reducing anvil movement. This should be done only as a last resort because it may reduce pile-driving effectiveness. The influence of the additional weight should be checked by wave equation analysis.

2.7 FACTORS AFFECTING PERFORMANCE

Like any machine, a diesel pile-driving hammer is subject to wear and deterioration which may affect performance adversely. Fortunately, sub-standard hammer performance usually manifests itself in easily observable operating characteristics. For instance, a hammer with a malfunctioning fuel system or worn compression rings will fail to achieve a full stroke in conditions of high soil resistance. Overheating may result in erratic operation and uncontrolled preignition. Preignition will result in a reduction in peak pile deflection, which can be detected by pencil set-graphs made by drawing a pencil horizontally across a paper attached to the pile as it is being driven.

High ambient temperatures may lead to overheating after long periods of continuous running. Cold temperatures, however, have little effect on performance. Starting may be a problem, although a highly volatile starting fluid (ether) is usually effective in initiating combustion.

CHAPTER 3

COMPUTER SIMULATION

3.1 INTRODUCTION

The development of a method for computerized, mathematical simulation of diesel pile-driving was considered essential to this investigation. Computer simulation of pile driving, commonly known as wave equation analysis, is a method for studying the dynamic response of the pile and soil to a hammer blow. The method is used routinely by geotechnical engineers to correlate pile bearing capacity with soil penetration resistance, expressed as hammer blows/inch. In addition, the method is a useful means for performing a comprehensive investigation of hammer operation under a wide range of simulated driving conditions. Further, it provides a framework of theoretically sound concepts within which actual hammer performance measurements can be analyzed and evaluated.

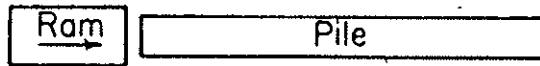
Currently available methods for wave equation analysis, however, are not adequate for simulation of diesel pile-driving. Although the mathematical models of pile and soil used in current methods are sufficiently accurate for purposes of this investigation, the hammer model is not. Therefore, development of a more accurate hammer model was a prerequisite to the study of diesel pile-driving.

In this chapter the basic concepts relating to wave equation analysis are summarized briefly in order to provide a basis for the subsequent discussion of hammer modeling. The improved hammer model, which has been incorporated into the DIESEL1 computer program, is described in detail with particular emphasis on gas-force simulation. Problems associated with simulation of steel-on-steel impact are explored and a method for dealing with these problems is presented. Friction and inclined driving are discussed and methods of simulation are proposed. Finally, the accuracy of the solution is evaluated by comparison with test data.

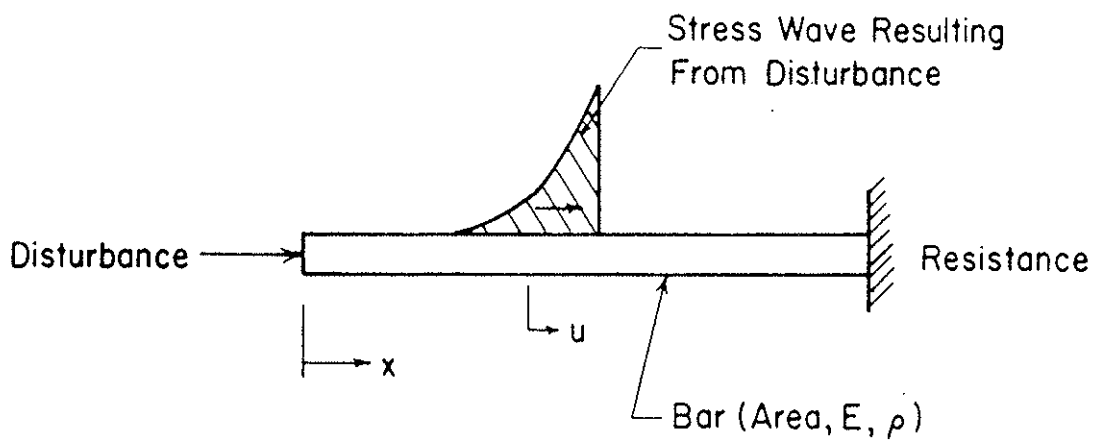
3.2 WAVE EQUATION ANALYSIS

Wave Phenomena

Ram-on-pile impact is properly represented, for analytical purposes, as the coaxial impact of a short rod (ram) and a longer rod (pile), as shown in Figure 3.1a. Ram impact generates a stress wave, or pulse, in the pile head. This pulse travels down the pile toward the tip, at which point it is reflected upward toward the pile head, where it is reflected once more. The process continues until all the energy contained in the force pulse is dissipated by plastic soil deformation, soil damping, internal damping in the pile and other losses. The back-and-forth motion of the force pulse through the pile is described by the one-dimensional wave equation as follows (Figure 3.1b):



a. Longitudinal Impact Of Rods



b. Wave Phenomena

Figure 3.1 RAM-PILE IMPACT

$$\frac{\partial u}{\partial t^2} = \frac{E}{\rho} \frac{\partial^2 u}{\partial x^2} \quad (3.1)$$

where u = particle displacement in direction of pile axis.

x = distance of particle from pile head.

E = Young's modulus of pile material.

ρ = mass density of pile material.

t = time.

Analysis of pile driving by solution of this equation is known as wave equation analysis.

Numerical Method

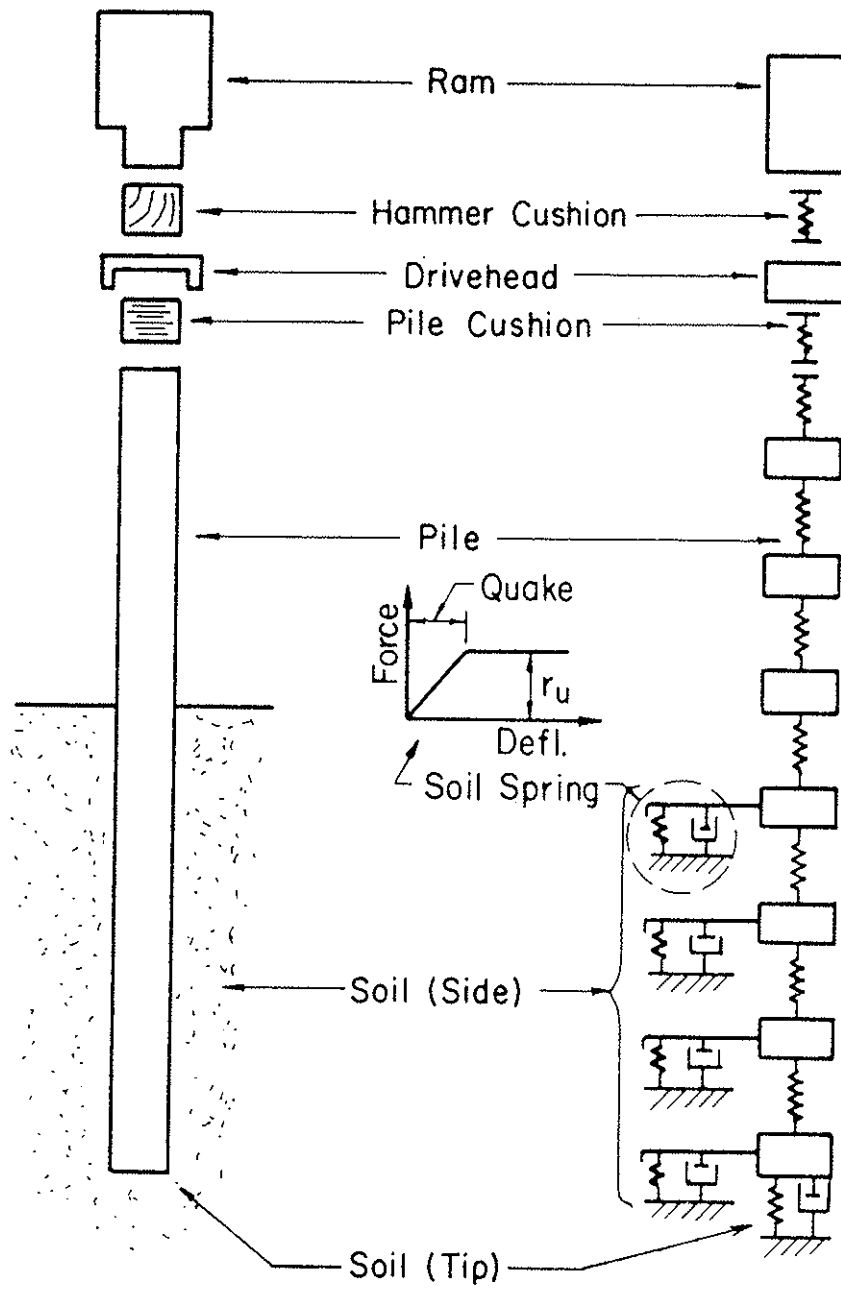
In mathematical terms, wave equation analysis can be described as the solution of a second order partial differential equation with initial values. A closed-form solution is possible for highly idealized problems, such as the ram-on-rod impact depicted in Figure 3.1a (Donnell, 1930). For more realistic problems, however, the following boundary conditions are encountered:

1. Non-prismatic pile; presence of anvil, cushion and drivehead.
2. Slack (no tension) at some points in the system.
3. Elastic-plastic, stress-strain characteristics of soil.
4. Inelastic stress-strain characteristics of hammer cushion and other elements in the system.
5. Distributed soil resistance.
6. Damping at various points in the system.

Due to the complexity of these boundary conditions, closed-form solutions of the wave equation as applied to real pile-driving problems are not feasible. However, Smith (1955, 1962) developed a method for solution of these problems by step-by-step finite difference techniques suitable for use with a digital computer. Smith's method for analysis of impact pile-driving has been modified for analysis of diesel pile-driving.

The first step in wave equation analysis is the identification of all the significant elements of the pile-driving problem to be solved. In the example shown in Figure 3.2a, the basic elements are the hammer, hammer cushion, drivehead, pile cushion, pile, and soil. The next step is the conversion of the elements into discrete masses, springs and dashpots. As shown in Figure 3.2b, the hammer ram is represented by a concentrated mass, the hammer and pile cushions by weightless springs, and the drivehead by a second point mass. The pile is broken into segments, each represented by a point mass equal to the mass of the segment and by a spring of stiffness equal to the stiffness of the segment.

Soil resistance is modeled by elastic-plastic springs and linear dashpots acting in parallel with the springs. The location and ultimate resistance, r_u , of each of the soil springs is specified so as to approximate the estimated distribution and total value of soil resistance. The total soil resistance, R_u , is by definition equal to the ultimate pile bearing capacity under static load. The maximum elastic



a. Elements Of Pile-Driving System

b. Model

Figure 3.2 CONSTRUCTION OF MASS-SPRING-DASHPOT MODEL

deformation (quake) of each soil spring and the damping factor of the associated dashpot are specified.

Calculations begin the instant the ram contacts the hammer cushion. The hammer ram is assigned an initial velocity, V_o , which is equal to the estimated velocity at impact. V_o is calculated by use of the following equation:

$$V_o = \sqrt{2 g s_t e_h} \quad (3.2)$$

where

g = acceleration due to gravity.

s_t = ram stroke.

e_h = estimated hammer efficiency.

All other masses are assigned an initial velocity equal to zero.

A time interval of calculation is selected. Calculations describing the motions of the masses and the compressions of the springs are performed at times corresponding to the selected time intervals during the hammer blow, continuing until pile deflections have maximized. The interval to be used must be small relative to the shortest natural period of oscillation of the adjacent spring-mass combinations within the system in order that all movements can be predicted accurately and that the calculation remain mathematically stable. Simple criteria for selection of a suitable time interval are available.

Calculations proceed sequentially, with the calculated motions and forces for the end of one interval becoming the starting point for the calculations in the following interval. For one interval, a set of calculations is performed for each mass segment, starting with the ram and proceeding downward to the pile tip segment. The calculations for each mass are as follows:

1. Calculate the new position of the mass, which is equal to the initial position (at beginning of time interval) plus the initial velocity multiplied by the time interval.
2. Using the specified spring stiffnesses and damping coefficients, calculate the compression and force in all adjacent pile springs, soil springs and dashpots.
3. Calculate the net force on the mass.
4. Calculate the acceleration of the mass.
5. Calculate a new velocity for the mass by adding to the initial velocity the product of acceleration and time interval.

Time is incremented by one interval, and the series of calculations described above is repeated. This process continues until pile tip deflection reaches a maximum and begins to decrease, at which time the wave equation analysis for the assumed value of R_u is complete. In the case of concrete piles, calculations may continue for additional time intervals in

order to determine peak tensile stresses, which often occur after peak tip penetration.

Results

The end result of wave equation analysis is a record of the response of each of the model segments to the hammer blow, as well as a record of ram movements during impact. Net pile penetration is calculated as the maximum gross tip deflection less the maximum elastic tip deflection (quake). Record is kept of the peak compressive and tensile forces occurring within each of the pile springs. These peak forces, when divided by the corresponding pile area, equal the peak dynamic pile stresses.

In normal practice, the above calculation is repeated for several values of R_u , and the results are summarized on a plot of R_u and peak stress vs blows/inch, as described in Chapter 1. An example plot of wave equation analysis results is included as Figure 3.3.

It is important to note that the predicted pile bearing capacity, R_u , is the capacity immediately after driving is completed. In some soils, pile capacity changes with time after driving as a result of time-dependent variations in soil strength. Such changes are not accounted for by wave equation analysis.

For research purposes, a great deal of additional information can be derived from the calculations described above. By examination of the mass motions and spring forces at each

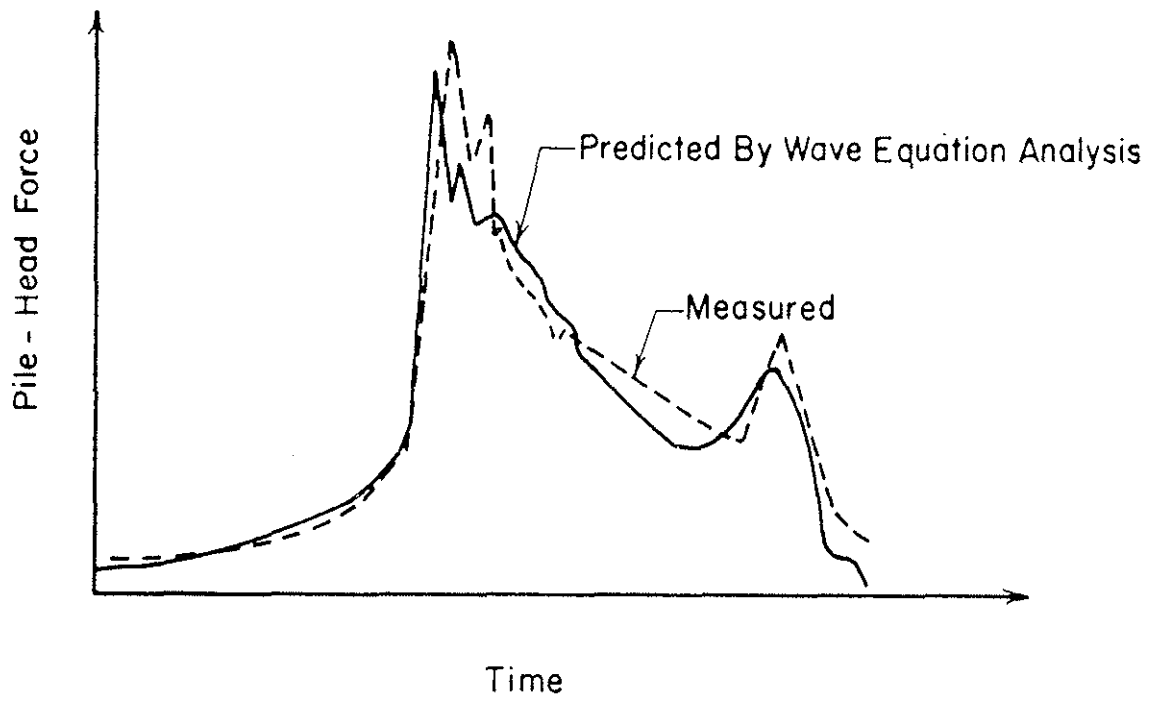


Figure 3.4 EXAMPLE PLOT OF PILE-HEAD FORCE PULSE

pile bearing capacity, comparisons of measured versus predicted capacity are often confused by incorrect input data, by inconsistent or irrational definitions of pile test failure criteria, and by time-dependent changes in pile capacity. In practice, however, if all variables are documented with reasonable accuracy, errors in prediction of pile capacity of less than 10 percent are normal.

3.3 MODELING THE DIESEL HAMMER

In order to analyze diesel pile-driving, it is necessary to replace the impact-hammer model described above with one that accurately simulates diesel-hammer operation. In this section the requirements for effective modeling will be discussed, and one commonly used model will be evaluated in terms of these requirements. A revised model, which meets the requirements, will be presented and discussed.

Requirements

It is essential that the hammer model simulate the interaction of impact and gas forces with the dynamic response of interface equipment, pile and soil. The model must reproduce the changes in hammer force-output which accompany variations in interface equipment stiffnesses and weights, pile materials and configuration, and soil resistance characteristics. For example, the model must respond to simulated soft-ground driving in the same way that the hammer does; that is, large

pre-impact deflections, reduced impact velocity, and decreased upstroke.

Gas-force effects must be simulated realistically prior to, during and after impact. Therefore, the iterative calculations must begin as the ram enters the power cylinder in order to account for the effects of gas force on ram and anvil motion prior to impact.

Finally, the model must be sufficiently flexible that it can easily be modified to reflect differences in design among the many hammer types and sizes currently in use. For example, the model must be capable of simulating preignition, prolonged fuel injection, and bounce- or vacuum-chamber effects.

Existing Model

A modification of Smith's model of the impact hammer for use in the simulation of diesel pile-driving was proposed by Edwards (1967). As depicted in Figure 3.5, the diesel hammer is modeled as follows:

1. Ram, anvil and drivehead are considered to be discrete masses separated by weightless springs. The ram may be segmented.
2. The spring between the ram and anvil is assigned a stiffness equal to the overall axial stiffness of the ram (Area x Modulus/Length).
3. Impact velocity, V_0 is calculated from the following equation:

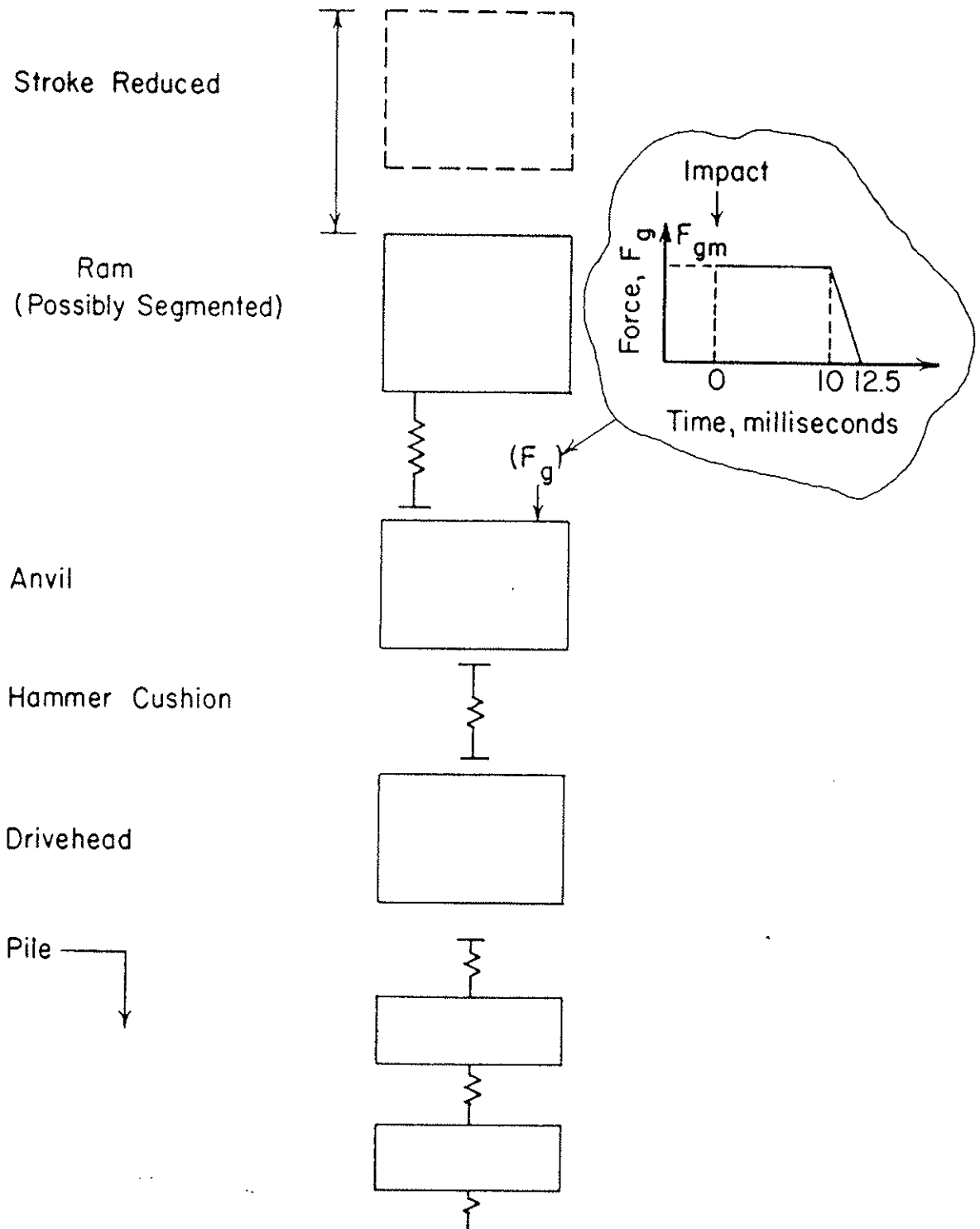


Figure 3.5 DIESEL HAMMER MODEL (EDWARDS, 1967)

$$v_o = \sqrt{2 g (s_t - s_p) e_h} \quad (3.3)$$

where g , s_t and e_h are as previously defined (e_h is set equal to 1.00), and s_p = the distance traveled by the ram between port closure and impact.

4. Calculations begin at the instant of impact. After impact, the force in the ram-anvil spring is held at a predetermined minimum value, F_{gm} , for 10 milliseconds, then allowed to decay to zero over an interval of 2.5 milliseconds. This provision is intended to simulate the gas force. The value of the above mentioned minimum force is selected either by judgement or upon the recommendation of the hammer manufacturer. No provision is made for adjusting the minimum force to simulate variations in driving resistance and hammer stroke.
5. Examples cited by those proposing the method include the use of coefficients of restitution, e , for the ram-anvil spring and the first pile spring which are less than normally-used values.

This model has been given a thorough trial over a period of years, during which time several serious deficiencies have become apparent. Specifically, the shortcomings can be summarized as follows:

1. Incorrect simulation of the gas-force pulse during and after impact. No attempt to simulate pre-impact gas force.
2. Incorrect provision for effect of gas force on ram movement prior to and during impact.
3. Absence of provision for the interdependence of gas force and anvil movement prior to, during and after impact.
4. Absence of provision for damping of spurious model oscillations arising from simulation of steel-on-steel impact.

As a result of these deficiencies, use of this model leads to potentially large errors in the prediction of pile capacities and stresses. Typically, load capacities are over-estimated by up to 20 percent (more in certain conditions); predicted peak pile stresses can be more than 50 percent higher than measured values. This is illustrated by a comparison between predicted and measured force in the head of a concrete-filled pipe pile being driven by a Link-Belt 520 diesel hammer (Davisson and McDonald, 1969). In Figure 3.6 the measured and predicted force is plotted versus time. Peak pile force predicted by wave equation analysis, using the model described above, is far in excess of the measured value. The oscillatory nature of the predicted force pulse, which is related to the steel-on-steel impact, will be explained later.

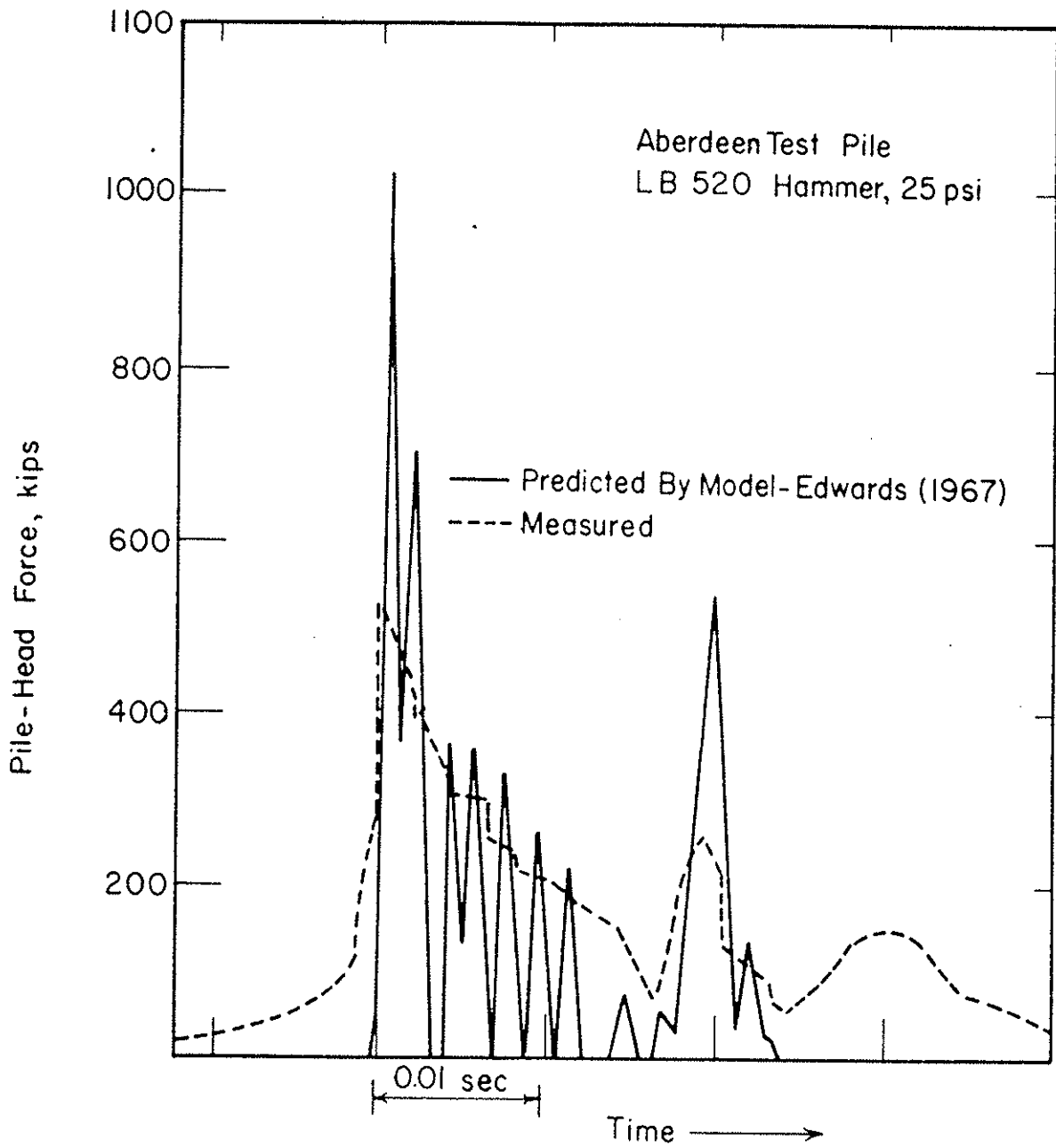


Figure 3.6 PREDICTED VS MEASURED FORCE-PULSE,
EXISTING HAMMER MODEL

The amount of error introduced by Edwards' hammer model is not consistent from case to case. In general, driving conditions leading to maximum error in the wave equation solution have been identified as follows:

1. High pile impedance relative to hammer energy rating.
2. High driving resistance.
3. Low ram stroke, as compared to rated value.
4. Preignition.
5. Stiff hammer and pile cushioning.

In general it is impossible to estimate the error, and thereby to correct the computer output in order to bring the results close to reality. Clearly this model is inadequate for general use in wave equation analysis and, particularly, for an investigation of hammer performance.

3.4 IMPROVED MODEL

An improved mathematical model of the diesel hammer was developed for the purposes of this investigation and incorporated in a computer program named DIESEL1. The significant features of the improved model are as follows:

1. Simulation of the entire hammer cycle, including downstroke, power stroke and upstroke, by means of iterative calculations which begin at port closure and continue through exhaust.

2. Realistic approximation of gas force, incorporating compression, combustion and expansion phases and accounting for all hammer design features affecting gas force.
3. Automatic adjustment of gas force for equality of downstroke and upstroke, taking into account the effects of the dynamic response of interface equipment, pile and soil.
4. Segmented ram.
5. Simulation of closed-top operation.
6. Provision for damping spurious oscillations.

The main components of the model are shown schematically in Figure 3.7. Details relating to the gas force and control of oscillations will be presented later in this chapter.

Normally the calculation begins with assumptions of total ram stroke. (It will be shown later that gas energy, rather than stroke, can be used as starting point.) Ram velocity at port closure is calculated from the stroke, with correction for estimated friction losses. At port closure the step-by-step calculation begins. As the ram moves downward toward the anvil, the simulated gas force causes deceleration of the ram and downward acceleration of the anvil. Anvil deflection results in forces and movements in the mass-spring system below the anvil such that, at the time of impact of ram on anvil, the entire system is in motion.

During the period of ram-anvil contact, the total force on the anvil is the sum of impact and gas forces. Ram motion

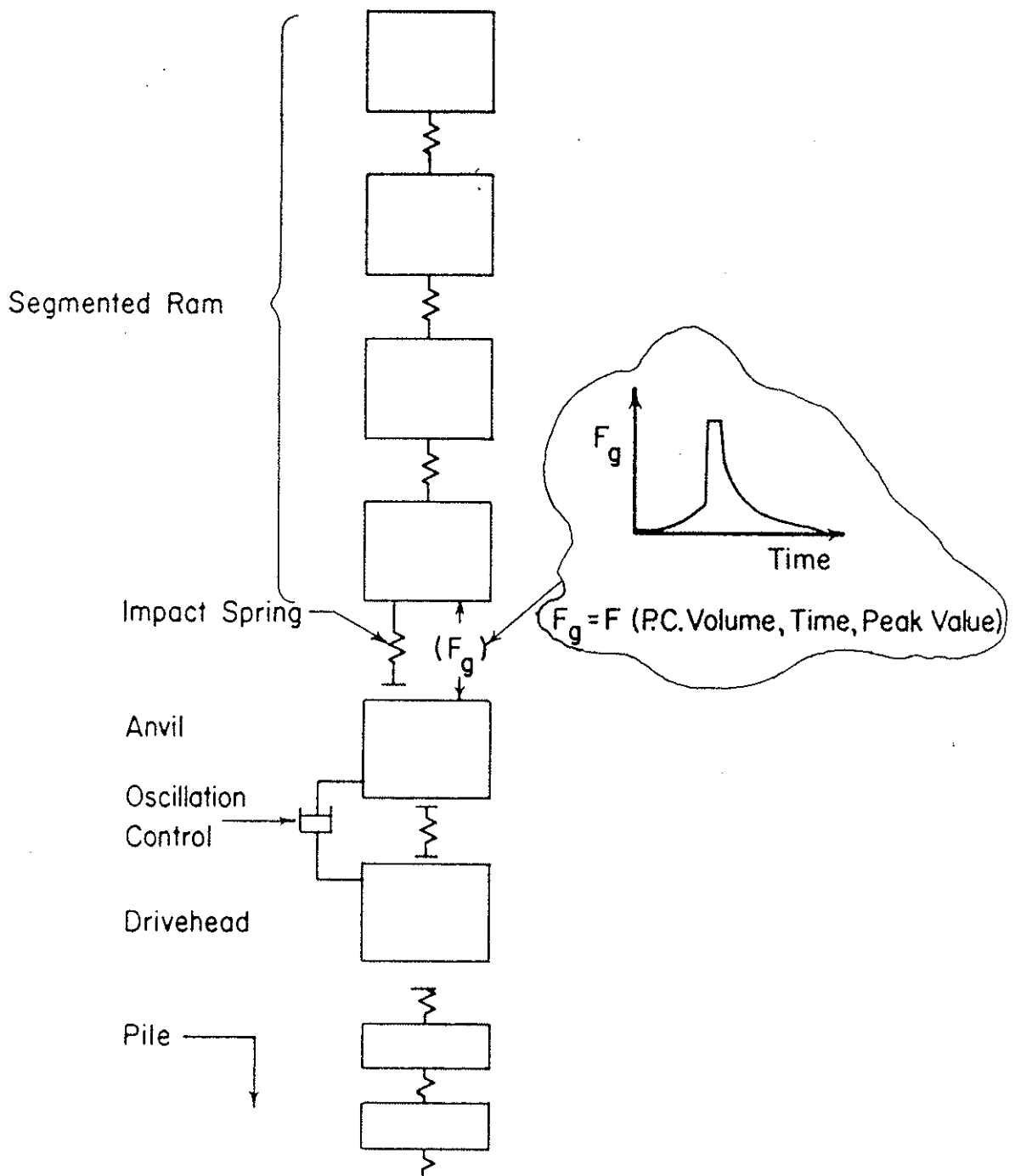


Figure 3.7 IMPROVED HAMMER MODEL

during this period is controlled by the forces of gas and impact acting upward and gravity acting downward.

Step-by-step calculations continue through the expansion phase of the power stroke, during which time the ram is accelerated upward by gas force and pile rebound. When the ram reaches the exhaust ports the iterative calculations are terminated. By this time the pile has reached maximum penetration and rebounded, and the dynamic stresses have maximized. Ram velocity at the instant of termination is used to calculate total upstroke, with correction for estimated friction loss.

The calculated upstroke will be equal to the specified downstroke only if the estimated gas force is accurate. For reasons to be discussed later, it is not practical to determine, in advance of the first calculation, the correct gas force. Therefore a trial-and-error process is required; this is an essential feature of the model. If the calculated upstroke is different from the assumed downstroke, gas force is adjusted automatically and the calculation repeated. In this manner, the correct gas energy input is obtained.

The ram, like the pile, is broken into several segments. This procedure increases computation time somewhat, but is justified by increased accuracy. Simulation of the ram with a single concentrated mass can be justified only in cases wherein the fundamental period of vibration of the ram is small compared to the duration of impact. This is generally the case in the simulation of impact hammers, which have a

relatively short ram and a relatively soft hammer cushion. The short ram length leads to a short fundamental period, whereas the low cushion stiffness increases the duration of impact.

Diesel hammers usually have a comparatively long ram, with a correspondingly longer fundamental period of vibration. Impact duration is short due to the presence of the anvil and the relatively high hammer cushion stiffness. As a result, segmentation is required for acceptable computational accuracy. In general, four equal segments are sufficient. Errors in the prediction of peak force on the order of 15 percent are possible if the ram is not segmented.

When bounce-chamber effects (closed-top hammers) occur during the power stroke of the hammer, the program has the capability of simulating these effects. For instance, in Link-Belt hammers the bounce-chamber pressure acts on the ram until the ram is within approximately one inch of the anvil. The program calculates the bounce-chamber pressure at each time interval and takes the resulting force into account in the calculation of ram acceleration.

The dashpots shown in Figure 3.7 serve to damp oscillations which may occur in the mass-spring model under certain conditions, but which do not occur in the real hammer-pile-soil system. The source of this oscillation and methods for controlling it are discussed later in this chapter.

3.5 GAS FORCE SIMULATION

An exact simulation of the gas-force pulse is impossible because of the numerous factors involved, many of which are not highly predictable because they vary with driving resistance, fuel type, hammer temperature, and other factors. Therefore, the problem of simulating the gas force was approached as follows:

1. Identification of fundamental physical and chemical processes controlling the buildup and decay of gas force.
2. Approximation of gas force by a mathematical model based on the fundamental processes.
3. For each solution, adjustment of gas force for overall balance of energy, as manifested by equality of downstroke and upstroke.
4. Check and modification of the method of force simulation by comparison with test data.

It was shown in Chapter 2 that the gas-force pulse can be divided into three phases: compression, combustion and expansion. In this section, the model developed for each phase will be described and discussed. At the end of this chapter the simulation method will be evaluated by comparison of predicted and measured force pulses.

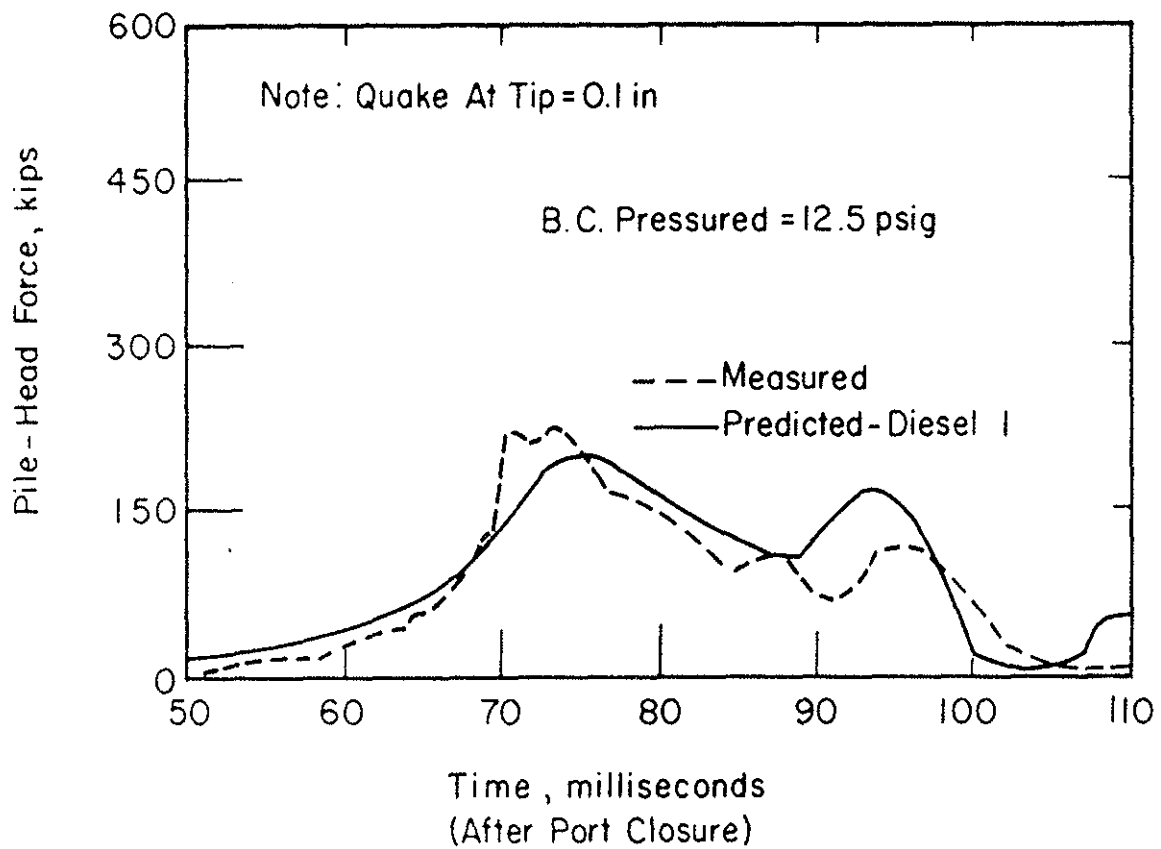


Figure 3.19 PREDICTED VS MEASURED FORCE PULSE, ABERDEEN TEST PILE, 12.5 PSIG BOUNCE-CHAMBER PRESSURE

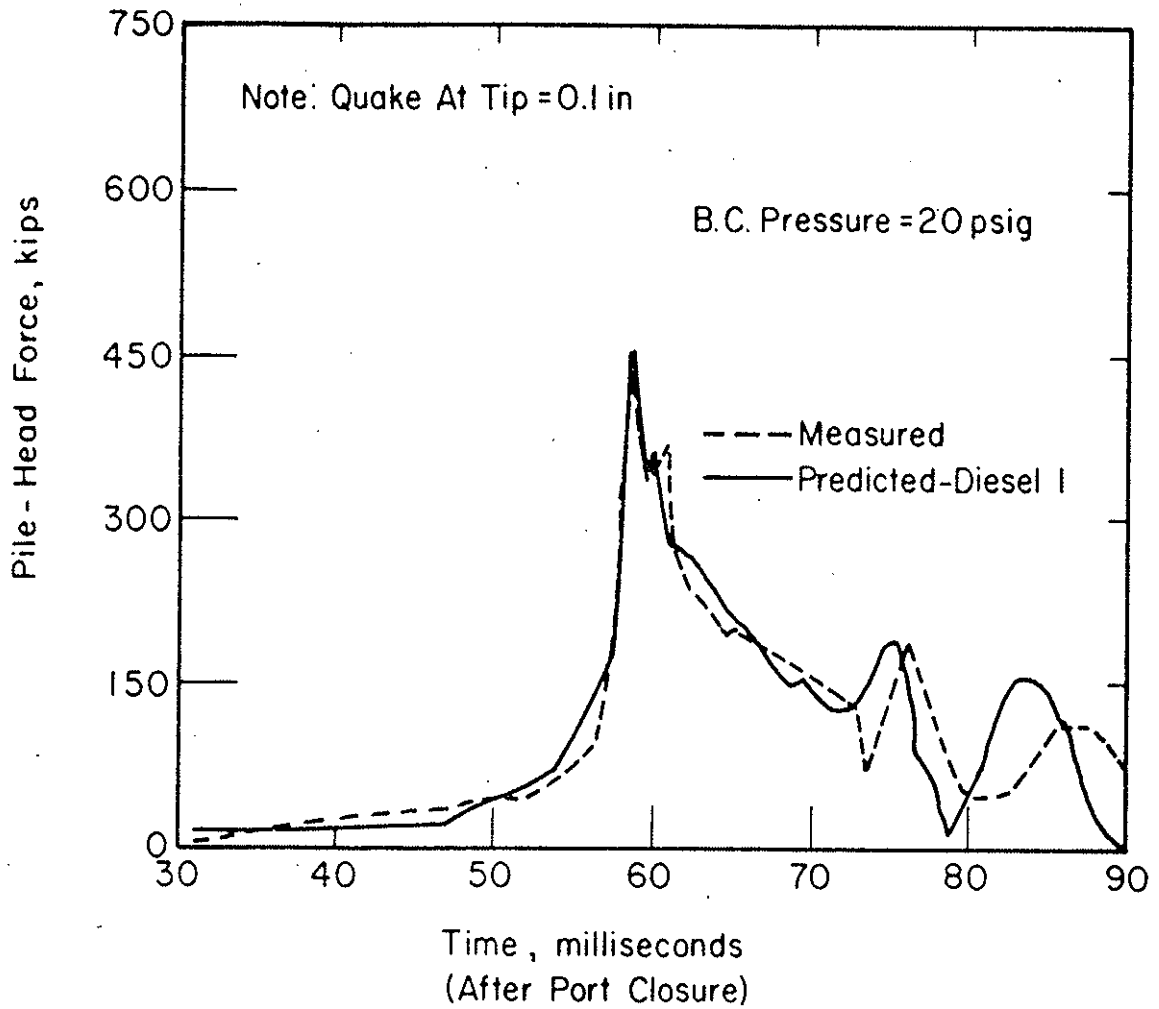


Figure 3.20 PREDICTED VS MEASURED FORCE PULSE, ABERDEEN TEST PILE, 20 PSIG BOUNCE-CHAMBER PRESSURE

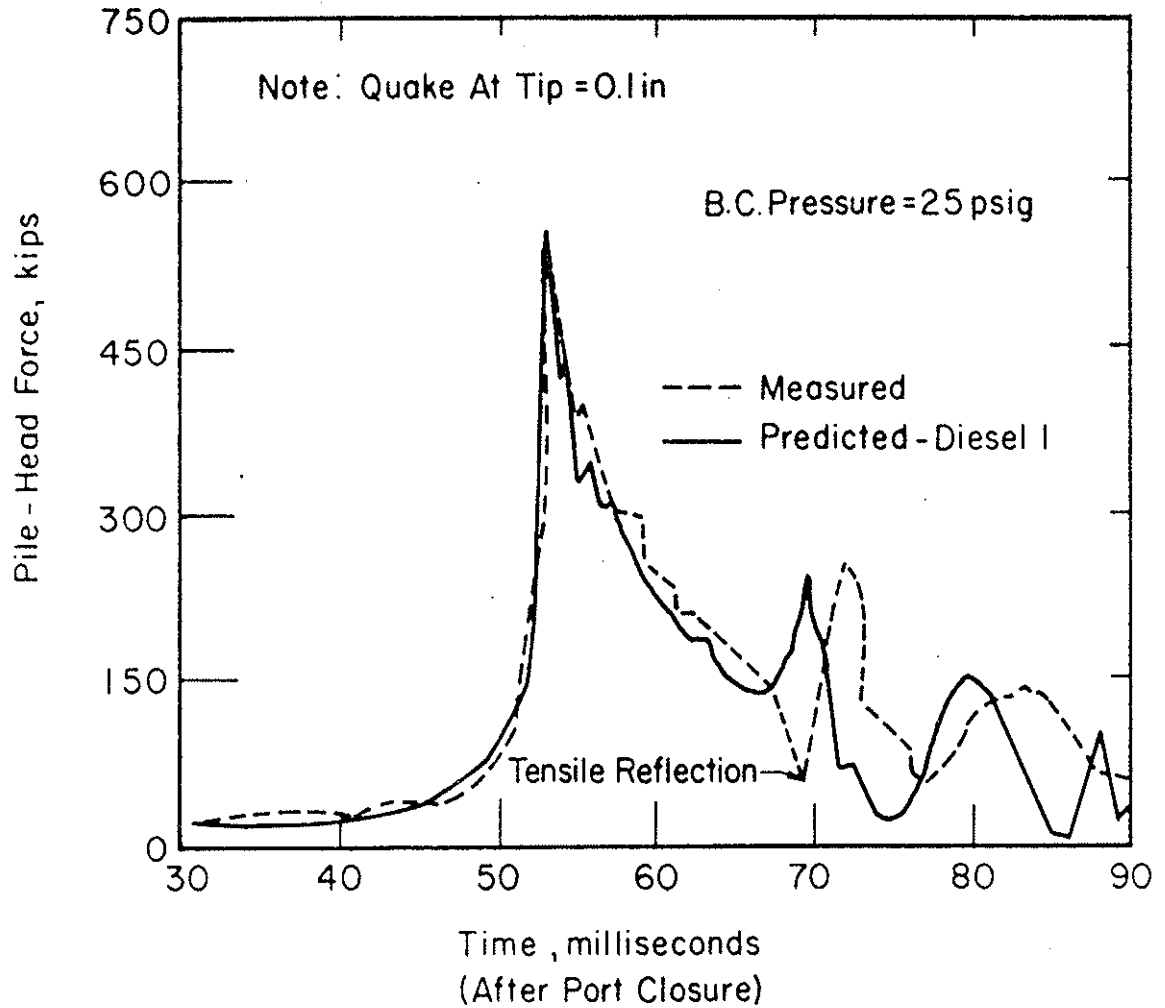


Figure 3.21 PREDICTED VS MEASURED FORCE PULSE, ABERDEEN TEST PILE, 25 PSIG BOUNCE-CHAMBER PRESSURE

In order to estimate the effect of pile tip damage or rock fracture on the force pulse, an additional DIESEL1 simulation was performed assuming a quake at the pile tip of 0.5 inch, as compared to 0.1 inch assumed in the simulations shown in Figures 3.19 through 3.21. The effect of the higher quake is to reduce the effective stiffness of the tip soil-spring below what is normally encountered. Results of the simulation are shown in Figure 3.22. The predicted force pulse is similar to that corresponding to normal quake (Figure 3.21) up to 65 milliseconds after port closure. At 70 milliseconds, approximately, a tensile wave followed by a compressive wave is predicted, very similar to those actually measured. This supports the possibility of tip damage or rock fracturing.

The Aberdeen test pile was driven to refusal with a Bodine Resonant Driver and then load tested to an estimated failure load of 268 tons, prior to the hammer tests. Total penetration during the hammer tests was 3.25 inches under a total of 437 blows, indicating essential refusal. The DIESEL1 prediction of capacity is 285 tons.

A second set of data pertinent to a Delmag D12 hammer operating on an H-section steel pile was reported by Goble, Kovacs and Rausche (1972). The Delmag D12 is an open-top hammer with constant fuel volume. Figure 3.23 is a comparison plot of the pile-head force pulse as predicted by DIESEL1 and as measured. The correlation is generally good, with a peak-force error of - 7 percent.

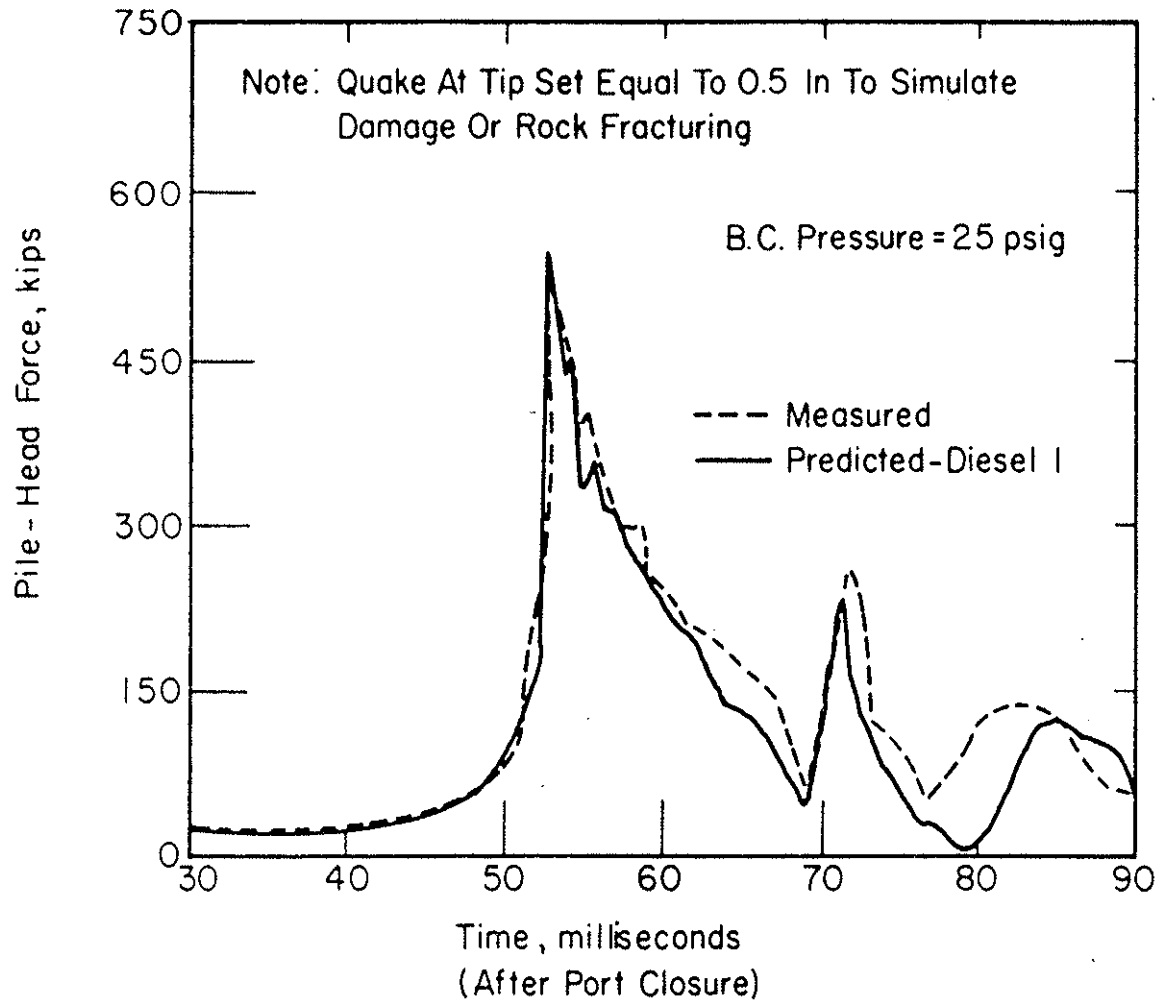


Figure 3.22 PREDICTED VS MEASURED FORCE PULSE, ABERDEEN TEST PILE, 25 PSIG BOUNCE-CHAMBER PRESSURE, SIMULATED TIP DAMAGE

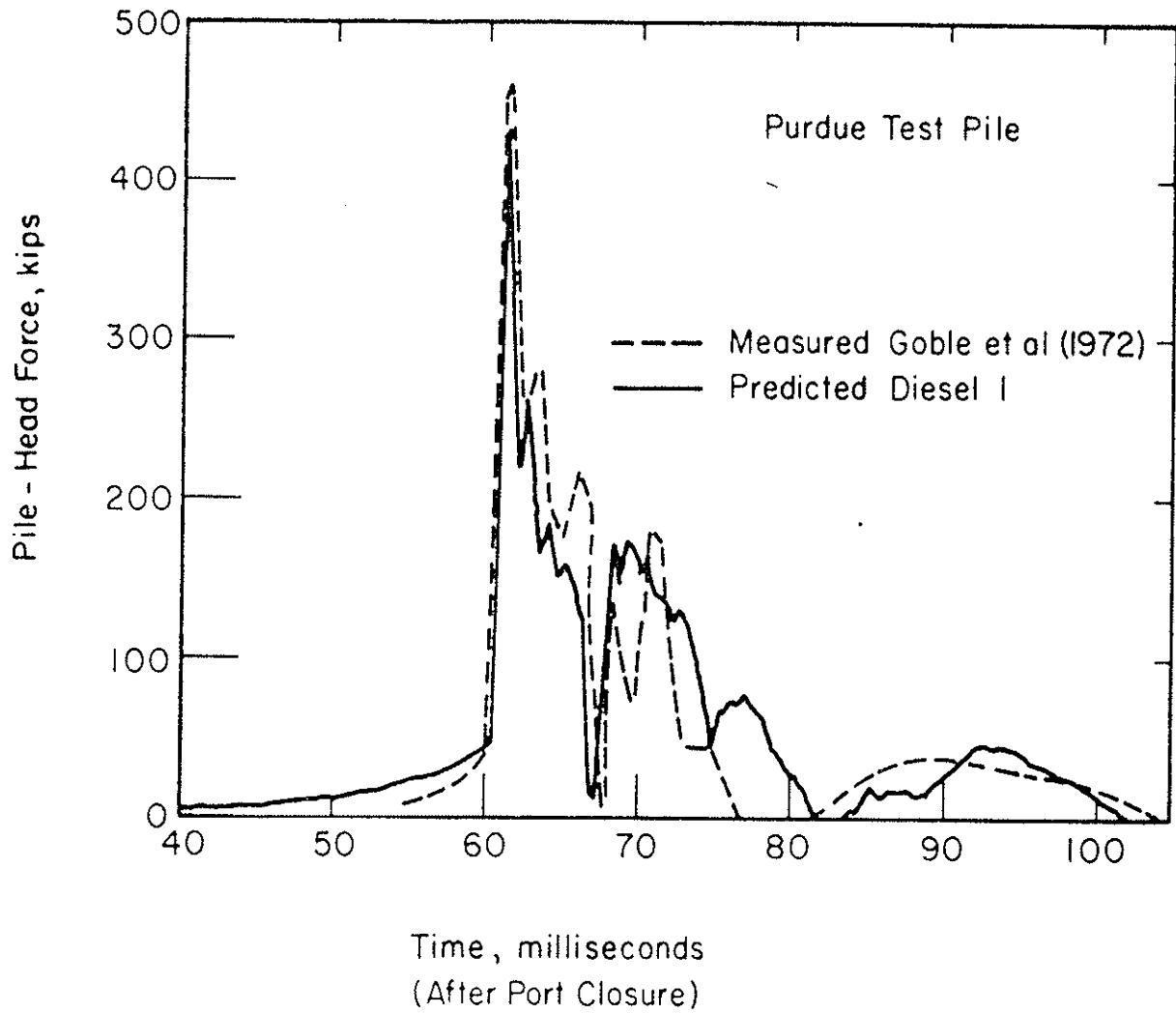


Figure 3.23 PREDICTED VS MEASURED FORCE PULSE,
PURDUE TEST PILE

A static pile load test was performed on the test pile. The pile capacity prediction by DIESEL1 was 83 tons. Pile capacity as determined by the Davisson criteria (Davisson, 1973) was 85 tons.

Comparison of Predicted and Measured Pile Capacity

The primary check on the hammer model was provided by instrumented-hammer and instrumented-pile tests such as those just described. As a check on the performance of the simulation method as a whole, data was accumulated relative to comparisons of pile capacity as predicted by DIESEL1 and as measured by static load tests. This information is summarized on Figure 3.24. In general the error in prediction of capacity is less than 10 percent of measured pile capacity which is consistent with the error to be expected in wave equation analysis of pile driving with impact hammers.

Conclusion

It is concluded that the simulation methods described herein are adequate for analysis of diesel hammer performance and prediction of pile stress and capacity. Confidence in the results is equal to that pertaining to wave equation analysis of pile driving with impact hammers.

- Note: 1. Aberdeen, Ohio (Davisson & McDonald 1969)
2. Purdue (Goble et al, 1972)
3. Aberdeen, Ohio (Davisson, 1975 a)
4. Sioux Station (Davisson, 1975 a)
5. Springfield, Ill. (Davisson, 1975 a)
6. Honolulu, Hawaii (Davisson, 1975 a)

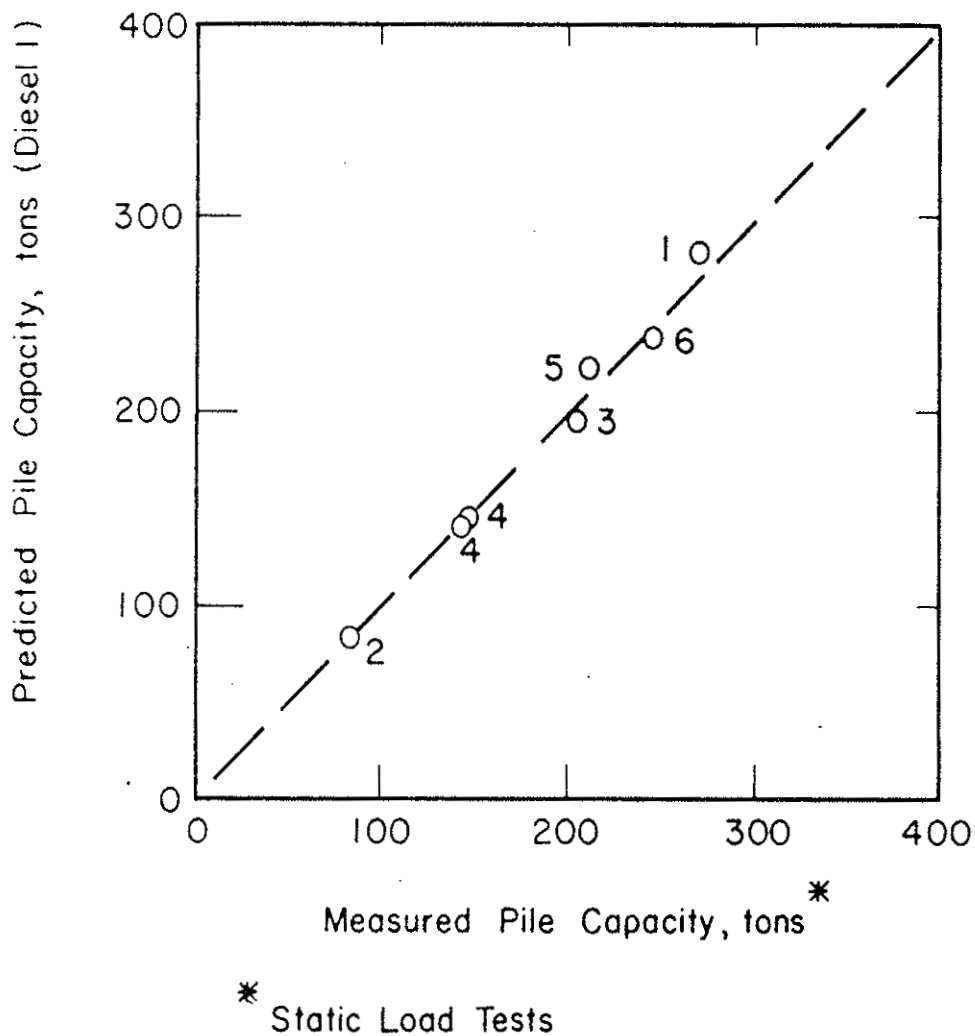


Figure 3.24 PREDICTED VS MEASURED PILE CAPACITY

CHAPTER 4

FUNDAMENTAL ASPECTS OF DIESEL HAMMER PERFORMANCE

4.1 INTRODUCTION

In the process of pile driving, energy contained in the hammer is transmitted through the interface equipment to the pile, causing penetration. The role of the hammer in this process can be examined according to three fundamental aspects of hammer performance: first, the quantity of energy available in the hammer for transmission to the pile; second, the efficiency with which the energy is transmitted through the interface equipment to the pile; and third, the form of energy delivered to the pile head, defined by the shape and duration of the incident force pulse plotted versus time. In this chapter, each aspect of performance is explained and discussed in relation to diesel hammer operation.

4.2 AVAILABLE ENERGY

A distinction should be made between available peak energy, E_{avp} , and available net energy, E_{avn} . Available peak energy is defined as available energy contributing to the peak transmitted energy at the pile head, that is, the energy at peak deflection prior to rebound. Available net energy is

defined as available energy contributing to the net transmitted energy at the pile head after rebound has occurred.

For impact hammers both E_{avp} and E_{avn} are equal to E_{wh} , the potential energy of the ram at the top-of-stroke position, relative to the bottom-of-stroke position. Additional energy, for lifting the ram, is supplied to the hammer via air, steam or hydraulic pressure; however, this occurs sufficiently long after impact that pile penetration is not affected. Therefore, the added energy is unproductive and should not be considered as part of the available energy.

In diesel hammers, available net energy, E_{avn} , is equal to E_{lf} , the latent energy contained in the fuel to be burned during a single cycle of operation. In this case, fuel energy qualifies for inclusion in available energy because combustion occurs approximately at impact and thus contributes to pile penetration. Ram potential energy, E_{wh} , is present in the diesel hammer, as in the impact hammer, at the beginning of the hammer cycle. However, for continuous operation of the hammer, energy equal to E_{wh} must be returned to the ram after impact. Thus ram potential energy should not be considered as part of net available energy, E_{avn} .

A portion of ram potential energy, βE_{wh} , may be transmitted to the pile and stored temporarily as elastic strain energy in the pile and soil. Although this energy is ultimately returned to the hammer, it does contribute to available peak energy, E_{avp} . Thus E_{avp} can be expressed as follows:

$$E_{avp} = E_{lf} + \beta E_{wh}$$

The factor β is variable for a given hammer, depending on ram stroke, pile length and impedance, and soil resistance. In general, β increases with increasing stroke, pile length and soil resistance, and decreases with increasing pile impedance. Based on the computer studies described in Chapter 5, β is estimated to vary from zero to 0.2.

4.3 TRANSMISSION OF ENERGY

Energy is transmitted from hammer to pile in a complex process involving the interaction of hammer, interface equipment, pile and soil. Therefore, in order to investigate energy transmission it was necessary to consider the entire pile-driving system. In this section the flow of energy through the system will be examined, the influence of impedance matching on transmission of energy will be discussed, and transmission efficiency will be defined.

Energy Flow

The flow of energy and work through the hammer-pile-soil system can be described by reference to Figure 4.1. In Figure 4.1a the boundary of the system is shown to encompass the hammer, the pile, and all the soil within the zone of influence of pile-induced forces and deflections. For purposes of discussion to follow, a subsystem known as the hammer subsystem is defined

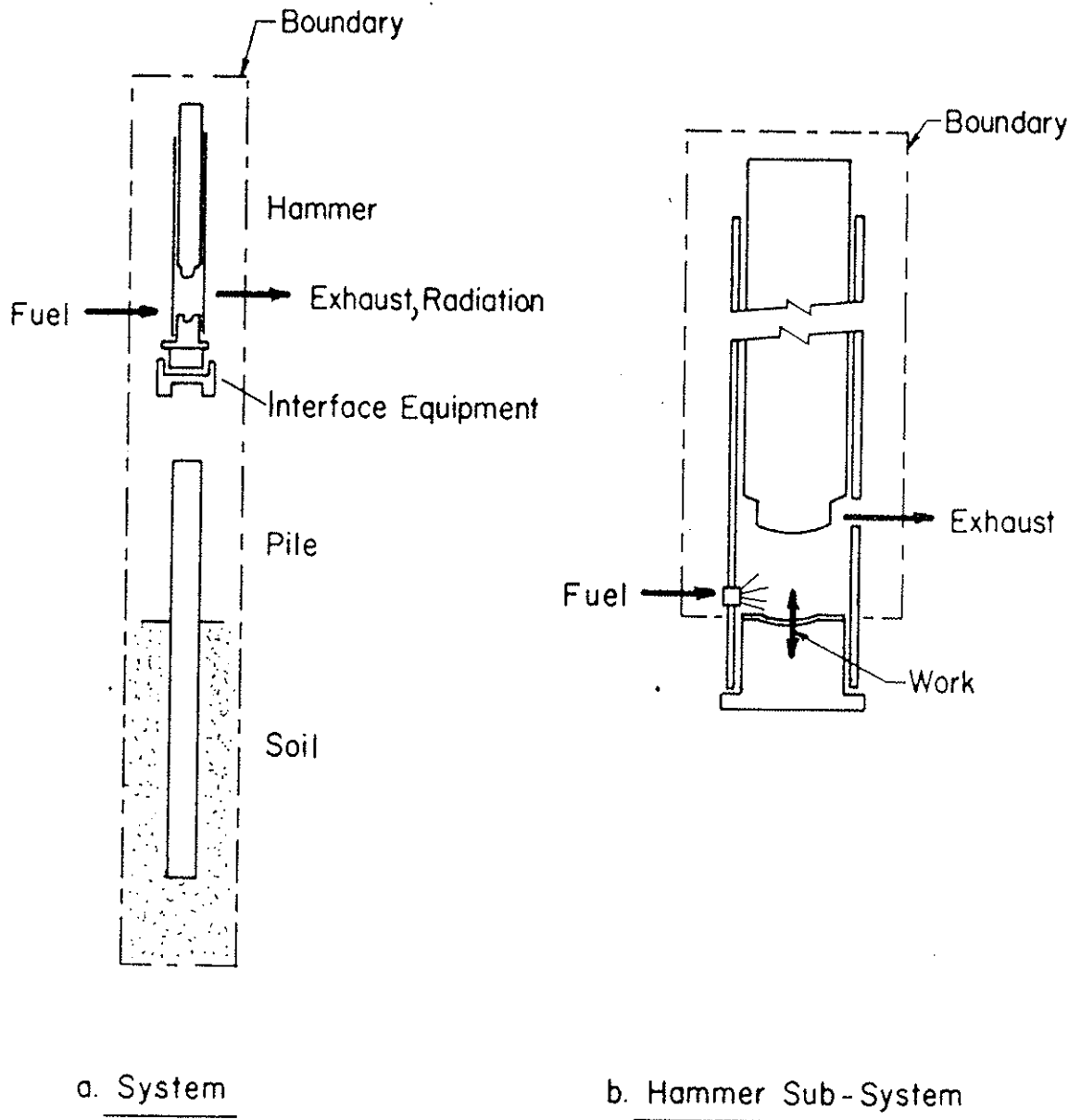


Figure 4.1 HAMMER-PILE-SOIL SYSTEM

to include the ram and power cylinder, and to exclude the anvil, interface equipment, pile and soil (Figure 4.1b).

Energy enters the hammer-pile-soil system in the form of unburned fuel and leaves the system via heat radiation and exhaust. Consider first the flow of energy in and out of the system over a period which includes several hammer blows. In Figure 4.2 total energy, including energy transferred as work, is plotted versus time. At each hammer blow, total energy increases sharply during the combustion phase of the gas-force pulse, remains approximately constant during the expansion phase, and drops abruptly during exhaust. There is a net gain in energy with each blow as more energy is absorbed by the system than is released. A portion of the net energy gain within the system is attributable to the plastic deformation of the soil which results from pile penetration. The remainder consists of losses within the hammer-pile-soil system.

In order to examine hammer operation in detail, energy vs time relationships for the hammer subsystem depicted in Figure 1.1b were studied. The operation of this subsystem cannot be studied without reference to the rest of the system. However, by isolating the ram and power cylinder with respect to energy accounting, it is possible to analyze the interaction of the gas and impact forces with the dynamic response of the elements outside the hammer subsystem.

Only a single hammer cycle was considered, because the time interval between one blow and the next is sufficiently long

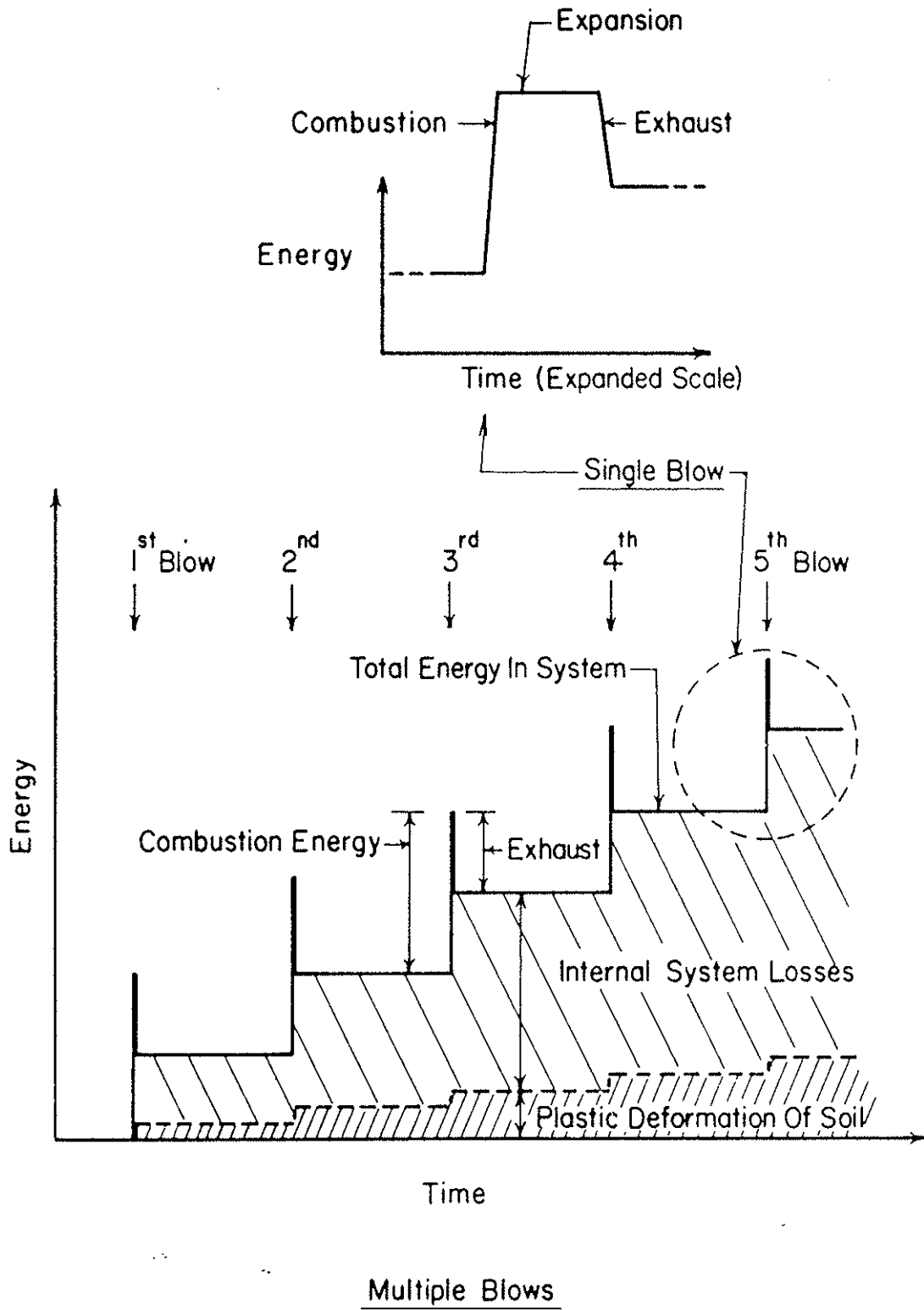


Figure 4.2 ENERGY VS TIME, HAMMER-PILE-SOIL SYSTEM

that there is no dynamic interaction. Within a single hammer cycle, the period of interest begins with port closure on the downstroke and ends with exhaust on the upstroke. This interval lasts approximately 100 to 250 milliseconds and encompasses essentially the entire force pulse at the pile head.

The DIESEL1 program was designed to keep a detailed accounting of the distribution of energy within the hammer subsystem at all times during the cycle. Thus, it is possible to generate charts of energy distribution vs time, such as that illustrated in Figure 4.3. This energy chart is a valuable means for gaining insight into hammer operation.

In the interest of simplicity, both energy and energy transferred as work are incorporated under the title "Energy" in the ordinate of the chart. Further, for this example, friction and radiation losses have been neglected and combustion characteristics have been idealized. Fuel energy is considered to be added when combustion occurs. Total energy within the hammer subsystem, plus energy transmitted to the anvil in the form of work, is plotted as the uppermost solid line. Note this total is constant between port closure and ignition (points a to b) at which point it increases sharply, reflecting the addition of energy to the system via combustion (b to c). From the completion of combustion to the beginning of exhaust (c to d) total energy is constant. At exhaust (d to e), total energy drops to a residual value which is equal to the initial total energy plus the net amount transferred to the anvil during the hammer blow.

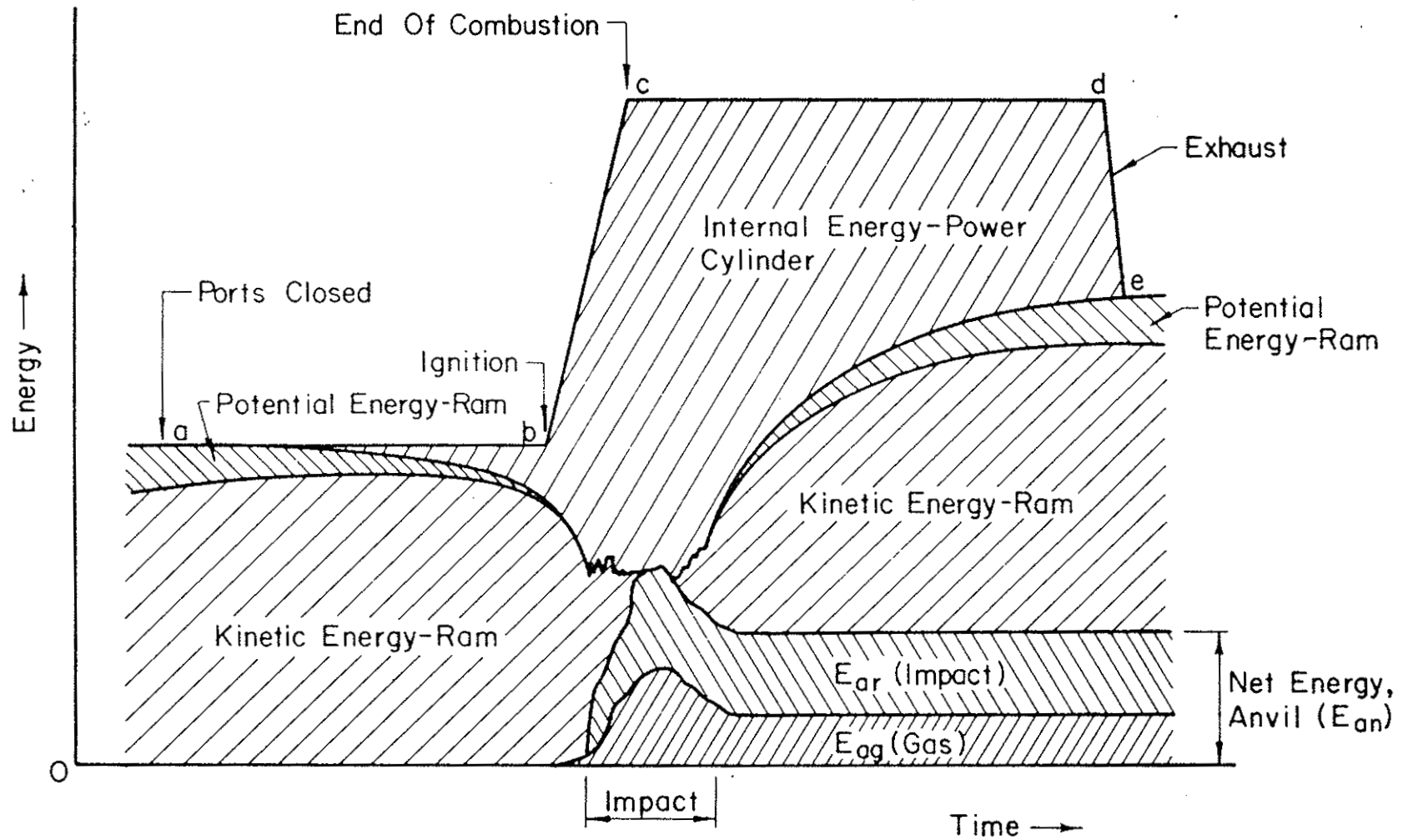


Figure 4.3 EXAMPLE ENERGY CHART FOR DIESEL HAMMER

The components of total energy are designated on Figure 4.3 as follows:

1. Potential energy of the ram, which for purposes of this plot is taken to include elastic strain energy as well as potential energy with reference to the ram-anvil impact position.
2. Kinetic energy of ram.
3. E_{ar} : Net work done on the anvil by the impact force, considered positive downward.
4. E_{ag} : Net work done on the anvil by the gas force, considered positive downward.
5. Internal energy of the power cylinder, which is a function of the pressure, volume and temperature of the power-cylinder gases (approximation).

At port closure the ram retains only a small portion of the potential energy it had at the top of stroke. As ram-to-anvil distance diminishes, potential energy decreases correspondingly, becoming equal to zero shortly after the instant of impact. The ram regains potential energy during the upstroke, such that the value at exhaust is equal to the value at port closure.

Ram kinetic energy is zero at the top of stroke and increases during the downstroke due to the acceleration of gravity. After port closure, ram acceleration is opposed by increasing gas force in the power cylinder. At the point where the gas force balances the acceleration due to gravity, kinetic

energy begins to decrease. In normal operation the ram retains significant kinetic energy at impact. However, when operating at reduced stroke or in soft-ground driving, the gas force alone may be sufficient to bring the ram velocity to zero, such that ram kinetic energy is also reduced to zero and impact does not occur.

In the example shown, ram kinetic energy drops to zero shortly after impact, and remains equal to zero until gas and anvil force combine to accelerate the ram upward. After separation of ram and anvil the gas force continues to act upon the ram, such that at the time of exhaust the ram has sufficient velocity to carry it to the top-of-stroke position. Assuming equality of downstroke and upstroke, ram kinetic energy at the exhaust position is equal to that at port closure. Note that in a non-idealized case, the presence of friction results in slightly greater kinetic energy at exhaust, as compared to that at port closure.

Internal energy of the power cylinder is zero at port closure, at which time the power-cylinder gas is nominally at atmospheric pressure and temperature. Internal energy increases during the compression phase due to work done on the gas by the falling ram. During combustion, internal energy increases rapidly to a peak value; during expansion, it decreases. At exhaust the pressure in the power cylinder is reduced to atmospheric and the remaining internal energy is lost to the atmosphere.

Total work done on the anvil, E_a , consists of the gas and ram impact components, E_{ag} and E_{ar} . The gas component, E_{ag} , is very small until a few milliseconds prior to impact at which time gas force causes downward movement. At impact E_{ar} is added. The relative proportion of E_{ag} and E_{ar} varies widely with driving conditions.

E_a maximizes several milliseconds after impact at the time of peak anvil deflection, then decreases to a net value, E_{an} . The difference between the peak and net values of E_a is a measure of the elastic strain energy stored temporarily in the interface equipment, pile and soil. During rebound the anvil is forced upward and this energy is returned to the hammer. The portion which is not returned, i.e. E_{an} , is indicative of the energy absorbed by the hammer-pile-soil system. This includes net work done on the pile head, plus losses in the interface equipment.

The relative values of the impact and gas components of E_{an} vary with hammer design and driving conditions. In easy driving with spray-atomization hammers, impact may not occur, in which case the ram impact component of E_{an} is zero. In hard driving on high-impedance piles, the ram impact component of E_{an} greatly exceeds the gas component in magnitude.

Net gas energy added to the system, E_{gn} , is equal to the difference between the energy added during combustion, E_{gt} (points b to c, Figure 4.3), and the energy lost during exhaust, E_{gl} (points d to e). Because energy is conserved,

and recalling that ram kinetic and potential energies at exhaust are approximately equal to the corresponding values at port closure, neglecting friction, it can be concluded that the net work done on the anvil, E_{an} , is approximately equal to E_{gn} .

Thermal efficiency of the hammer can be defined as the ratio E_{gn}/E_{gt} . Under normal operating conditions, i.e. when ram impact occurs and fuel volumes are within the normal operating range, thermal efficiency can be expected to remain approximately constant. Assuming that thermal efficiency is constant and that E_{an} is equal to E_{gn} , it follows that the ratio E_{an}/E_{gt} is also constant. Thus, in general, the work done on the anvil is approximately proportional to the amount of fuel burned per blow. Furthermore, if interface-equipment losses are assumed constant, work done on the pile is also approximately proportional to fuel burned; this will be demonstrated in Chapter 5.

In summary, the energy chart demonstrates the interaction of impact and gas forces in the transmission of energy to the anvil. Further, it illustrates the approximate relationship of fuel volume per blow to net work done on the anvil.

Impedance Matching

The concept of impedance matching can be useful in the selection of hammer and hammer cushions so as to obtain optimum energy transfer from anvil to pile. Parola (1970) applied the concept to pile driving with impact hammers. The impedance ratio of hammer to pile, I_r , was defined as follows:

$$I_r = \frac{\text{Pile impedance}}{\text{Hammer impedance}} = \frac{\rho ca}{\sqrt{M_1 K_C}}$$

where ρ = mass density of pile material.

$c = \sqrt{E/\rho}$, where E is Young's modulus of elasticity for the pile material.

a = cross-sectional area of pile.

M_1 = mass of ram.

K_C = spring stiffness of hammer cushion.

Parola concluded that optimum energy-transmission efficiency occurred for values of I_r between 0.6 to 1.1, under the following conditions:

1. Infinite pile length (no reflections).
2. Ratio of ram weight to drivehead weight equal to 5:1, approximately.
3. Elastic hammer cushion.

In the case of diesel hammers, impedance matching is much more complicated. Due to the presence of the anvil and the addition of the gas-force pulse, the number of variables involved is increased and generalization becomes difficult. As an approximation, it is possible to apply Parola's conclusions directly to diesel hammers, considering only ram weight and cushion stiffness without regard to the complicating factors, and thus to gain a basis for judgement in selection of hammer and cushioning. The approximation thus obtained should be refined on the basis of wave equation analysis, taking into account the real properties of the diesel hammer.

Transmission Efficiency

For the diesel hammer, transmission efficiency should be defined, ideally, as the ratio of E_{hm} , peak energy delivered to the pile head, to E_{avp} , the available peak energy. However, due to the difficulty in determining E_{avp} , it is more convenient to use the following arbitrary definition:

$$e_f = E_{hm}/E_{wh}$$

where e_f = transmission efficiency. This is the same definition commonly used for impact hammers and thus allows comparison of the two types of hammer. However, with respect to diesel hammers, e_f should be interpreted in light of the following considerations:

1. In easy driving, at maximum fuel flow, e_f theoretically can exceed 1.0.
2. Efficiency, e_f , is strongly affected by fuel volume, impedance matching, and driving conditions.

For the above reasons, e_f is not considered a useful indicator of the relative performance of various types of hammer. Suggestions for a more valid method of rating diesel hammers are included in Chapter 6.

4.4 FORM OF ENERGY

In this section, the force-pulse characteristics which describe the form in which energy is delivered to the pile will

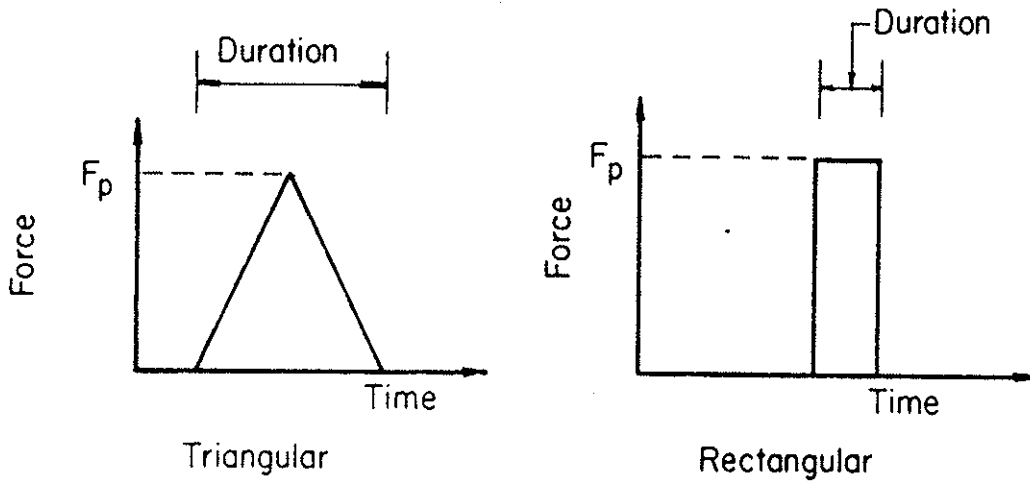
be identified. The gas and impact components of pile-head force, and their interaction, will be described. Finally, the influence of soil resistance on the form of energy will be discussed.

Force-Pulse Characteristics

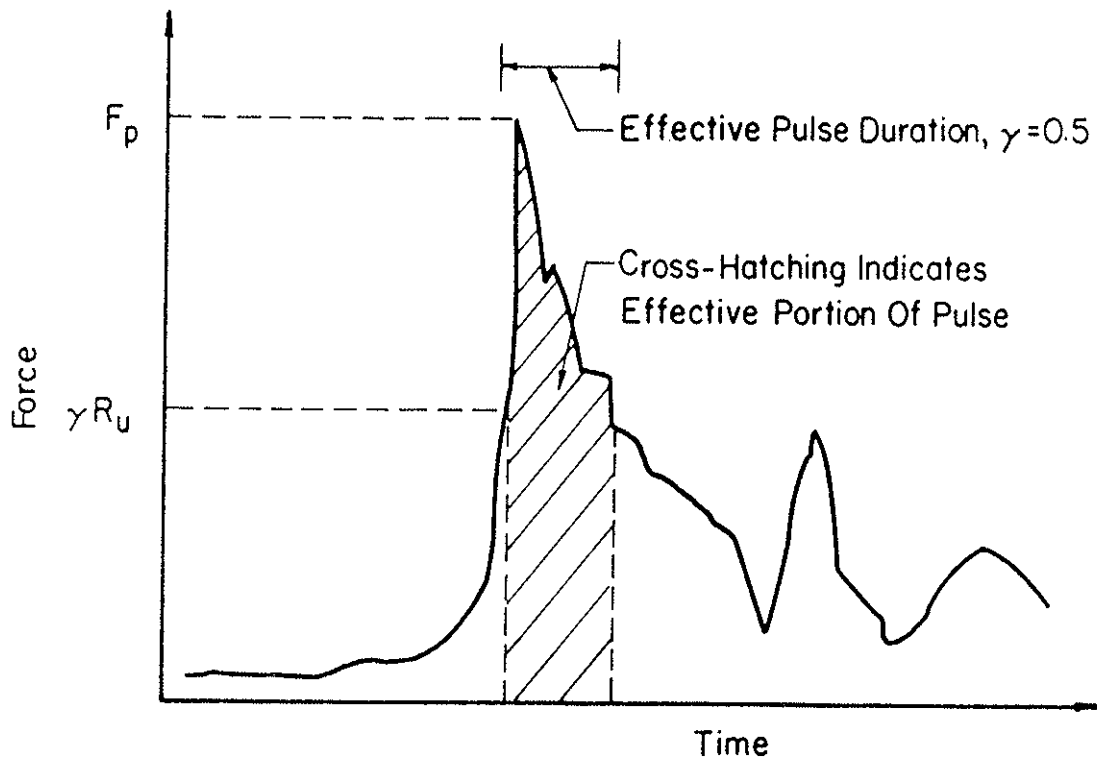
Parola (1970) demonstrated that force pulses of equal energy but of varying peak force, shape and duration produce differing pile penetration. Parola concluded that optimum peak force, shape and duration characteristics are a function of soil resistance, R_u , as follows:

1. For peak force, F_p , greatly exceeding R_u (easy driving), variations in F_p have little effect on penetration. Pulse shape and duration are critical, with the long-duration, triangular shape producing greater penetration than the short-duration, rectangular shape (Figure 4.4a).
2. For F_p equal to or less than R_u (hard driving), F_p is critical; an increase in F_p produces an increase in penetration. No penetration will occur if F_p is less than $R_u/2$. The most effective shape is that which results in the longest duration near the peak. Thus the rectangular shape, which has the shortest overall duration but longest duration near the peak, produces the greatest penetration.

The force pulse generated by a diesel hammer, an example of which is illustrated in Figure 4.4b, can be evaluated according to the above criteria. It is necessary, however, to consider



a. Idealized Force - Pulse Shapes



b. Example Force Pulse Produced By Diesel Hammer

Figure 4.4 FORM OF ENERGY, FORCE-PULSE SHAPES

the duration and shape of that portion of the pulse which is of primary significance in causing penetration. The low-amplitude portions of the pulse occurring prior to and after the period of significant pile-head motion have only a secondary effect on penetration, and should be excluded from the effective pulse duration. Although a precise, general definition of effective duration is not possible, an arbitrary definition such as that shown in Figure 4.4b can be applied. Only the duration of pile-head force greater than γR_u is considered effective, wherein γ ranges from 0.50 to 1.0, approximately, depending primarily on soil resistance distribution and soil damping. A low value of γ corresponds to point-bearing piles, with normal soil damping, i.e. most soils of low plasticity. Increases in side friction and soil damping result in higher values of γ .

Components of Pile-Head Force

In diesel pile driving, total force on the pile head is composed of a gas-force component and an impact-force component. In this section the gas and impact components of the force will be discussed separately in order to identify their unique characteristics. The interaction of the two components will then be discussed.

Gas Force. The fundamental nature of the gas-force pulse was discussed in Chapter 2. In typical diesel hammers the duration of the pulse is 100 to 250 milliseconds, which is

sufficiently long to allow several round trips of the stress wave from the anvil to the pile tip. Further, the rise time of the gas force is sufficiently long that very little distortion of the pulse occurs between anvil and pile. As a result, the gas-force pulse is reproduced in the pile head with little change in peak force or duration. Interface-equipment properties, pile impedance and soil resistance have little direct effect on the gas component of pile-head force.

The indirect effect of pile impedance and soil resistance can be large, however. The portion of the gas-force pulse which occurs prior to ignition is essentially unaffected by variations in soil resistance or pile impedance, provided impact occurs. After ignition the amplitude of the pulse is strongly affected by soil resistance and pile impedance; an increase in either of these quantities results in a reduction of the peak gas force, because less fuel is required and combustion pressures are lower (Figure 4.5).

Impact Force. The generation of the impact component of force in a diesel hammer is closely related to force generation in an impact hammer. The peak force generated in the pile head is fundamentally a function of ram-impact velocity, pile impedance and interface-equipment properties.

Compared to the gas-force pulse, the impact-force pulse in the diesel hammer is short in duration and has a very short rise time. Dynamic response characteristics of the interface

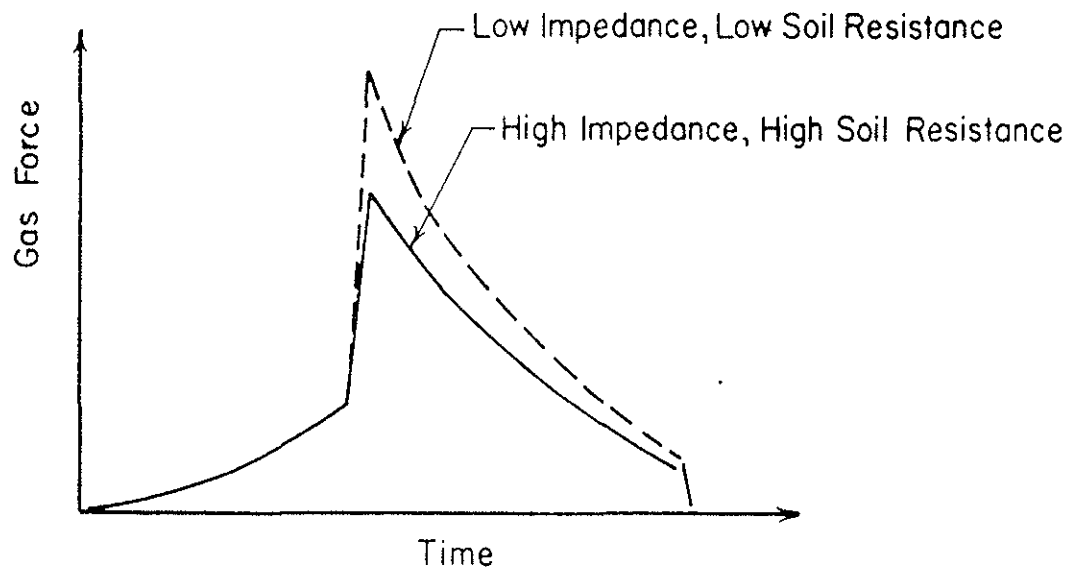


Figure 4.5 EFFECTS OF PILE IMPEDANCE AND SOIL RESISTANCE ON GAS-FORCE PULSE, CONSTANT STROKE

equipment, which have very little effect on the gas-force pulse, can cause significant distortion of the impact-force pulse.

Parola (1970) investigated the influence of interface equipment on the generated force pulse for impact hammers. Despite the presence of the anvil in the diesel hammer, a complication not present in impact hammers, it has been found by experience that Parola's conclusions relative to peak force generation apply approximately to diesel hammers operated at the stroke corresponding to maximum rated energy. Exceptions are those diesel hammers in which preignition occurs; in such hammers the preignition causes a reduction in ram-impact velocity and a corresponding diminution of peak force. The influence of preignition on peak force is discussed in Chapter 5.

Parola concluded that, in general, hammer-cushion stiffness is the most critical characteristic of the interface equipment with respect to peak force; an increase in stiffness results in higher peak force, up to a point of diminishing returns, beyond which increasing stiffness has little effect on peak force. The stiffness corresponding to maximum peak force may be higher than the stiffness resulting in maximum transmission of energy from ram to pile. The influence of hammer-cushion stiffness on performance is investigated in Chapter 5.

The effects of force reflections, changes in pile cross-section, and other factors can be of major significance in the determination of impact force. Therefore conclusions

reached on the basis of elemental theory should be checked by wave equation analysis.

Interaction of Gas and Impact Forces. Total pile force is a result of interaction of the ram and anvil movements with the gas force. Interaction results in the following phenomena:

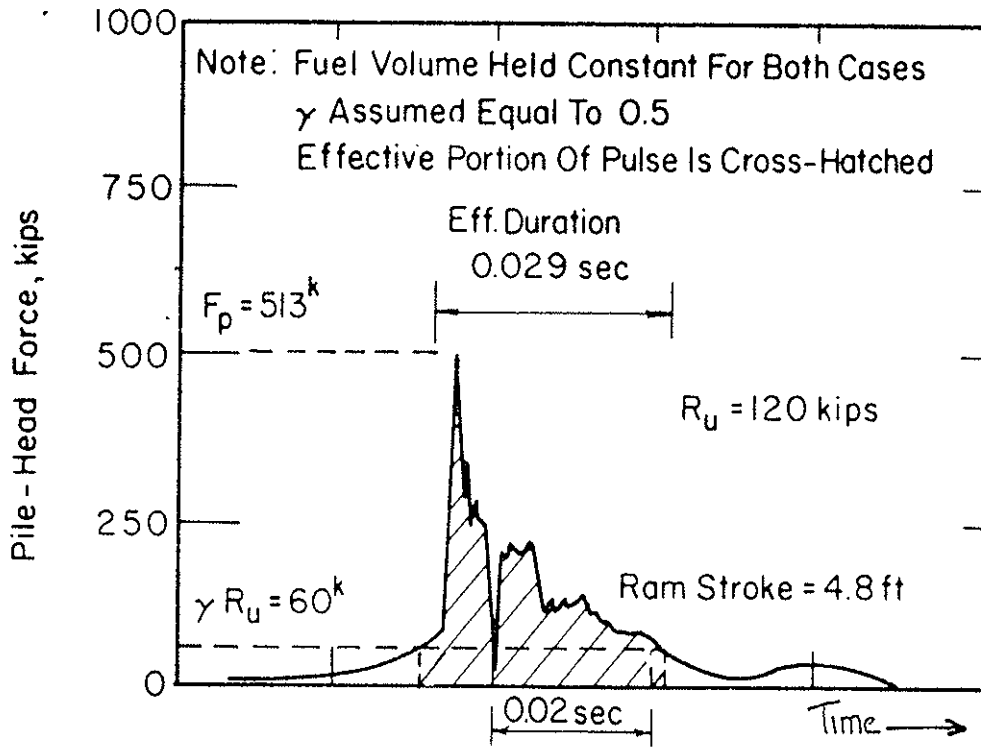
1. Pre-impact anvil acceleration.
2. Pre-impact ram deceleration.
3. Reduction of impact duration.

Pre-impact anvil acceleration and ram deceleration result from gas force and cause a reduction in the relative velocity of the ram and anvil at impact. This in turn results in a reduction in peak pile force. In normal driving, with moderate to high soil resistance, the reduction in velocity is on the order of 10 to 20 percent. In easy driving the reduction can be up to 100 percent.

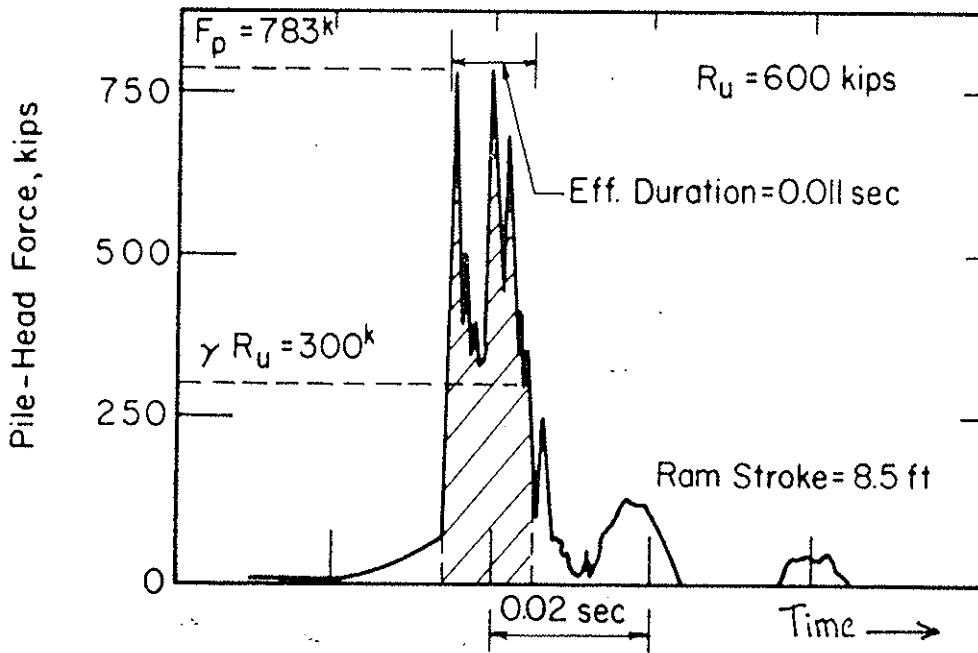
Because gas force acts on the anvil and ram throughout the period of contact, tending to separate the two masses, the duration of impact is reduced. Impact-force duration is correspondingly reduced; however, this is compensated by the presence of the gas force after separation.

Influence of Soil Resistance on Form of Energy

Soil resistance has an important, indirect effect on the form of energy delivered to the pile head by a diesel hammer. The effect is illustrated in Figure 4.6, in which the force pulse corresponding to easy driving (Figure 4.6a) is compared



a. Easy - Driving Case



b. Hard - Driving Case

Figure 4.6 INFLUENCE OF SOIL RESISTANCE ON FORM OF ENERGY

to that corresponding to hard driving (Figure 4.6b). The pulses are those predicted by the DIESEL1 simulation of a hammer operated with constant fuel volume per blow, with soil resistance varied as shown.

In the easy-driving case a low ram-stroke occurs, resulting in a low peak force and a long effective pulse duration. This is favorable with respect to pile penetration and the potential for pile damage.

For the hard-driving case a higher ram-stroke is obtained and thus peak force is increased. Although the effective pulse duration is reduced, a large percentage of the pulse falls within the effective (cross-hatched) zone. The increased peak force and change in pulse shape are both favorable to pile penetration. Peak compressive pile stresses are larger in the hard-driving case, and thus the potential for pile damage is increased.

The response of the diesel hammer to variations in soil resistance is an important aspect of performance, and will be examined further in Chapter 5.

00000

CHAPTER 5

FACTORS AFFECTING DIESEL HAMMER PERFORMANCE

5.1 INTRODUCTION

The most important factors affecting diesel hammer performance were identified on the basis of field experience and preliminary studies. DIESEL1 analyses, simulating variations in these factors, were used to investigate their influence on performance.

Factors were classified as either job controlled or hammer controlled. Job-controlled factors include pile length and impedance, inclination, total soil resistance and expended fuel energy. Hammer-controlled factors include combustion timing, power-cylinder area, compression ratio, component weights and cushioning.

In the following sections, procedures for the study are described and results of the analyses are presented and discussed.

5.2 PROCEDURE

In this section the hammer, pile and soil conditions considered in the study are described and the criteria for evaluation of hammer performance are identified and discussed.

Hypothetical Hammer

Throughout the study a single, hypothetical diesel hammer was considered, on the assumption that hammers of all sizes exhibit similar performance characteristics. The specifications of the hypothetical hammer, as listed below, approximate those of commonly used open-top hammers. Closed-top operation was not considered, because the closed top has little effect on performance characteristics other than blow rate.

In most of the analyses, specifications of the hypothetical hammer were assumed as follows:

1. Rated energy	40,000 lbs
2. Ram weight	5,000 lbs
3. Stroke	8.0 ft
4. Anvil weight	1,500 lbs
5. Drivehead weight	1,000 lbs
6. Compression ratio	12:1
7. Power-cylinder area	190 in ²
8. Combustion-chamber volume	200 in ³
9. Ram length	8.0 ft
10. Preignition distance	0.00 ft
11. Delay time	0.000 sec
12. Rise time	0.003 sec
13. Hold time	0.002 sec
14. Friction factor, vertical operation	5 %
15. Gas constant, compression	1.40
16. Gas constant, expansion	1.35

17. Hammer-cushion stiffness	20×10^6 lb/in
18. Coefficient of restitution, ram-anvil	0.85
19. Coefficient of restitution, hammer-cushion	0.80
20. Coefficient of restitution, drivehead-pile	1.00

In certain analyses the above specifications were varied in order to investigate the resulting affect on performance. These changes are noted in the discussions to follow. In all cases the peak gas force, F_{gm} , was adjusted so as to obtain equality of downstroke and upstroke.

For each of the analyses wherein stroke was specified as an input constant, unlimited fuel energy was considered available for lifting the ram. Thus it was possible to investigate hypothetical operating conditions such as the infinitely long pile without regard to fuel energy limits. In reality the amount of fuel which can be burned is limited by the quantity of air in the power cylinder, fuel injection capability, and other hammer design factors. Therefore, the fuel energy limit varies widely from hammer to hammer.

The analytical results presented herein should be interpreted in light of the fuel energy which might be available in an actual hammer equivalent to the hypothetical hammer. For this purpose the maximum available fuel energy, assuming 4.0 cc of fuel with 28,800 ft-lbs of latent energy per cc, is 115,200 ft-lbs. If a thermal efficiency of 32 percent is

assumed, the maximum available net expended fuel energy $(E_{gn})_{max}$, is approximately 37,000 ft-lbs. The quantity $(E_{gn})_{max}$ does not enter the calculations of hammer performance; it is marked on some figures in order to aid interpretation. No documented information relative to the value of $(E_{gn})_{max}$ for various hammers is available. Recommendations for accumulation of such data are discussed in Chapter 6.

Piles

Pile impedance was held constant throughout the study with the exception of the investigation of impedance effects. An impedance of 2900 lb-sec/in was used, corresponding to a steel pile with 20 in² cross-sectional area. This impedance was selected in order to provide proper matching of hammer energy and pile impedance, as occurs on a well-engineered foundation project. Davisson (1975) suggests 1000 to 2000 ft-lbs of energy per square inch of steel area, depending on pile length, soil resistance distribution and final blows per inch. Experience with diesel hammers indicates a somewhat higher range of values is appropriate: approximately 1250 to 2500 ft-lbs/in². For 20 in² of steel area, the 40,000 ft-lbs rated energy of the hypothetical hammer falls midway in this range.

Various pile lengths, ranging from 40 to infinity, were considered. In short piles force reflections are an important factor in dynamic pile response; as pile length increases reflections become less important. In the case of the

infinitely long pile it is possible to investigate hammer performance in the total absence of reflections.

The infinitely long pile was simulated by a dashpot, as suggested by Parola (1970). The force-velocity relationship of the dashpot (Figure 5.1) was specified in the DIESEL1 program as follows:

$$F_h = \rho c a v \quad (5.1)$$

where v = drivehead velocity. Because the pile is modeled exactly by this dashpot, spurious oscillations do not occur and internal damping is not required.

It is important to recognize certain peculiarities of the infinitely long pile:

1. Maximum pile-head deflection, D_{hm} , is strictly related to total impulse, I_h , as follows:

$$D_{hm} = I_h / \rho c a \quad (5.2)$$

Thus the quantity and form of transmitted energy have no effect on pile-head deflection.

2. Due to the absence of reflections, total pile-head deflections are much larger than in the case of short piles. Thus large anvil deflections occur.
3. As a result of the large anvil deflections, which consume large amounts of energy, the calculated

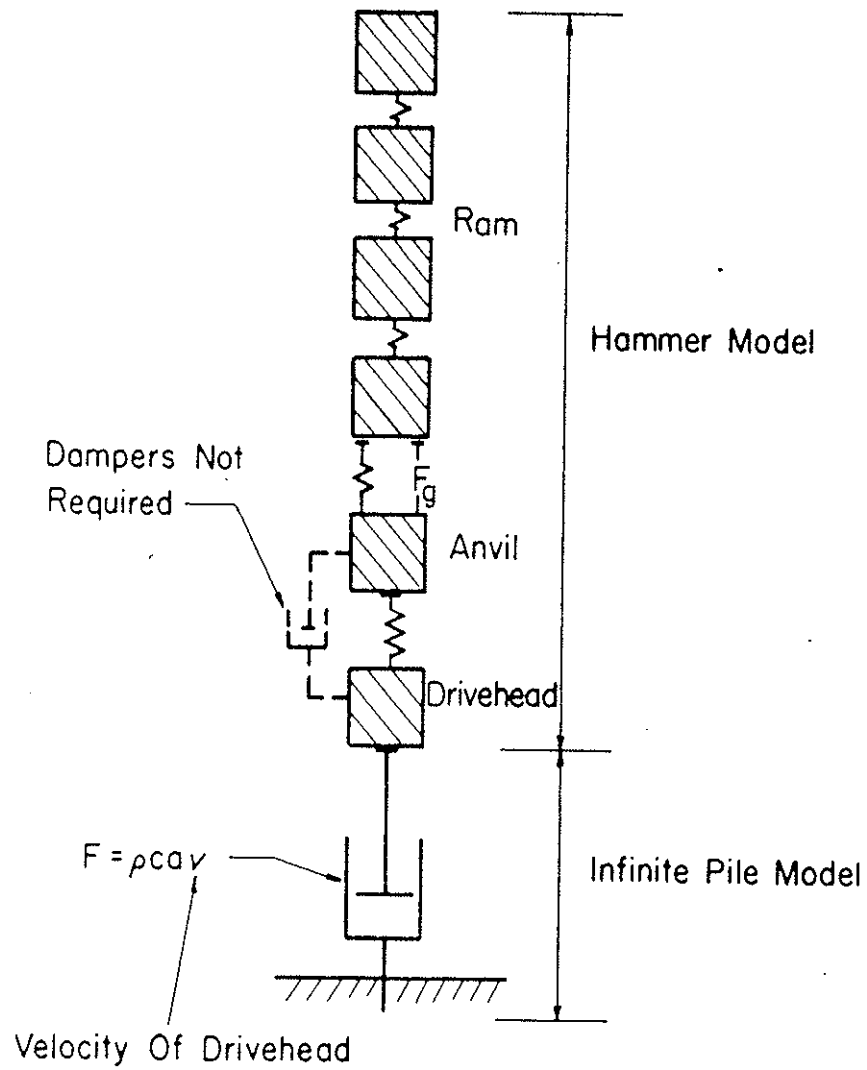


Figure 5.1 SIMULATION OF DRIVING INFINITELY LONG PILE

gas-force pulse is of higher amplitude relative to the impact-force pulse than is the case when driving short piles. Similarly, the calculated value of net expended fuel energy is much larger than that corresponding to the short-pile case.

4. Soil-resistance effects cannot be evaluated.

Because of the foregoing peculiarities the infinitely long pile case is not totally representative of long-pile driving. Therefore, in some parts of the study, pile lengths of 160 and 320 ft were considered to be representative of long-pile driving. By examining the cases of long piles of finite length it is possible to study hammer performance under conditions of diminished force-reflection effects, without the large pile deflections and high fuel energy requirements associated with the infinitely long pile. Additionally, soil resistance effects can be investigated.

Soil

In all cases wherein a finite pile length was assumed, 80 percent of the static soil resistance was considered to be concentrated at the pile tip, with the remainder distributed uniformly along the side of the pile. The following soil parameters were assumed:

1. Quake at tip of pile, $Q_t = 0.10$ in.
2. Quake at side of pile, $Q_s = 0.10$ in.
3. Damping factor at tip, $J_t = 0.15$ sec/ft.
4. Damping factor at side, $J_s = 0.05$ sec/ft.

These are commonly used values, appropriate to most soils, and to piles on the order of 1 ft^2 tip area. The soil resistance distribution and soil parameters were held constant throughout the study because variations in these factors have a negligible effect on fundamental hammer performance characteristics.

Total static soil resistance, R_u , was set equal to 60, 120, 240 or 300 tons (2000 lbs/ton) in order to simulate easy, moderate, moderately-hard and hard driving conditions, respectively.

Criteria

In evaluation of the results of the analyses, emphasis was placed on the fundamental aspects of hammer performance as identified in Chapter 4. Energy transmitted to the pile and the form of the energy, as indicated by peak force, total impulse and pulse shape, were given primary consideration. Pile deflections were examined and fuel energy expended in the hammer was investigated.

The following quantities will be mentioned in discussions of the results of the analyses:

E_{hm} = Maximum energy transmitted to the pile head in the form of work. Some of this energy is returned to the hammer during pile rebound.

E_{hn} = Net energy transmitted to the pile head at the completion of the hammer blow. In the case of the infinitely long pile there is no rebound and therefore $E_{hn} = E_{hm}$.

- E_{am} = Maximum energy transmitted to the anvil in the form of work. E_{am} will be discussed in terms of the contribution of impact and gas forces to transmitted energy.
- E_{gn} = Net energy transmitted to the ram and anvil in the form of work done by the gas force, i.e. the total fuel energy expended in the form of work within the hammer. This is an indicator of the volume of fuel injected.
- $(E_{gn})_{max}$ = Estimated maximum value of E_{gn} , indicating the performance limit.
- F_{hm} = Maximum (peak) pile head force. This normally occurs at ram impact, but can occur later due to reflections. F_{hm} is a key indicator of the form of energy delivered at the pile head.
- F_{tm} = Maximum force at the pile tip. This is particularly significant in hard driving.
- I_a = Total impulse on the anvil, due to both gas and impact forces.
- I_h = Total impulse on the pile head. I_h is approximately equal to I_a ; for the cases studied the small difference between I_h and I_a , in general less than 1 percent, is due to energy losses and inertial effects in the anvil, drivehead and cushioning.

For purposes of this study, I_h and I_a are considered equal.

D_{hm} = Maximum deflection of pile head.

D_{tm} = Maximum deflection of pile tip. Net pile penetration is determined from D_{tm} as follows:

$$\text{Net penetration} = D_{tm} - \text{soil quake } (Q_t)$$

BPI = Blows per inch of penetration. BPI is the reciprocal of the net penetration of the pile due to a single hammer-blow.

5.3 JOB-CONTROLLED FACTORS

Pile Length

Analyses were performed relative to the hypothetical hammer operating on piles from 40 to 320 ft in length, plus an infinitely long pile. Pile impedance was set equal to 2900 lb-sec/in. For piles of finite length, soil resistance, R_u , was varied from 60 to 300 tons, simulating the range from easy to hard driving. Results of the analyses are summarized in Figures 5.2 through 5.5.

Transmitted Energy vs Length. The variation of maximum pile-head energy, E_{hm} , and net pile-head energy, E_{hn} , with pile length is illustrated in Figure 5.2. At low values of R_u , E_{hm} and E_{hn} decrease with increasing pile length; this can be attributed to the effects of force reflections. Pile-head

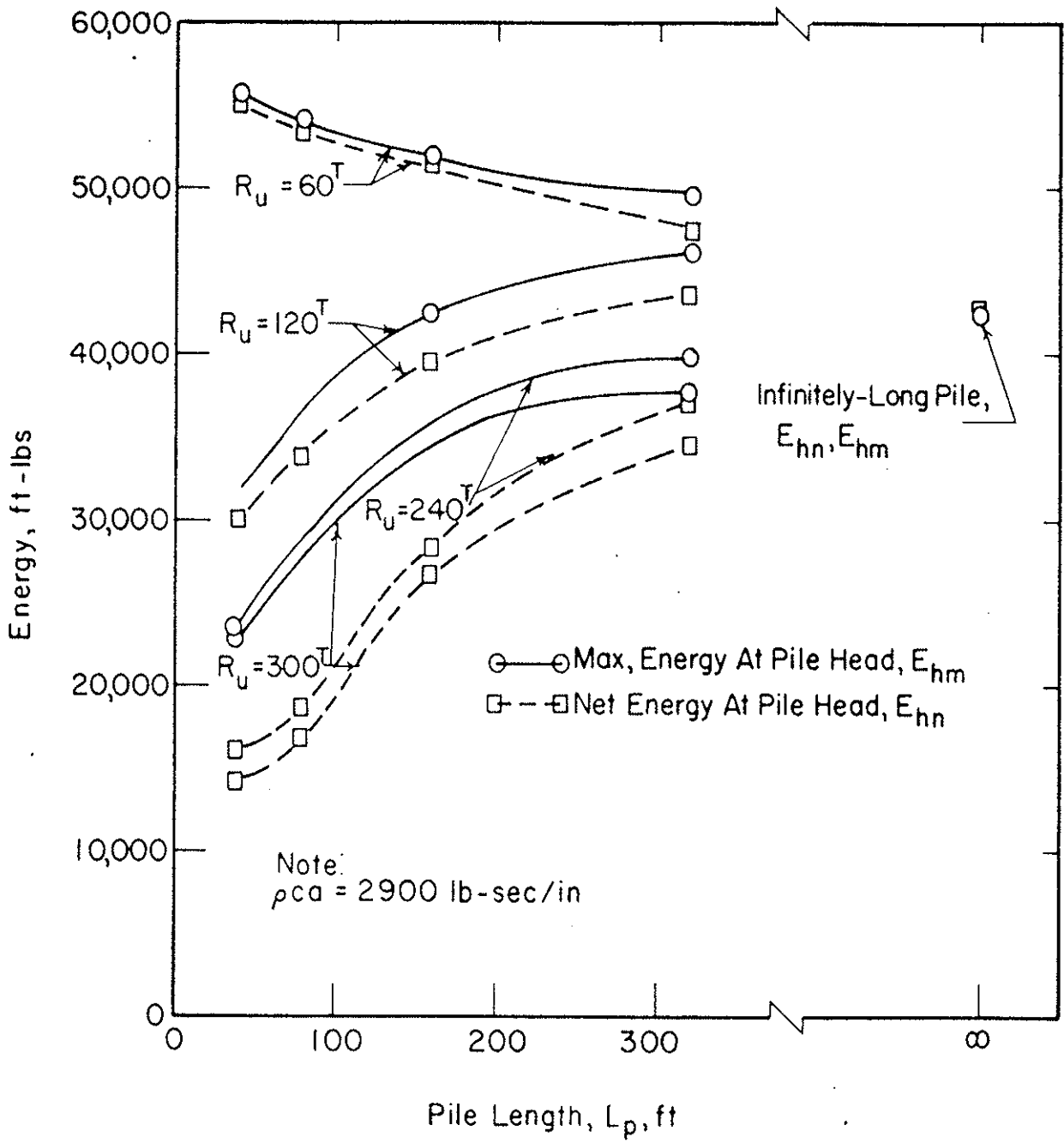


Figure 5.2 TRANSMITTED ENERGY VS PILE LENGTH

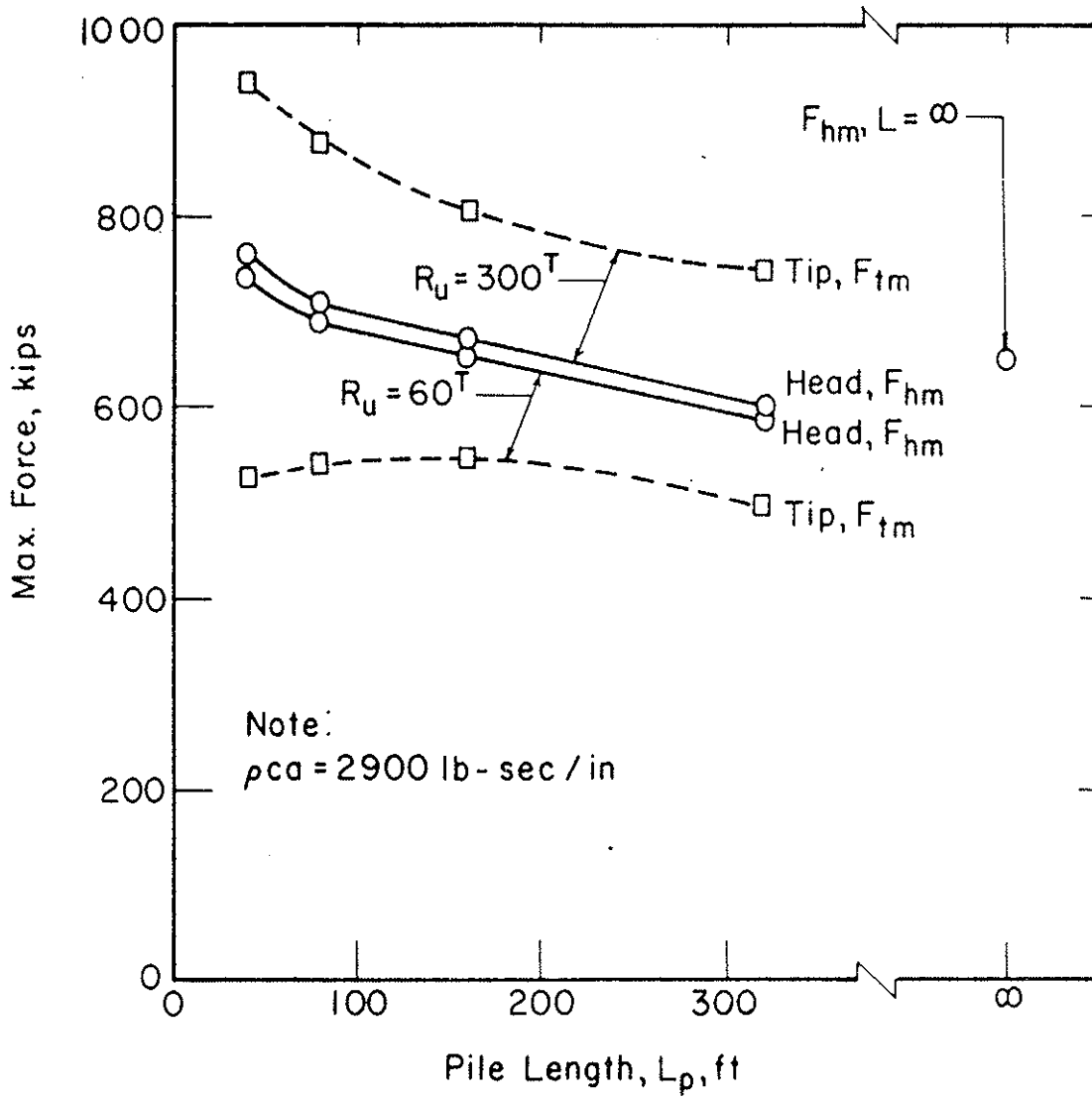


Figure 5.3 PEAK FORCE VS PILE LENGTH

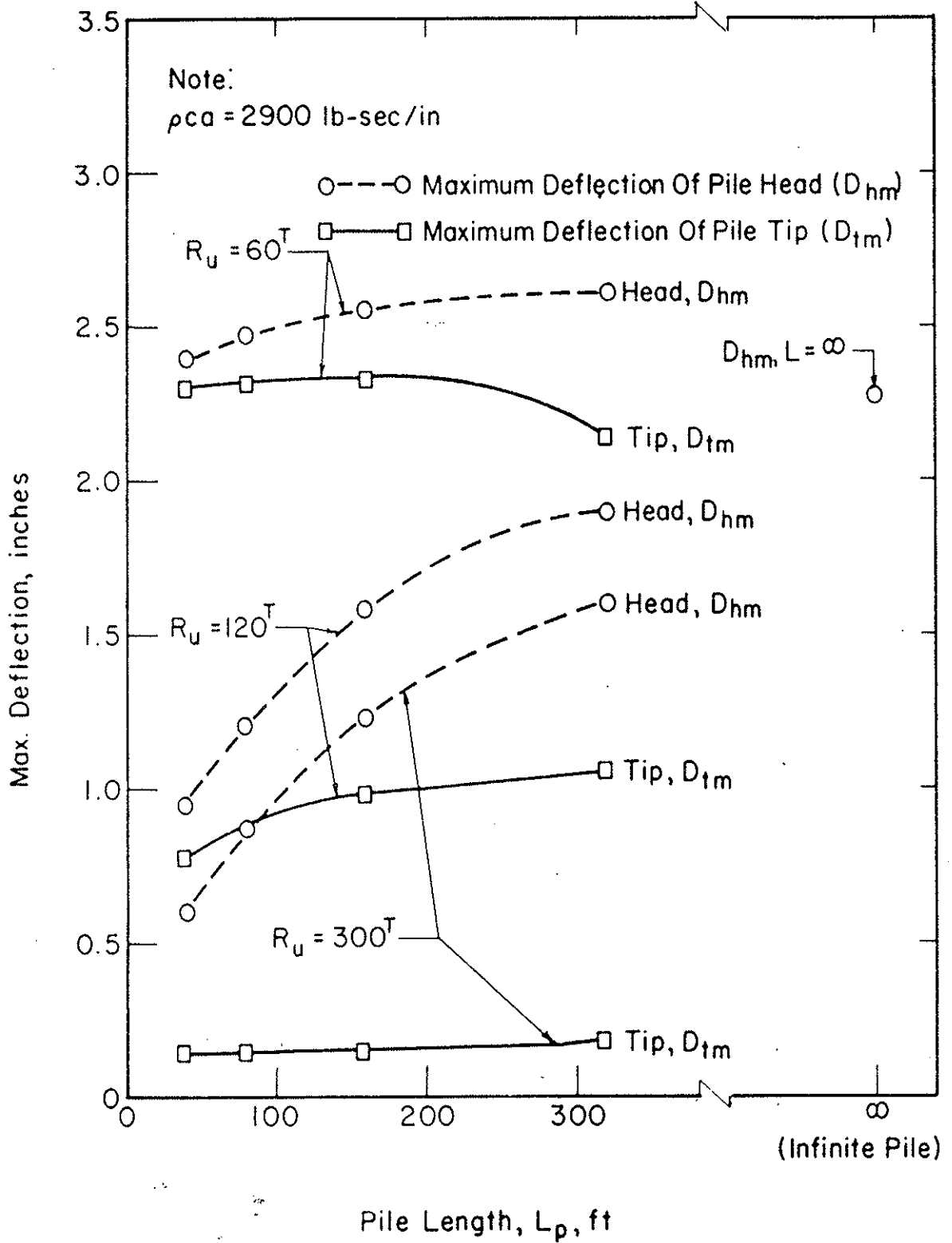


Figure 5.4 PILE DEFLECTION VS PILE LENGTH

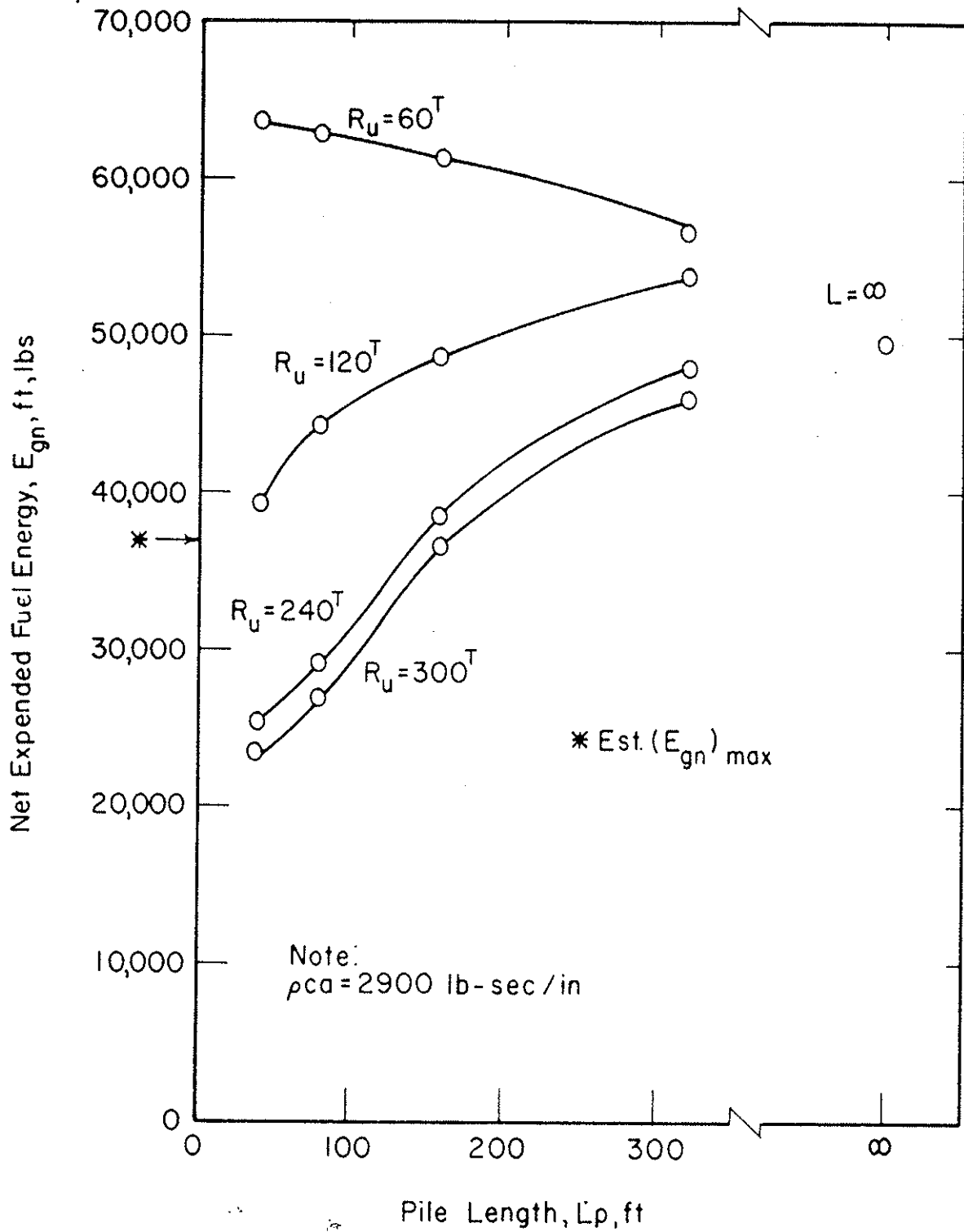


Figure 5.5 NET EXPENDED FUEL ENERGY VS PILE LENGTH

forces (Figure 5.3) decrease due to the diminishing effect of reflections, whereas reflections at the pile head are approximately constant with increasing pile length (Figure 5.4). Thus transmitted energy, which is the integral of force times deflection, also decreases.

At high values of R_u , pile-head deflections increase with increasing pile length due to increased elastic strain energy stored in the pile. Much of this energy remains in the pile at the completion of the blow, due to residual stresses. Thus both maximum and net pile-head energy increase with increasing pile length. As length increases the influence of force reflections decreases and, therefore, the transmitted energy, for all values of R_u , converges on the value corresponding to the infinitely long pile. Note that R_u has no relevance to the case of the infinitely long pile.

For several of the cases at low values of R_u , both maximum and net transmitted energy exceed the assumed $(E_{gn})_{max}$ (37,000 ft-lbs). In reality, unless additional fuel energy is available, the ram stroke and transmitted energy will be below the values calculated for the 8 ft stroke.

Peak Force vs Length. Peak force at the pile head, F_{hm} , and pile tip, F_{tm} , are plotted versus pile length in Figure 5.3. In general, peak forces at the head and tip of the pile decrease with increasing length because of the reduced influence of reflections. In diesel driving, reflections of pre-impact gas forces have the effect of reducing anvil movement. The result

in the case of short piles is that the relative velocity of ram and anvil at impact is increased and, thus, peak force also is increased. In the case of very long piles, for all values of R_u , pile-head peak force approaches that calculated for the infinitely long pile.

The relationship of F_{tm} to F_{hm} is a function of soil resistance distribution and impedance matching at the pile tip and, as such, is not dependent on hammer performance characteristics. In the examples shown, F_{tm} is less than F_{hm} at low R_u due to side resistance on the pile. At high R_u , however, F_{tm} exceeds F_{hm} as a result of compressive reflections at the pile tip.

Pile Deflection vs Length. Maximum deflections of the pile head, D_{hm} , and the pile tip, D_{tm} , are plotted versus pile length in Figure 5.4. D_{hm} increases with increasing length as a result of elastic compression of the pile. For high values of R_u , D_{tm} increases slightly with increasing length, indicating that force reflections in the shorter-length piles are detrimental to pile penetration for the case analyzed.

Fuel Energy vs Length. Net expended fuel energy, E_{gn} , is plotted versus pile length in Figure 5.5. Because E_{gn} is a measure of the amount of fuel burned, the plot can be interpreted as an indication of the effect of pile length on fuel requirements at constant stroke. Because E_{gn} is approximately proportional to net pile-head energy, E_{hn} (Chapter 4), variations in pile length affect E_{gn} and E_{hn} similarly. Therefore

the preceding discussion of the influence of pile length on transmitted energy applies equally to fuel energy.

As noted previously, values of E_{gn} in excess of $(E_{gn})_{max}$ could not be achieved by a real hammer equivalent to the hypothetical hammer. Ram stroke would decrease to a value which results in E_{gn} equal to $(E_{gn})_{max}$.

Pile Impedance

For the study of impedance effects, analyses were performed relative to the hypothetical hammer operating on piles with impedances ranging from 1450 to 11,600 lb-sec/in, corresponding to a steel area of 10 in² to 80 in². This represents the extreme range of impedances for which a hammer equivalent to the hypothetical hammer might be used, and exceeds the range for which it is properly used. In the case of the 40 ft pile, R_u was set equal to 240 tons. Results of the analyses are summarized in Figures 5.6 through 5.8.

Transmitted Energy vs Pile Impedance. For the infinitely long pile (Figure 5.6), transmitted energy (E_{hm} , E_{hn}) decreases sharply with increasing impedance, reflecting the decrease in elastic compression which accompanies high impedance. For the 40 ft pile (Figure 5.8), E_{hm} is essentially unaffected by impedance and E_{hn} increases somewhat with increasing impedance due to increased penetration, D_{tm} . The difference between long and short pile performance is due to increased force reflections and reduced elastic compression in the short pile.

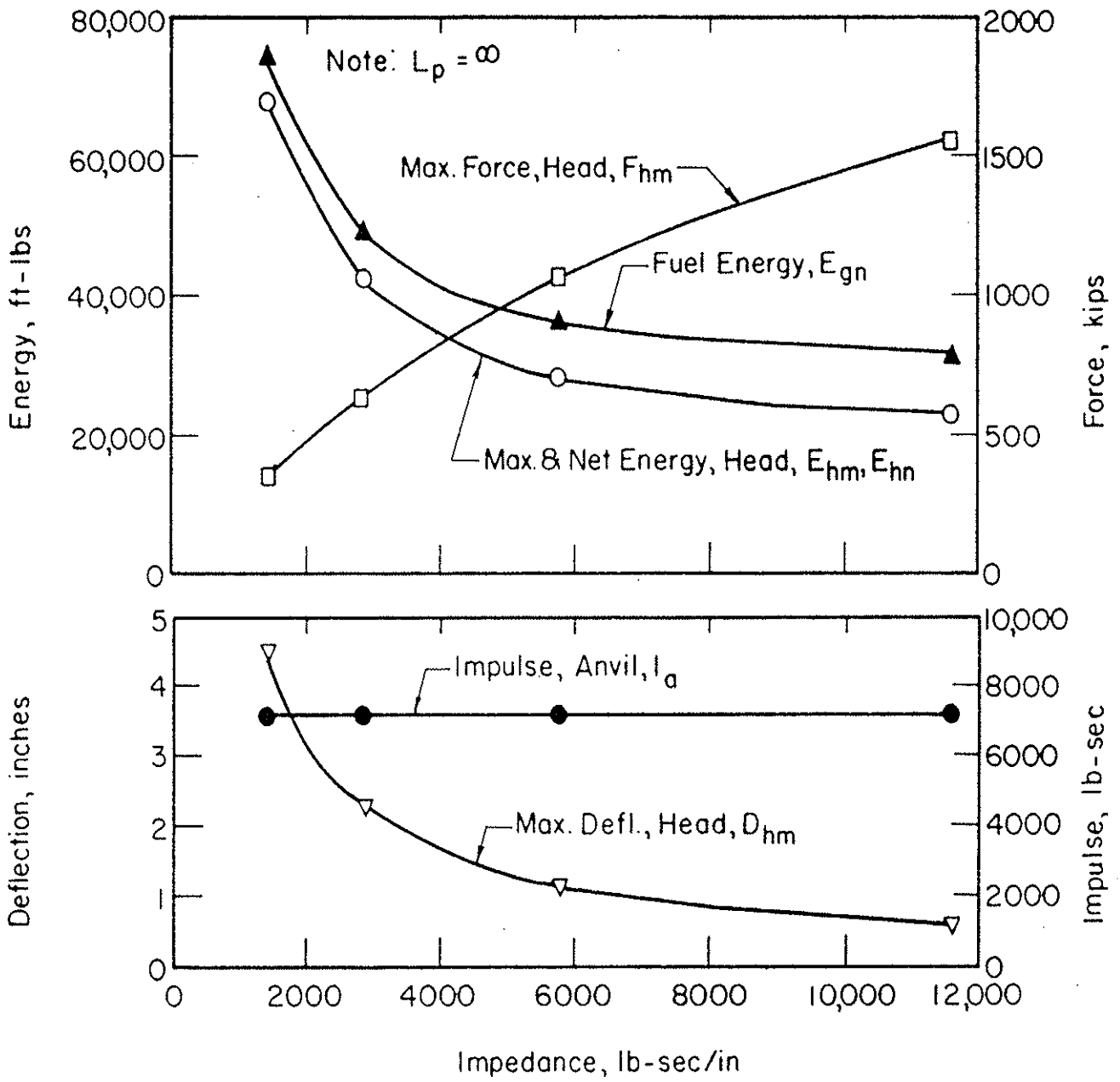


Figure 5.6 IMPEDANCE EFFECTS, INFINITELY LONG PILE

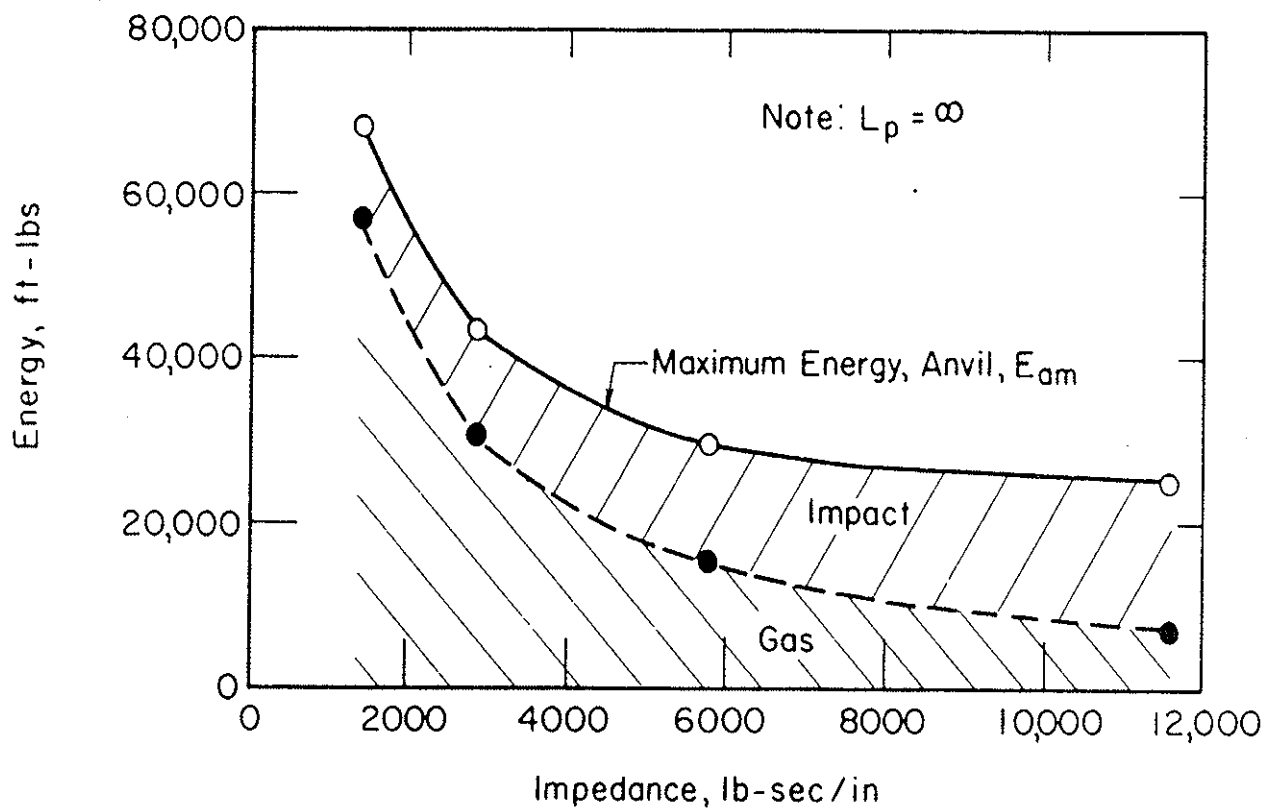


Figure 5.7 COMPONENTS OF WORK DONE ON ANVIL, INFINITELY LONG PILE

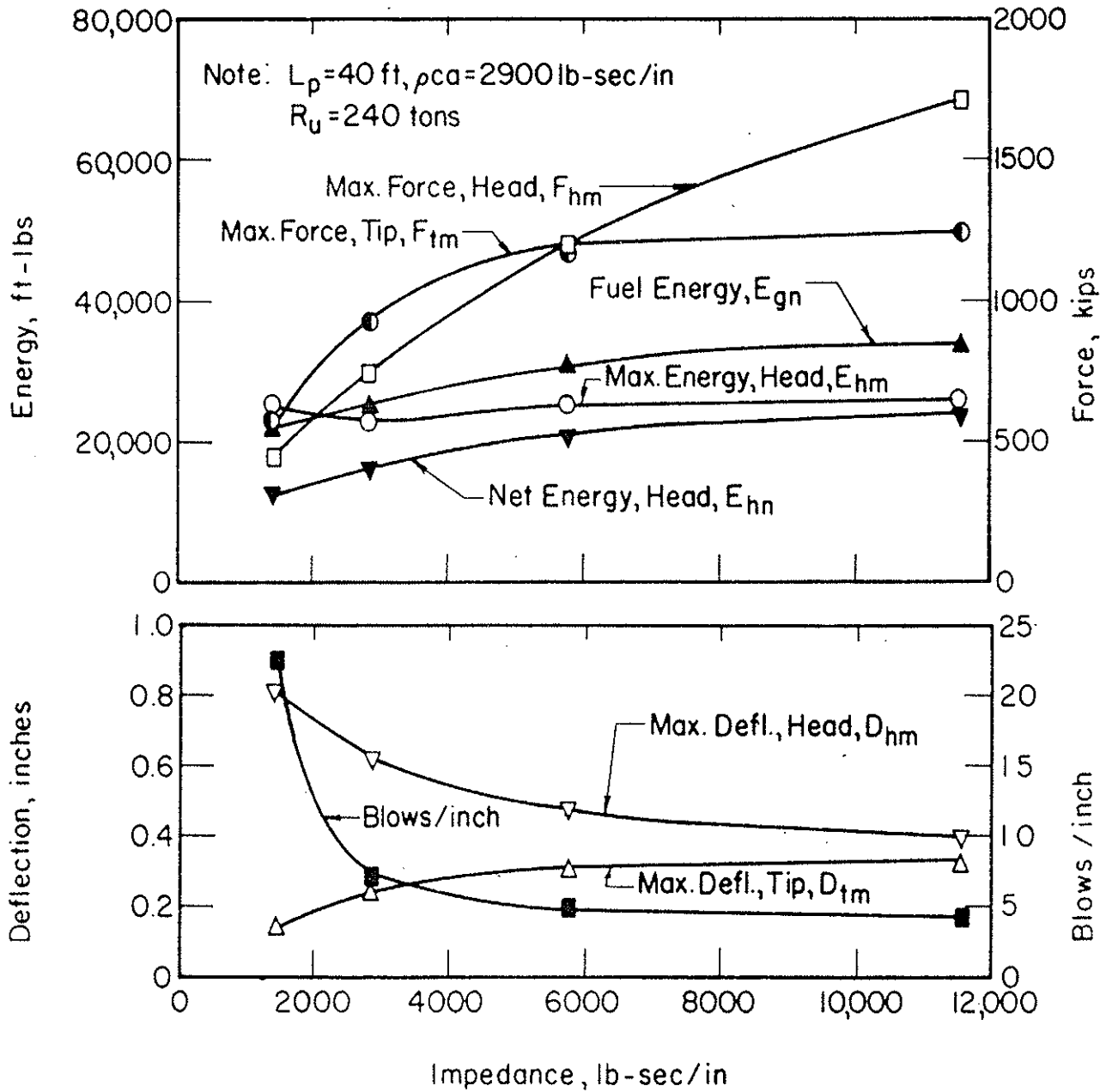


Figure 5.8 IMPEDANCE EFFECTS, 40 FT PILE, 240 TONS SOIL RESISTANCE

Peak Force vs Impedance. In the cases of both the infinitely long and 40 ft piles, peak forces are strongly affected by pile impedance. Peak pile-head force, F_{hm} , increases with increasing impedance for both pile lengths, as predicted by fundamental wave theory, assuming constant impact velocity and ideal impact conditions. However, due to the presence of interface equipment, variation of impact velocity with impedance, and other non-ideal conditions, F_{tm} and impedance are not strictly proportional.

For the 40 ft pile, peak pile-tip force, F_{tm} , exceeds F_{hm} at low impedance and is less than F_{hm} at high impedance, due to the effects of the ratio of pile impedance to maximum soil resistance at the pile tip. As pile impedance is increased relative to soil resistance, reflections change from compressive to tensile, thus reducing F_{tm} relative to F_{hm} .

Pile Deflection vs Pile Impedance. For both the infinitely long and 40 ft piles, D_{hm} decreases with increasing pile impedance because of decreasing elastic compression of the pile. For the infinitely long pile, total impulse at the anvil, I_a , remains constant over the range of impedance values; therefore D_{hm} is inversely proportional to impedance (Equation 5.2). For the 40 ft pile length, D_{tm} increases with increasing impedance, as a result of the higher peak force associated with increased impedance.

Fuel Energy vs Pile Impedance. For both pile lengths, the variation of net expended fuel energy, E_{gn} , with impedance

is similar to the variation of E_{hn} with impedance, reflecting the approximate proportionality of E_{gn} and E_{hn} . The relative contributions of the gas and impact forces to energy at the anvil are shown in Figure 5.7. Maximum energy through the anvil, E_{am} , is plotted versus impedance; the gas and impact components of E_{am} are also shown. At low impedance the gas component accounts for the majority of transmitted energy, whereas at high impedance the impact component predominates.

Inclined (Batter) Operation

In Chapter 3 the influence of inclination on hammer performance was discussed and a method for simulating inclined operation was described. In order to examine the effect of inclination angle, α , and batter friction factor, C_{fb} , as defined in Chapter 3, analyses were performed for the hypothetical hammer operating at various values of α . C_{fb} was varied from zero to 0.10, the estimated upper limit of sliding friction. Pile impedance was set equal to 2900 lb-sec/in; pile lengths of 40 to 160 ft were considered. In all cases ram stroke as measured along the axis of the hammer was held constant, and R_u was set equal to 240 tons. Results of the analyses are summarized in Figures 5.9 and 5.10.

Transmitted Energy, Peak Force and Deflection vs α .

Net energy and peak force at the pile head decrease with increasing inclination for both the 40 ft pile (Figure 5.9) and the 160 ft pile (Figure 5.10), reflecting a decrease in

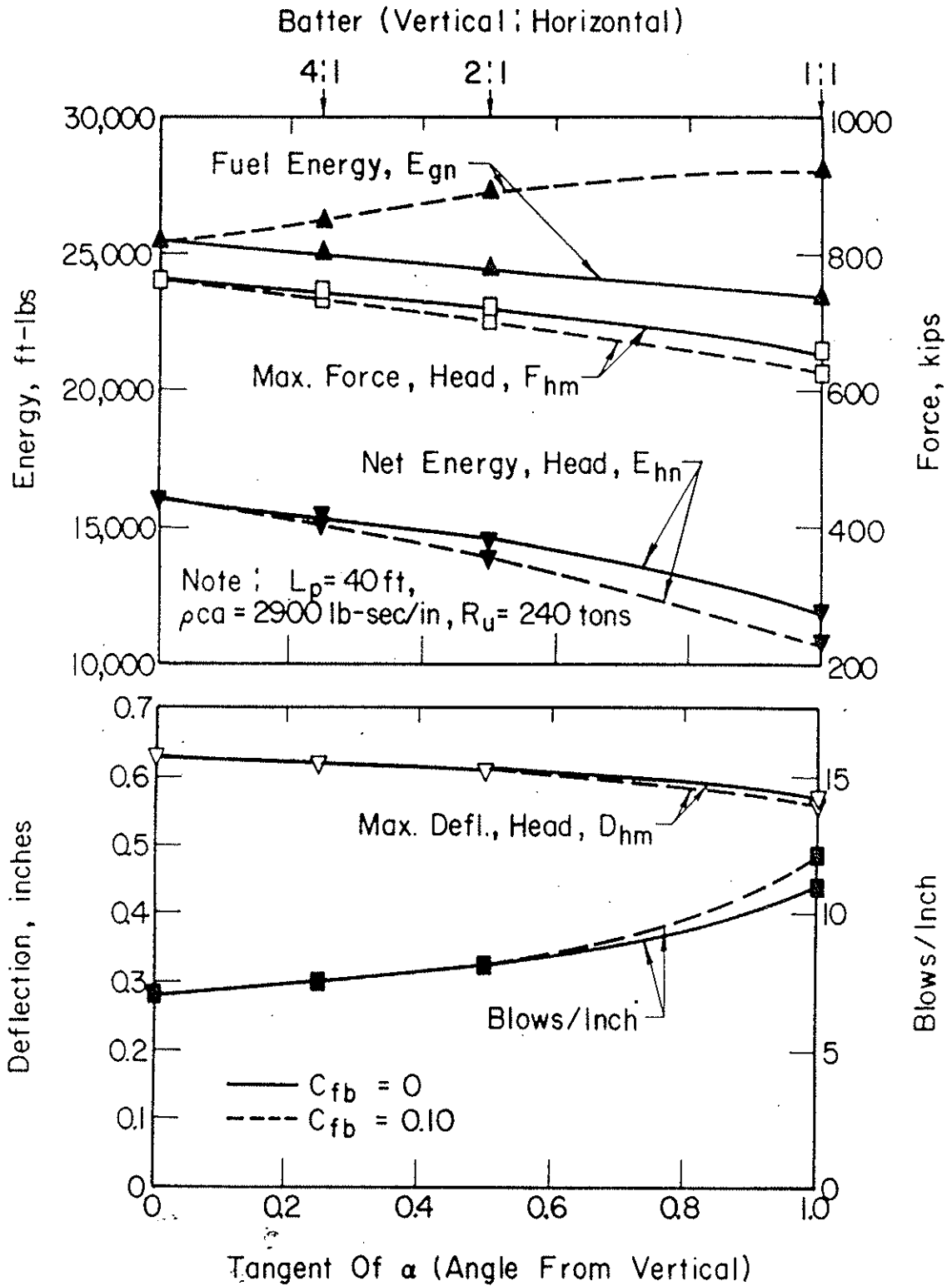


Figure 5.9 EFFECTS OF INCLINATION, 40 FT PILE, 240 TONS SOIL RESISTANCE

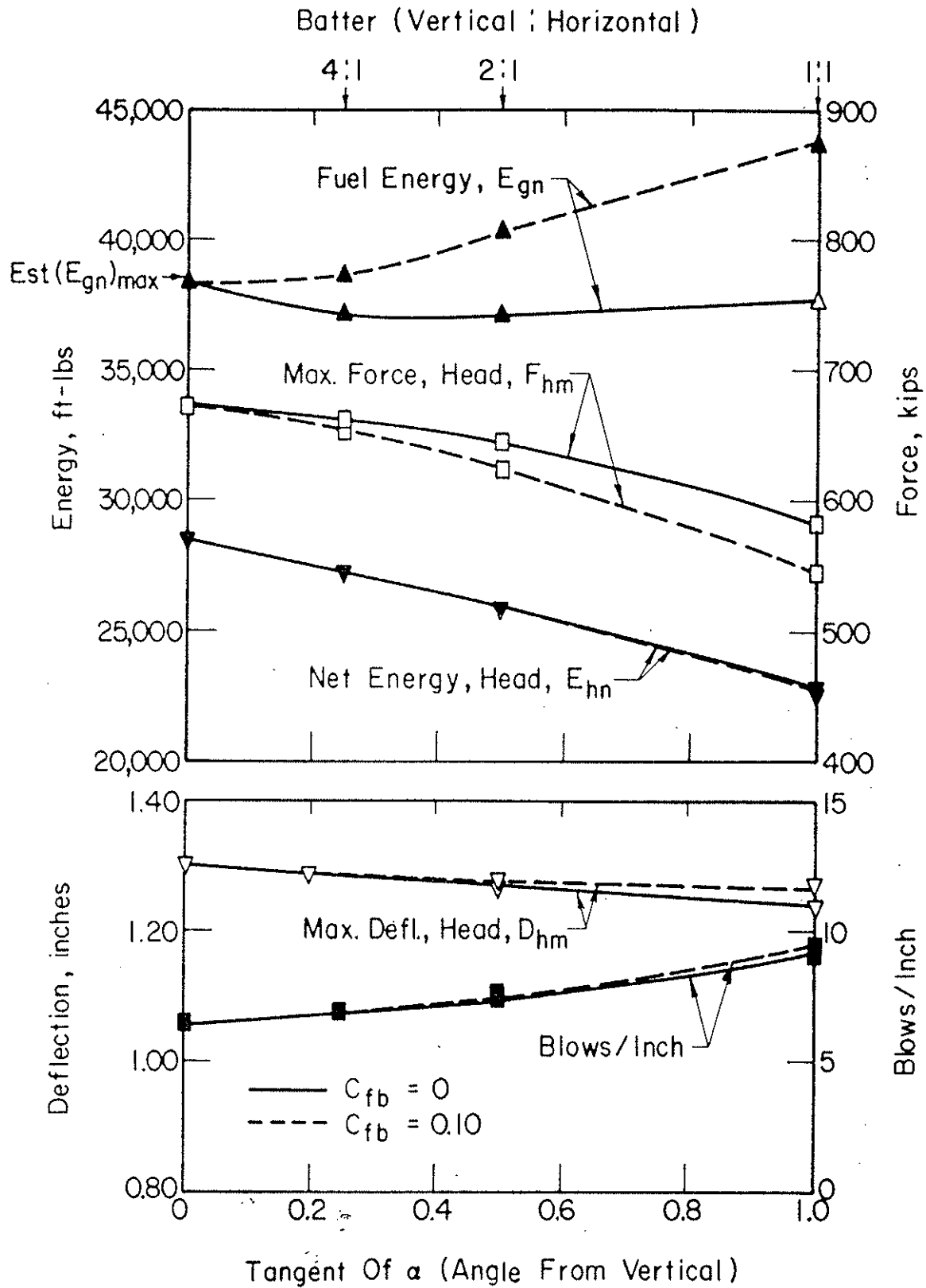


Figure 5.10 EFFECTS OF INCLINATION, 160 FT PILE, 240 TONS SOIL RESISTANCE

impact velocity. Net tip deflection, as indicated by blows per inch of penetration, showed less than 10 percent change as α was increased from zero to 14° (4:1), indicating that performance is not sensitive to batter at batter angles steeper than 4:1, for a given ram stroke.

Fuel Energy vs α . The effect of inclination on net expended fuel energy, E_{gn} , depends on C_{fb} . For C_{fb} equal to zero, E_{gn} decreases with increasing α ; for C_{fb} equal to 0.10 the reverse is true. Field experience indicates that, for constant ram stroke, fuel volume decreases with increasing α . Thus, on an empirical basis, C_{fb} should be set equal to a value less than 0.10; a value of 0.05 is considered reasonable. The results of the analyses indicate that variations in C_{fb} from zero to 0.10 have negligible effect on calculated performance for α less than 27° (2:1).

Soil Resistance

Analyses were performed relative to the hypothetical hammer operating on piles with impedance of 2900 lb-sec/in, with R_u ranging from 60 to 300 tons in order to simulate easy to hard driving conditions. Pile lengths of 40 ft and 160 ft were investigated. Results of the analyses are summarized in Figure 5.11 (40 ft pile) and Figure 5.12 (160 ft pile).

Transmitted Energy vs Soil Resistance. Maximum and net energy at the pile head, E_{hm} and E_{hn} , decrease with increasing R_u for both pile lengths, as a result of decreasing penetration.

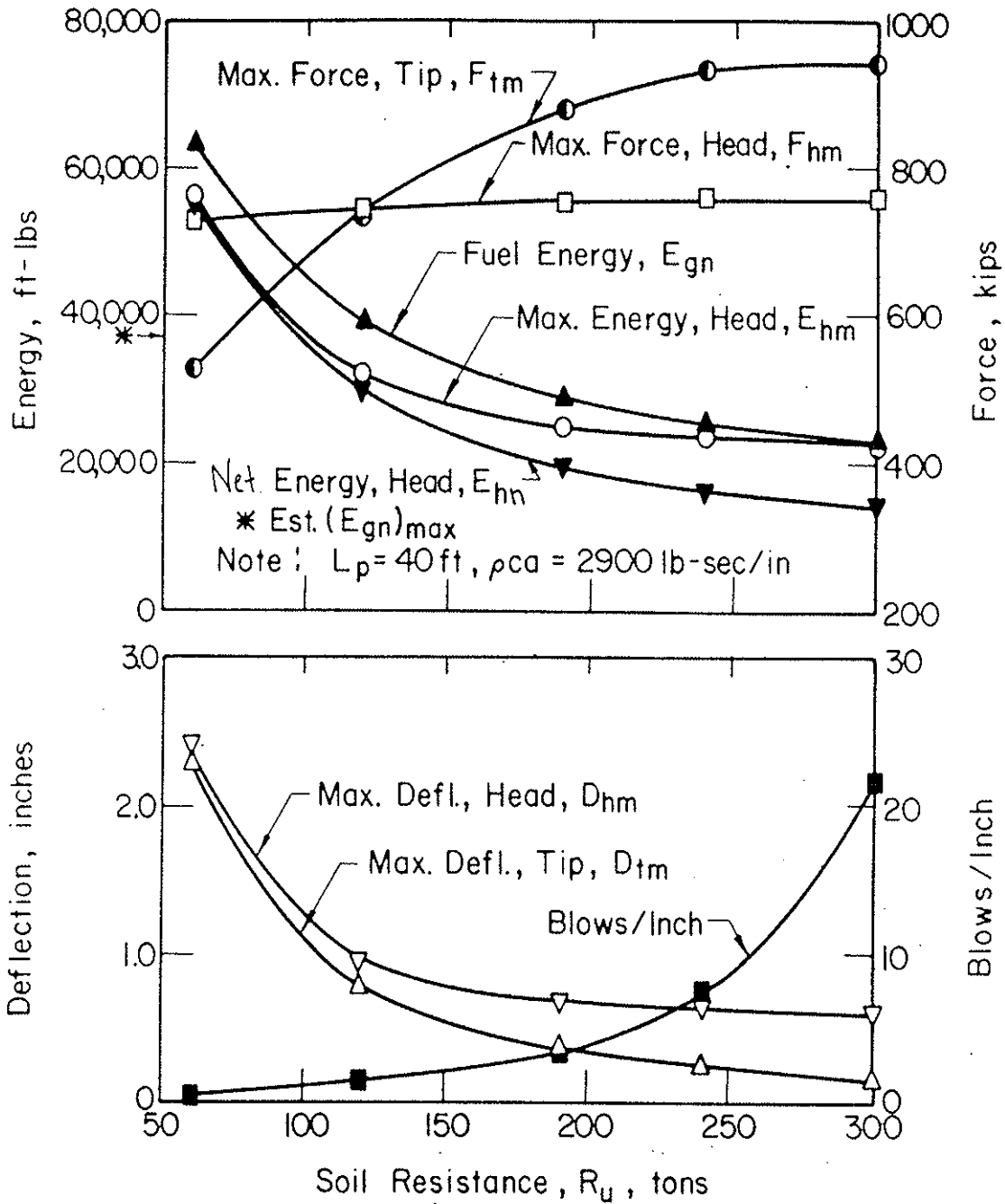


Figure 5.11 SOIL RESISTANCE EFFECTS, 40 FT PILE

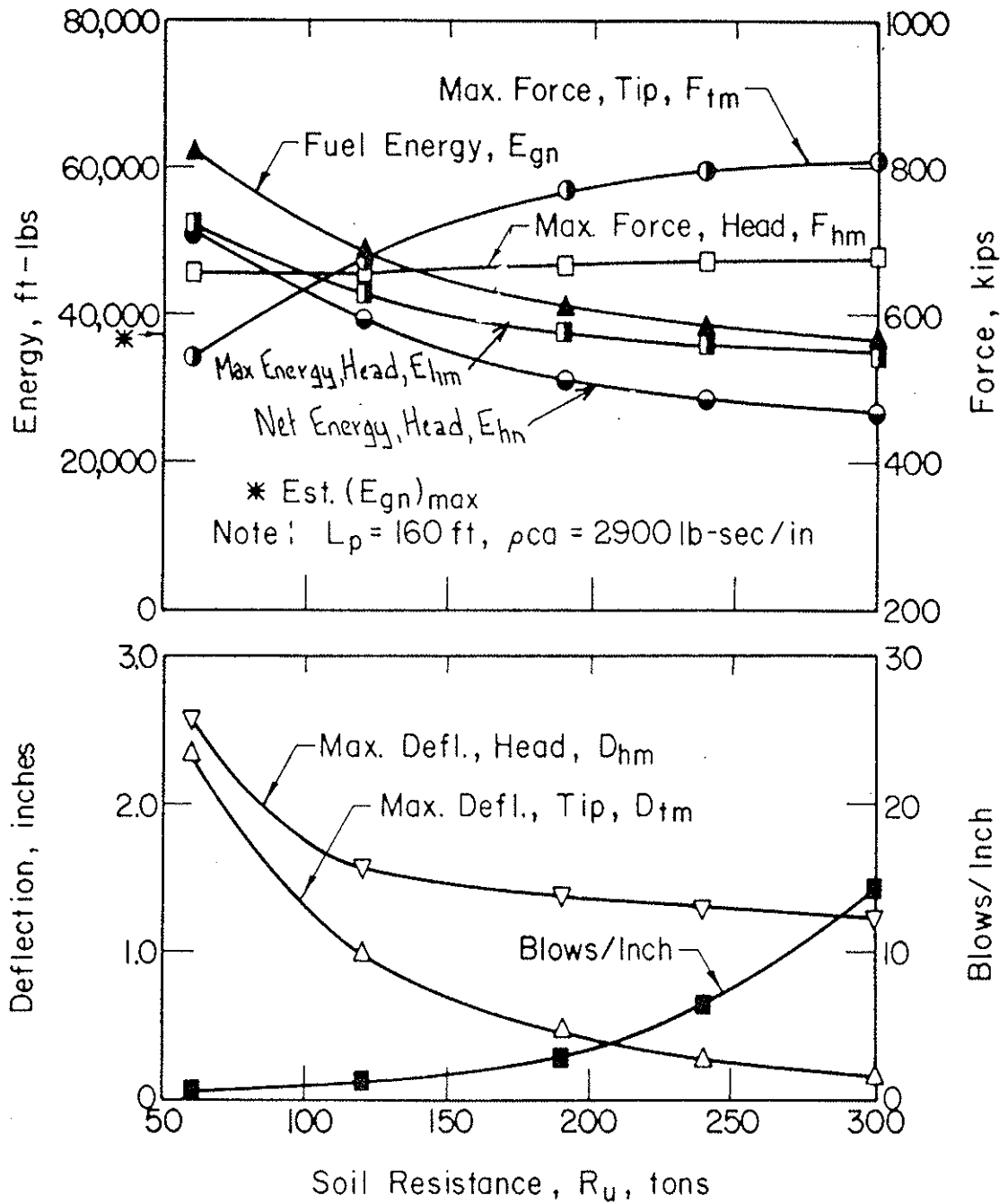


Figure 5.12 SOIL RESISTANCE EFFECTS, 160 FT PILE

The difference between E_{hm} and E_{hn} increases with increasing R_u as more and more energy is returned to the hammer during rebound. The 160 ft pile drives more efficiently; penetration and transmitted energy are somewhat higher than for the shorter pile.

Peak Force vs Soil Resistance. An increase in R_u has very little effect on the peak force at the pile head, F_{hm} . At the tip, however, low R_u results in tensile reflection and a low value of F_{tm} . For high R_u compressive reflections result in a high value of F_{tm} . In both cases the effect is more pronounced for the shorter pile length.

Pile Deflection vs Soil Resistance. Maximum deflection at the pile tip, D_{tm} , decreases with increasing R_u because a greater amount of energy is consumed in soil damping and in elastic compression of pile and soil. The difference between maximum pile-head deflection, D_{hm} , and D_{tm} increases with increasing R_u due to increased elastic compression of the pile. Tip deflections are somewhat greater for the 160 ft pile as compared to the 40 ft pile because of more favorable force-reflection conditions.

Fuel Energy vs Soil Resistance. Net expended fuel energy, E_{gn} , decreases with increasing R_u ; therefore with low R_u more fuel is required to maintain a given stroke than at high R_u . In soft soil conditions a large amount of energy is expended in anvil movement. Note that for the examples shown,

fuel energy in excess of rated energy would be required in order to maintain full stroke.

Constant Fuel Energy. A second series of analyses was performed wherein soil resistance was varied and net expended fuel energy, E_{gn} , was held constant. For this purpose the energy-input type of analysis was used (Chapter 3). Thus the ram stroke was adjusted in order to achieve the desired value of E_{gn} . The hypothetical hammer was assumed to operate on a 40 ft pile with impedance equal to 2900 lb-sec/in. This series of analyses simulates the variations in hammer performance which are encountered in driving through soft soil (easy driving) to firm bearing (hard driving) with no adjustment of the fuel control on the hammer. Results of the analyses are summarized in Figures 5.13 and 5.14.

As shown in Figure 5.13, stroke increases with an increase in R_u because less energy is expended in anvil movement and, therefore, more energy is available for lifting the ram. Maximum energy transmitted to the pile head, E_{hm} , is fairly constant with increasing R_u ; net transmitted energy, E_{hn} , decreases somewhat due to decreased penetration. Peak pile-head force, F_{hm} , increases as R_u increases as a result of the increased stroke. The pile-head force pulses corresponding to R_u values of 60, 120, and 300 tons (Figure 5.14) are indicative of the tendency of diesel hammers to adjust output automatically to meet changing soil resistance conditions; as R_u increases

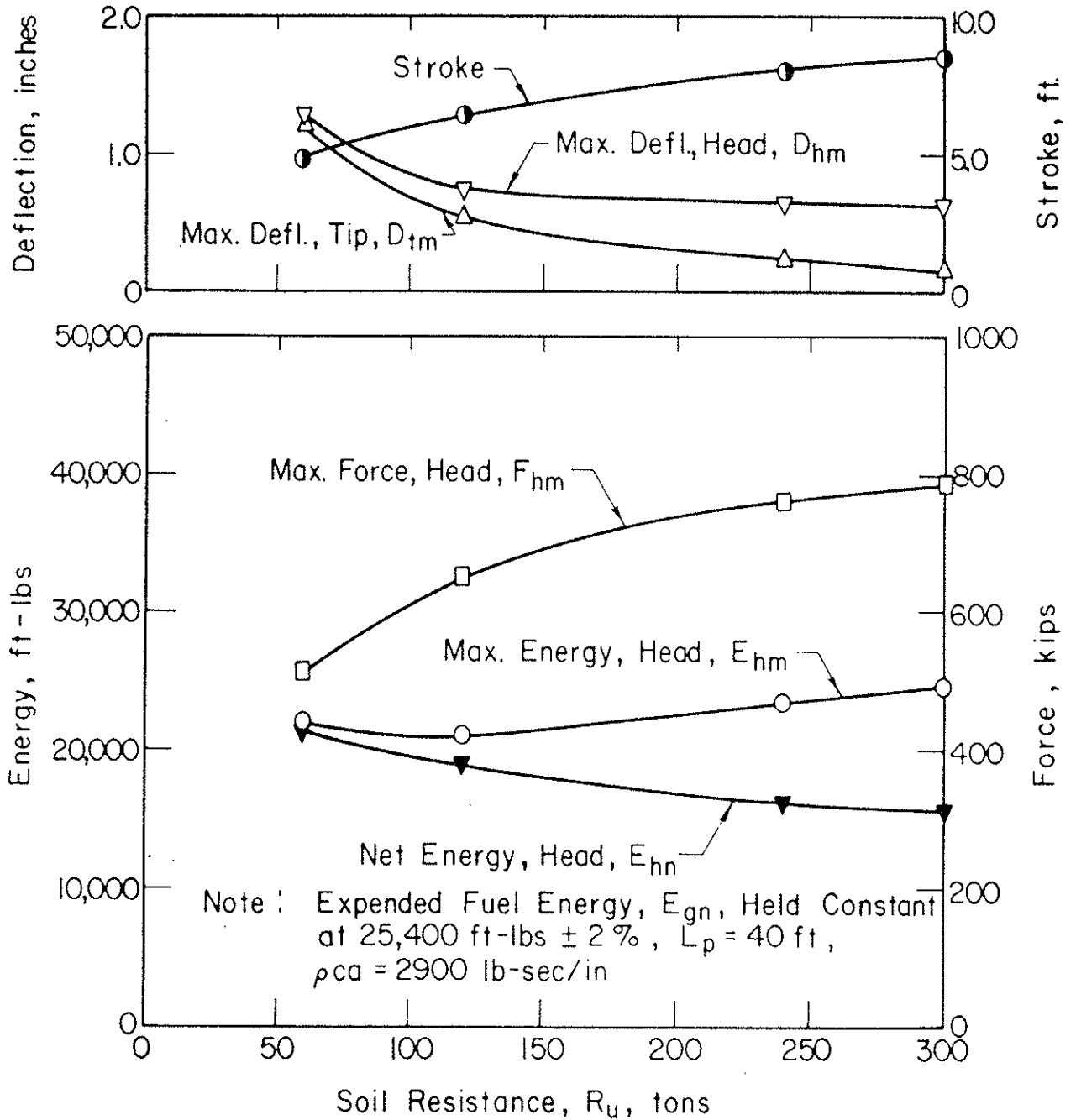


Figure 5.13 EFFECTS OF VARIATION IN SOIL RESISTANCE, CONSTANT FUEL ENERGY

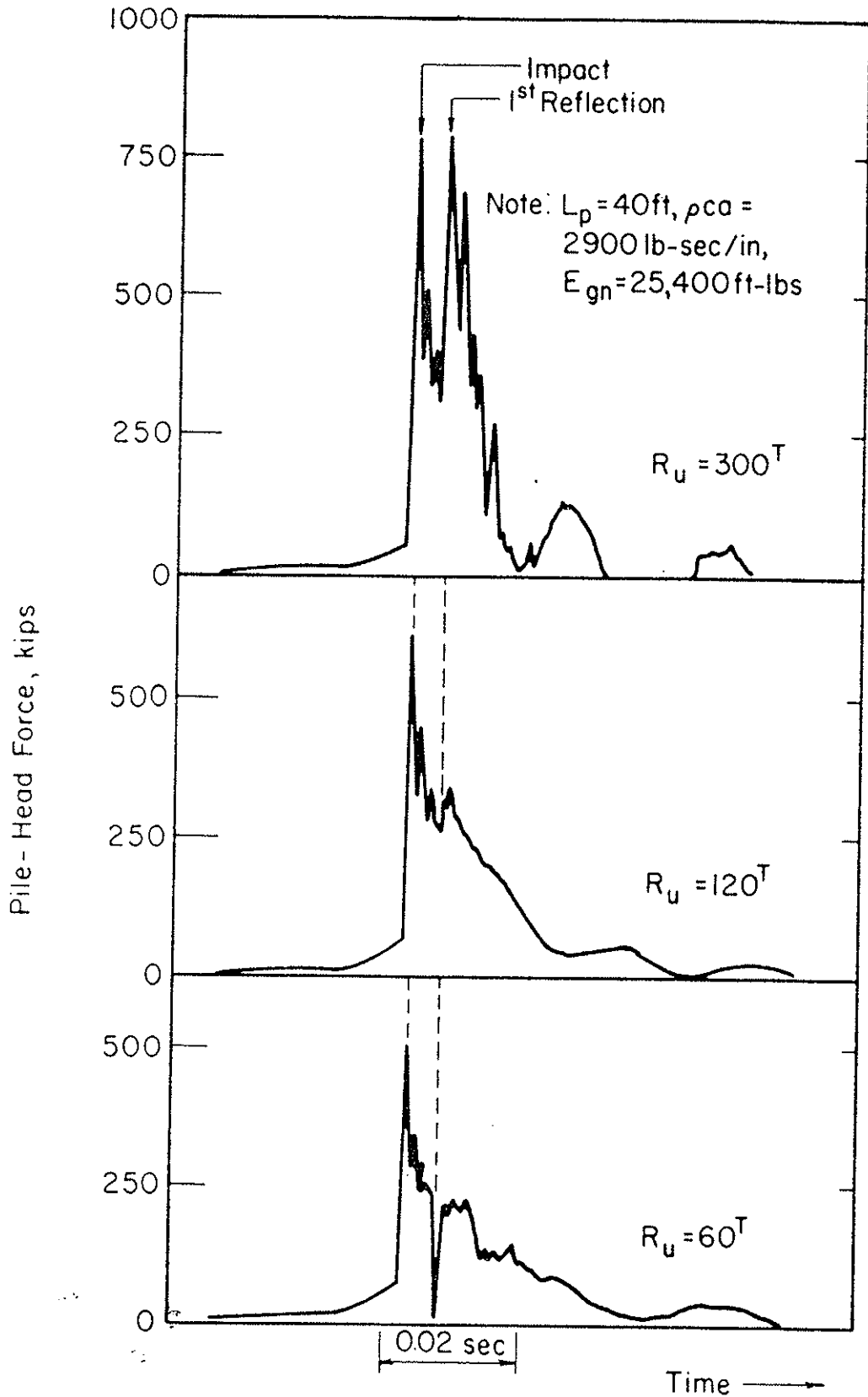


Figure 5.14 COMPARISON OF FORCE PULSES - VARYING SOIL RESISTANCE, CONSTANT FUEL ENERGY, 40 FT PILE

peak forces increase and the pulse duration decreases. This example illustrates the degree to which hammer performance can vary even though fuel volume is held constant.

Fuel Energy

In order to examine the influence of fuel energy on hammer performance, analyses were performed wherein soil resistance was held constant and fuel energy was varied (Figure 5.15). The hypothetical hammer was assumed to operate on a 40 ft long pile with impedance of 2900 lb-sec/in; ram stroke was varied in order to obtain the desired values of E_{gn} .

This series of analyses simulates the changes in hammer performance which accompany adjustment of the fuel control on the hammer. In Figure 5.15, a line has been drawn at 45° to the E_{gn} axis, representing energy equal to E_{gn} . The curves connecting the E_{hm} and E_{hn} points are below and roughly parallel to the 45° line; thus it can be concluded that energy transmitted to the pile is approximately proportional to the amount of fuel burned. This is consistent with the performance fundamentals outlined in Chapter 4.

For any given value of E_{gn} , the difference between E_{gn} and E_{hn} is indicative of the energy losses between anvil and pile head. These losses increase slightly with increasing E_{gn} mainly as a result of greater hysteresis losses in the hammer cushion. As E_{gn} increases, more energy is available for raising the ram and, therefore, stroke also increases. The result is

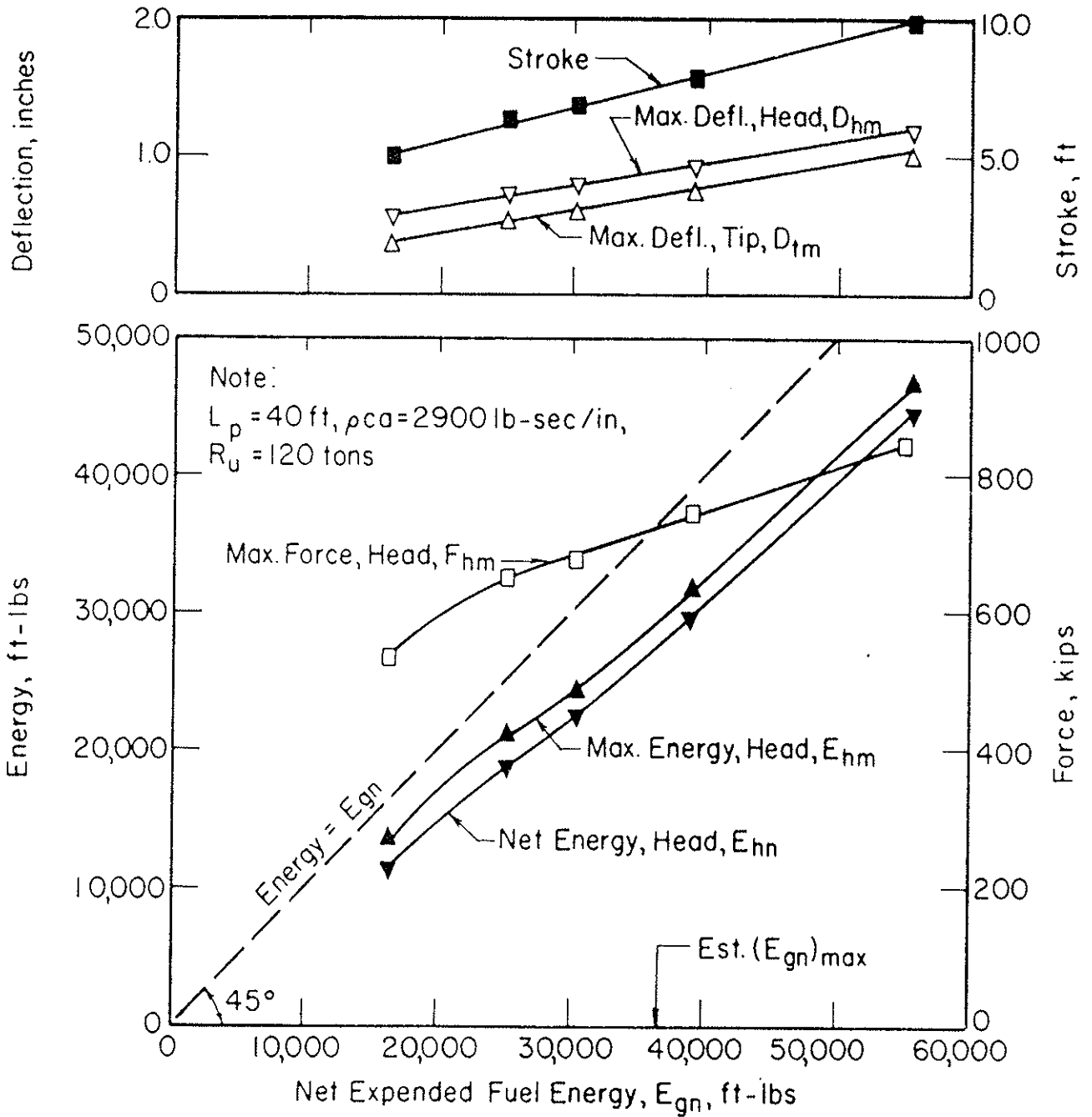


Figure 5.15 EFFECTS OF VARIATION IN FUEL ENERGY, CONSTANT SOIL RESISTANCE

higher peak force and greater deflection at the head and tip of the pile.

5.4 HAMMER-CONTROLLED FACTORS

Combustion Timing

A series of analyses were performed pertaining to the hypothetical hammer operating with various values of preignition distance, D_p . As described in Chapter 3, D_p is the gap between ram and anvil when ignition occurs. For D_p equal to zero, ignition is simultaneous with impact. Increasing D_p has the effect of advancing the timing of ignition relative to impact.

Pile lengths of 40 ft and infinity were investigated; pile impedance was taken as 2900 lb-sec/in for all cases. For the 40 ft pile, R_u was set equal to 240 tons. For the infinitely long pile, a ram stroke of 5.0 ft, in addition to the standard 8.0 ft, was investigated. In addition to the above, analyses were performed with D_p equal to zero and peak gas force maintained for 10 milliseconds, simulating the prolonged combustion which occurs in hammers employing post-impact fuel injection.

Results of the analyses are summarized in Figures 5.16 through 5.20.

Transmitted Energy vs Preignition Distance. For the infinitely long pile with standard ram stroke (Figure 5.16), E_{hm} increases slightly as D_p increases from 0.00 in to 0.24 in,

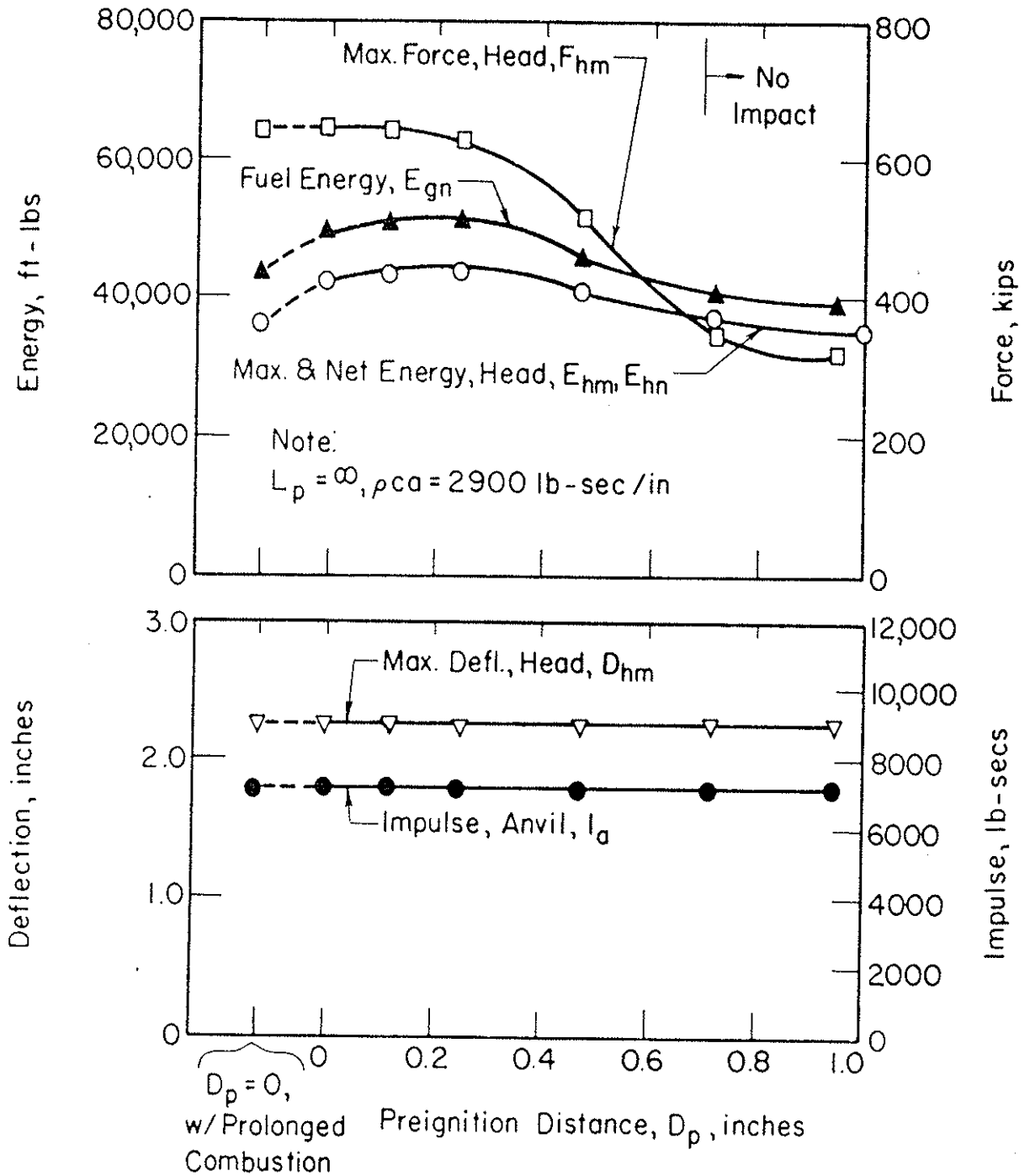


Figure 5.16 PREIGNITION EFFECTS, INFINITELY LONG PILE, 8 FT STROKE

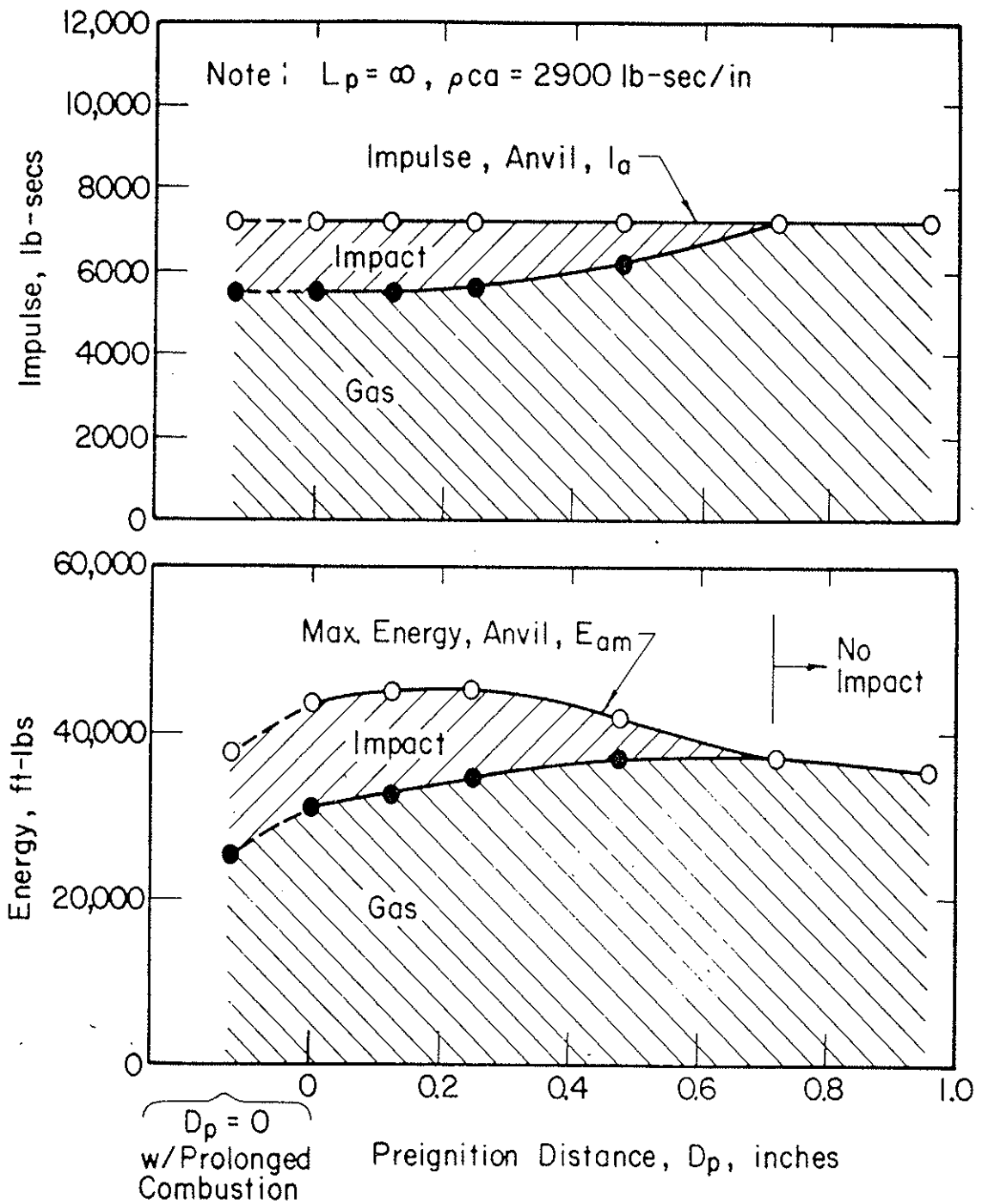


Figure 5.17 EFFECTS OF PREIGNITION DISTANCE ON CONTRIBUTION OF GAS AND IMPACT TO HAMMER OUTPUT, INFINITELY LONG PILE, 8 FT STROKE

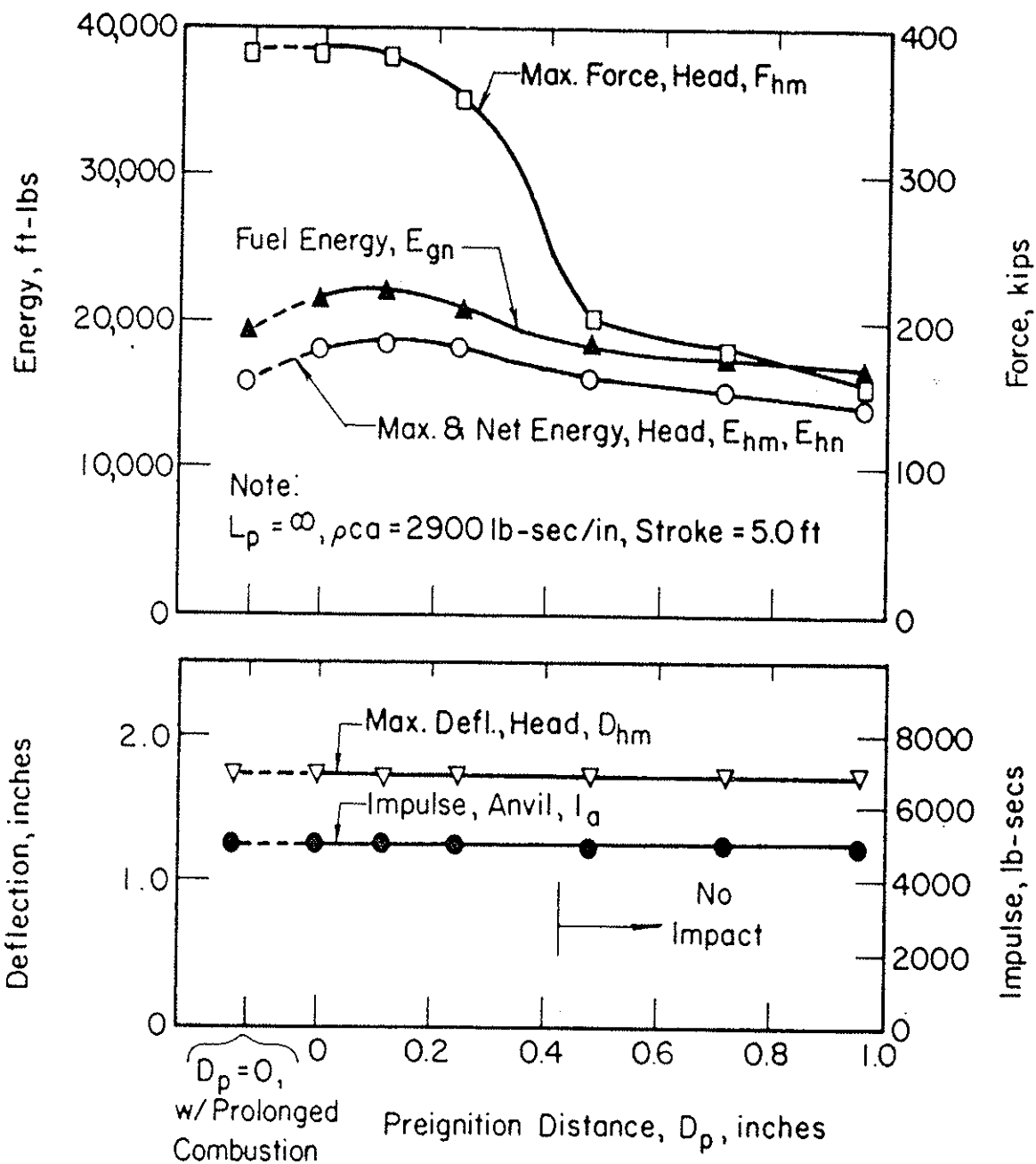


Figure 5.18 PREIGNITION EFFECTS, INFINITELY LONG PILE, 5 FT STROKE

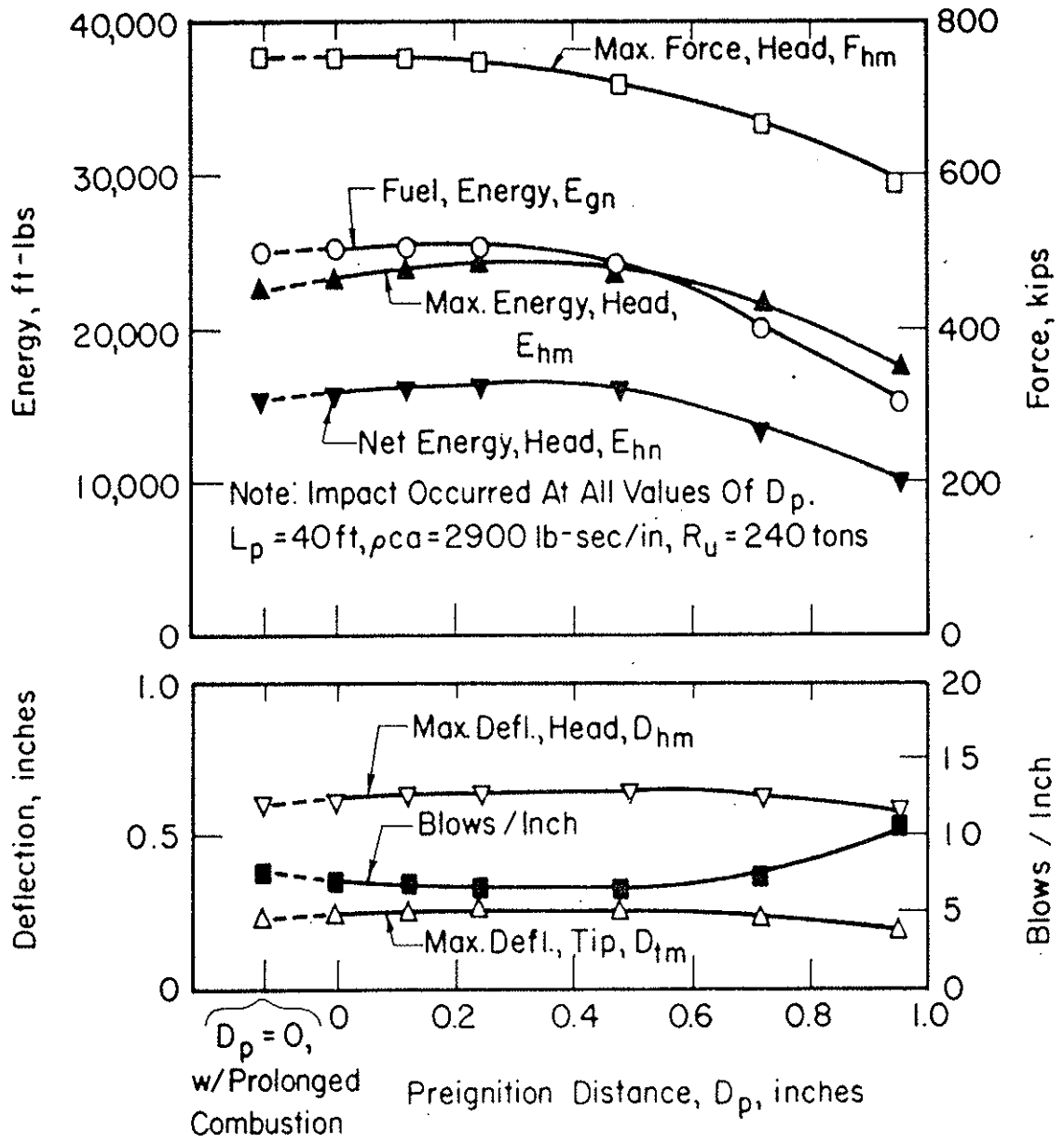


Figure 5.19 PREIGNITION EFFECTS, 40 FT PILE, 8 FT STROKE, 240 TONS SOIL RESISTANCE

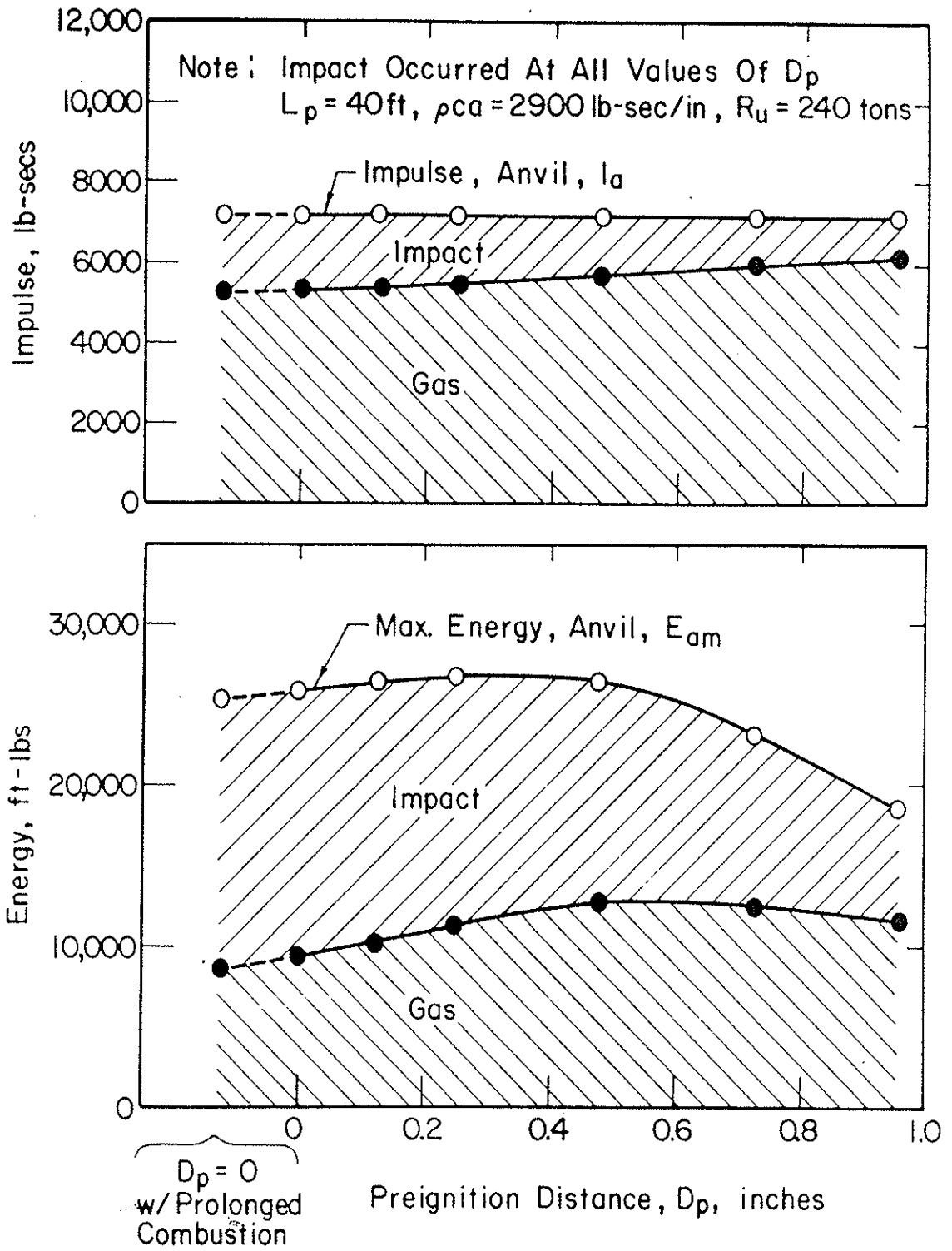


Figure 5.20 EFFECTS OF PREIGNITION DISTANCE ON RELATIVE CONTRIBUTION OF GAS AND IMPACT TO HAMMER OUTPUT, 40 FT PILE, 8 FT STROKE, 240 TONS SOIL RESISTANCE

then decreases with additional increase in D_p . A small amount of preignition is necessary in order to obtain simultaneous peaking of the impact and gas forces, which results in maximum energy transmission. Because the gas force has a longer rise time than the impact force, ignition must occur before impact in order for the gas and impact force-peaks to occur simultaneously.

The relative contributions of gas and impact forces to the transmitted energy are illustrated in Figure 5.17, in which maximum energy at the anvil, E_{am} , and its impact and gas components are plotted versus D_p . In the same figure, total anvil impulse and its gas and impact components are also plotted versus D_p . For the example shown, the impact contribution to energy and impulse decreases with increasing D_p , becoming zero at D_p equal to 0.72 in, at which point impact does not occur.

In the case of the infinitely long pile with 5.0 ft ram stroke (Figure 5.18), the value of D_p corresponding to maximum transmitted energy is approximately half of that corresponding to the 8.0 ft stroke. With the reduced ram-impact velocity that accompanies low stroke, a given value of D_p corresponds to a larger time lag between ignition and impact than would occur at high stroke. The result is that the hammer is more sensitive to preignition effects at low stroke.

For the 40 ft pile with standard stroke (Figure 5.19) the effect of preignition on transmitted energy was similar to the case of the infinitely long pile, except that E_{hm} maximized

at a greater value of D_p . The relative contributions of gas and impact forces to total energy and impulse (Figure 5.20) are somewhat less sensitive to D_p , as compared to the infinitely long pile.

Peak Force vs Preignition Distance. For the infinitely long pile, F_{hm} was strongly affected by D_p , decreasing sharply at values of D_p greater than 0.24 in for the 8.0 ft stroke and 0.12 in for the 5.0 ft stroke. At large values of D_p , the pre-ignition force was sufficient to prevent impact. For the 40 ft pile length, the effect of D_p on F_{hm} was qualitatively the same as for the infinitely long pile, however the variation of F_{hm} was not as great. Impact occurred at all values of D_p .

Pile Deflection vs Preignition Distance. For the 40 ft pile, pile-head and pile-tip deflections, D_{hm} and D_{tm} were slightly affected by D_p . Both maximized at the value of D_p corresponding to maximum E_{hm} . This example may not be representative of hard-driving conditions wherein penetration is largely controlled by peak force. In such cases, increases in D_p can be expected to result in sharply reduced penetration.

The infinitely long pile cases are not relevant to pile deflection, because deflection is strictly a function of impulse, and total impulse is unaffected by preignition distance.

Fuel Energy vs Preignition Distance. The variation of E_{gn} with D_p is similar to the variation of E_{hn} with D_p , for both the 40 ft and infinitely long piles. E_{gn} increases

slightly with increasing D_p up to a point corresponding to maximum E_{hn} , then decreases with further increases in D_p .

Prolonged Combustion. The effect of prolonged combustion, as compared to zero D_p and normal combustion, is to delay the application of the gas-force pulse to the anvil and thus to reduce slightly the maximum transmitted energy. Peak force at the pile head is unaffected and pile deflections are reduced somewhat. Fuel energy requirements are decreased because transmitted energy is diminished. Quantitative evaluation of prolonged combustion for a given hammer should be based on specific details of combustion timing.

Power-Cylinder Area and Power Stroke

The volume swept by the ram between port closure and impact is equal to the product of power-cylinder area, A_{pc} , and power stroke, S_p . Thus, for a given swept volume, A_{pc} is inversely proportional to S_p . In order to study the influence of the relative values of A_{pc} and S_p on hammer performance, analyses were performed wherein A_{pc} and S_p were varied such that the product of the two remained constant. A typical value of A_{pc} for hammers approximately equivalent to the hypothetical hammer is 190 in^2 ; for this study values of A_{pc} equal to 50, 100 and 150 percent of the typical value were used. Pile impedance was held constant at 2900 lb-sec/in. Pile lengths of 40 ft, 160 ft and infinity were investigated. Results of these analyses are summarized in Figures 5.21 through 5.25.

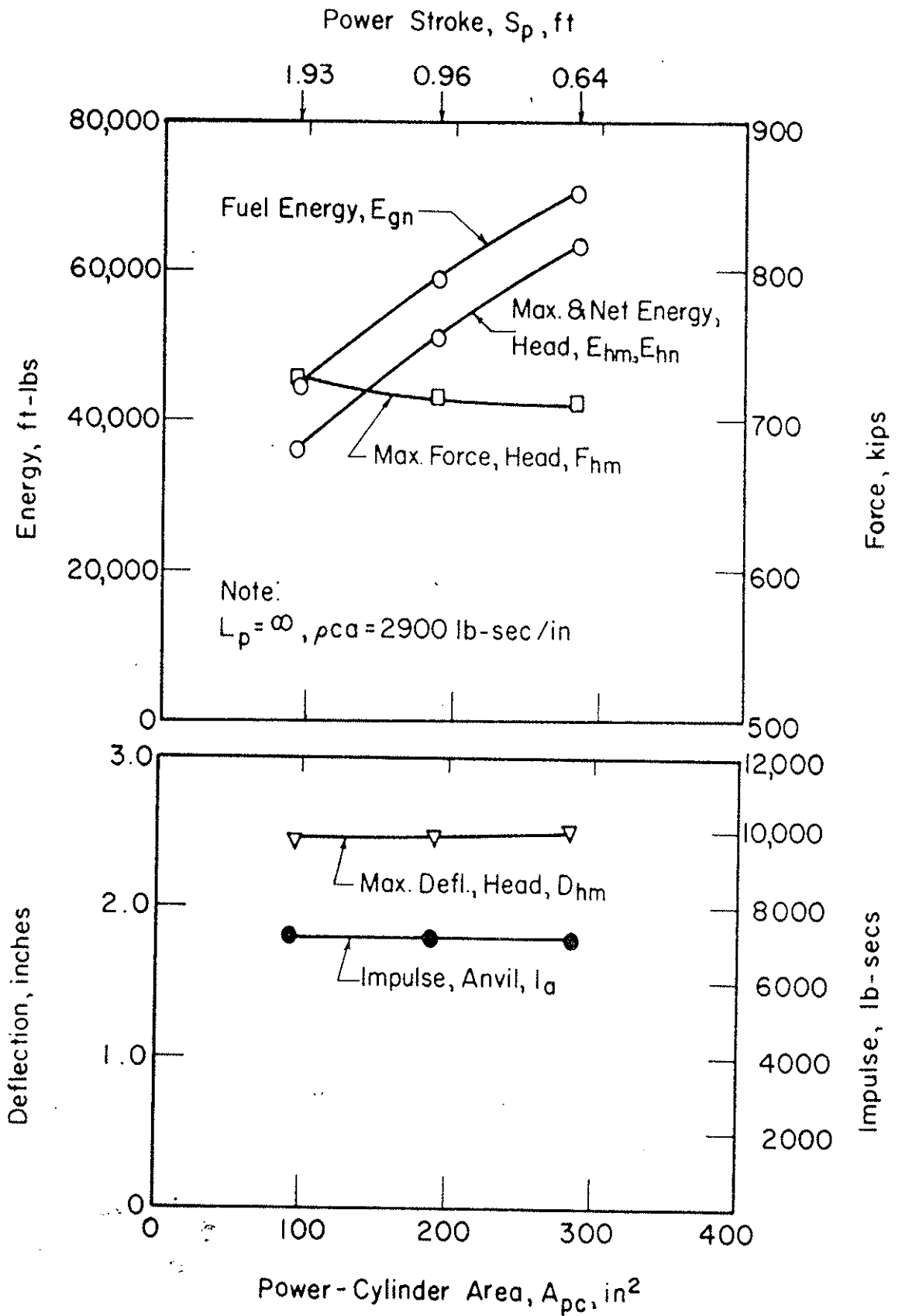


Figure 5.21 EFFECTS OF POWER-CYLINDER AREA, INFINITELY LONG PILE

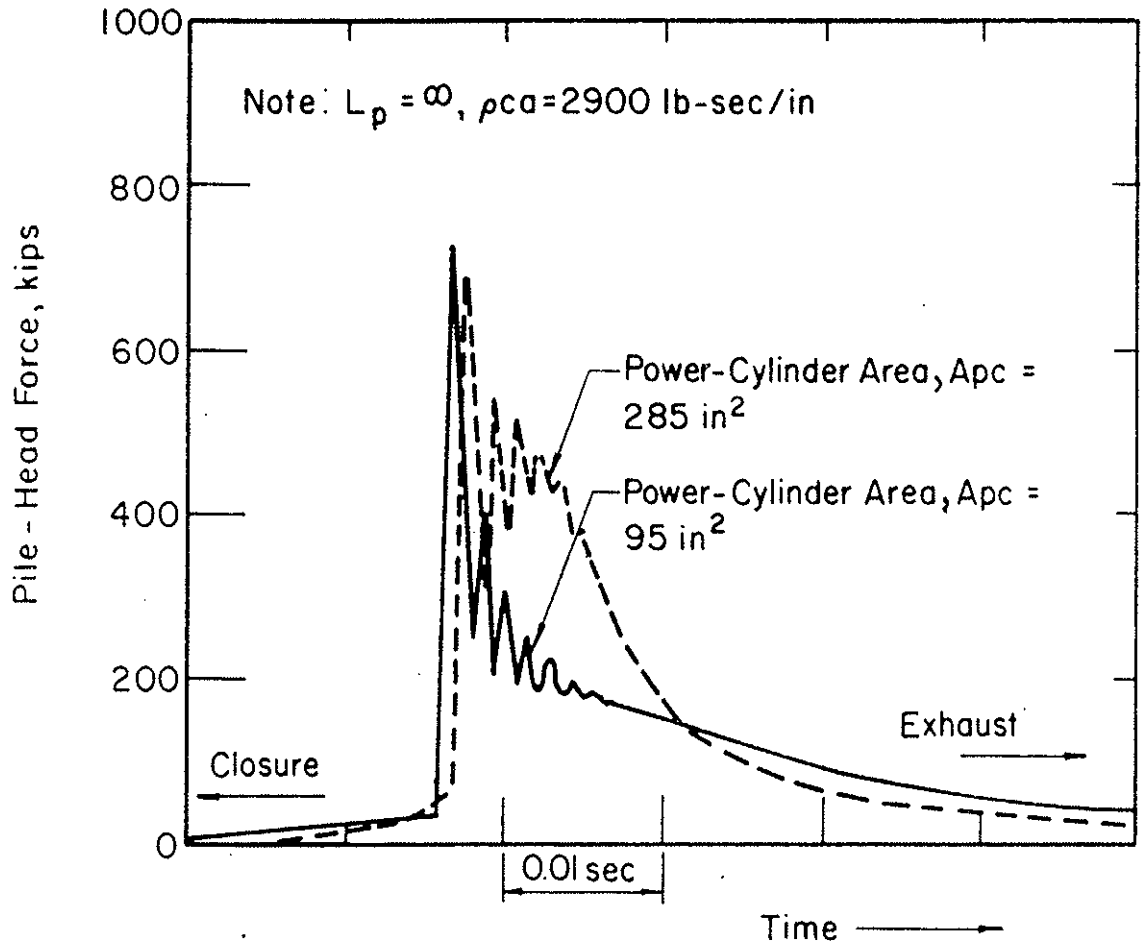


Figure 5.22 COMPARISON OF FORCE PULSES - VARYING POWER-CYLINDER AREA, INFINITELY LONG PILE

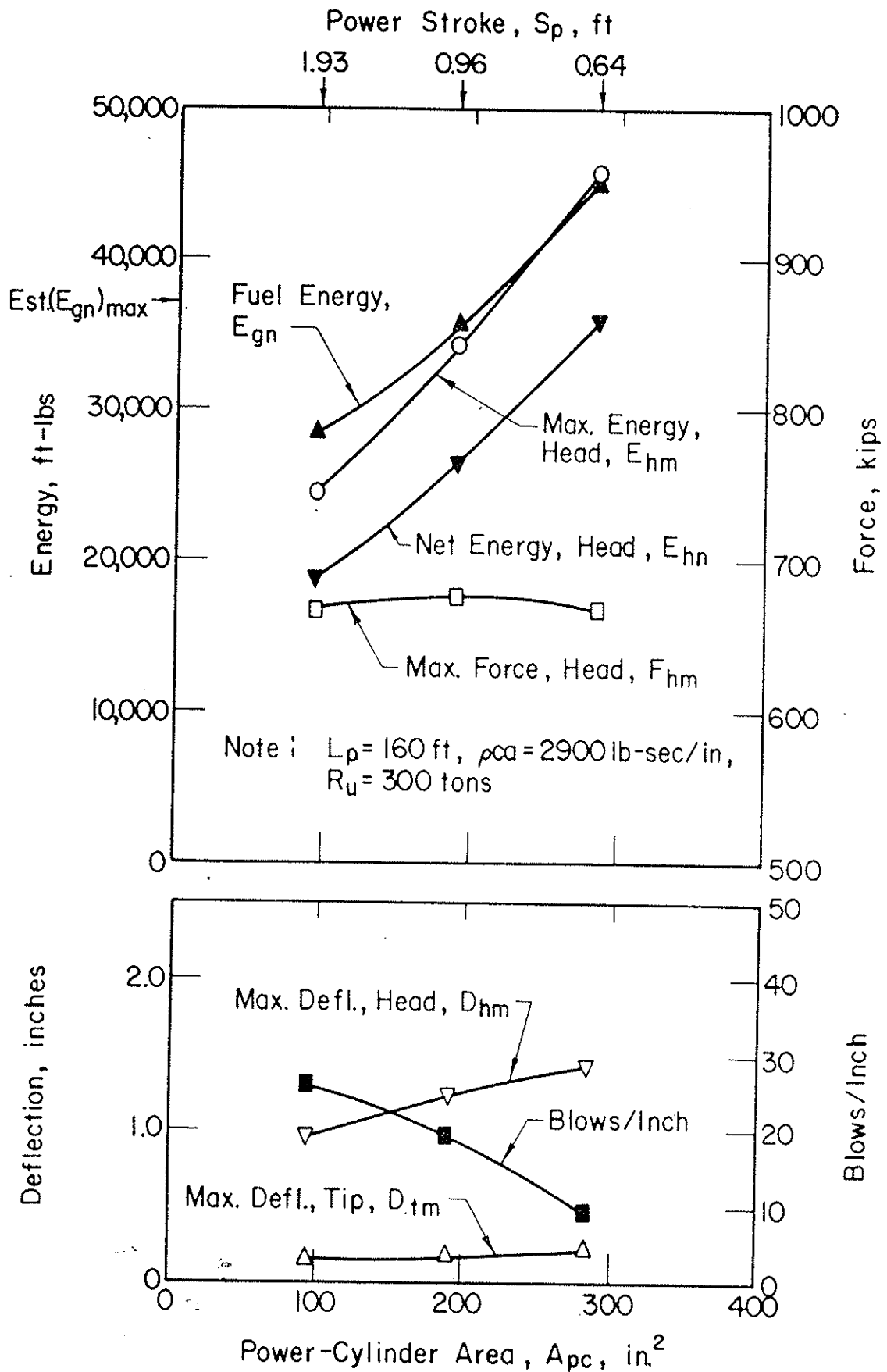


Figure 5.23 EFFECTS OF POWER-CYLINDER AREA, 160 FT PILE, 300 TONS SOIL RESISTANCE

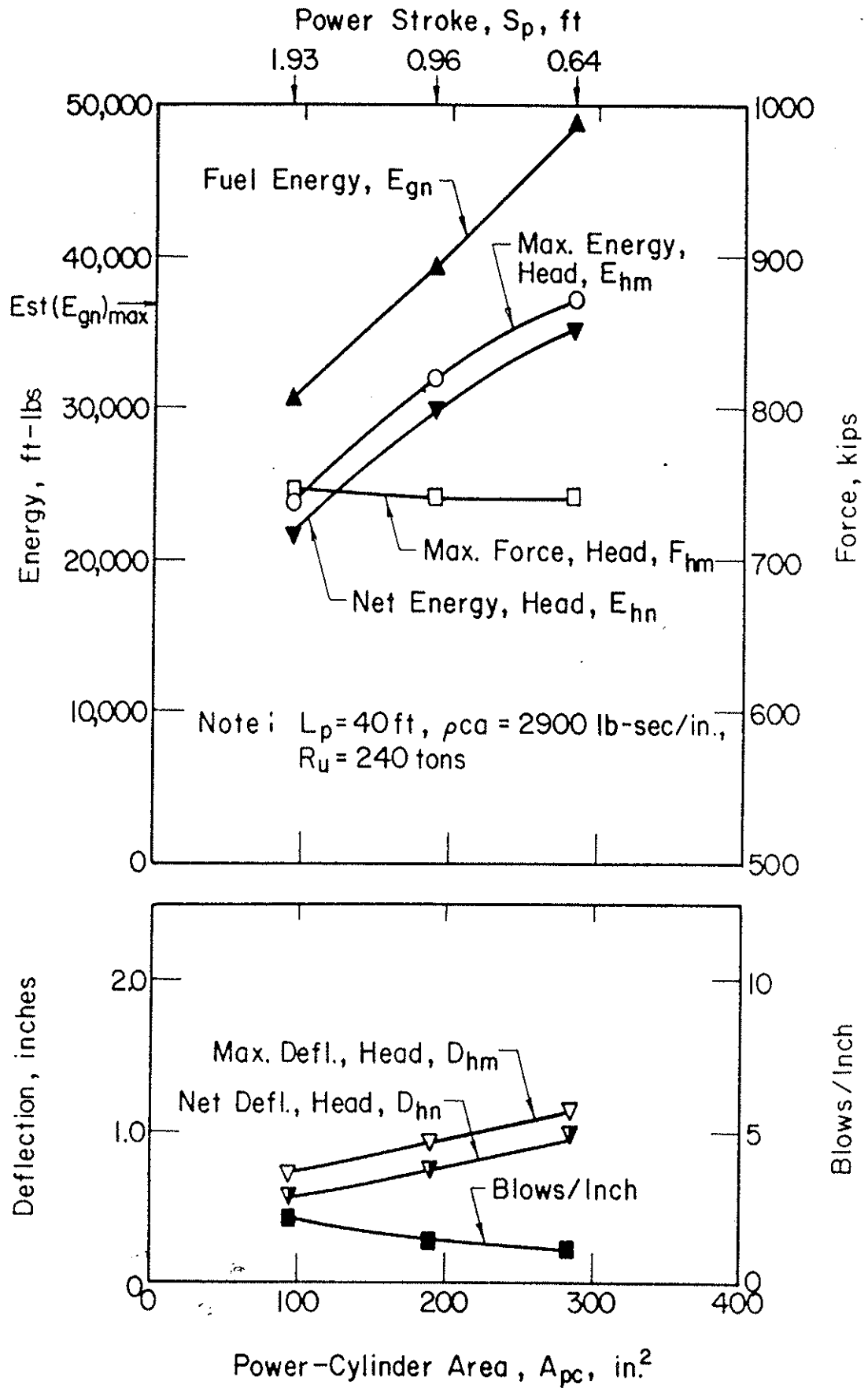


Figure 5.24 EFFECTS OF POWER-CYLINDER AREA, 40 FT PILE, 120 TONS SOIL RESISTANCE

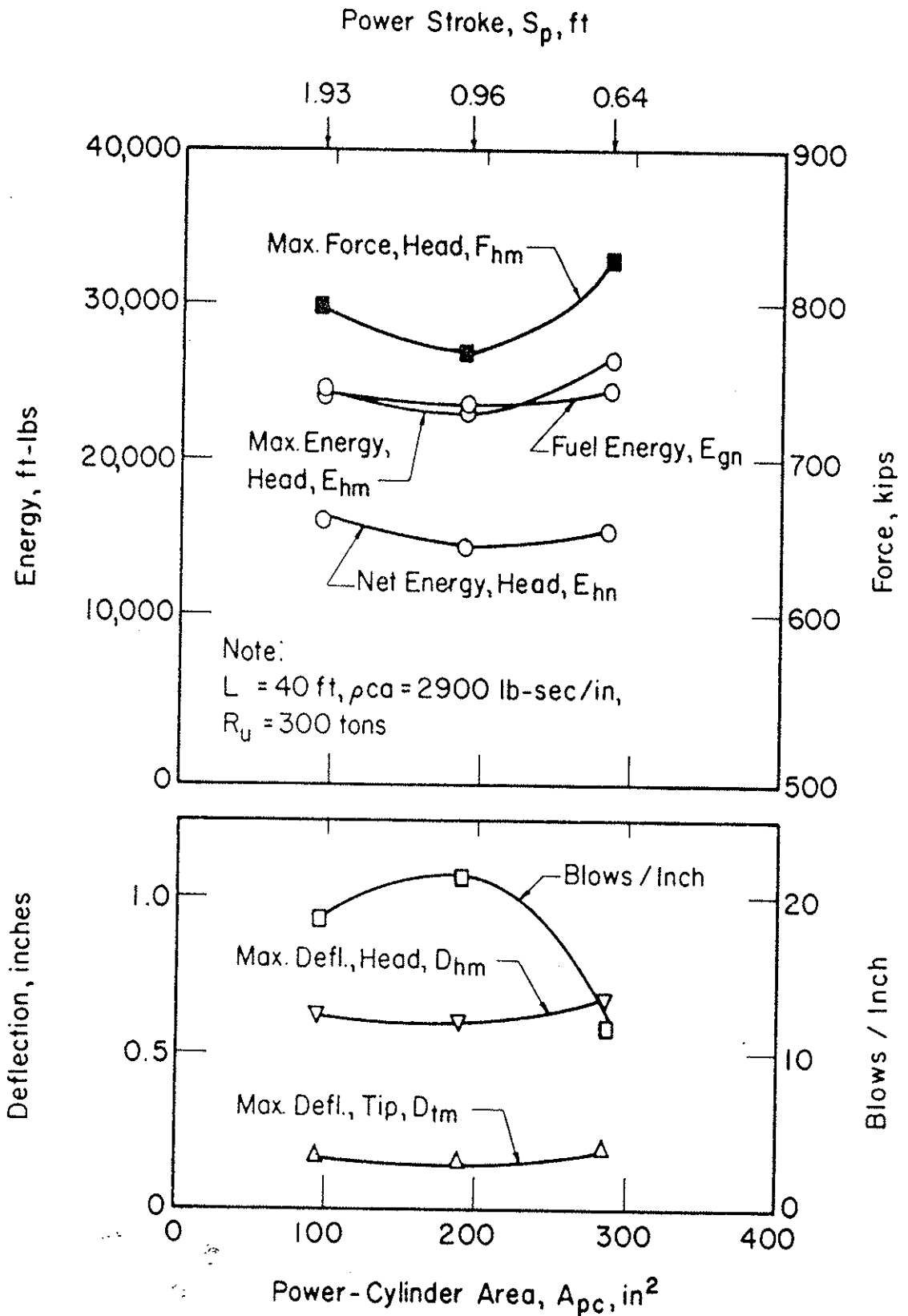


Figure 5.25 EFFECTS OF POWER-CYLINDER AREA, 40 FT PILE, 300 TONS SOIL RESISTANCE

Transmitted Energy vs Power-Cylinder Area. For the infinitely long pile (Figure 5.21), maximum and net energy at the pile head increase with increasing A_{pc} . The reason can be found in a plot of the force-time relationship at the pile head for the cases of A_{pc} equal to 95 and 285 in² (Figure 5.22). The increase in A_{pc} results in a change in the shape of the force pulse. Although peak force is approximately equal for both cases, the average force for .015 seconds following the peak is much higher for the higher value of A_{pc} , indicating a longer effective pulse duration (Chapter 4). The result is a more efficient force pulse and higher transmitted energy.

For the 160 ft pile (Figure 5.23), transmitted energy increases with increasing A_{pc} , as in the case of the infinitely long pile. The same is true for the 40 ft pile with R_u equal to 120 tons (Figure 5.24). However, at R_u equal to 300 tons (Figure 5.25) different results are obtained; transmitted energy is only slightly affected by A_{pc} . Best performance occurred at the highest and lowest values of A_{pc} due to higher pile deflections in these cases.

Peak Force vs Power-Cylinder Area. In general, peak force at the pile head, F_{hm} , is only slightly affected by A_{pc} . An exception is the case of the 40 ft pile with high soil resistance (Figure 5.25), wherein F_{hm} is somewhat higher at the highest and lowest values of A_{pc} as compared to the intermediate value. This exemplifies the importance of reflections

relative to the peak force generated in short piles with high soil resistance, and underscores the necessity for detailed examination of such cases.

File Deflections vs Power-Cylinder Area. Maximum pile deflections increased with increasing A_{pc} , except in the case of the 40 ft pile with high soil resistance (Figure 5.25). As a result of the higher peak forces corresponding to the highest and lowest values of A_{pc} , deflections in these cases were greater than at the intermediate value of A_{pc} .

The results are an indication that, in easy-to-moderate driving with long piles, pile deflection is increased by increasing A_{pc} . As driving gets harder or pile length decreases, the advantage of high A_{pc} diminishes.

Fuel Energy vs Power-Cylinder Area. In general the net expended fuel energy, E_{gn} , increases with increasing A_{pc} , reflecting the increase in transmitted energy. Again the exception is the case of the 40 ft pile with R_u equal to 300 tons, wherein E_{gn} minimizes at the intermediate value of A_{pc} .

Soft-Ground Operation vs Power-Cylinder Area. For soft-ground operation, the increased fuel requirements corresponding to large values of A_{pc} may exceed the fuel-burning capacity of the hammer, $(E_{gn})_{max}$, and the hammer will fail to operate. Thus it may be advantageous to decrease A_{pc} in order to improve soft-ground operation, even though this may decrease pile penetration-per-blow in some driving conditions.

Compression Ratio

Analyses were performed with compression ratio, C_r , varying from 11.0 to 17.0, encompassing the range of compression ratios encountered in currently available diesel hammers. Power-cylinder area and power stroke were held constant and pile impedance was set equal to 2900 lb-sec/in. Pile lengths of 40 ft and infinity were investigated. For the 40 ft pile, R_u values of 120 tons and 300 tons were studied, corresponding to moderate and hard driving conditions.

Results of the analyses are summarized in Figures 5.26 through 5.29.

Transmitted Energy vs Compression Ratio. For the infinitely long pile (Figure 5.26), maximum energy at the pile head, E_{hm} , increases with increasing C_r because the shape of the force pulse becomes more favorable. As shown in Figure 5.27, the higher C_r results in a higher average force for approximately .015 sec after the peak force occurs, indicating a longer effective pulse duration (Chapter 4). The result is a pulse which, on the infinitely long pile, is more efficient in transmitting energy.

In the case of the 40 ft pile with R_u equal to 120 tons (Figure 5.28), the effect of C_r on E_{hm} and E_{hn} is similar to the case of the infinitely long pile. For R_u equal to 300 tons (Figure 5.29), however, transmitted energy is relatively insensitive to C_r , as a result of peak force effects as will be discussed below.

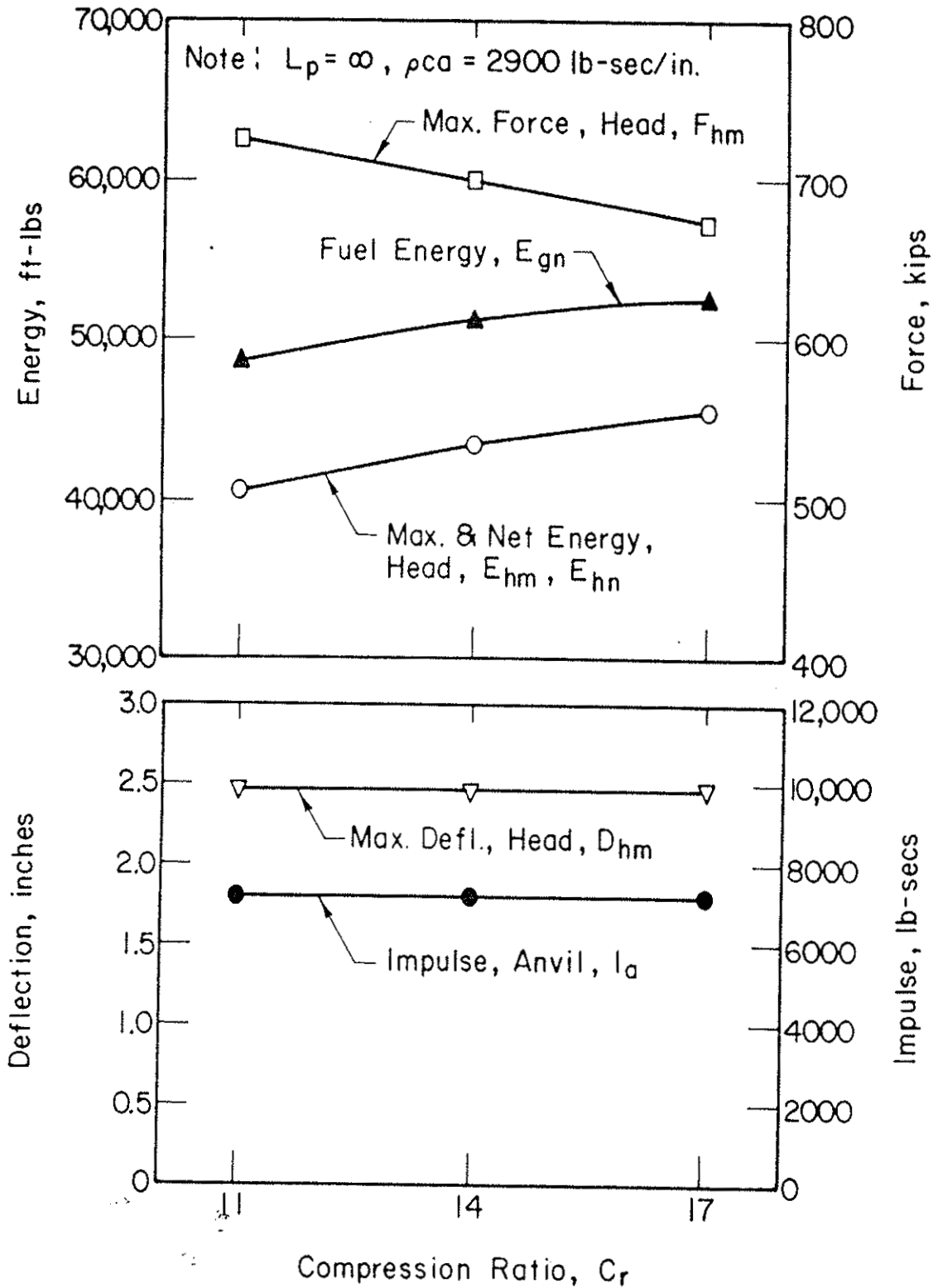


Figure 5.26 EFFECTS OF COMPRESSION RATIO, INFINITELY LONG PILE

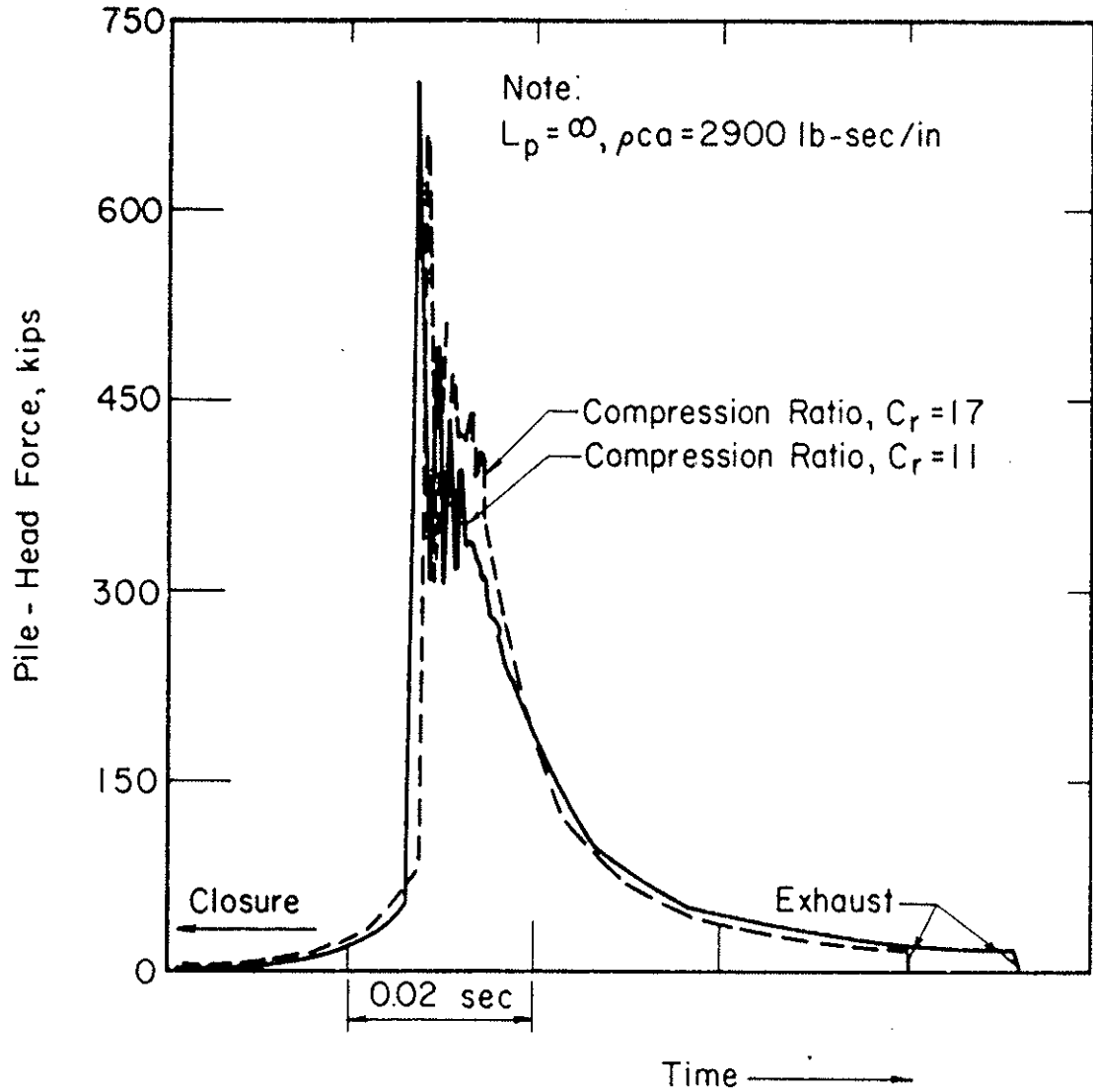


Figure 5.27 COMPARISON OF FORCE PULSES - VARYING COMPRESSION RATIO, INFINITELY LONG PILE

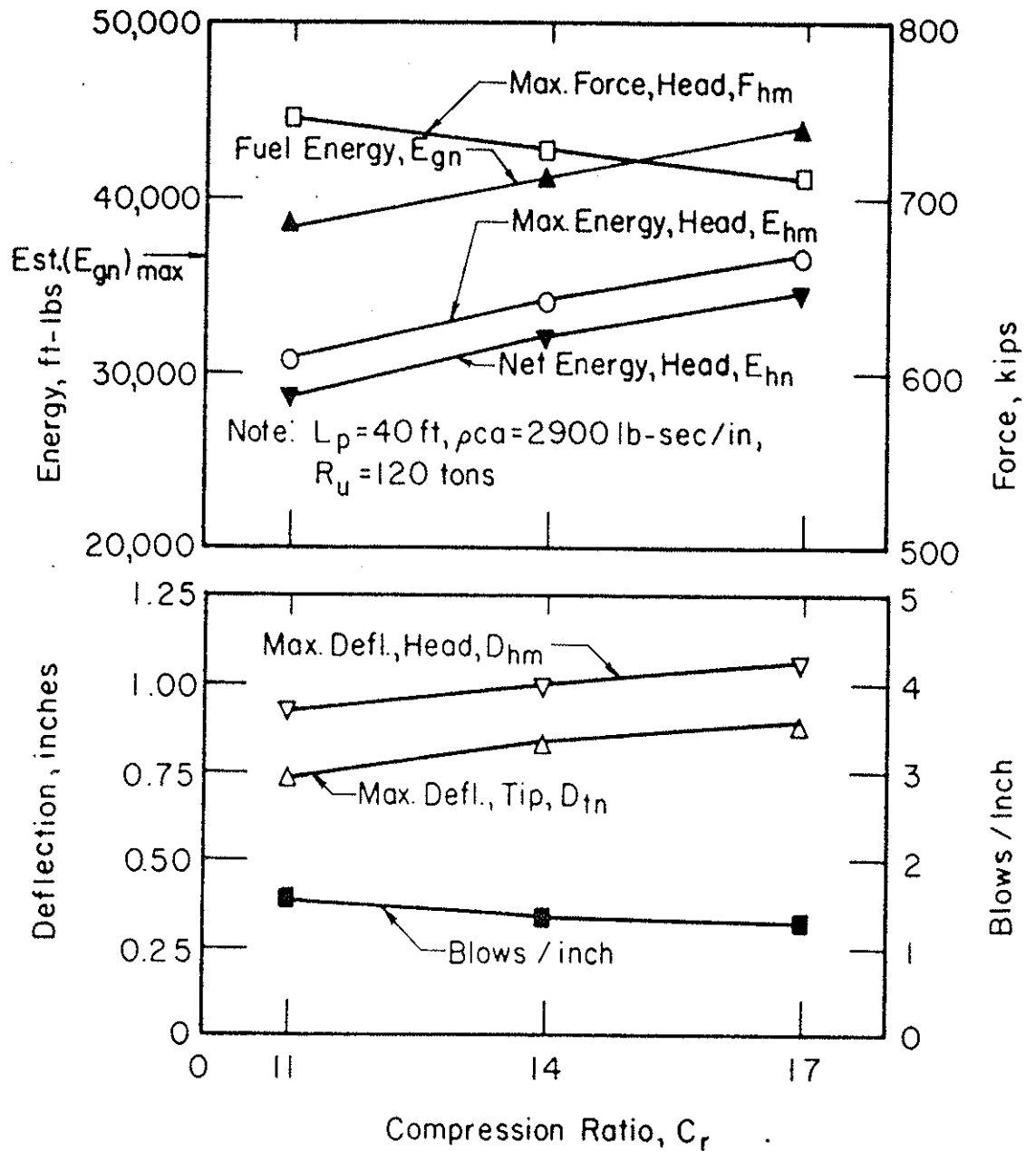


Figure 5.28. EFFECTS OF COMPRESSION RATIO, 40 FT PILE, 120 TONS SOIL RESISTANCE

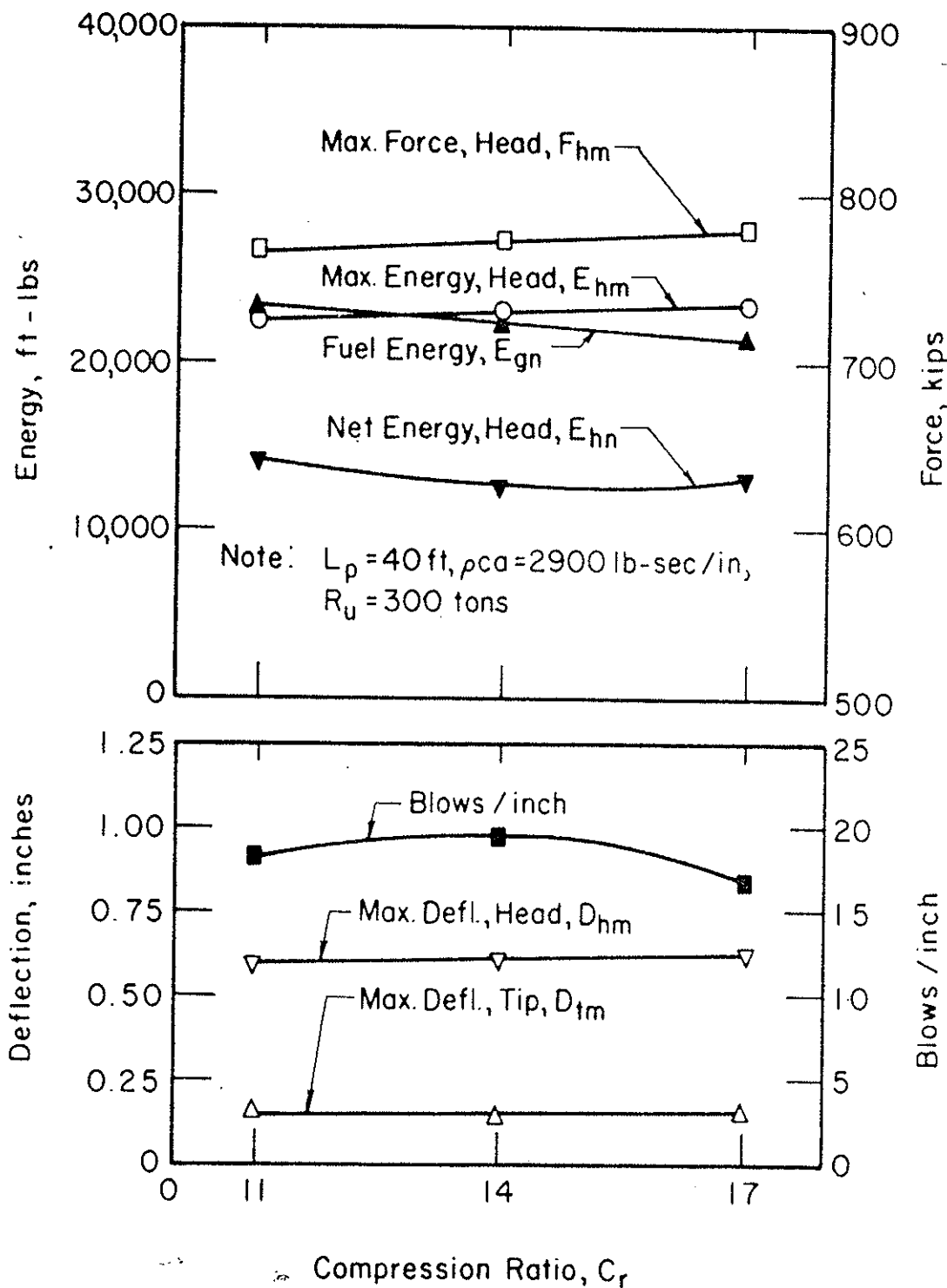


Figure 5.29 EFFECTS OF COMPRESSION RATIO, 40 FT PILE, 300 TONS SOIL RESISTANCE

Peak Force vs Compression Ratio. Increasing C_r has the effect of increasing pre-impact gas force and thereby reducing the relative velocity of ram and anvil at impact. Therefore, in the case of the infinitely-long and 40 ft pile at low R_u , peak force diminishes as C_r increases. In the case of the 40 ft pile at high R_u , impact velocity diminishes with increasing C_r as in the case of low R_u , but peak force increases due to reflection effects. Reflections are a function of pile length, soil resistance distribution and other factors; thus no general conclusions should be drawn relative to the influence of C_r on peak force for short piles.

Pile Deflections vs Compression Ratio. For the 40 ft pile at low R_u , deflections increase with increasing C_r , reflecting the increasing efficiency of energy transmission. At high R_u , however, peak force becomes more important and, because the increase in transmitted energy is offset by decreasing peak force, performance is less sensitive to C_r . For the case analyzed, best performance occurred at the intermediate value of C_r .

Fuel Energy vs Compression Ratio. Net expended fuel energy, E_{gn} , increases slightly with increasing C_r except in the case of high soil resistance (Figure 5.29), wherein E_{gn} is essentially unaffected by C_r . In general, the increase of E_{gn} with increasing C_r is a result of corresponding increases in pile deflection.

Soft-Ground Operation vs Compression Ratio. In soft-ground driving the small increase in E_{gn} which accompanies an increase in C_r can become significant, causing E_{gn} to exceed $(E_{gn})_{max}$. Further, the high pre-impact forces resulting from a high C_r will reduce ram-impact velocity, possibly causing a failure to ignite. In either case, the hammer will fail to operate. Thus, for soft-ground driving, a low value of C_r is advantageous.

Weight of Ram, Anvil and Drivehead

Ram weight is most important of the component masses because the ram is the striking mass. Anvil and drivehead weights are of secondary importance because, in combination with ram weight, cushioning characteristics, and the gas-force pulse, they determine the effective impedance of the hammer. As discussed previously, determination of effective impedance is much more complex in the case of diesel hammers than for impact hammers, due to the additional mass (anvil) and the presence of the gas force. No attempt was made in this study to evaluate effective hammer impedance because of the large number of variables involved. Example analyses illustrating the effect of variations in ram, anvil and drivehead weights are presented in order to demonstrate the potential effect on performance.

Weight of Ram. The influence of ram weight on hammer performance can be predicted on the basis of fundamental

considerations. For a given rated energy, a heavy ram can be expected to generate lower peak force and greater total impulse in the pile head. The reduction in peak force is due to decreased stroke and, therefore, lower impact velocity. The increase in total impulse can be predicted on the premise that, for a diesel hammer, total impulse on the anvil, I_a , is related to ram momentum as follows:

$$I_a = \frac{2 W_1}{g} \sqrt{2 g S_t}$$

where W_1 = ram weight.
 g = acceleration due to gravity
 S_t = total stroke.

Because rated energy, E_{wh} , equals the product of ram weight and total stroke, it follows that:

$$I_a = \frac{2 W_1}{g} \sqrt{2 g \frac{E_{wh}}{W_1}} = 2 \sqrt{\frac{2 E_{wh} W_1}{g}}$$

Thus if E_{wh} is held constant, I_a is proportional to $\sqrt{W_1}$.

Analyses were performed with ram weights varying from 3000 to 10,000 lbs; this exceeds the range of ram weights in existing diesel hammers with rated energies varying from 35,000 to 45,000 ft-lbs. Stroke was varied such that rated energy was equal to 40,000 ft-lbs. Piles 40 ft long and infinitely long were studied. Results of the analyses are summarized in Figures 5.30 through 5.33.

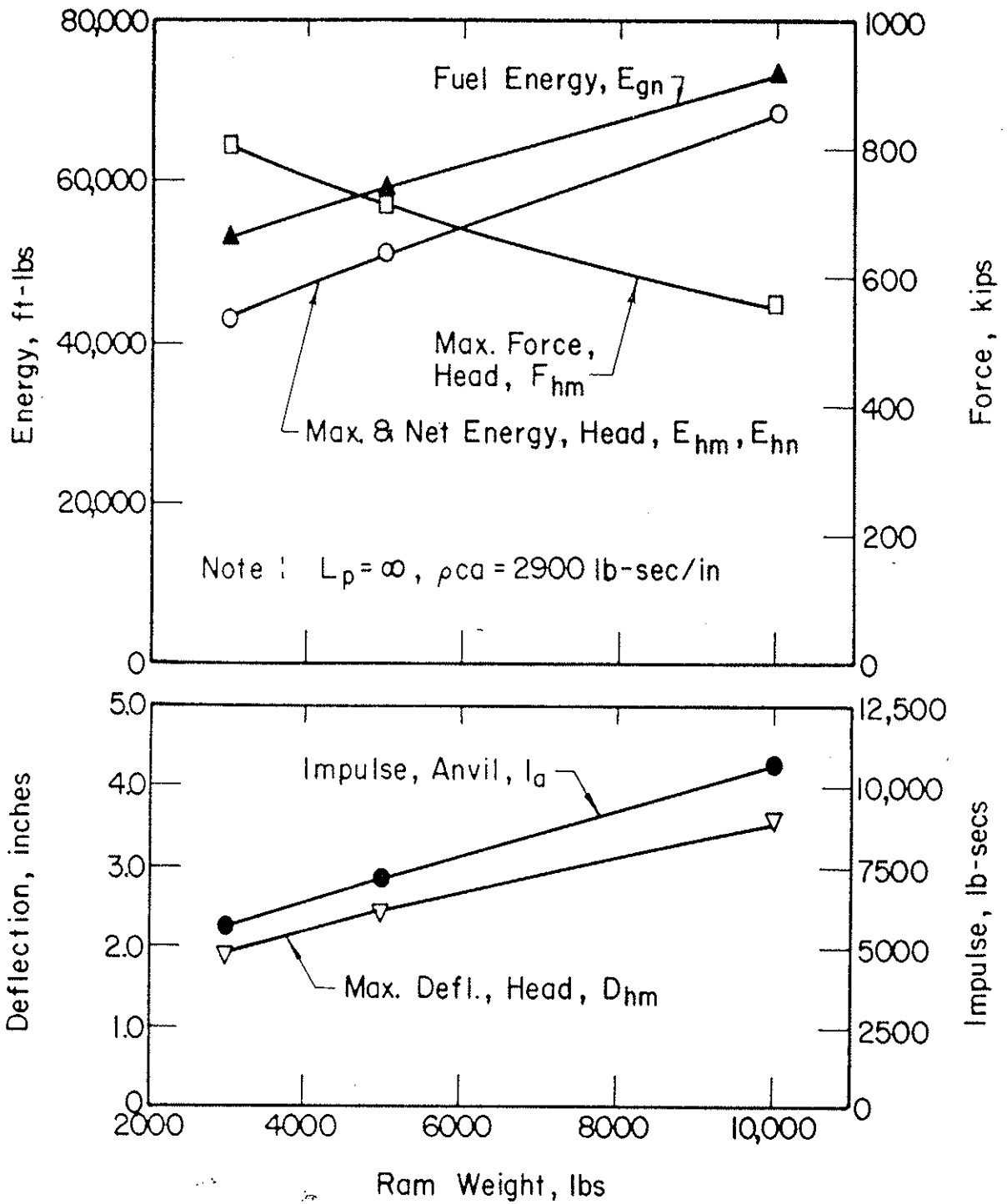


Figure 5.30 EFFECTS OF RAM WEIGHT, INFINITELY LONG PILE, CONSTANT RATED ENERGY

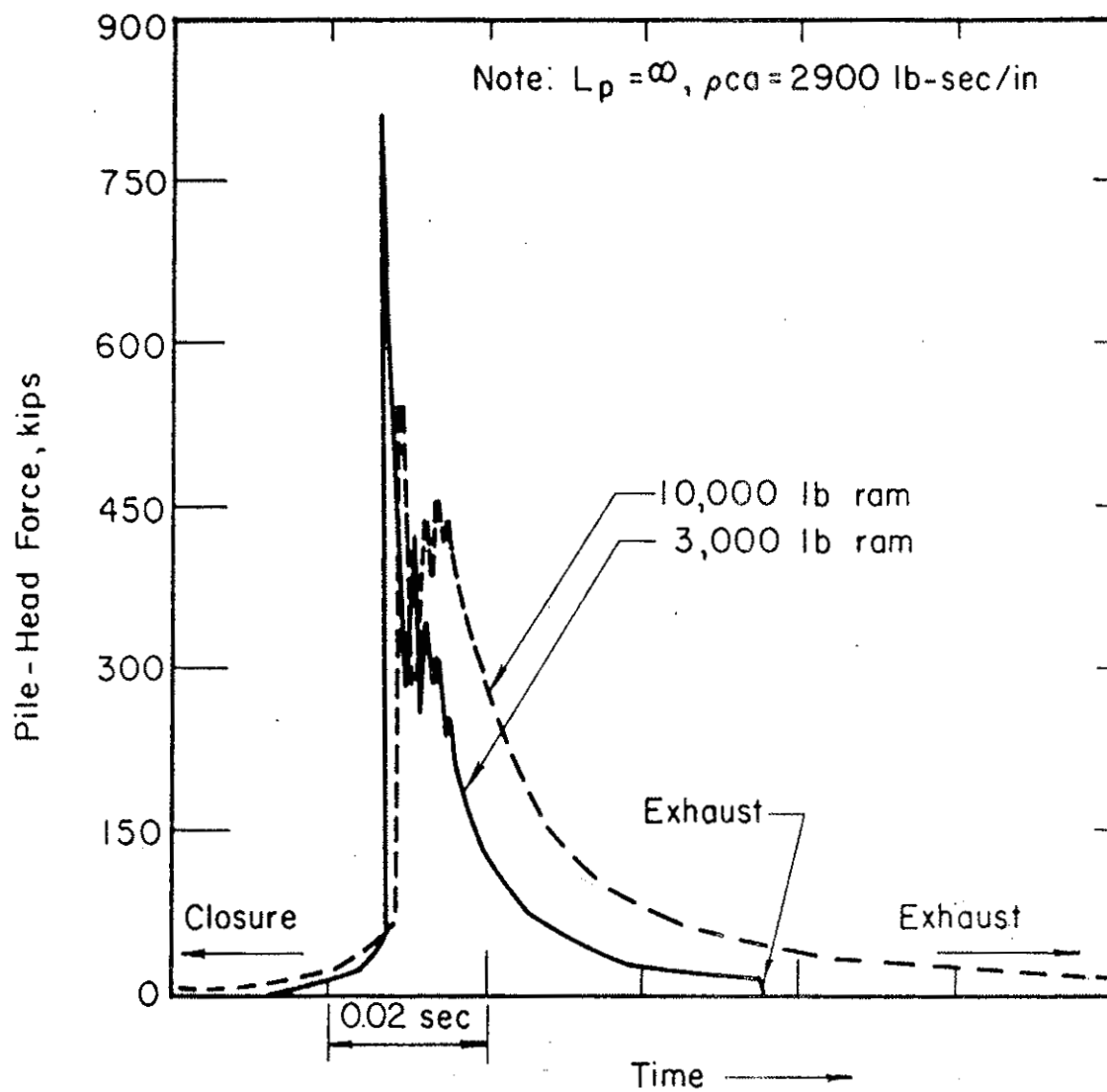


Figure 5.31 COMPARISON OF FORCE PULSES - VARYING RAM WEIGHT, INFINITELY LONG PILE

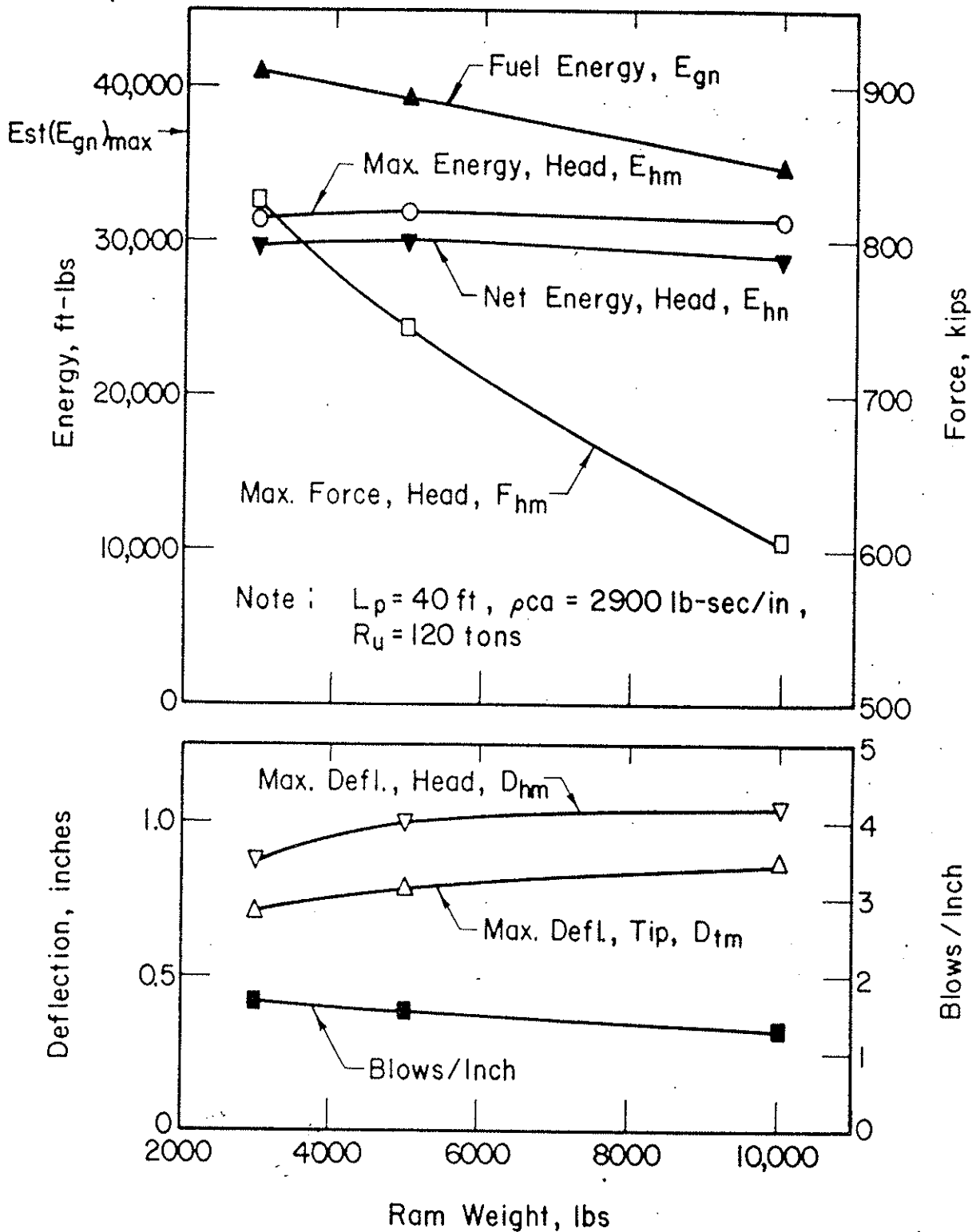


Figure 5.32 EFFECTS OF RAM WEIGHT, 40 FT PILE, 120 TONS SOIL RESISTANCE, CONSTANT RATED ENERGY

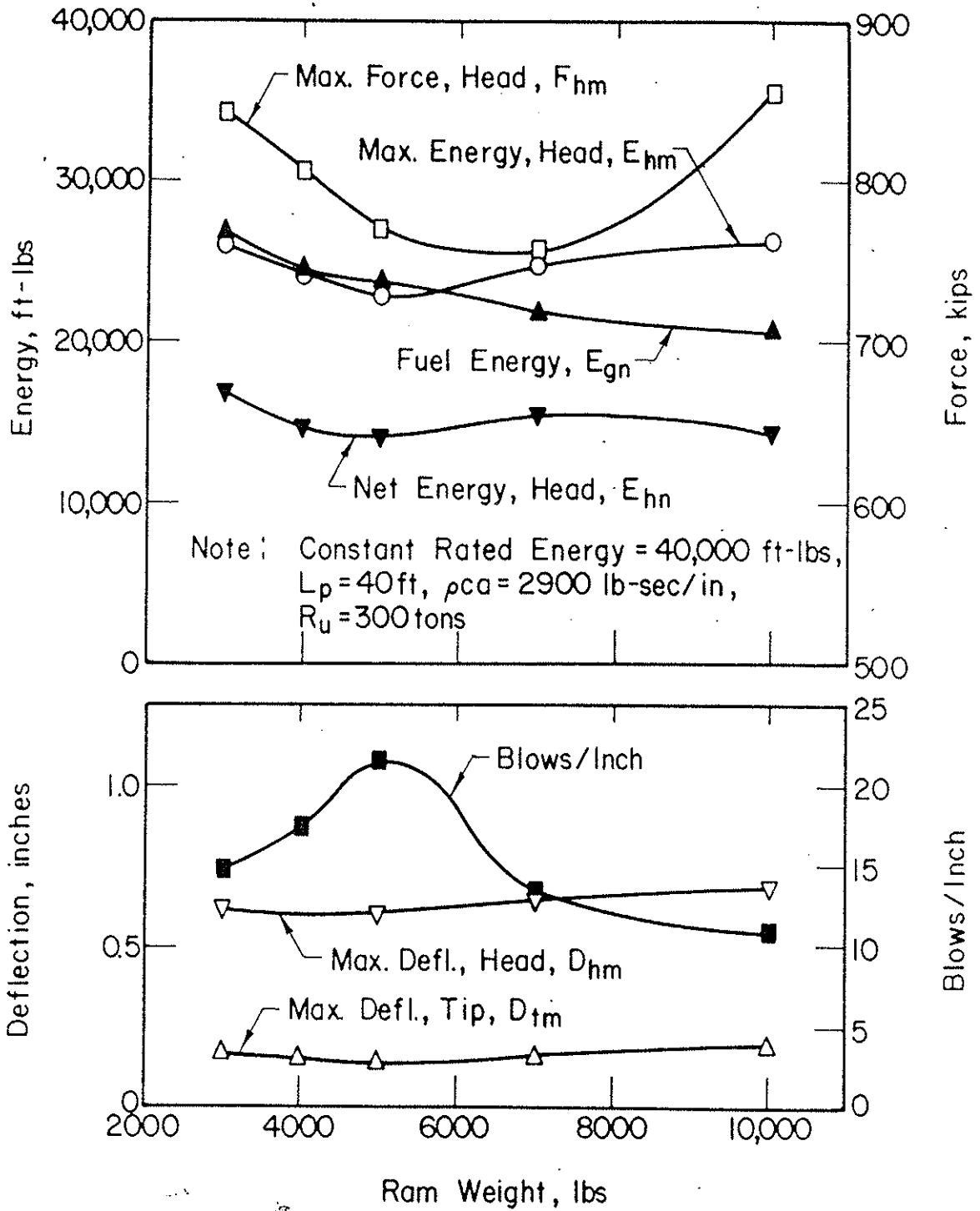


Figure 5.33 EFFECTS OF RAM WEIGHT, 40 FT PILE, 300 TONS SOIL RESISTANCE, CONSTANT RATED ENERGY

For the infinitely long pile (Figure 5.30) total impulse, I_a , increases with ram weight as predicted and, therefore, pile deflection and transmitted energy also increase. Peak force, F_{hm} , decreases with increasing ram weight. Net expended fuel energy, E_{gn} , increases with increasing ram weight because of additional energy absorbed by pile deflection. Note that for a given rated energy, the energy required to raise the ram is not affected by ram weight.

In Figure 5.31 the force pulses generated in the head of the infinitely long pile by the 3000 lb and 10,000 lb rams are compared. In the case of the lighter ram a comparatively high incident peak force is generated, due to a higher velocity at impact; for the heavy ram the initial peak force is smaller but the force decays more slowly, reflecting a longer duration of impact.

In the case of the 40 ft pile, the influence of ram weight depends upon the soil resistance, R_u . For R_u equal to 120 tons (Figure 5.32), maximum penetration occurs with the 10,000 lb ram, as in the case of the infinitely long pile. Transmitted energy is relatively insensitive to ram weight. Net expended fuel energy decreases slightly with increasing ram weight due to pile rebound which, in the case of the heavy ram, occurs while the ram is still in contact with the anvil, returning energy to the ram. At R_u equal to 3000 tons (Figure 5.33), the peak force becomes more critical in determining penetration. The incident peak force is high for the light

ram, due to high impact velocity. For the heavy ram, incident peak force is relatively low, but reflections which occur during the impact period increase the ultimate peak force to a value greater than that generated by the light ram. Therefore, best performance occurs with the heavy ram, as in the case of the infinitely long pile.

The irregularity of the blows/inch vs ram weight relationship in Figure 5.32 exemplifies the complexity of the effects of force reflections in pile driving, particularly in the case of short piles. Thus, conclusions drawn from the study of driving on infinitely long piles may not be applicable to the case of short piles, due to reflection effects.

Weight of Anvil. Analyses were performed with anvil weights ranging from 500 to 3000 lbs, approximately 30 to 200 percent of the typical anvil weight for hammers similar to the hypothetical hammer. The infinitely long pile, and the 40 ft pile, with R_u equal to 120 tons and 300 tons, were considered. Pile impedance was held constant at 2900 lb-sec/in. Results of the analyses are presented in Figures 5.34 through 5.37.

For the infinitely long pile (Figure 5.34), performance is not sensitive to anvil weight, the most significant effect being a slight decrease in peak force with increasing anvil weight. This could be important in hard driving, wherein peak force is critical. Figure 5.35 is a comparison of the force pulse generated in the head of the infinitely long pile by hammers with anvil weights of 500 and 3000 lbs. The pulses are

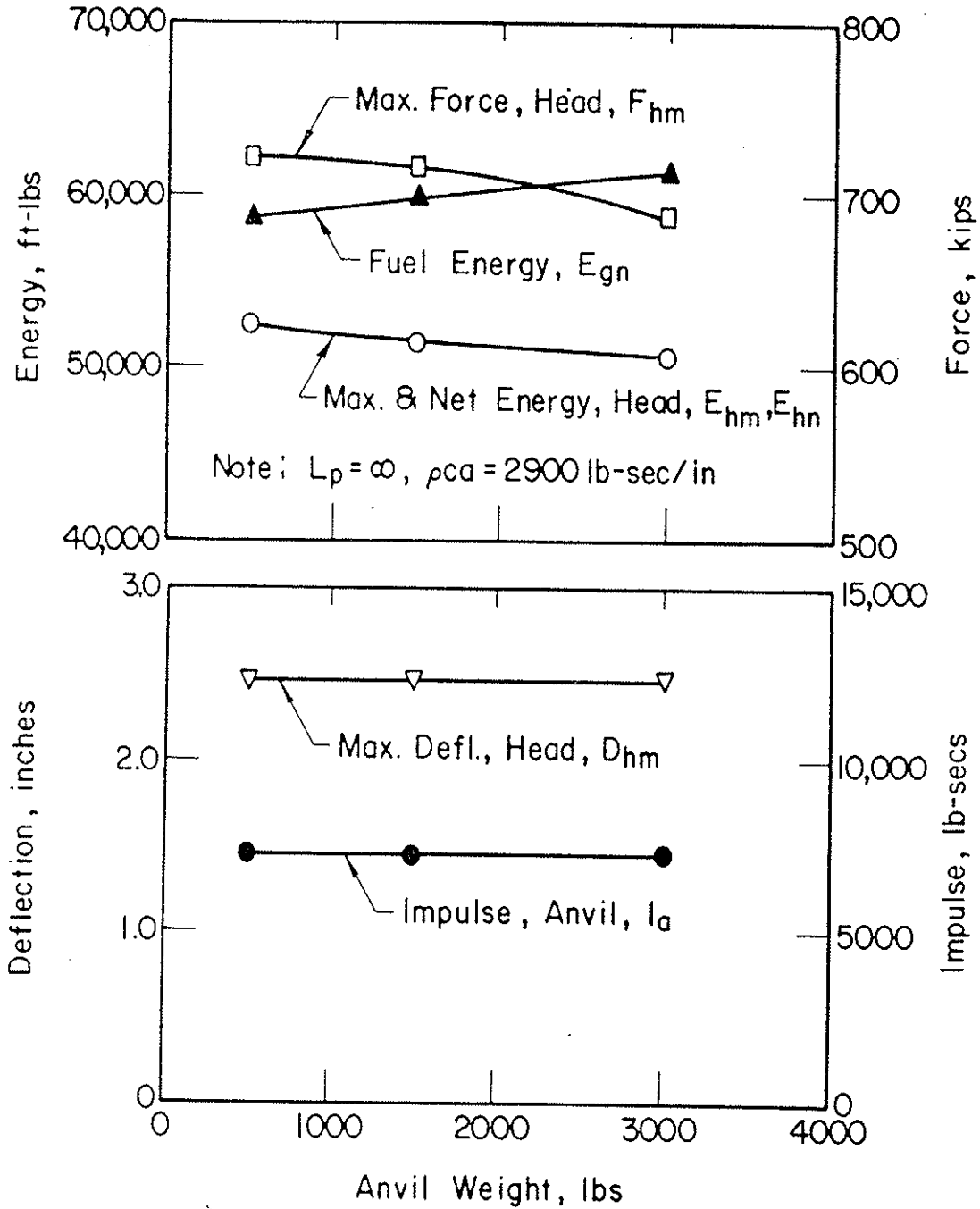


Figure 5.34 EFFECTS OF ANVIL WEIGHT, INFINITELY LONG PILE

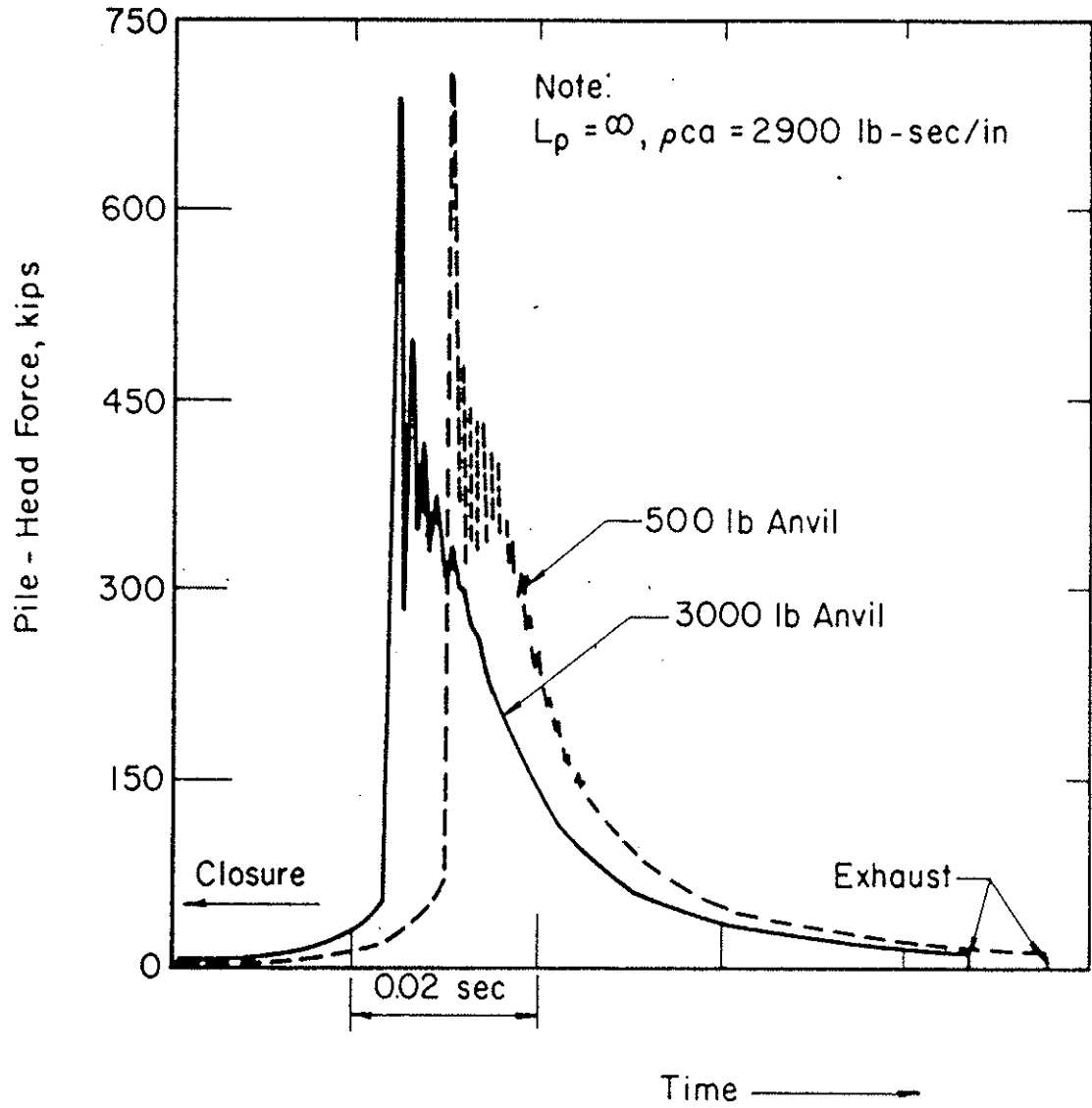


Figure 5.35 COMPARISON OF FORCE PULSES - VARYING ANVIL WEIGHT, INFINITELY LONG PILE

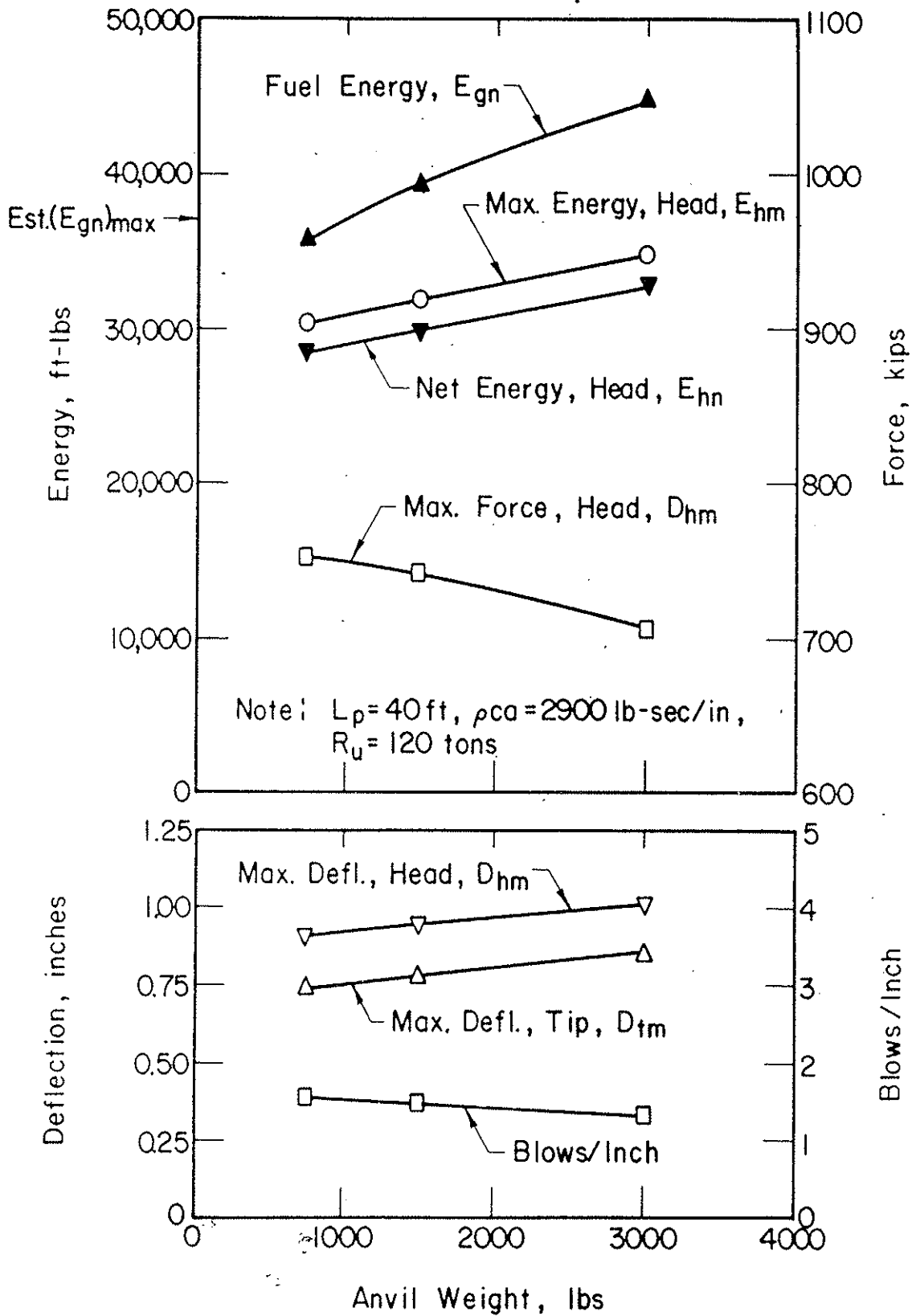


Figure 5.36 EFFECTS OF ANVIL WEIGHT, 40 FT PILE, 120 TONS SOIL RESISTANCE

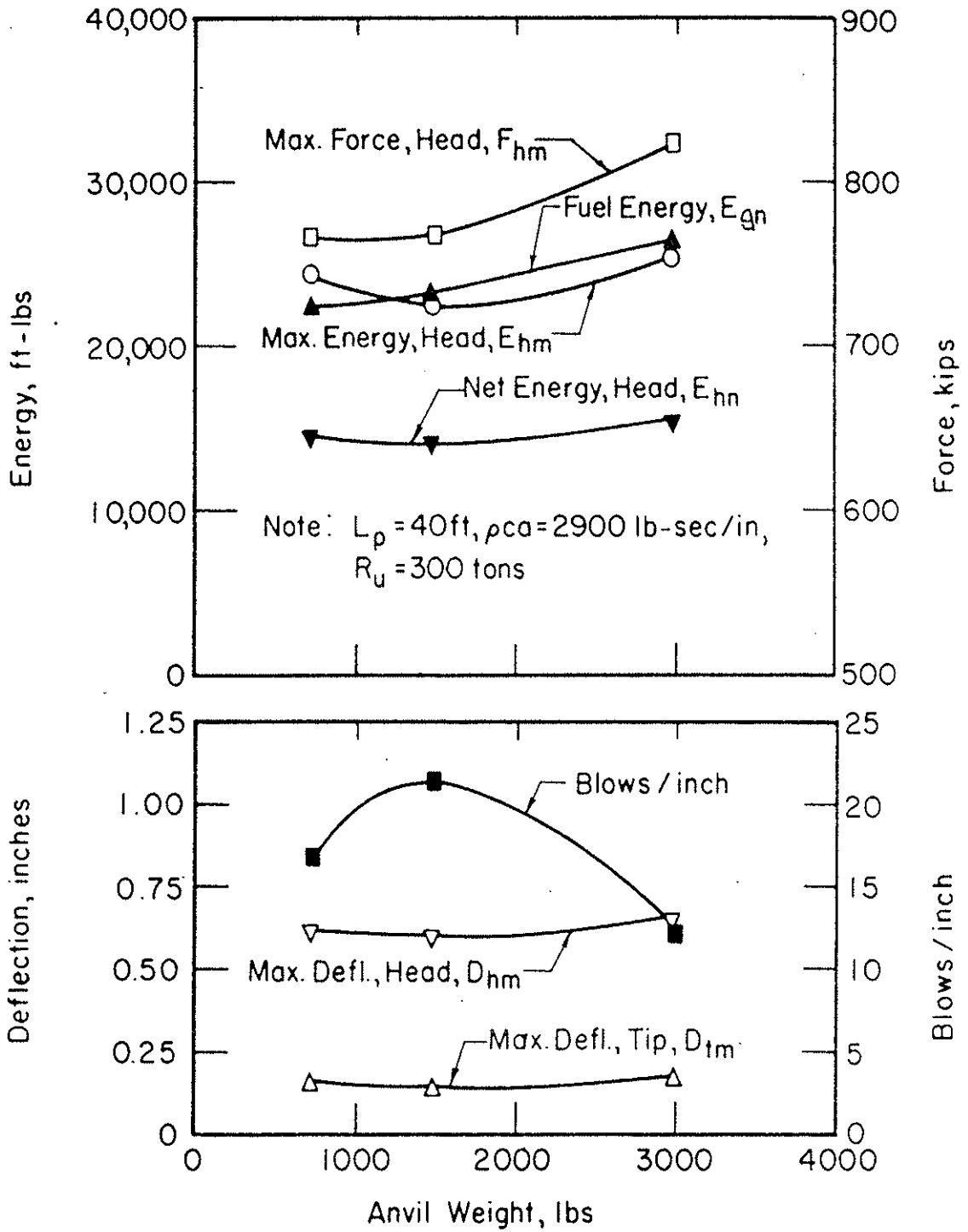


Figure 5.37

EFFECTS OF ANVIL WEIGHT, 40 FT PILE, 300 TONS SOIL RESISTANCE

essentially identical, with a slightly lower peak force in the case of the heavy anvil.

The case of the 40 ft pile illustrates the complications of real pile-driving cases, as compared to the infinitely long pile case. For R_u equal to 120 tons (Figure 5.36), anvil-weight effects are approximately similar to those of the infinitely long pile case. For R_u equal to 300 tons (Figure 5.37), however, impedance and force-reflection effects combine to produce somewhat greater energy transmission and deflection at the high and low extremes of anvil weight than at the intermediate anvil weight.

In general the effects of variations in anvil weight are secondary as compared to variations in ram weight. For short piles at high soil resistance the effects may be significant, and can be checked by wave equation analysis.

Weight of Drivehead. Analyses were performed with drivehead weights ranging from 500 to 3000 lbs, representing the extreme range of weights normally encountered for a hammer of 40,000 ft-lbs rated energy. The infinitely long pile and the 40 ft pile, with R_u equal to 120 tons and 300 tons were considered. Pile impedance was held constant at 2900 lb-sec/in. Results of the analyses are presented in Figures 5.38 through 5.41.

In the case of the infinitely long pile (Figure 5.38), peak pile-head force falls off sharply for the highest drivehead weight, indicating that the increased drivehead inertia

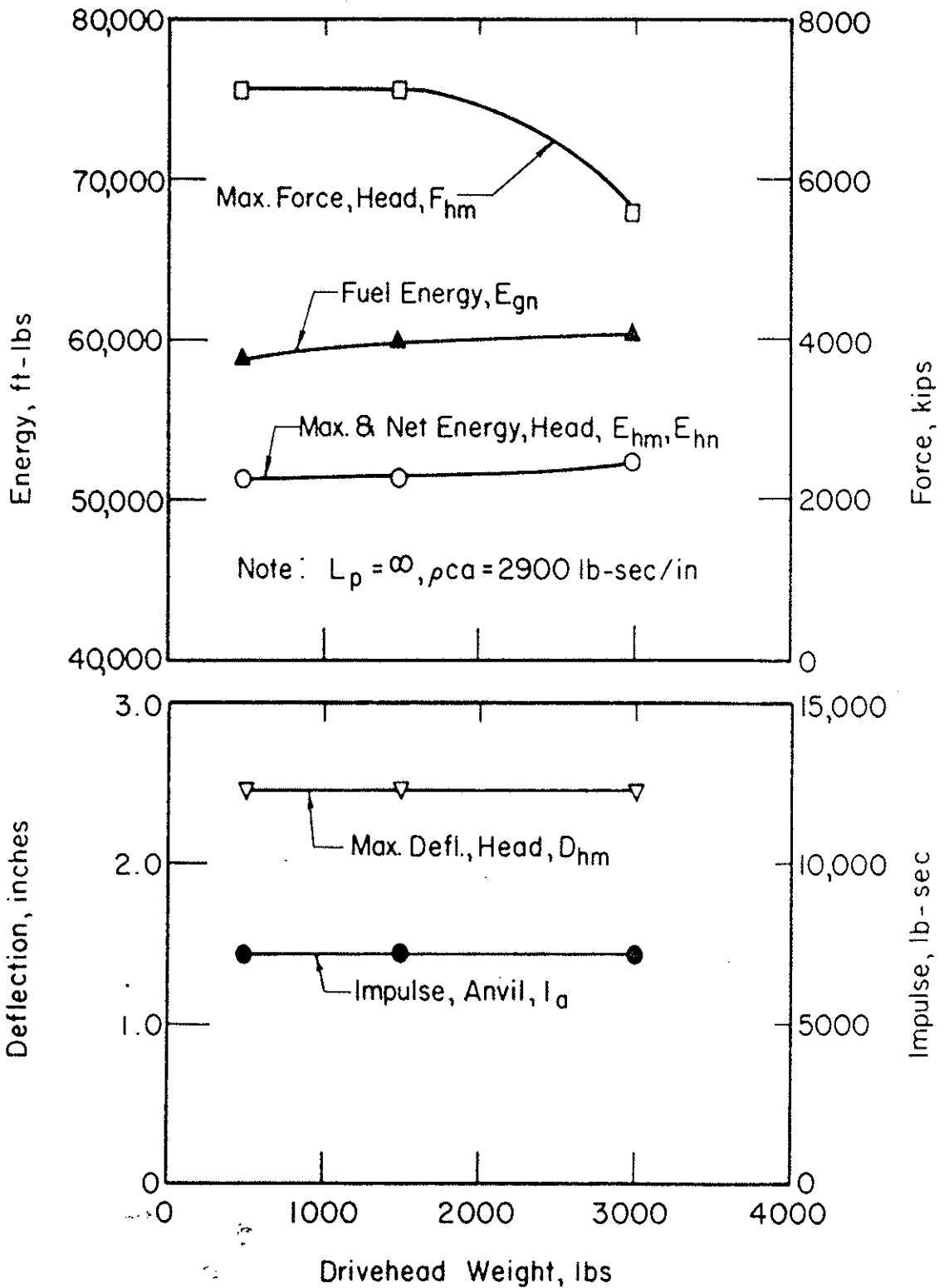


Figure 5.38 EFFECTS OF DRIVEHEAD WEIGHT, INFINITELY LONG PILE

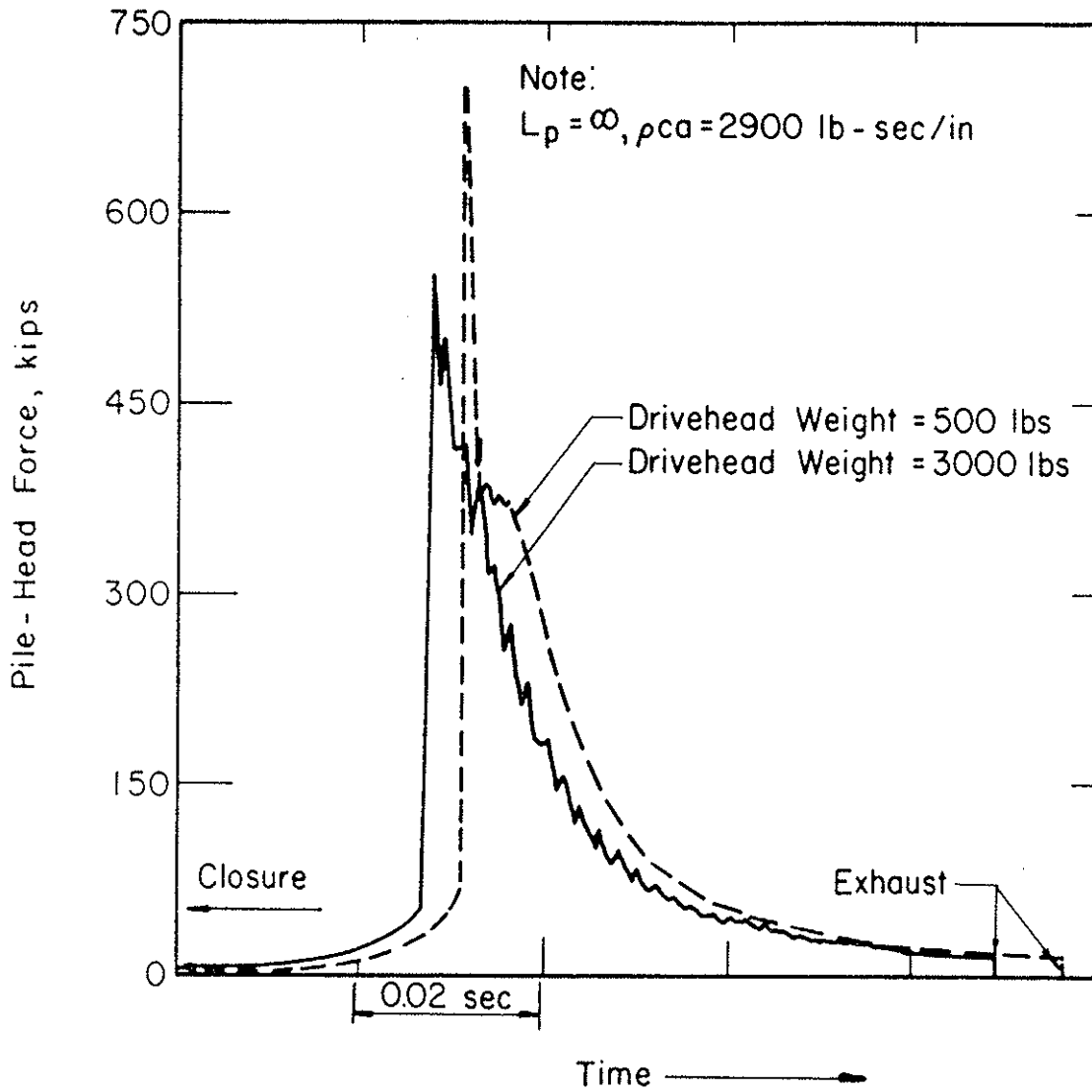


Figure 5.39 COMPARISON OF FORCE PULSES - VARYING DRIVEHEAD WEIGHT, INFINITELY LONG PILE

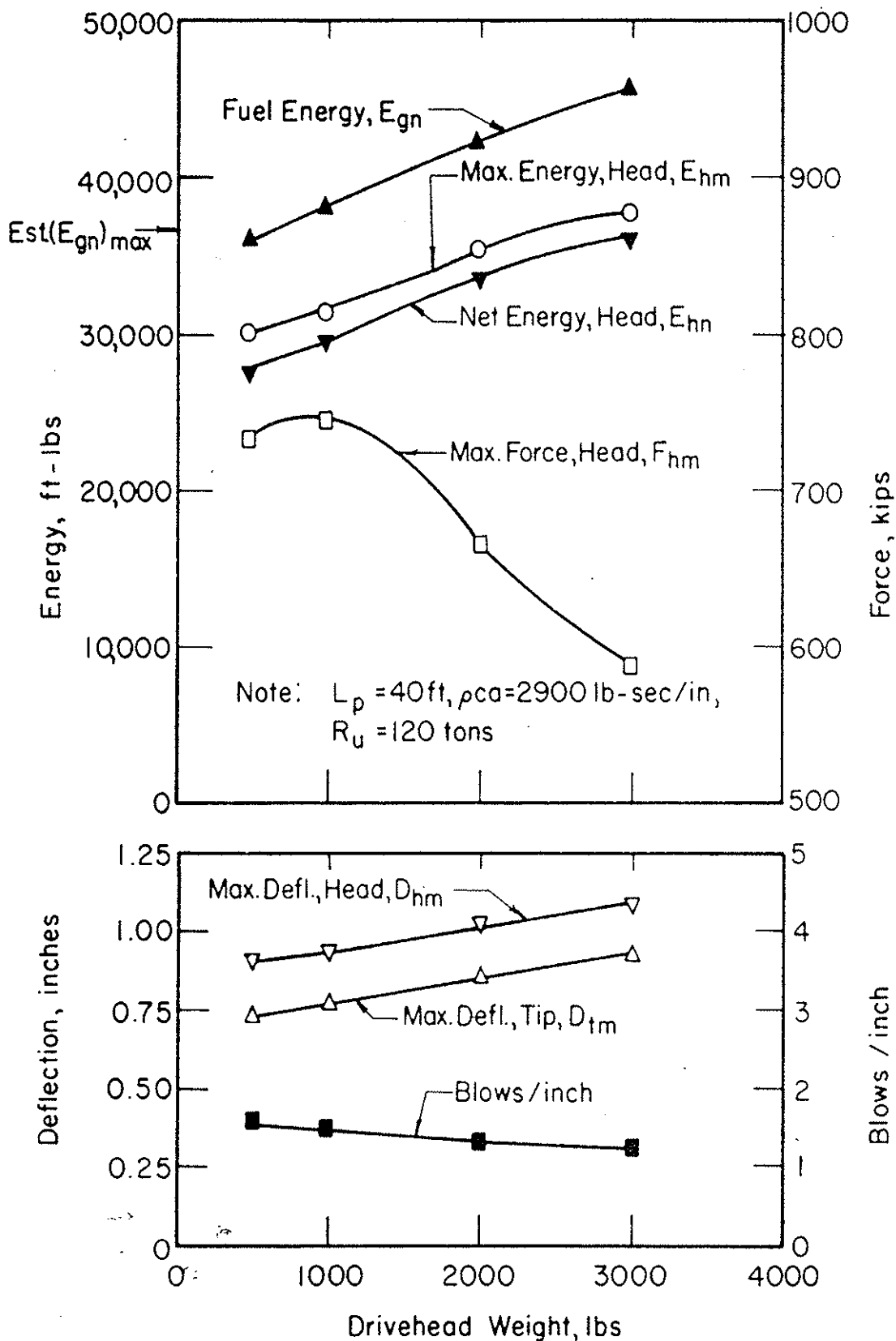


Figure 5.40 EFFECTS OF DRIVEHEAD WEIGHT, 40 FT PILE, 120 TONS SOIL RESISTANCE

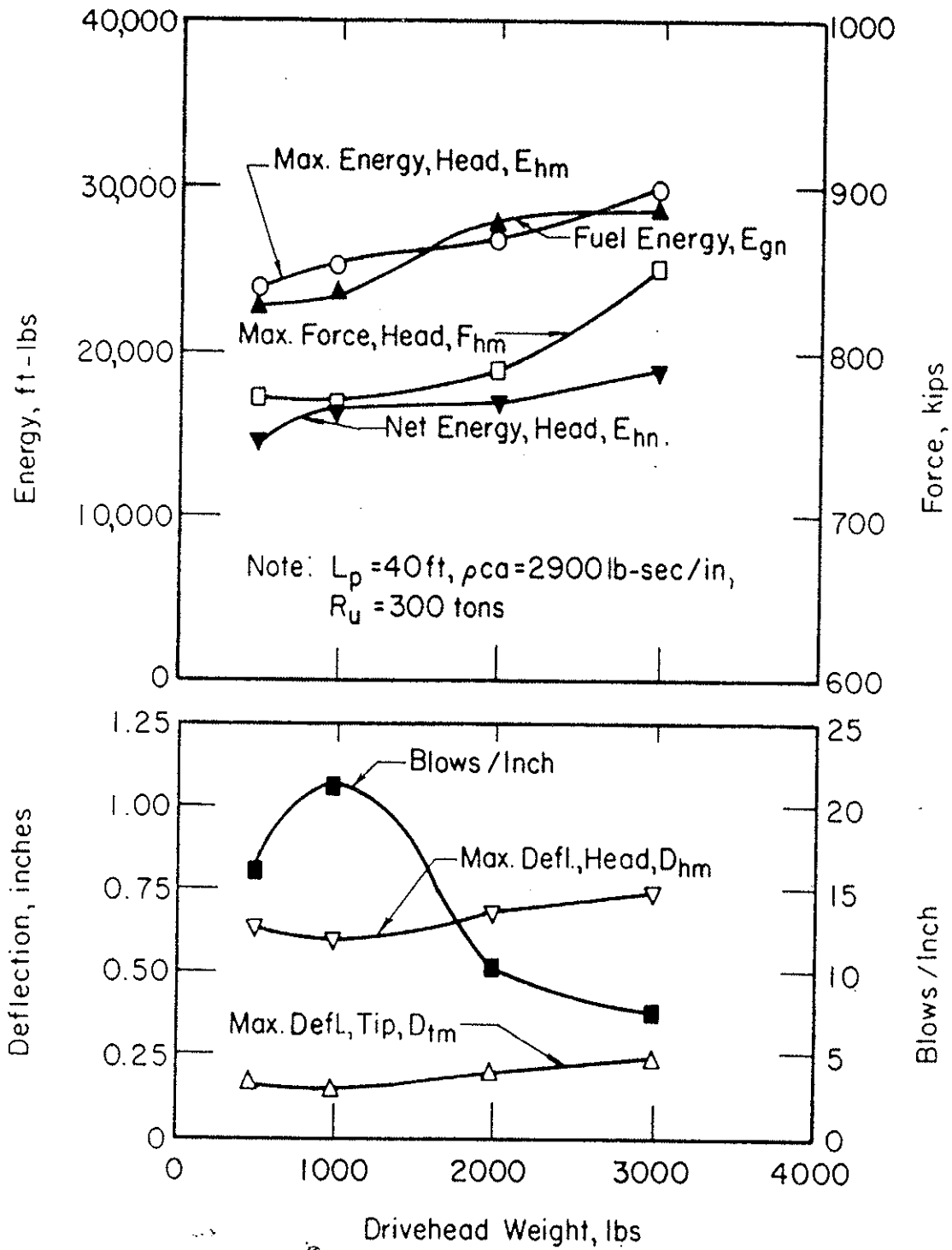


Figure 5.41 EFFECTS OF DRIVEHEAD WEIGHT, 40 FT PILE, 300 TONS SOIL RESISTANCE

reduces pile-head acceleration. Figure 5.39 is a comparison of the force pulses generated at the head of the infinitely long pile by the hypothetical hammer with drivehead weights of 500 lbs and 3000 lbs. The principal difference between the pulses is the magnitude of the peak force; the pulses are similar prior to and after the peak. In actual pile driving, this difference in peak force may or may not be of importance, depending upon whether peak force controls penetration.

The presence of the drivehead will affect the nature of the force reflections which occur at the top of the pile. A small drivehead weight will tend to cause tensile reflections, whereas a large drivehead weight will result in compressive reflections which, in the case of short piles, may increase pile penetration. This occurs in the case of the 40 ft pile at R_u equal to 120 tons (Figure 5.40) and 300 tons (Figure 5.41). As drivehead weight is increased from 500 to 1000 lbs, penetration decreases slightly due to increased incident peak force. At higher values of drivehead weight, penetration increases as a result of the reflection effects.

Stiffness of Hammer Cushion

Hammer-cushion stiffness, K_c , is a primary factor in the determination of the form of energy delivered to the pile head and, thus, in the impedance matching of hammer and pile. Although the precise relationship of K_c to hammer impedance has not been determined, insight into the influence of K_c on pile penetration and stress was gained by examination of several cases.

A series of analyses was performed pertaining to the hypothetical hammer operating on the infinitely long pile, with impedance of 2900 lb-sec/in; K_C was varied from 500,000 lb/in to 100,000,000 lb/in. For most diesel hammers, the stiffness of the manufacturer's recommended cushion falls in this range, with 15,000,000 lb/in to 70,000,000 lb/in being most common.

Results of the analyses are summarized in Figure 5.42. In the range of stiffnesses from 500,000 lb/in to 20,000,000 lb/in, performance was strongly affected by cushion stiffness; both transmitted energy and peak force increased with increasing stiffness. At higher stiffness, however, performance remained essentially constant, indicating that a point of diminishing returns had been reached.

As illustrated by the comparison of force pulses in Figure 5.43, the effect of a large increase in K_C is to increase the incident peak force. The influence of this change in the form of energy on pile penetration and stress depends on pile impedance, soil resistance distribution, total soil resistance and other factors. The influence of peak force is greatest in cases wherein peak force limits penetration, namely, the driving of high-impedance piles against high soil resistance.

To exemplify the influence of K_C on the driving of a finite-length pile, a second series of analyses was performed relative to the hypothetical hammer operating on 40 ft long piles with impedances equal to 2175, 2900 and 3625 lb-sec/in (15, 20, and 25 in² of steel, respectively). Results of the

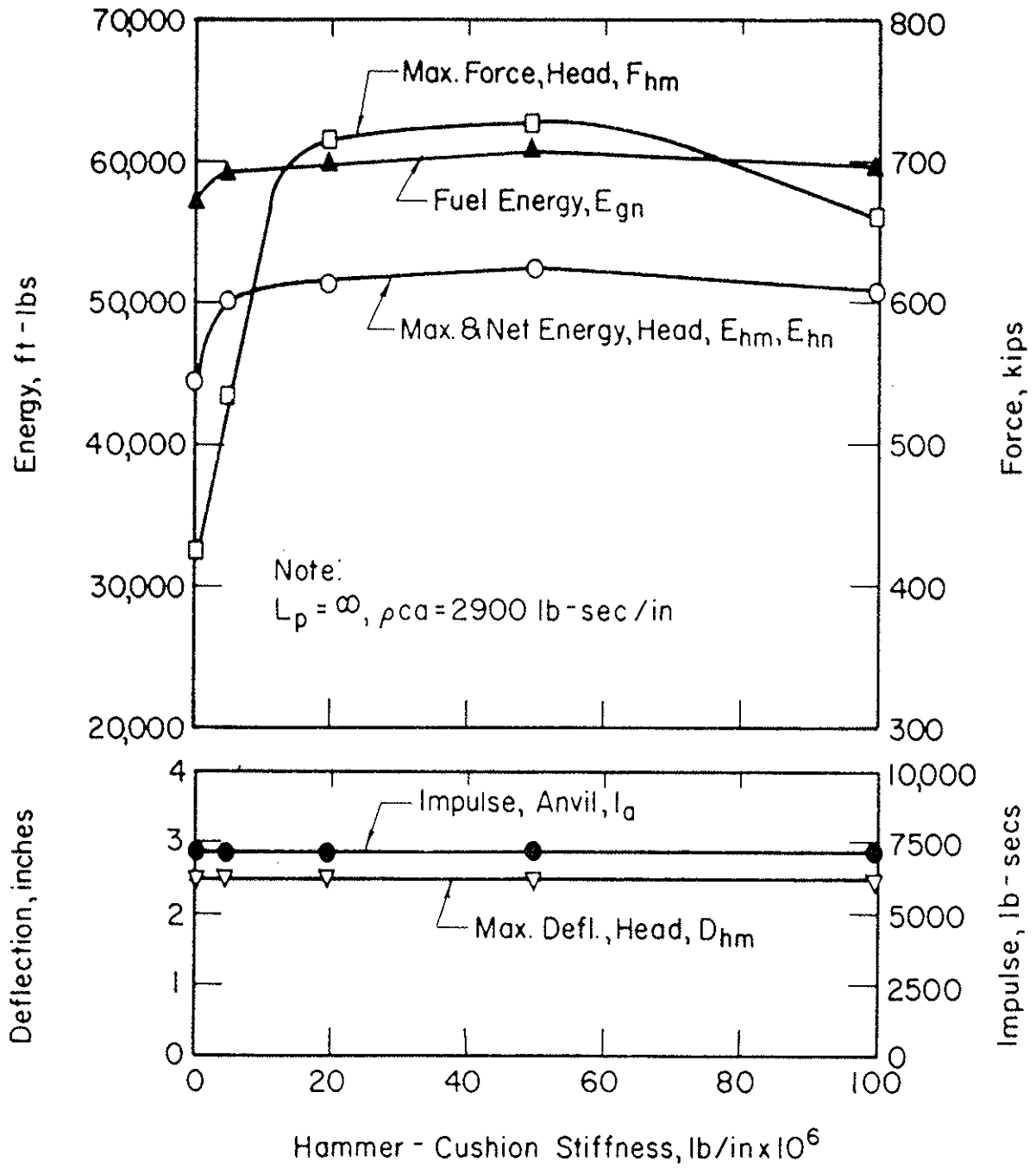


Figure 5.42

EFFECTS OF HAMMER-CUSHION STIFFNESS,
 INFINITELY LONG PILE

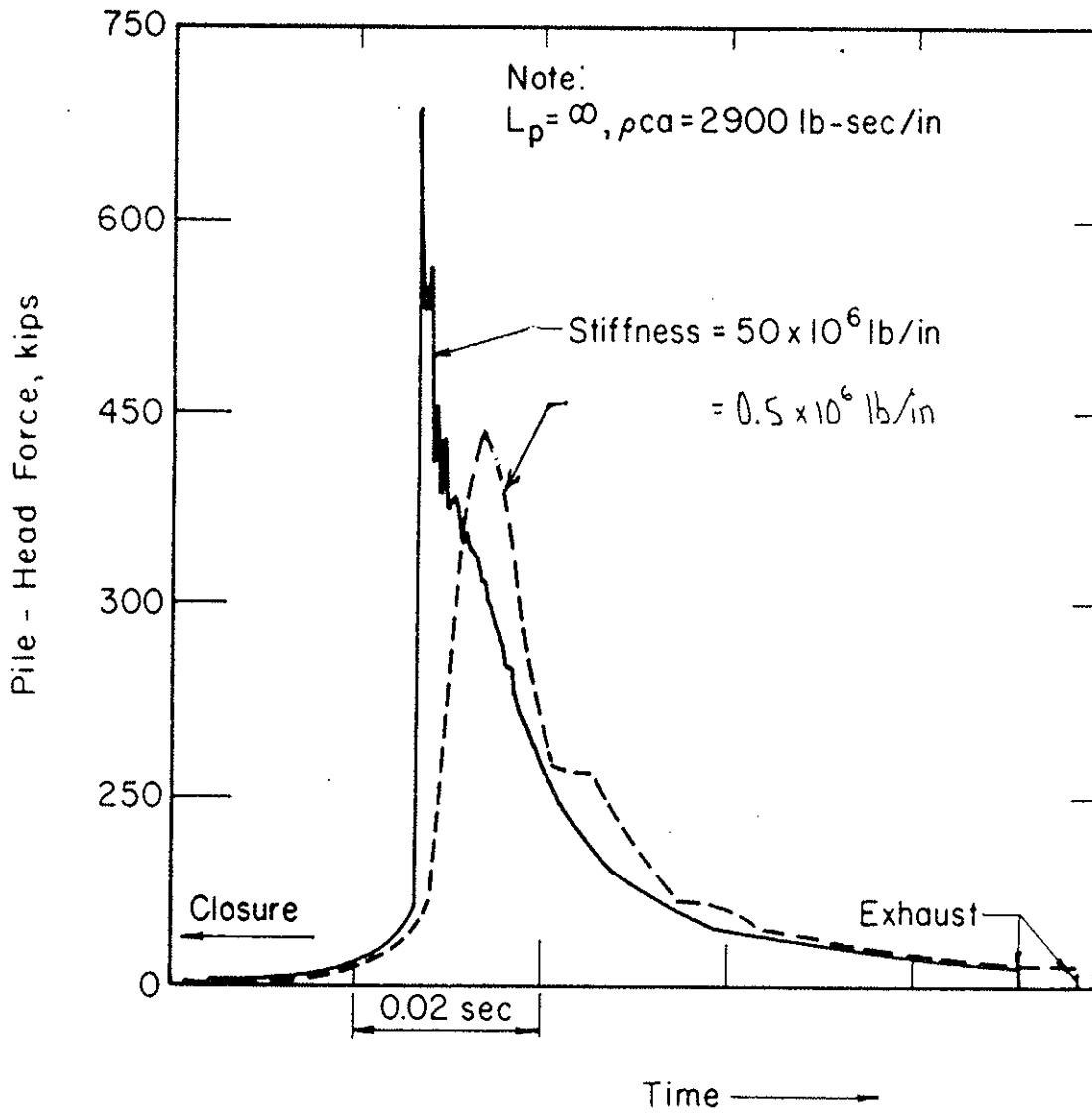


Figure 5.43 COMPARISON OF FORCE PULSES - VARYING
 HAMMER-CUSHION STIFFNESS, INFINITELY
 LONG PILE

analyses are summarized in Figure 5.44 wherein blows/inch and peak pile force are plotted versus K_c . For each of the impedances, maximum pile penetration occurred at K_c equal to 50,000,000 lb/in, approximately. For these examples, at least, the hammer cushions normally used in diesel hammers are near the optimum stiffness relative to pile penetration.

For the cases investigated, the optimum hammer-cushion stiffness is considerably higher than the stiffness corresponding to impedance matching in an impact hammer of equal ram weight. For example, to obtain matched impedance of impact hammer and pile, for a ram weight of 5000 lbs and pile impedance of 2900 lb-sec/in, K_c should be between 500,000 and 1,800,000 lb/in (Parola, 1970). The apparent difference between the stiffness corresponding to impedance matching in the impact hammer and the optimum stiffness for the cases investigated can be attributed to reflection effects and to the influence of the anvil and gas force on impedance matching in the diesel hammer.

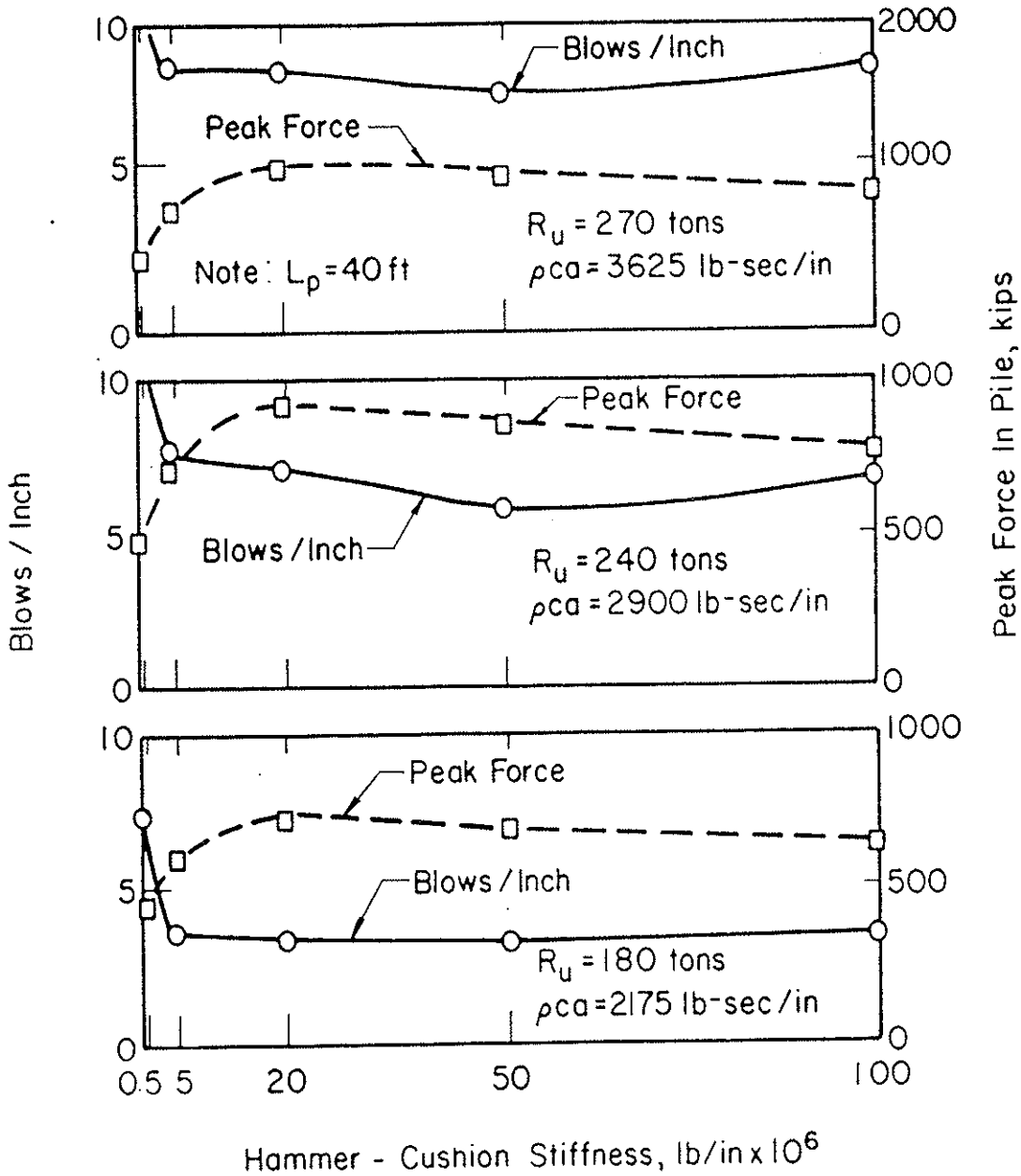


Figure 5.44 EFFECTS OF HAMMER-CUSHION STIFFNESS ON PERFORMANCE, 40 FT PILE, VARYING IMPEDANCE

CHAPTER 6

CONCLUSIONS AND RECOMMENDATIONS FOR RESEARCH

6.1 CONCLUSIONS

Conclusions relative to diesel hammer performance will be presented under three topics: simulation of performance by wave equation analysis; fundamental characteristics of performance; and factors affecting performance.

Simulation of Diesel Hammer Performance

1. Diesel hammer performance can be simulated by wave equation analysis with accuracy sufficient for both soil mechanics applications and hammer design.
2. Accurate simulation requires that the hammer model correctly account for gas-force effects, including the interaction of impact and gas force with the movement of the pile in the course of the hammer blow.
3. Gas-force effects can be simulated by application of basic thermodynamic laws to the compression and expansion of gas in the power cylinder, by utilization of appropriate pulse-shape factors describing the timing and characteristics of the combustion event, and by adjustment of the pulse amplitude to

achieve equality of downstroke and upstroke of the ram. By this method the influence of soil resistance, pile characteristics, fuel volume and other factors on the gas-force pulse are correctly taken into account.

4. If the amount of fuel energy expended within the hammer is known, it is possible to perform the energy-input analysis, wherein the ram stroke corresponding to the specified amount of fuel energy is calculated.
5. Provision should be made for minimizing the calculation error resulting from spurious oscillation of the spring-mass model used to represent the pile. This can be accomplished by the use of internal damping.

Characteristics of Diesel Hammer Performance

1. The diesel hammer is essentially a variable-stroke, free-piston diesel engine; the stroke of the piston (ram) varies with the load on the engine (pile-soil response) and the amount of fuel supplied. The variable-stroke characteristic has important implications with regard to field control of diesel pile driving, prevention of pile damage, and overall pile-driving performance.
2. For effective pile-driving control, field personnel must be provided with a means for estimating pile capacity on the basis of blows/inch, at various values of ram stroke. Wave equation analysis can be used to

generate curves of R_u vs blows/inch at three or more values of ram stroke. By interpolation, estimated pile capacity can be determined for any combination of blows/inch and stroke. For a given pile capacity, a single curve of blows/inch vs stroke can be used, in which case no interpolation is required.

3. The variable-stroke characteristic can be put to use in the prevention of pile damage, particularly in the driving of concrete piles. Because peak stress is a function of ram stroke, damage is less likely when the hammer is operated at reduced stroke. In soft-ground driving where tension stresses are critical, ram stroke automatically decreases because a large proportion of the fuel energy is absorbed by the pile. Additional control over stroke is afforded by hammers in which fuel flow can be controlled.
4. Net energy transmitted to the anvil is, in general, approximately equal to the net expended fuel energy and thus is proportional to the amount of fuel injected.
5. Both the impact and gas force contribute significantly to the total force output of the hammer. In general, the impact component increases relative to the gas component as ram stroke or soil resistance increases.

Factors Affecting Hammer Performance

Job-Controlled Factors. Pile characteristics, site conditions and fuel volume have an important effect on diesel hammer performance; therefore it is essential that these be taken into account. Specific conclusions regarding these factors are as follows:

1. As pile length increases, maximum and net transmitted energy tend to increase, peak pile-head force tends to decrease, and required fuel energy tends to increase.
2. Increasing pile impedance results in larger peak pile-head force, which in most cases results in increased pile penetration.
3. Based on the analyses described, the effects of inclination on hammer performance are probably negligible for inclinations less than 14° , measured from the vertical. At larger inclinations, reduced gravity and increased friction forces diminish the transmitted energy and peak force corresponding to a given ram stroke.
4. Soil resistance, R_u , has an important influence on hammer performance. At constant ram stroke, maximum and net transmitted energy decrease with increasing R_u , whereas peak pile-head force tends to increase. Peak pile-tip compressive forces increase significantly with increasing R_u , due to compressive reflections at the pile tip. Fuel energy required to

maintain constant stroke decreases with increasing R_u .

5. If fuel energy is held constant and soil resistance is increased, maximum transmitted energy remains approximately constant, and net transmitted energy tends to decrease slightly; stroke and peak force increase significantly. Thus in easy-driving conditions, even though the amount of fuel injected per blow is held constant.
6. If soil resistance is held constant, an increase in fuel energy results in a significant increase in stroke, peak force and transmitted energy. The ability to vary fuel energy during driving will result in more favorable performance characteristics in both easy and hard driving. This is especially important in soft-ground operation, wherein large amounts of fuel are required in order to prevent hammer shutdown.

Hammer-Controlled Factors. Certain characteristics of the hammer, drivehead and cushioning should be considered in the selection of equipment for a given job. The following conclusions relative to these characteristics were derived from the current research:

1. The effective impedance of diesel hammers involves several factors, including ram weight, cushion stiffness, combustion characteristics and the weights of

anvil and drivehead. Due to the large number of factors involved, no method has been developed for determining the effective impedance. Matching of hammer and pile impedance in order to optimize performance is best accomplished by wave equation analysis of trial hammer-pile combinations.

2. Increasing the ram weight, at constant rated energy, results in lower impact velocity and greater force-pulse duration. Although the incident peak force is reduced, the long pulse duration may result in reflected peak forces which are greater than those achieved with a lighter ram, particularly in the case of short piles. Increasing the ram weight may increase or decrease transmitted energy, depending on the impedance match and force-reflection effects.
3. Ignition timing has an important effect on peak force and energy transmission. Ignition occurring prior to impact decreases incident peak force; ignition after impact has little effect on incident peak force. For optimum energy transmission, ignition should be timed such that peak gas and impact forces occur simultaneously.
4. As compared to impact atomization, spray atomization has the advantage of closely-controlled ignition timing, which results in more predictable hot-weather performance and less sensitivity to the type of fuel used.

Furthermore, spray atomization makes possible low-stroke operation without impact, which is useful in driving concrete piles.

5. For a given swept volume, an increase in power-cylinder area will produce a force pulse of approximately equal peak force but of longer effective duration; the results are as follows:
 - a. In the case of long piles or low R_u , pile penetration will increase.
 - b. For short piles or high R_u , penetration may increase or decrease depending on other factors.
 - c. The minimum soil resistance at which the hammer will operate will increase, which is unfavorable for soft-ground operation.
6. An increase in compression ratio results in decreased peak force and increased transmitted energy for long piles and low values of R_u . However, the effects are secondary in importance. For short piles at high R_u , variations in compression ratio have negligible effect on performance. A high compression ratio is undesirable for soft-ground operation because it results in an increase in the minimum soil resistance at which the hammer will operate.
7. Cushion stiffness has an important effect on peak force and efficiency of energy transmission. In general an increase in stiffness results in increased peak force;

however there is a point of diminishing returns, beyond which further increases in stiffness have little effect. The influence of cushion stiffness on the efficiency of energy transmission depends on the impedance match of hammer and pile. For the cases investigated, stiffness on the order of 50,000,000 lb/in produced the greatest pile penetration.

8. In general, variations in the weights of anvil and drivehead, within the range of values normally encountered, have only a secondary effect on hammer performance. Large values of anvil or drivehead weight may, in some cases, significantly reduce the incident peak force in the pile head. In short piles, however, the presence of the heavy anvil or drivehead may produce force reflections which are favorable with respect to pile penetration.

6.2 RECOMMENDATIONS FOR RESEARCH

With respect to simulating the diesel hammer for purposes of wave equation analysis, measurements should be performed which will facilitate accurate correlation of expended fuel energy with the amount of fuel injected. This requires measurement of fuel volume, ram and anvil movements, and anvil force under a variety of well-documented driving conditions for several representative hammer sizes and models. Information of this nature will allow prediction of obtainable ram stroke in advance of

driving. Then, hammer operation could be specified and controlled more competently.

For all hammers of the spray-atomization type, the timing and duration of the injection should be documented in order that the effective ignition timing and force-pulse shape factors may be determined for use in wave equation analysis. Predicted gas-force pulses should be checked by measurement.

A practical means should be developed for detection of uncontrolled preignition due to overheating. Currently, preignition can be detected only by measurements indicating a decrease in pile deflection, or by the observations of personnel experienced in the symptoms of overheating. Neither means is satisfactory for routine job control. If undetected, such preignition will result in diminished hammer performance and reduced pile capacity.

For simulation of inclined operation, measurements of ram velocity and pile-head force pulse under a variety of fully-documented driving conditions are needed in order to evaluate friction coefficients to be used in wave equation analysis.

A rational system for comparative rating of pile driving hammers, of both the diesel and impact type, is needed. This system should be based on measured performance of each hammer operating under one or more of a limited number of standardized driving conditions. Probably a minimum of five test stands should be used, each consisting of an

instrumented pile driven to firm bearing and each with a different impedance.

The hammer manufacturer would select the pile upon which his hammer would be tested; then the hammer would be operated under controlled conditions of stroke, fuel flow, temperature, etc. Hammer performance would be evaluated on the basis of the quantity and form of energy transmitted to the pile. The hammer ratings developed from such tests would replace the present "rated energy" and would thus contribute to more competent hammer utilization.

REFERENCES

- Baumeister, T., and L. S. Marks, eds., (1967), Standard Handbook for Mechanical Engineers, 7th ed., New York, McGraw-Hill, pp. 3-35.
- Biggs, J. M., (1964), Introduction to Structural Dynamics, New York, McGraw-Hill, pp. 140-147.
- Chellis, R. D., (1961), Pile Foundations, 2nd ed., New York, McGraw-Hill, p. 564.
- Cummings, A. E., (1940), "Dynamic Pile Driving Formulas," Contributions to Soil Mechanics 1925-1940, Boston Society of Civil Engineers, Boston, pp. 392-413.
- Davisson, M. T., (1973), "High Capacity Piles," Innovations in Foundation Construction, Illinois Section, ASCE, May, Chicago, pp. 81-112.
- Davisson, M. T., (1974), "Pile Foundations and the Computer," Seminar on Use of Computers in Foundation Design and Construction, Metropolitan Section, ASCE, New York City, April.
- Davisson, M. T., (1975a), Personal Communication.
- Davisson, M. T., (1975b), "Pile Load Capacity," Proceedings, Seminar on Design, Construction and Performance of Deep Foundations, University of California, Berkeley.
- Davisson, M. T., and V. J. McDonald, (1969), "Energy Measurements for a Diesel Hammer," Performance of Deep Foundations, ASTM STP 444, pp. 295-337.
- Davisson, M. T., and D. M. Rempe, (1974), "Wave Theory Simplified," Piletalk Seminar, Associated Pile and Fitting Corp., 15 February.
- Degler, H. E., (1939), Diesel Engines - Theory and Design, Chicago, American Technical Society, p. 44.
- Donnell, L. H., (1930), "Longitudinal Wave Transmission and Impact," Transactions ASME, Vol. 52, Paper APM-52-14.
- Edwards, T. C., (1967), "Piling Analysis Wave Equation Computer Program Utilization Manual," Texas Transportation Institute, Research Report 33-11, Texas A & M University, August, 40 p.

- Goble, G. G., W. D. Kovacs, and F. Rausche, (1972), "Field Demonstration: Response of Instrumented Piles to Driving and Load Testing," Proceedings ASCE Conference on Performance of Earth and Earth-Supported Structures, Purdue, Vol. III, pp. 3-38.
- I. H. I., (1970), "Outline of IDH-J Type Diesel Pile Hammer," Ishikawajima-Harima Heavy Industries Co., Ltd., Tokyo, (Sales Literature).
- Isaacs, D. V., (1931), "Reinforced Concrete Pile Formulae," Journal of the Institution of Engineers, Australia, Transactions, Vol. 12, pp. 305-323.
- Kobe, (1969), "Pile Driving Data of Model K22 Diesel Pile Hammer," Kobe Steel Ltd., Kobe, Japan.
- Lichty, L. E., (1967), Combustion Engine Processes, New York, McGraw-Hill.
- Link-Belt, (Undated), "Diesel Pile Hammer Comparative Analysis," Brochure, Link-Belt Speeder Corp., Cedar Rapids, Iowa.
- Murtha, J. P., (1961), "Discrete Mass Mathematical Models for One-Dimensional Stress Waves," Ph.D. Thesis, University of Illinois, Urbana, Illinois.
- Obert, E. F., (1968), Internal Combustion Engines, 3rd ed., Scranton, Pennsylvania, International Textbook Company.
- Parola, J. F., (1970), "Mechanics of Impact Pile Driving," Ph.D. Thesis, University of Illinois at Urbana-Champaign.
- S. A. E., (1964), Digital Calculations of Engine Cycles, Vol. 7, SAE Special Publication Progress in Technology (TP7), New York, MacMillan Company.
- Smart, J. D., (1969), "Vibratory Pile Driving," Ph.D. Thesis, University of Illinois, Urbana, Illinois.
- Smith, E. A. L., (1955), "Impact and Longitudinal Wave Transmission," Transactions ASME, August, pp. 963-973.
- Smith, E. A. L., (1962), "Pile-Driving Analysis by the Wave Equation," Transactions ASCE, Vol. 127, Part I, pp. 1145-1193.
- Taylor, C. F., and E. S. Taylor (1961), The Internal-Combustion Engine, 2nd ed., Scranton, Pennsylvania, International Textbook Company.

APPENDIX A

OSCILLATION ERROR IN SPRING-MASS MODEL

A.1 INTRODUCTION

Pile hammers incorporating stiff internal cushioning, or no cushioning at all, are capable of generating a pile-head force pulse which has a very short rise time (less than 1 millisecond). In simulating the operation of such hammers by wave equation analysis, the use of a conventional spring-mass model may result in large computational error. Typically, both peak pile force and penetration are overpredicted; in extreme cases, the peak-force error may exceed 50 percent.

The source of the error is oscillation within the spring-mass model which has no counterpart in reality. In sections to follow, the cause of the oscillation and a method for minimization of the computational error will be discussed. An example problem will be examined.

A.2 CAUSE OF OSCILLATION

If a force pulse with short rise time is applied to a spring-mass model, such as that used to simulate the pile, the resulting motion of the masses in the system may be oscillatory. Murtha (1961) noted that a step pulse applied to a spring-mass model will cause the system to oscillate

predominantly in its highest mode. Further, Murtha demonstrated that the vibration of the model exactly simulates that of an equivalent continuous rod only in the fundamental mode of vibration, and that the disparity between the dynamic response of the model and rod increases with the frequency of vibration. It follows that the participation of the higher modes in the response of the spring-mass model detracts from the accuracy of the simulation.

A.3 DAMPING

An effective method for minimizing the error resulting from spurious oscillation is to prevent the model from oscillating in its higher modes. This can be accomplished by the introduction of internal damping elements (dashpots) into the model. A variety of dashpot arrangements are possible.

The writer uses an arrangement which has yielded satisfactory results. Dashpots are arranged in parallel with the springs representing the stiffness of the system elements (Figure A.1). Not all springs are damped; normally two dashpots, connecting the anvil to the drivehead and the drivehead to the first pile mass, are used.

Dashpots consume energy, thus simulating an energy loss which does not occur in reality. Therefore, it is necessary to design the dashpot such that a minimum of energy is consumed. For routine calculations a linear dashpot is

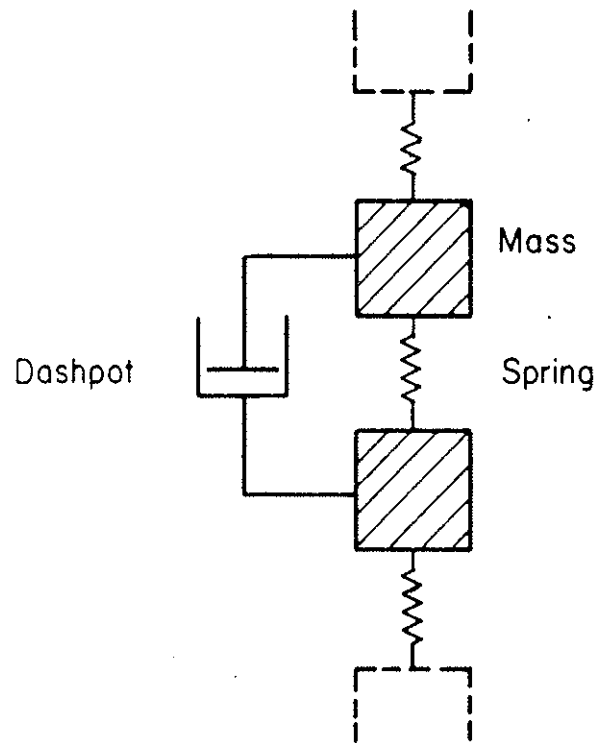


Figure A.1 DAMPING ELEMENT FOR CONTROL OF SPURIOUS OSCILLATION

assumed, such that the force F , in the dashpot is calculated as follows:

$$F = C_d (\dot{e})$$

where C_d is the damping coefficient and \dot{e} is the rate of strain. An important advantage of this type of dashpot is that the selection of the constant C_d can be done automatically, without trial and error. C_d is calculated according to the following relationship (Biggs, 1964):

$$C_d = \frac{2 C_p}{100 \omega}$$

where C_p = desired percentage of critical damping in highest mode of vibration, percent.

ω = highest natural frequency of vibration of the system consisting of the pile and interface equipment, radians/sec.

Normally C_p is set equal to 200 - 300 percent. The result is to damp the highest modes without materially affecting vibration in the lower modes. Using this method, the energy absorbed by the dashpots is normally less than 5 percent of the rated energy of the hammer. If higher values of C_p are used the dashpots may consume excessive amounts of energy, the result being underprediction of pile stress and penetration.

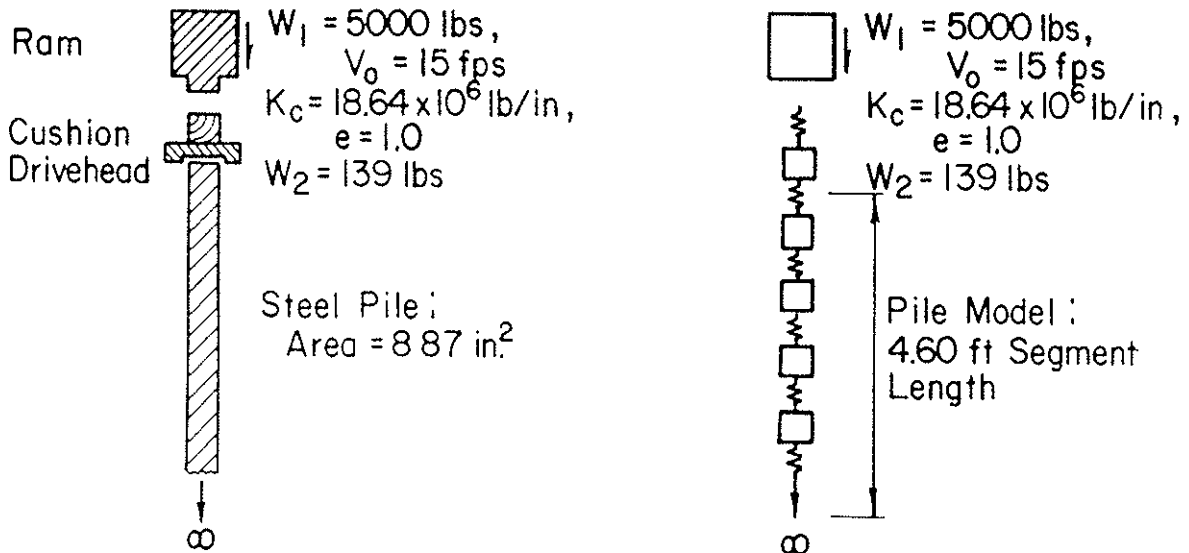
Use of internal damping as described above leads to a solution which is sufficiently accurate for soil mechanics

applications and hammer design. The error introduced by energy losses in the dashpots is small compared with the errors inherent in the assumed soil properties and other input variables. It is important to recognize, however, that the internal damping is an imperfect solution to the oscillation problem and should be used with judgement. For instance, it is necessary to ensure that the dashpots serve to damp only the spurious oscillations of the model. This is accomplished by selection of pile segment lengths which are sufficiently short that the highest natural frequency of the spring-mass model will be higher than that of the real system. If this is done, the spurious oscillations will occur at frequencies higher than the real oscillations of the pile-hammer-soil system. Thus the small amount of damping required to eliminate the high-frequency oscillation will have little effect upon the real oscillations.

A.4 EXAMPLE

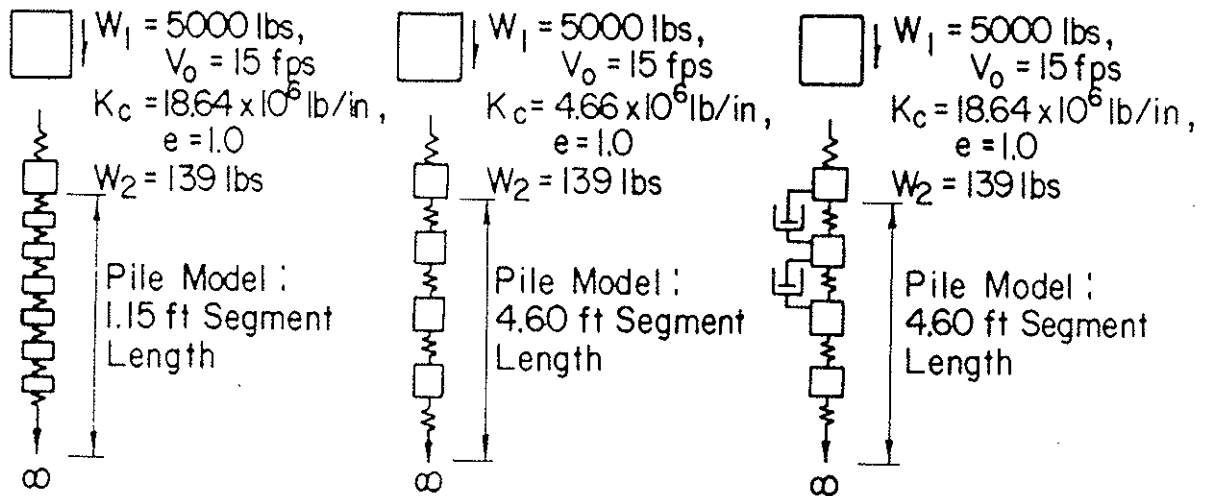
A hypothetical problem will illustrate the various methods for minimizing the oscillation error, including the method described in the preceding section. The problem has been idealized for simplicity, but is directly related to the oscillation problems encountered in the wave equation analysis of diesel pile driving.

The problem (Figure A.2a) involves the cushioned impact of a ram on an infinitely long steel pile. The



(a) Hypothetical Problem

(b) Model I



(c) Model II

(d) Model III

(e) Model IV

Figure A.2 HYPOTHETICAL PROBLEM AND ANALYTICAL MODELS

cushion, with a stiffness of 18.64×10^6 lb/in, rests on a 139-lb drivehead, which is in direct contact with the pile head.

The force pulse generated in the pile head by the ram impact was calculated by wave equation analysis, using four different analytical models. Model I (Figure A.2b) is representative of the "standard" approach to spring-mass modeling; the true cushion stiffness is used, and a pile segment length (4.6 ft) is selected. The pile-head force pulse calculated by this method is shown as a solid line in Figure A.3. Also shown in the figure is the exact solution to the problem, calculated by simulating the pile with an equivalent dashpot. Clearly, spurious oscillation has occurred in the model, resulting in a totally unrealistic calculated force pulse.

Model II (Figure A.2c) is similar to Model I, except that the pile is broken into segments one-fourth as long. As shown in Figure A.4, the force pulse calculated using this model shows no evidence of spurious oscillation and is almost identical to the true pulse. However, the computer time required for this solution was far greater than that required using Model I.

Model III (Figure A.2d) is similar to Model I, except that a cushion stiffness equal to one-fourth of the true value was used. The results of the solution (Figure A.5) indicate that spurious oscillation was avoided. However, the calculated incident peak force is significantly less than the true value;

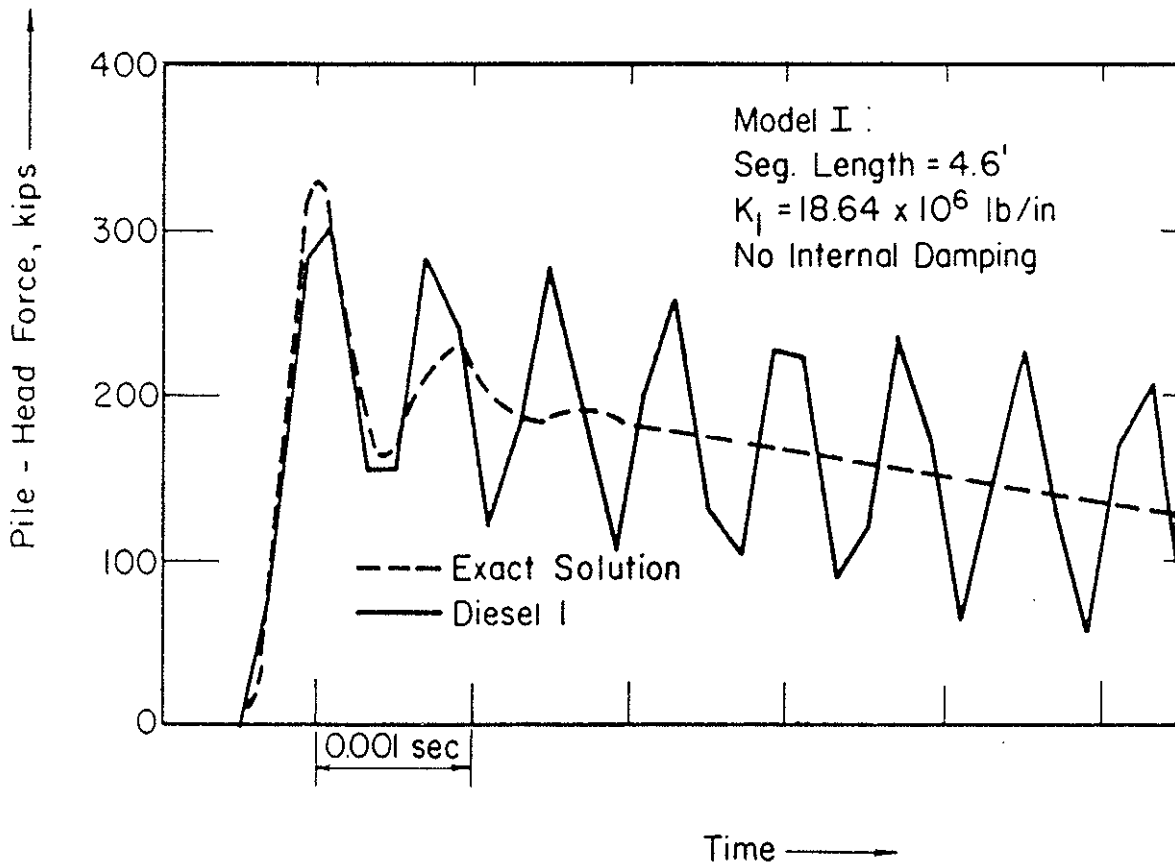


Figure A.3 HYPOTHETICAL PROBLEM, DIESEL I SOLUTION USING MODEL I

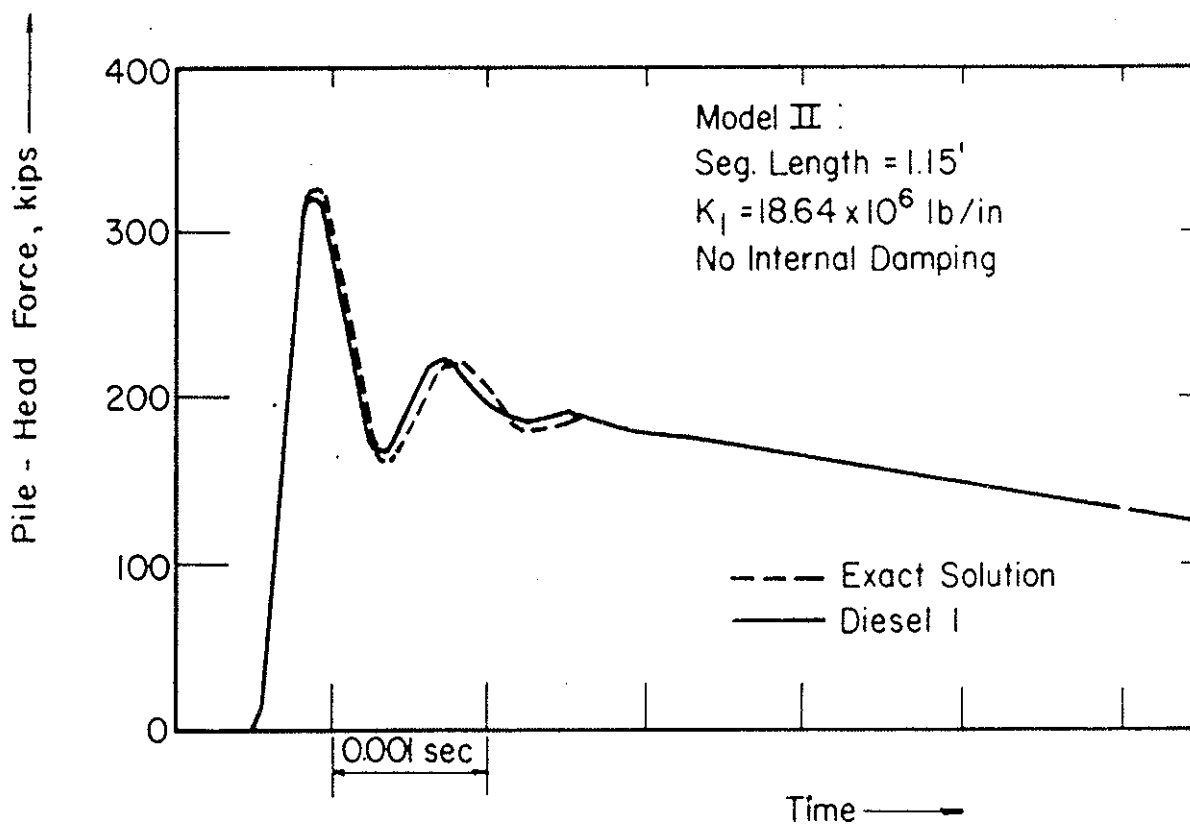


Figure A.4 HYPOTHETICAL PROBLEM, DIESEL I SOLUTION USING MODEL II

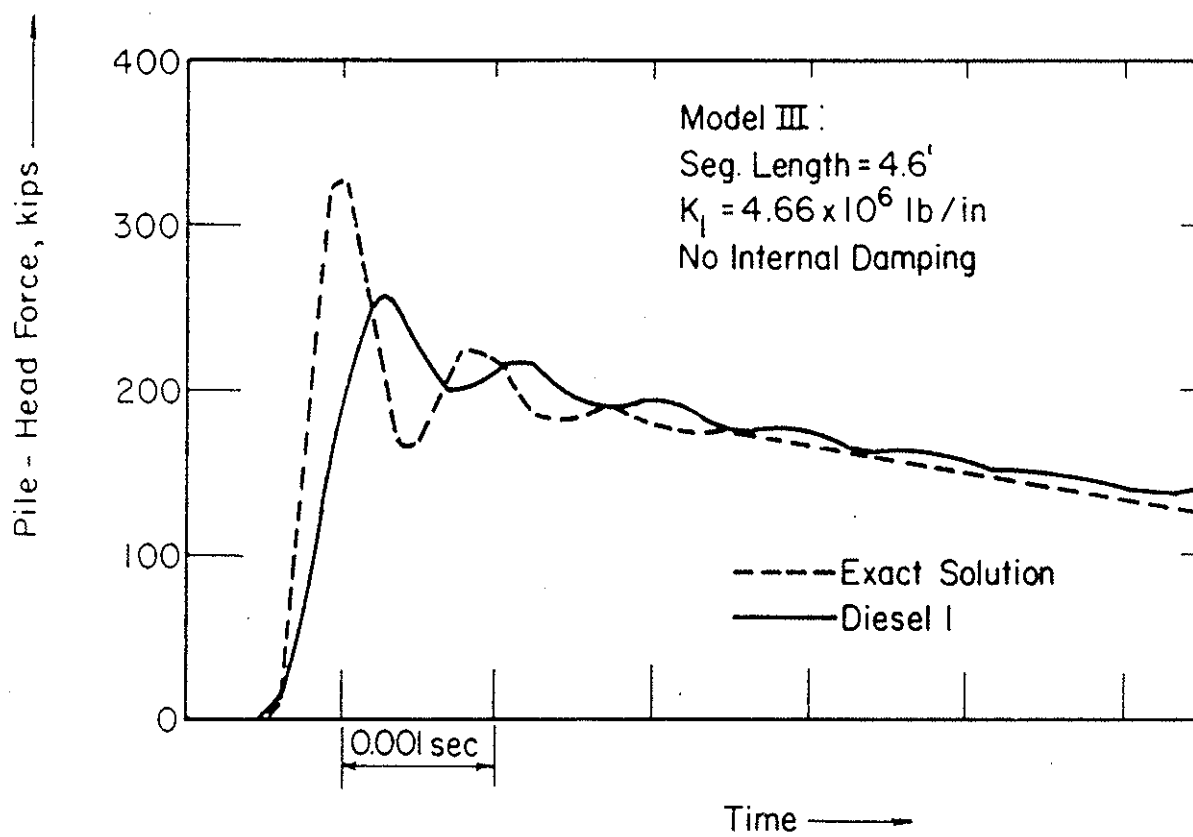


Figure A.5 HYPOTHETICAL PROBLEM, DIESEL I SOLUTION USING MODEL III

this is a serious deficiency. Computer time was equal to that required using Model I.

Model IV (Figure A.2e) also is similar to Model I, but incorporates internal damping as described in the previous section. The results obtained using this model (Figure A.6) are nearly as good as those obtained with Model II, yet the computer time was no greater than that required for Model I.

A.5 CONCLUSION

It is concluded that the use of internal damping is an effective and economical method for minimizing the error due to spurious oscillation. An alternate method, using extremely short pile segments, can produce slightly more accurate results, however excessive computer time is required.

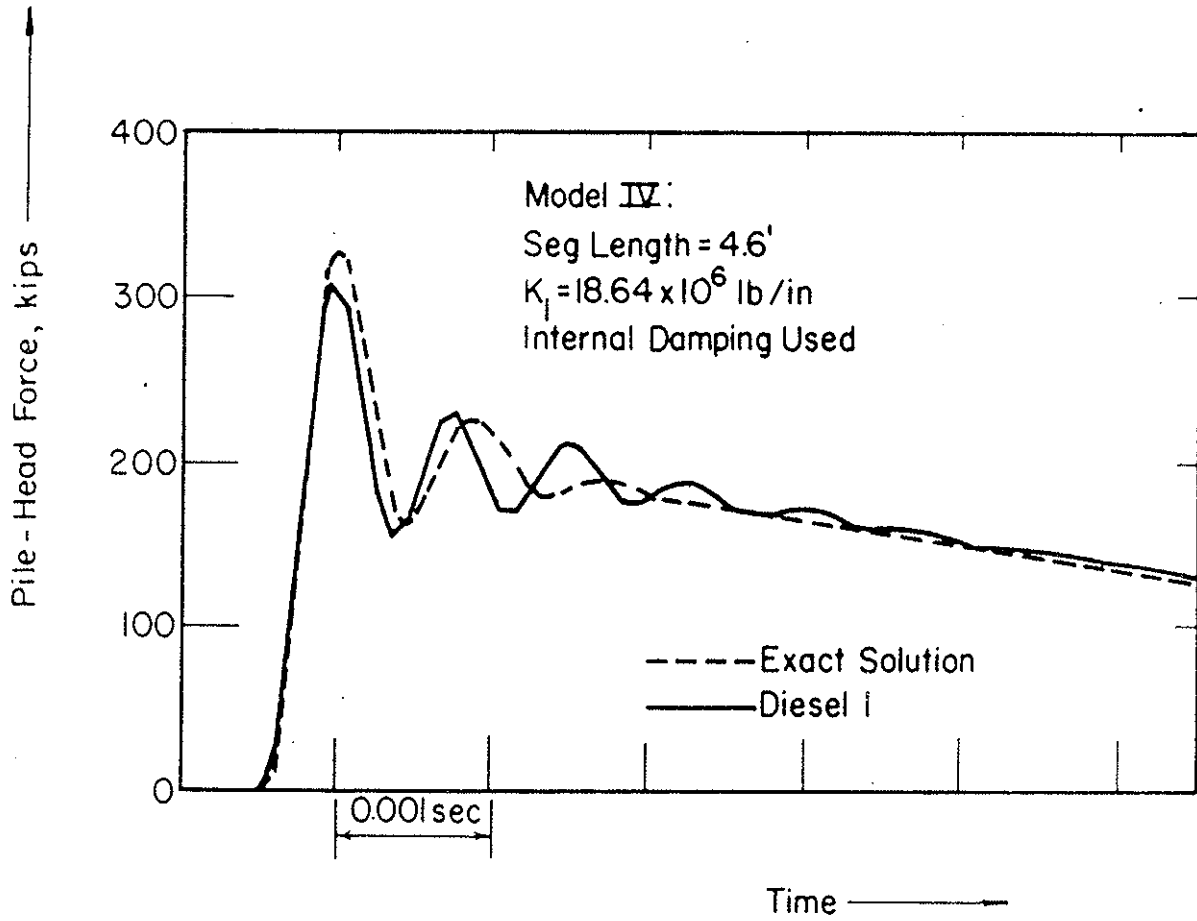


Figure A.6 HYPOTHETICAL PROBLEM, DIESEL I SOLUTION USING MODEL IV

APPENDIX B

SUMMARY FLOW CHART FOR DIESEL1 PROGRAM

DIESEL1 is a computer program for wave equation analysis of diesel pile driving. The program is based on the wave equation solution developed by Smith (1962) for impact hammers. Major modifications were required in order to simulate diesel hammer operation; these are described in Chapter 3.

Fundamental program logic is outlined in the summary flow chart (Figure B.1). Normally, the stroke-input type of analysis is used, wherein downstroke is specified and the peak gas force is adjusted so as to achieve equality of downstroke and upstroke. If the net expended fuel energy is known, the energy-input type of analysis can be used (Chapter 3). In this case, fuel energy is an input quantity; stroke is adjusted in order to obtain the required value of fuel energy.

The program is written in the FORTRAN computer language and consists of approximately 3000 statements.

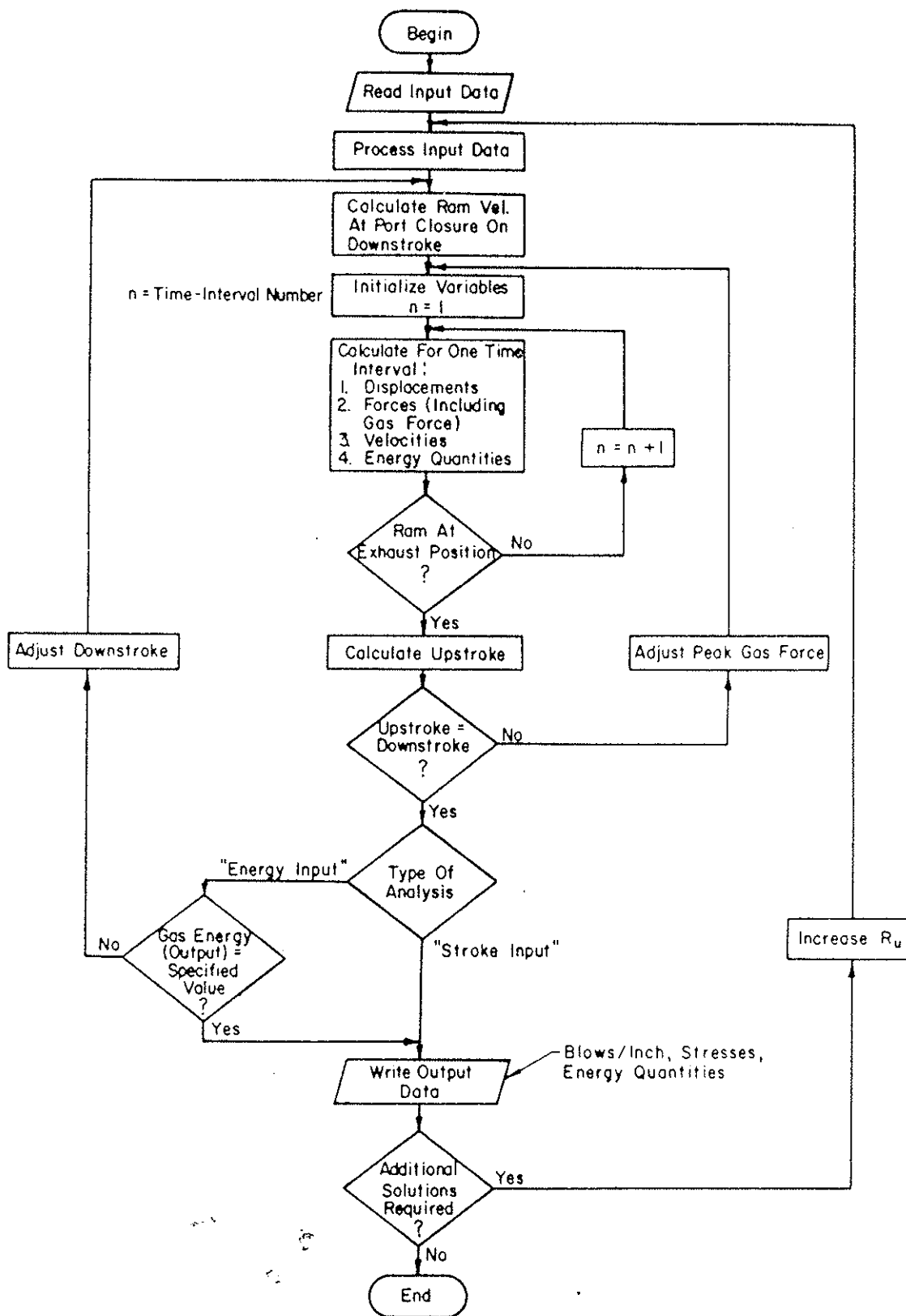


Figure B.1 SUMMARY FLOW CHART FOR DIESEL1 PROGRAM

VITA

David Maher Rempe was born on September 4, 1937 in Yonkers, New York. He graduated from Bethesda-Chevy Chase High School in Bethesda, Maryland in 1955. He graduated from Cornell University in 1960 with a Bachelor of Science degree in Civil Engineering. He entered the University of Illinois at Urbana-Champaign in 1968 and received a Master of Science degree in Civil Engineering in 1969.

He was employed by Raymond International Inc. as a construction engineer and superintendent on heavy construction projects in Liberia, Jamaica, and the U. S. A. During his graduate studies he worked as a private consultant, and for a private consultant, in Geotechnical Engineering.

He is a member of Chi Epsilon and Tau Beta Pi honorary societies, and a Member of the American Society of Civil Engineers, the American Society for Testing and Materials, and the International Society of Soil Mechanics and Foundation Engineering.

